FEEDBACK PARTICLE FILTER AND ITS APPLICATIONS

BY

TAO YANG

DISSERTATION

Submitted in partial fulfillment of the requirements
for the degree of Doctor of Philosophy in Mechanical Engineering
in the Graduate College of the
University of Illinois at Urbana-Champaign, 2014

Urbana, Illinois

Doctoral Committee:

Professor Prashant G. Mehta, Chair and Director of Research
Professor Tamer Başar
Professor Venugopal V. Veeravalli
Professor Pierre Moulin

Abstract

The purpose of nonlinear filtering is to extract useful information from noisy sensor data. It finds applications in all disciplines of science and engineering, including tracking and navigation, traffic surveillance, financial engineering, neuroscience, biology, robotics, computer vision, weather forecasting, geophysical survey and oceanology, etc.

This thesis is particularly concerned with the nonlinear filtering problem in the continuous-time continuous-valued state-space setting (diffusion). In this setting, the nonlinear filter is described by the Kushner-Stratonovich (K-S) stochastic partial differential equation (SPDE). For the general nonlinear non-Gaussian problem, no analytical expression for the solution of the SPDE is available. For certain special cases, finite-dimensional solution exists and one such case is the Kalman filter. The Kalman filter admits an innovation error-based feedback control structure, which is important on account of robustness, cost efficiency and ease of design, testing and operation. The limitations of Kalman filters in applications arise because of nonlinearities, not only in the signal models but also in the observation models. For such cases, Kalman filters are known to perform poorly. This motivates simulation-based methods to approximate the infinite-dimensional solution of the K-S SPDE. One popular approach is the particle filter, which is a Monte Carlo algorithm based on sequential importance sampling. Although it is potentially applicable to a general class of nonlinear non-Gaussian problems, the particle filter is known to suffer from several well-known drawbacks, such as particle degeneracy, curse of dimensionality, numerical instability and high computational cost. The goal of this dissertation is to propose a new framework for nonlinear filtering, which introduces the innovation error-based feedback control structure to the particle filter. The proposed filter is called the *feedback particle filter* (FPF).

The first part of this dissertation covers the theory of the feedback particle filter. The filter is defined by an ensemble of controlled, stochastic, dynamic systems (the "particles"). Each particle evolves under feedback control based on its own state, and the empirical distribution of the ensemble. The feedback control law is obtained as the solution to a variational problem, in which the optimization criterion is the Kullback-Leibler divergence between the actual posterior, and the common posterior of any particle. The following conclusions are obtained for diffusions with continuous observations: 1) The optimal control solution is exact: The two posteriors match exactly, provided they are initialized with identical priors. 2) The optimal filter admits an innovation error-based gain feedback structure. 3) The optimal feedback gain is obtained via a solution of an Euler-Lagrange boundary value problem; the feedback

gain equals the Kalman gain in the linear Gaussian case. The feedback particle filter offers significant variance improvements when compared to the bootstrap particle filter; in particular, the algorithm can be applied to systems that are not stable. No importance sampling or resampling is required, and therefore the filter does not suffer sampling-related issues and incurs low computational burden.

The theory of the feedback particle filter is first developed for the continuous-time continuous-valued state-space setting. Its extensions to two other settings are also studied in this dissertation. In particular, we introduce feedback particle filter-based solutions for: i) estimating a continuous-time Markov chain with noisy measurements, and ii) the continuous-discrete time filtering problem. Both algorithms are shown to admit an innovation error-based feedback control structure.

The second part of this dissertation concerns the extensions of the feedback particle filter algorithms to address additional uncertainties. In particular, we consider the nonlinear filtering problem with i) model uncertainty, and ii) data association uncertainty. The corresponding feedback particle filter algorithms are referred to as the *interacting multiple model-feedback particle filter* (IMM-FPF) and the *probabilistic data association-feedback particle filter* (PDA-FPF). The proposed algorithms are shown to be the nonlinear non-Gaussian generalization of their classic Kalman filter-based counterparts. One remarkable conclusion is that the proposed IMM-FPF and PDA-FPF algorithm retains the innovation error-based feedback structure even for the nonlinear non-Gaussian case. The results are illustrated with the aid of numerical simulations.

To my parents.

Acknowledgments

Above all I would like to thank my advisor, Professor Prashant G. Mehta, for his infinite support, enthusiasm, encouragement and guidance through my doctoral study at the University of Illinois at Urbana-Champaign. Special thanks also go to Professor Sean P. Meyn at the University of Florida for his directions and insights on many of the research works included in this thesis. I also greatly appreciate the guidance from Professor Henk A. P. Blom at the Delft University of Technology and National Aerospace Laboratory in Amsterdam, the Netherlands. I've benefited a lot from his instructive comments as well as his great passion about scientific research. I feel lucky and privileged to have worked with them in the past few years. I would like to thank Professor Tamer Başar, Professor Venugopal V. Veeravalli, and Professor Pierre Moulin for serving on my committee and providing valuable suggestions. I feel honored to have them as my defense committee.

I would like to thank the Coordinated Science Laboratory (CSL) for providing me the working space and research facilities. The CSL is an exceptional place to be a graduate student at. The research environment is interdisciplinary and spectacular. I would like to thank the staff and students of CSL for maintaining such a friendly atmosphere. I especially wish to thank Angie Ellis and Becky Lonberger for their help. I am also grateful to the Department of Mechanical Science and Engineering for admitting me to the PhD program. I would like to thank Kathy Smith for her patience to answer all my questions related to the graduate program. This research was funded by several institutions. I am deeply grateful to the National Science Foundation, and the Air Force Office of Scientific Research for their support of my entire doctoral program.

I would not survive the long journey without my friends along the way. I would like to thank Kun Deng for his selfless help and valuable guidance ever since I met him. It is really a blessing to have him both as an academic mentor and a life counselor. I would like to thank Yu Sun, Huibing Yin and Dayu Huang, Bo Tan for their useful suggestions on my research and career development. I would like to thank Adam Tilton who has been an inspiring lab mate and an amazing entrepreneur. Thank you for saving me from the bicycle trip at Montréal, Canada. I would like to thank the brain trust whom I sat with everyday. Thank you Shane Ghiotto, Chi Zhang, Rohan Arora, Amir taghvaei, Sahand Hariri, Geng Huang, Krishna Medarametla for all the good collaboration and friendship.

I would like to thank Xun Gong, Yunwen Xu, Jiamin Xu, Rui Wu, Quan Geng, Mindi Yuan, Qiaomin Xie, Ji Zhu,

Yun Li, Lili Su, Ge Yu, Xiaoyu Guang, Yifei Yang for all the meals and laughters we have together. I would like thank my basketball buddies at the U of I for the good memories on and off the court. I would also like to thank my small groups at both TCBC and CFC. It is my honor to have the fellowship with you and your prayers have always been a great support to me. All your friendship is greatly appreciated and treasured.

I am grateful to my girlfriend, Weiran Zhao, for showing up in my life and falling love with me. It is one of the most beautiful things that have ever happened in my life. It would be impossible for me to finish this work without you. I would also like to thank my parents, Yajian Yang and Jianqiu Tao, for their deep and unconditional love along the way. They give me the freedom to pursue my own interest and the trust to make decisions. They also teach me the value of hard working, time-managing, and self-control. Their supports and encouragements always give me the strength and perseverance to deal with any difficulties I encountered in my research and life.

Lastly, I would like to thank God my savior, for your word is a lamp to my feet and a light to my path.

Table of Contents

List of Figures

Chapter 1

Introduction

Nonlinear filtering is the science of extracting useful information from noisy sensor data. It is fundamental to many application domains including target tracking and surveillance, air traffic management, weather surveillance, ground mapping, geophysical surveys, remote sensing, autonomous navigation and robotics [10].

Prior to mid-1990s, the primary tool for filtering was a Kalman filter or one of its extensions (e.g., extended Kalman filter, interacting multiple model filter). The limitations of these tools in applications arise on account of nonlinearities, not only in signal models (e.g., drag forces acting on ballistic objects, whose estimation is of interest in surveillance applications) but also in the measurement models (e.g., range or bearing sensing modalities in radar-based target tracking systems). The nonlinearities can lead to a non-Gaussian multimodal conditional distribution. For such cases, Kalman and extended Kalman filters are known to perform poorly; cf., [132].

Since the advent and wide-spread use of particle filters [3, 39, 55, 74], such filters are becoming increasingly relevant to nonlinear filtering applications; cf., [132] and references therein. While rapid increases in computational capacity has provided an impetus to development of particle methods, currently these are simulation-based approaches grounded in importance sampling techniques. In applications, these approaches can be non-robust on account of variance issues [4, 15, 51, 132].

Significantly, simulation-based approaches do *not* have the (innovation error-based) feedback structure of the Kalman filter. Arguably, *the structural aspects of the Kalman filter have been as important as the algorithm itself in design, integration, testing and operation of the overall system.* Without such structural features, it is a challenge to create scalable cost-effective solutions.

The central theme of this thesis is to describe feedback-based algorithms for particle filtering. The core algorithm, referred to as the *feedback particle filter* (FPF), is presented for the continuous-time continuous-valued state-space models described by stochastic differential equations (SDEs). Several extensions of the core algorithm are discussed. The two most important extensions address additional uncertainties in models and in data association. The corresponding algorithms are referred to as the interacting multiple model-feedback particle filter (IMM-FPF) and the probabilistic data association-feedback particle filter (PDA-FPF), respectively. Although the main focus of this thesis is on nonlinear filtering problems described by SDEs, feedback-based particle filtering algorithms are also discussed

for continuous-time Markov chain models and for certain discrete-time models.

The organization of the remainder of this chapter is as follows. Sec. 1.1 presents the mathematical problem of nonlinear filtering considered in this thesis along with an enumerated list of its applications. Sec. 1.2 summarizes the classic Kalman filter as well as the conventional particle filter algorithm. Sec. 1.3 presents the feedback-control based architecture for filtering together with a discussion of relevant prior literature. Sec. 1.4 and Sec. 1.5 describes the main contributions and the layout of this thesis, respectively.

1.1 Problem Statement

Consider the filtering problem:

$$\mathrm{d}X_t = a(X_t)\,\mathrm{d}t + \sigma(X_t)\,\mathrm{d}B_t, \tag{1.1a}$$

$$\mathrm{d}Z_t = h(X_t)\,\mathrm{d}t + \mathrm{d}W_t, \tag{1.1b}$$

where $X_t \in \mathbb{R}^d$ is the state (signal), $Z_t \in \mathbb{R}^m$ is the observation (measurement), $a(\cdot)$, $h(\cdot)$ are C^1 functions, and $\{B_t\}$, $\{W_t\}$ are mutually independent standard Wiener processes of appropriate dimension. Unless otherwise noted, the SDEs in this thesis are expressed in Itô form.

The objective of the filtering problem is to compute the posterior distribution of X_t given the filtration (history of observations) $\mathscr{Z}_t := \sigma(Z_s : s \le t)$. The posterior p^* is defined so that, for any measurable set $A \subset \mathbb{R}^d$,

$$\int_{x\in A} p^*(x,t)\,\mathrm{d}x = \mathsf{P}\{X_t \in A \mid \mathscr{Z}_t\}. \tag{1.2}$$

The theory of general nonlinear filtering is described in the classic monograph [91]. The evolution of the posterior p^* is described by the Kushner-Stratonovich (K-S) equation [100, 135]:

$$\mathrm{d}p^* = \mathscr{L}^\dagger p^*\,\mathrm{d}t + (h-\hat{h})^T(\mathrm{d}Z_t - \hat{h}\,\mathrm{d}t)p^*, \tag{1.3}$$

where $\hat{h} = \int h(x)p^*(x,t)\,\mathrm{d}x$ and $\mathscr{L}^\dagger p^* = -\nabla\cdot(p^* a) + \frac{1}{2}\sum_{l,k=1}^{d}\frac{\partial^2}{\partial x_l \partial x_k}\left(p^*[\sigma\sigma^T]_{lk}\right)$.

The filter (1.3) is infinite-dimensional since it defines the evolution, in the space of probability measures, of $\{p^*(\cdot,t) : t \ge 0\}$. Under few circumstances, (1.3) reduces to a finite-dimensional filter. If $a(\cdot)$, $h(\cdot)$ are linear functions, the solution is given by the finite-dimensional Kalman-Bucy filter [34, 92]. If the underlying state evolves as a continuous-time Markov chain, the solution is given by the Wonham filter [148]. Another example of the finite-dimensional filter is the Beneš filter [12]. For infinite-dimensional filter, numerical methods are used to approximate

the nonlinear filter (1.3) (see survey [36]).

In nonlinear filtering, there are two major problems of research interest:

(i) **Numerical methods for solving the nonlinear filtering problem** (1.3). This involves numerical approximation of the posterior distribution p^*, which is typically an infinite-dimensional object. Several class of numerical methods have been developed for this purpose, such as the projection filter/moment methods [31], spectral methods [109], PDE methods [38] and the particle methods (also known as *particle filters* or *sequential Monte Carlo methods*) [74]. Although successfully applied to a variety of settings, particle filters often yield high variance, suffer particle degeneracy and are known to be unstable even in low-order models [13]. Therefore it is essential to come up with new computational methods which overcome these difficulties.

(ii) **Algorithms for nonlinear filtering in the presence of model and data association uncertainties**. It has been recognized that there can be additional uncertainties associated with the filtering problem in addition to process/observation noise. In applications involving tracking a maneuvering target, the target's dynamic model can randomly switch from one to another. In multiple target tracking applications, the measurement-to-target relationship is not apriori known in a cluttered environment. Nonlinear filtering algorithms that can handle such uncertainties are therefore of significant practical importance.

This thesis is devoted to solving these two problems stated above. For the first problem, a new framework for nonlinear filtering is proposed based on ideas from optimal control and mean-field game theory. The proposed feedback particle filter admits an innovation-error based feedback control structure and requires no importance sampling or resampling. For the second problem, the filter is generalized for problems involving additional uncertainties, including model uncertainty and data association uncertainty. The feedback control structure is shown to be preserved for both cases, even for the nonlinear non-Gaussian setting. Details on these topics appear in the following chapters.

1.1.1 Applications

Before proceeding to the next section, it is useful to list some practical applications of nonlinear filtering. The list is far from exhaustive and it serves mainly to show the wide usage and impact of filtering.

1. **Navigation and target tracking:** One classic application of filtering is to navigate an object through unknown terrain by estimating its current position based on sensor measurements [6, 35, 40, 77, 132]. Well-known applications include tracking and navigation of the Apollo spacecraft and the Mars orbiter. In recent years, the wide-spread use of new sensors based on infrared, laser and other technologies requires novel approaches to data fusion and tracking. More complicated applications also arise in problems with additional uncertainties,

such as model uncertainty (maneuvering target tracking) [10,21,112], and data association uncertainty (multiple target tracking) [5,8,73]. Although the primary tool for tracking and navigation is a Kalman filter or an extended Kalman filter, particle filters are becoming increasingly relevant to this field [28, 80, 101, 121, 151, 153].

2. **Data assimilation:** Given a computer-based model of a real system, data assimilation is the process by which observations are incorporated into the model to estimate system states. Applications of data assimilation originally arose in meteorology. For example, in weather forecasting, historical observations are taken into account to predict the state of the atmosphere for a given location [62, 72, 144]. The scope of data assimilation has now been extended to the fields of oceanology and geoscience [76, 123, 147]. Nonlinear filtering has been proposed as a suitable framework for the data assimilation task. One of the widely used algorithms is the ensemble Kalman filter (EnKF) introduced by Evensen [62, 63].

3. **Computer vision:** Nonlinear filtering is used for visual tracking, shape correspondence and motion estimation in computer vision [11, 17, 68]. In the problem of tracking outlines and features of foreground objects as they move in substantial clutter, the conditional density of the object is typically multimodal and therefore non-Gaussian. The development of particle filtering has provided a framework to handle non-Gaussian posteriors [84]. Particle filters (also referred to as the *CONDENSATION algorithm* by the authors in [83, 85]) have been successfully applied to track the contour of an object moving in a cluttered environment.

4. **Biology:** Bayesian inference is an important paradigm in systems neuroscience; cf., [58, 98, 128]. It has been proposed as a model of certain neuronal circuits in the brain [111, 129, 133]. Lee and Mumford [**?**] proposed a conceptual inference framework for the visual cortex based on particle filtering. Recent biology-related filtering applications include gait cycle estimation and human activity recognition, where coupled oscillator models are used to solve Bayesian inference problems [139, 140].

5. **Quantitative finance:** Given the stochastic volatility model, filtering is used to estimate the volatility of an asset's return based on stock market data [46]. In financial time series analysis, the Kalman filter is applied to estimate the trend of the stock price [141]. Particle filters have also found applications in derivative pricing [127] and portfolio optimization [149].

1.2 A Review of Common Approaches to Filtering

In this section, we briefly review two common approaches to filtering: the Kalman filter (KF) and the particle filter (PF). The Kalman filter expresses the closed form solution for the linear Gaussian problem, while the particle filter is a simulation-based algorithm to approximate the filtering task for the nonlinear non-Gaussian case. Each approach

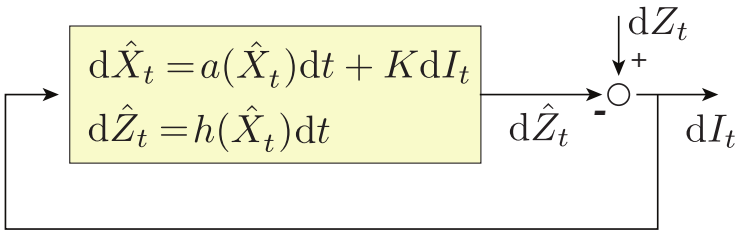

Figure 1.1: Innovation error-based feedback structure for the Kalman filter.

has its own advantages and disadvantages. The discussion here is intended to provide a brief overview of the two approaches, and to set the stage for the following chapters.

1.2.1 Kalman Filter

Consider a linear system,

$$\mathrm{d}X_t = A\,X_t\,\mathrm{d}t + \mathrm{d}B_t \tag{1.4a}$$

$$\mathrm{d}Z_t = H\,X_t\,\mathrm{d}t + \mathrm{d}W_t \tag{1.4b}$$

where A is an $d \times d$ matrix, and H is an $m \times d$ matrix. The initial distribution $p^*(x,0)$ is Gaussian with mean vector μ_0 and covariance matrix Σ_0.

The Kalman filter [94] gives the closed form solution to the linear system (1.4a)-(1.4b). It turns out that the posterior distribution p^* is Gaussian with conditional mean μ_t and covariance matrix Σ_t. Their evolutions are governed by the Kalman filtering equations:

$$\mathrm{d}\mu_t = A\mu_t\,\mathrm{d}t + \Sigma_t H^T(\mathrm{d}Z_t - H\mu_t\,\mathrm{d}t), \tag{1.5}$$

$$\frac{\mathrm{d}\Sigma_t}{\mathrm{d}t} = A\Sigma_t + \Sigma_t A^T + I - \Sigma_t H^T H\Sigma_t, \tag{1.6}$$

where I is the d-dimensional identity matrix.

The Kalman filter admits an innovation error-based feedback control structure. The correction part of μ_t (second term on the RHS of (1.5)) is the product of the Kalman gain ($K_t = \Sigma_t H^T$) and the innovation error ($\mathrm{d}I_t = \mathrm{d}Z_t - H\mu_t\,\mathrm{d}t$). This structural feature is illustrated in Fig. 1.1.

The Kalman filter has been widely used in applications for the following reasons:

1. **Optimality:** The Kalman filter (1.5)-(1.6) is the optimal (minimum variance) filter of the linear filtering problem (1.4a)-(1.4b) [90]. It is the best "guess" we can make regarding the underlying system state.

2. **Robustness:** The Kalman filter is guaranteed to be stable under very mild conditions (e.g., controllability and observability of the system model) [93]. The feedback control structure of the Kalman filter makes it robust to a certain degree of uncertainty inherent in any model [158].

3. **Cost efficiency:** Only the conditional mean and covariance matrix are propagated at each time step (see (1.5)-(1.6)). Therefore it is much more efficient compared to sampling-based algorithms, where the entire distribution is propagated through particles [57, 158].

4. **Ease of design, testing and operation:** On account of the structural features, Kalman filter-based solutions can be easily extended to other problems, such as the probabilistic data association filter for the data association problem [8], and the interacting multiple model filter for the estimation problem of stochastic hybrid systems [21]. The separate treatment for the gain function and the innovation error is also helpful for debugging and testing of large-scale problems [158].

The biggest limitation of the Kalman filter is the linear Gaussian assumption. For nonlinear systems in particular, the Kalman filter is known to perform poorly; cf., [132]. One remedy is the extended Kalman filter (EKF), which uses the linearized model in the update equations [1]. Other KF-based approaches for nonlinear filtering include the unscented Kalman filter (UKF) [146], ensemble Kalman filter (EnKF) [62]. Nevertheless, in all these approaches, the performance deteriorates as the nonlinearity becomes severe [89]. This motivates the study of sampling-based particle filter algorithms.

1.2.2 Particle Filter

For nonlinear systems, the particle filter is a simulation-based algorithm to approximate the filtering task (1.1a)-(1.1b) (see survey articles [36, 55, 74, 78]). The key step is the construction of N stochastic processes $\{X_t^i : 1 \le i \le N\}$. The value $X_t^i \in \mathbb{R}^d$ is the state for the i^{th} particle at time t. For each time t, the empirical distribution formed by, the "particle population" is used to approximate the conditional distribution. It is defined for any measurable set $A \subset \mathbb{R}^d$ by,

$$p^{(N)}(A,t) = \frac{1}{N}\sum_{i=1}^{N} \mathbb{1}\{X_t^i \in A\}. \tag{1.7}$$

A common approach in particle filtering is called *sequential importance resampling* (SIR), where particles are generated according to their importance weight at every time stage [36, 55]. By choosing the sampling mechanism properly, particle filtering can approximately propagate the posterior distribution, with the accuracy improving as N increases [44].

We sketch the implementation for the SIR particle filter (also known as the bootstrap particle filter), which is based on an algorithm taken from Chap. 9 of [7]. The Euler discretization is used and the resulting discrete-time algorithm

is as follows: Consider the evolution of the ensemble

$$(X_t^i, w_t^i) \longrightarrow (X_{t+\delta}^i, w_{t+\delta}^i),$$

as new observations are obtained; here δ is the time-step and w_t^i is the importance weight of the i^{th} particle at time t. This evolution is carried out in three steps [138]:

1. Prediction: Prediction involves using the SDE model (1.1a) to *push-forward* the particles, $X_t^i \longrightarrow X_{t+\delta}^{i-}$. This is accomplished by numerically integrating the SDE using Euler method. The weights $w_{t+\delta}^{i-} = w_t^i$.

At the end of prediction step, the particles are denoted as $(X_{t+\delta}^{i-}, w_{t+\delta}^{i-})$.

2. Update: The update step involves application of the Bayes' formula to update the weights. Given a new observation, $Z_{t+\delta}$, the unnormalized weights are obtained as,

$$\tilde{w}_{t+\delta}^{i-} = w_{t+\delta}^{i-} \, L(\delta Z | X_{t+\delta}^{i-}), \tag{1.8}$$

where $\delta Z := Z_{t+\delta} - Z_t$ and $L(\delta Z | X_{t+\delta}^{i-}) := (2\pi)^{-\frac{m}{2}} \delta^{-\frac{1}{2}} \exp\left[-\frac{\|\delta Z - h(X_{t+\delta}^{i-})\delta\|^2}{2\delta} \right]$. The weights at time $t+\delta$ are then obtained by normalization,

$$w_{t+\delta}^i = \frac{\tilde{w}_{t+\delta}^{i-}}{\sum_{j=1}^N \tilde{w}_{t+\delta}^{j-}}. \tag{1.9}$$

3. Resampling: The resampling step involves sampling $X_{t+\delta}^i$ with replacement from the set of particle positions $\{X_{t+\delta}^{i-}\}_{i=1}^N$ according to the probability vector of normalized weights $\{w_{t+\delta}^i\}_{i=1}^N$. After resampling, the particles are set to be equally-weighted for the next iteration: $w_{t+\delta}^i = \frac{1}{N}$. The resampling step is required in SIR particle filter because of the issue of *particle degeneracy*, whereby only a few particles have insignificant weight values. Other popular methods for resampling are surveyed in [4], including systematic resampling, stratified resampling and residual resampling.

The SIR particle filter approximates the true posterior p^* by the empirical measure $p^{(N)}$ defined in (1.7). The expectation of any test function $\phi : \mathbb{R}^d \to \mathbb{R}$ given by

$$I(\phi) := \int \phi(x) p^*(x) \, \mathrm{d}x,$$

is thus estimated by:

$$\hat{I}(\phi) := \int \phi(x) p^{(N)}(x) \, \mathrm{d}x = \frac{1}{N} \sum_{i=1}^N \phi(X_t^i), \tag{1.10}$$

Its straightforward to check that the SIR estimator (1.10) is unbiased and consistent. The variance of this estimator is

defined as

$$\mathrm{Var}_{\mathrm{SIR}}\left[\hat{I}(\phi)\right] := \mathsf{E}\left[(\hat{I}(\phi) - I(\phi))^2\right]. \tag{1.11}$$

The particle filter algorithm, as opposed to the linear Kalman filter, is applicable to a general class of nonlinear non-Gaussian problems. However, this sampling-based approach suffers from several notable drawbacks:

1. **Particle degeneracy:** It refers to the case where after a few (even one) observations, nearly all particles have zero weight values (one particle has unity weight). With a reduced effective sampling size, large computational effort is devoted to updating particles whose contribution is almost zero. It has been shown that the degeneracy phenomenon is impossible to avoid in importance sampling [56]. The root cause for particle degeneracy is the point-by-point multiplication implementation of Bayes' rule; cf., [13, 52, 57]. Common remedy is to occasionally "rejuvenate" the particle population via resampling: i.e., eliminate particles that have small weights and reproduce particles that have larger weights.

2. **Sample impoverishment:** Although resampling can potentially alleviate particle degeneracy, the benefit comes at the cost of reducing the quality of the path-space representation [4, 57]. This is because after resampling, the particles that have high weights w_t^i are statistically selected many times. This leads to a loss of diversity among the particles as the resultant sample will contain many repeated points. This problem, which is known as *sample impoverishment*, is severe in the case of small process noise.

3. **Curse of dimensionality:** As a result of particle degeneracy, the number of particles required to achieve a certain accuracy grows exponentially with the dimensionality of the state space [37, 47]. It is a fundamental problem with the importance sampling-based particle filter. As expected, when applied to geophysical models of high dimension, the classic particle filter is known to behave poorly after a few (or even one!) observation cycles [2, 143].

4. **Computational cost:** The importance sampling step (requires point-by-point multiplication) and the resampling step (requires the entire particle population) incurs high computational burden [53]. Resampling also limits the opportunity for parallel computation since all the particles must be combined [4].

5. **Variance:** A issue common to sampling-based particle filters is the high variance of the resulting estimator (1.10) [56, 70]. Under certain conditions, it is shown in [57] that the variance of the estimator defined in (1.11) satisfies:

$$\mathrm{Var}_{\mathrm{SIR}}\left[\hat{I}(\phi)\right] \leq \frac{D}{N},$$

where the constant D typically increases exponentially with the dimension of the state-space of X_t. The root

cause is the particle degeneracy which causes highly varying importance weights [13]. The variance of the particle filter estimator can only be expected to be reasonable if the variance of the sample weights is small.

6. **Numerical instability:** The particle filter implementation is generally fragile for unstable systems, in contrast to the Kalman filter, which is guaranteed to be stable under very mild conditions [51]. When the signal process (1.1a) is unstable, individual particle can exhibit numerical instabilities due to time-discretization, floating point representation, etc [158]. Recent efforts to understand the lack of stability for particle filters for unstable systems are surveyed by Ramon van Handel in [142].

7. **Difficulty in design, test and implementation:** The innovation error in the Kushner's equation (and in the Kalman filter) does not appear explicitly in the sampling-based particle filters. Without such a feedback control structure, it is a challenge to create scalable cost-effective solutions [158]: the optimal proposal density for importance sampling is difficult to design [56]; and the choice of resampling step is often ad-hoc [57].

Readers are referred to [4, 57] for more details on both the theory and implementation of the convectional particle filter.

1.3 Control-Oriented Particle Filtering

The objective of this work is to introduce an alternative approach to the construction of a particle filter for (1.1a)-(1.1b) inspired by mean-field optimal control techniques; cf., [79, 160]. In this approach, the model for the i^{th} particle is defined by a controlled system,

$$\mathrm{d}X_t^i = a(X_t^i)\,\mathrm{d}t + \sigma(X_t^i)\,\mathrm{d}B_t^i + \mathrm{d}U_t^i, \tag{1.12}$$

where $X_t^i \in \mathbb{R}^d$ is the state for the i^{th} particle at time t, U_t^i is its control input, and $\{B_t^i\}$ are mutually independent standard Wiener processes. Certain additional assumptions are made regarding admissible forms of the control input.

Throughout the thesis we denote conditional distribution of a particle X_t^i given $\mathscr{Z}_t$ by p, where for any measurable set $A \subset \mathbb{R}^d$,

$$\int_{x\in A} p(x,t)\,\mathrm{d}x = \mathsf{P}\{X_t^i \in A \mid \mathscr{Z}_t\}. \tag{1.13}$$

Recall the actual posterior of the system state X_t is denoted as p^* (defined in (1.2)). The initial conditions $\{X_0^i\}_{i=1}^N$ are assumed to be i.i.d., and drawn from initial distribution $p^*(x,0)$ of X_0 (i.e., $p(x,0) = p^*(x,0)$).

The control problem is to choose the control input U_t^i so that p approximates p^*, and consequently $p^{(N)}$ (defined in (1.7)) approximates p^* for large N. The synthesis of the control input is cast as a variational problem, with the Kullback-Leibler metric serving as the cost function. The optimal control input is obtained via analysis of the first

variation. The main objective is to derive an explicit formula for the optimal control input, and demonstrate that under general conditions we obtain an exact match: $p = p^*$ under optimal control. Details for the proposed filter appear in the following chapters.

1.3.1 Related Work

In recent years, there has been a burgeoning interest in application of ideas and techniques from statistical mechanics to nonlinear estimation and control theory. Although some of these applications are classic (see e.g., Del Moral [54]), the recent impetus comes from explosive interest in mean-field games, starting with two papers from 2007: Lasry and Lions' paper titled "Mean-field games" [103] and a paper by Huang, Caines and Malhamé [79]. These papers spurred interest in analysis and synthesis of *controlled interacting particle systems*.

The nonlinear estimation problem is a (mathematical) dual to the mean-field game control problem. Over the years, Mitter has a number of publications on duality between estimation and control [30, 67, 116–118]. Mitter's 2003 SIAM paper explicitly focused on a variational formulation of the nonlinear filtering problem with the objective of constructing a particle filtering algorithm based on duality considerations [117]. The variational construction in [117] was inspired by the variational formulation of the Fokker-Planck equation in the paper by Otto and collaborators [88]. The feedback particle filter algorithm (our approach) is a solution to the variational filtering problem (see also [104]). Given the variational underpinnings, there are also close parallels with the optimal transportation theory [61, 145]. For image processing applications, this theory has been used extensively by Tannenbaum and collaborators [96, 102, 115].

Apart from our work, there have also been a number of papers on *control-oriented* approaches to particle filtering: For the continuous-time filtering problem, an approximate particle filtering algorithm appears in the 2009 paper of Crisan and Xiong [45]. In the 2003 paper of Mitter, an optimal control problem for particle filtering is formulated based on duality [117]. Certain mean-field game inspired approximate algorithms for nonlinear estimation appear in the recent papers by other groups [64, 65, 125]. In discrete-time settings, Daum and Huang have introduced the *particle flow* algorithm [48–51]. A comparison of our work to Daum's particle flow filter appears in [152]. Despite the similarity, *important differences* exist between our approach and theirs, which are clarified in later chapters.

The innovative control structure in particle filtering is shown to be beneficial in terms of filter performance, robustness, stability as well as computational cost. There are by now a growing list of papers on application of such controlled algorithms to: physical activity recognition [139, 140], estimation of soil parameters in dredging applications [134], estimation and control in the presence of communication channels [110], target state estimation [138], weather forecasting [130].

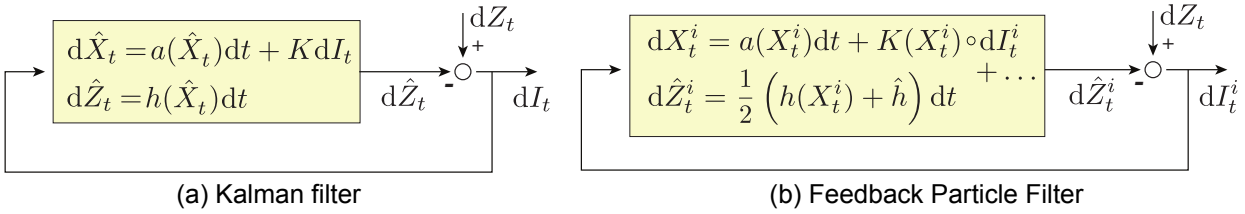

(a) Kalman filter (b) Feedback Particle Filter

Figure 1.2: Innovation error-based feedback structure for (a) the Kalman filter and (b) the feedback particle filter.

1.4 Main Contributions of the Thesis

As discussed in Sec. 1.1, there are two major problems of research interest in nonlinear filtering: 1) Numerical methods for solving the nonlinear filtering problem (1.3), and 2) Algorithms for nonlinear filtering in the presence of model and data association uncertainties. Both subjects are studied in this thesis. The original contributions are as follows:

1. **Feedback particle filter (FPF) algorithm:** The proposed filter is defined by an ensemble of controlled particle systems. Each particle evolves under feedback control based on its own state, and features of the empirical distribution of the ensemble. The feedback control law in (1.12) is obtained as the solution to a variational problem, where the optimization criterion is the Kullback-Leibler divergence between the actual posterior, and the common posterior of any particle. The optimal control solution is shown to be exact in the sense that the two posteriors match exactly, provided they are initialized with identical priors. The optimal filter admits an innovation error-based feedback structure, and the optimal feedback gain is obtained via a solution of an Euler-Lagrange boundary value problem (E-L BVP). See Fig. 1.2 for an illustration of the feedback control structure. The feedback gain equals the Kalman gain in the linear Gaussian case. For the nonlinear case, the Kalman gain is replaced by a nonlinear function of the state. These results have been published in [156–158].

2. **Existence and uniqueness of FPF:** Consistency is established in the general multivariate setting, as well as the well-posedness of the associated BVP to obtain the filter gain function. The admissibility of the control input in (1.12) is proved as a corollary. These results have been published in [154].

3. **Numerical algorithms for gain function approximation:** Several approaches have been proposed to solve the BVP, including the direct numerical approximation, constant gain approximation and the Gaussian mixture approximation. Motivated by a weak formulation of the BVP, a Galerkin finite-element algorithm has been proposed to approximate the gain function. These results have been published in [154, 156].

4. **FPF for discrete-time observation:** The FPF algorithm is introduced for the continuous-discrete time nonlinear filtering problem. A continuous-discrete time analogue of the feedback control structure is derived. Comparisons to existing continuous-discrete time algorithms, specifically the particle flow filter by Daum and Huang [51], are also provided. These results have been published in [152].

5. **FPF for a continuous-time Markov chain:** The Wonham filter is shown to be approximated by the FPF algorithm for the problem of estimating a continuous-time Markov chain. A complete characterization of the feedback mechanism that defines the FPF is obtained, which leads to tractable algorithms for the nonlinear filtering problem, even for large state space. These results have been published in [159].

The second half of this thesis focuses on the algorithms for nonlinear filtering with additional uncertainties in models and in data association. Contributions are as follows:

6. **Interacting Multiple Model-Feedback Particle Filter (IMM-FPF):** The IMM-FPF is an algorithm for nonlinear filtering in the presence of model uncertainty. The uncertainty is modeled using a stochastic hybrid system (SHS) framework. The proposed filter is shown to be the nonlinear generalization of the classic Kalman filter-based IMM filter. The theoretical results are illustrated with numerical examples for tracking a maneuvering target. These results have been published in [151].

7. **Probabilistic Data Association-Feedback Particle Filter (PDA-FPF):** The PDA-FPF is an approximating algorithm for nonlinear filtering in the presence of data association uncertainty. The proposed filter is shown to represent a generalization - to the nonlinear non-Gaussian case - of the classic Kalman filter-based PDA filter (PDAF). Numerical examples motivated by multiple target tracking applications are used to illustrate the PDA-FPF. These results have been published in [153, 155].

One remarkable conclusion is that both the IMM-FPF and PDA-FPF retain the innovation error-based feedback structure as in the FPF, even for the nonlinear non-Gaussian case.

1.5 Layout of the Thesis

The remainder of the thesis is comprised of two parts. Part I covers the theory of the feedback particle filter: Chap. 2 contains an introduction to the fundamentals of the feedback particle filter. For pedagogical purpose, only the simplest scalar case is presented. The multivariable feedback particle filter appears in Chap. 3, where well-posedness results are also derived. The continuous-discrete time FPF algorithm is developed in Chap. 4, while the FPF for a continuous-time Markov chain is discussed in Chap. 5.

Part II of this thesis concerns two applications of the feedback particle filter in the presence of additional uncertainties. Specifically, Chap. 6 develops the IMM-FPF algorithm for the estimation problem of stochastic hybrid systems, where model uncertainty is present. To deal with data association uncertainty, Chap. 7 first proposes the PDA-FPF algorithm for the problem of tracking a single target in the presence of clutter. The JPDA-FPF for multiple target tracking case follows as a straightforward extension. All proofs are summarized in appendices.

Part I

Feedback Particle Filter

Chapter 2

Fundamentals of the Feedback Particle Filter*

2.1 Introduction

In this chapter, the basic feedback particle filter is introduced for the continuous-time continuous-valued state-space nonlinear filtering problem. The scalar case is described for pedagogical purposes and for ease of presentation. The general multivariable case appears in Chap. 3.

The scalar filtering problem is modeled using stochastic differential equations (SDEs):

$$\mathrm{d}X_t = a(X_t)\,\mathrm{d}t + \sigma_B\,\mathrm{d}B_t, \tag{2.1a}$$

$$\mathrm{d}Z_t = h(X_t)\,\mathrm{d}t + \sigma_W\,\mathrm{d}W_t, \tag{2.1b}$$

where $X_t \in \mathbb{R}$ is the state at time t, $Z_t \in \mathbb{R}$ is the observation, $a(\,\cdot\,)$, $h(\,\cdot\,)$ are C^1 functions, and $\{B_t\}$, $\{W_t\}$ are mutually independent standard Wiener processes. Unless otherwise noted, SDEs are expressed in Itô form.

The objective of the filtering problem is to compute or approximate the posterior distribution of X_t given the history $\mathscr{Z}_t := \sigma(Z_s : s \le t)$. The posterior p^* is defined so that, for any measurable set $A \subset \mathbb{R}$,

$$\int_{x\in A} p^*(x,t)\,\mathrm{d}x = \mathsf{P}\{X_t \in A \mid \mathscr{Z}_t\}. \tag{2.2}$$

The feedback particle filter is an alternative approach to the construction of a particle filter for (2.1a)-(2.1b) inspired by mean-field optimal control techniques; cf., [79, 160]. In this approach, the model for the i^{th} particle is defined by a controlled system,

$$\mathrm{d}X^i_t = a(X^i_t)\,\mathrm{d}t + \sigma_B\,\mathrm{d}B^i_t + \mathrm{d}U^i_t, \tag{2.3}$$

where $X^i_t \in \mathbb{R}$ is the state for the i^{th} particle at time t, U^i_t is its control input, and $\{B^i_t\}$ are mutually independent standard Wiener processes. Certain additional assumptions are made regarding admissible forms of control input.

*This chapter is an extension of the published paper [158].

We denote the conditional distribution of a particle X_t^i given $\mathscr{Z}_t$ by p where:

$$\int_{x\in A} p(x,t)\,\mathrm{d}x = \mathsf{P}\{X_t^i \in A \mid \mathscr{Z}_t\}. \tag{2.4}$$

The initial conditions $\{X_0^i\}_{i=1}^N$ are assumed to be i.i.d., and drawn from initial distribution $p^*(x,0)$ of X_0 (i.e., $p(x,0) = p^*(x,0)$).

The control problem is to choose the control input U_t^i so that p approximates p^*, and consequently $p^{(N)}$ (the empirical distribution formed by the "particle population", as defined in (1.7)) approximates p^* for large N. The synthesis of the control input is cast as a variational problem, with the Kullback-Leibler metric serving as the cost function. The optimal control input is obtained via analysis of the first variation.

The main result of this chapter is to derive an explicit formula for the optimal control input, and demonstrate that under general conditions we obtain an exact match: $p = p^*$ under optimal control. The optimally controlled dynamics of the i^{th} particle have the following Itô form,

$$\mathrm{d}X_t^i = a(X_t^i)\,\mathrm{d}t + \sigma_B\,\mathrm{d}B_t^i + \underbrace{\mathsf{K}(X_t^i,t)\,\mathrm{d}I_t^i + \Omega(X_t^i,t)\,\mathrm{d}t}_{\text{optimal control, } \mathrm{d}U_t^{i*}}, \tag{2.5}$$

in which I_t^i is a certain modified form of the *innovation process* that appears in the nonlinear filter,

$$\mathrm{d}I_t^i := \mathrm{d}Z_t - \frac{1}{2}\big(h(X_t^i) + \hat{h}_t\big)\,\mathrm{d}t, \tag{2.6}$$

where $\hat{h}_t := \mathsf{E}[h(X_t^i)|\mathscr{Z}_t] = \int h(x)p(x,t)\,\mathrm{d}x$. In a numerical implementation, we approximate

$$\hat{h}_t \approx \hat{h}_t^{(N)} := \frac{1}{N}\sum_{i=1}^N h(X_t^i)\,. \tag{2.7}$$

The gain function K is shown to be the solution to the following Euler-Lagrange boundary value problem (E-L BVP):

$$\frac{\partial}{\partial x}(p\mathsf{K}) = -\frac{1}{\sigma_W^2}(h-\hat{h}_t)p, \tag{2.8}$$

with boundary conditions $\lim_{x\to\pm\infty} p(x,t)\mathsf{K}(x,t) = 0$, where $h'(x) = \frac{\mathrm{d}}{\mathrm{d}x}h(x)$. Note that the gain function needs to be obtained for each value of time t.

Finally, $\Omega(x,t)$ is the Wong-Zakai correction term where $\Omega(x,t) := \frac{1}{2}\sigma_W^2\mathsf{K}(x,t)\mathsf{K}'(x,t)$ and $\mathsf{K}'(x,t) = \frac{\partial\mathsf{K}}{\partial x}(x,t)$. The controlled system (2.5)-(2.8) is called the *feedback particle filter*.

The contributions of this chapter are as follows:

• **Variational Problem.** The construction of the feedback particle filter is based on a variational problem, where the

cost function is the Kullback-Leibler (K-L) divergence between $p^*(x,t)$ and $p(x,t)$. The feedback particle filter (2.5)-(2.8), including the formula (2.6) for the innovation error and the E-L BVP (2.8), is obtained via analysis of the first variation.

• **Consistency.** The particle filter model (2.5) is consistent with nonlinear filter in the following sense: Suppose the gain function $\mathsf{K}(x,t)$ is obtained as the solution to (2.8), and the priors are consistent, $p(x,0) = p^*(x,0)$. Then, for all $t \geq 0$ and all x,

$$p(x,t) = p^*(x,t).$$

• **Algorithms.** Numerical techniques are proposed for synthesis of the gain function $\mathsf{K}(x,t)$. If $a(\cdot)$ and $h(\cdot)$ are linear and the density p^* is Gaussian, then the gain function is simply the Kalman gain. At time t, it is a constant given in terms of variance alone. The variance is approximated empirically as a sample covariance.

In the nonlinear case, numerical approximation techniques are described. A Galerkin finite-element algorithm appears in Chap. 3. Another approach based on the Gaussian mixture approximation is discussed in [156].

In recent decades, there have been many important advances in importance sampling based approaches for particle filtering; cf., [36,55,150]. A crucial distinction here is that there is no importance sampling or resampling of particles.

We believe that the introduction of control in the feedback particle filter has several useful features/advantages:

Does not require sampling. There is no importance sampling or resampling required as in the conventional particle filter. This property allows the feedback particle filter to be flexible with regards to implementation and does not suffer from sampling-related issues, such as particle degeneracy or sample impoverishment.

Innovation error. The innovation error-based feedback structure is a key feature of the feedback particle filter (2.5). The innovation error in (2.5) is based on the average value of the prediction $h(X_t^i)$ of the i^{th}-particle and the prediction $\hat{h}_t$ due to the entire population.

The feedback structure is easier to see when the filter is expressed in its Stratonovich form:

$$\mathrm{d}X_t^i = a(X_t^i)\,\mathrm{d}t + \mathrm{d}B_t^i + \mathsf{K}(X^i,t) \circ \left(\mathrm{d}Z_t - \frac{1}{2}(h(X_t^i) + \hat{h}_t)\,\mathrm{d}t \right). \tag{2.9}$$

Given that the Stratonovich form provides a mathematical interpretation of the (formal) ODE model [122, Section 3.3], we also obtain the ODE model of the filter. Denoting $Y_t \doteq \frac{\mathrm{d}Z_t}{\mathrm{d}t}$ and white noise process $\dot{B}_t^i \doteq \frac{\mathrm{d}B_t^i}{\mathrm{d}t}$, the ODE model of the filter is given by,

$$\frac{\mathrm{d}X_t^i}{\mathrm{d}t} = a(X_t^i) + \dot{B}_t^i + \mathsf{K}(X^i,t) \cdot \left(Y_t - \frac{1}{2}(h(X_t^i) + \hat{h}_t) \right).$$

The "innovation" of the feedback particle filter thus lies in the (modified) definition of innovation error for a particle filter (see (2.6)). Moreover, the feedback control structure that existed thusfar only for the Kalman filter now

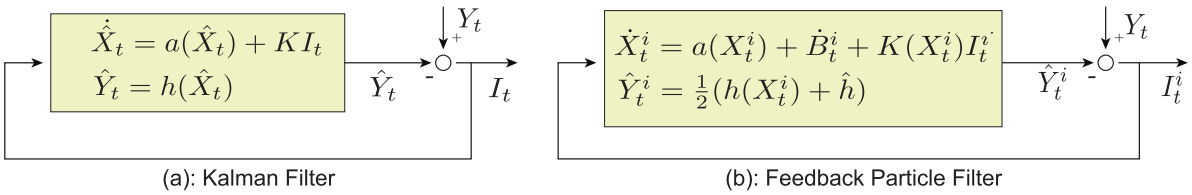

Figure 2.1: Innovation error-based feedback structure for (a) the Kalman filter and (b) the feedback particle filter (in ODE model).

also exists for particle filters (compare parts (a) and (b) of Fig. 2.1). For the linear case, the optimal gain function is the Kalman gain. For the nonlinear case, the Kalman gain is replaced by a nonlinear function of the state.

Feedback structure. Feedback is important on account of the issue of *robustness*. A filter is based on an idealized model of the underlying dynamic process that is often nonlinear, uncertain and time-varying. The self-correcting property of the feedback provides robustness, allowing one to tolerate a degree of uncertainty inherent in any model.

In contrast, a conventional particle filter is based upon importance sampling. Although the innovation error is central to the Kushner-Stratonovich's stochastic partial differential equation (SPDE) of nonlinear filtering, it is conspicuous by its absence in a conventional particle filter.

Arguably, the structural aspects of the Kalman filter have been as important as the algorithm itself in design, integration, testing and operation of the overall system. Without such structural features, it is a challenge to create scalable cost-effective solutions.

Variance reduction. Feedback can help reduce the high variance that is sometimes observed in the conventional particle filter. Numerical results in Sec. 2.5 support this claim — See Fig. 2.3 for a comparison of the feedback particle filter and the bootstrap particle filter.

Ease of design, testing and operation. On account of structural features, feedback particle filter-based solutions are expected to be more robust, cost-effective, and easier to debug and implement.

Applications. Bayesian inference is an important paradigm used to model functions of certain neural circuits in the brain [58, 105]. Compared to techniques that rely on importance sampling, a feedback particle filter may provide a more neuro-biologically plausible model to implement filtering and inference functions. It is illustrated in this chapter with the aid of a filtering problem involving nonlinear oscillators. Another application appears in [139, 140].

The remainder of this chapter is organized as follows: The variational setup is described in Sec. 2.2: It begins with a discussion of the continuous-discrete filtering problem: the equation for dynamics is defined by (2.1a), but the observations are made only at discrete times. The continuous-time filtering problem (for (2.1a)-(2.1b)) is obtained as a limiting case of the continuous-discrete problem.

The feedback particle filter is introduced in Sec. 2.3. Algorithms are discussed in Sec. 2.4, and numerical examples are described in Sec. 2.5, including the neuroscience application involving coupled oscillator models. These models

(also considered in our earlier mean-field control paper [160]) provided some of the initial motivation for the present work.

2.2 Variational Problem

The precise formulation of the variational problem begins with the continuous time model, with sampled observations. The equation for dynamics is given by (2.1a), and the observations are made only at discrete times $\{t_n\}$:

$$Y_{t_n} = h(X_{t_n}) + W^{\triangle}_{t_n}, \tag{2.10}$$

where $\triangle := t_{n+1} - t_n$ and $\{W^{\triangle}_{t_n}\}$ is i.i.d and drawn from $\boldsymbol{N}(0, \frac{\sigma_W^2}{\triangle})$.

The particle model in this case is a hybrid dynamical system: For $t \in [t_{n-1}, t_n)$, the i^{th} particle evolves according to the stochastic differential equation,

$$\mathrm{d}X^i_t = a(X^i_t)\,\mathrm{d}t + \sigma_B\,\mathrm{d}B^i_t\,, \quad t_{n-1} \le t < t_n\,, \tag{2.11}$$

where the initial condition $X^i_{t_{n-1}}$ is given. At time $t = t_n$ there is a potential jump that is determined by the input $U^i_{t_n}$:

$$X^i_{t_n} = X^i_{t_n^-} + U^i_{t_n}\,, \tag{2.12}$$

where $X^i_{t_n^-}$ denotes the right limit of $\{X^i_t : t_{n-1} \le t < t_n\}$. The specification (2.12) defines the initial condition for the process on the next interval $[t_n, t_{n+1})$.

The filtering problem is to construct a control law that defines $\{U^i_{t_n} : n \ge 1\}$ such that $p(\,\cdot\,, t_n)$ approximates $p^*(\,\cdot\,, t_n)$ for each $n \ge 1$. To solve this problem we first define "belief maps" that propagate the conditional distributions of X_t and X^i_t.

2.2.1 Belief Maps

The observation history is denoted $\mathscr{Y}_n := \sigma\{Y_{t_k} : k \le n, k \in \mathbb{N}\}$. For each n, various conditional distributions are considered:

1) p^*_n and p^{*-}_n: The conditional distribution of X_{t_n} given $\mathscr{Y}_n$ and $\mathscr{Y}_{n-1}$, respectively.

2) p_n and p^-_n: The conditional distribution of $X^i_{t_n}$ given $\mathscr{Y}_n$ and $\mathscr{Y}_{n-1}$, respectively.

These densities evolve according to recursions of the form,

$$p_n^* = \mathscr{P}^*(p_{n-1}^*, Y_{t_n}), \qquad p_n = \mathscr{P}(p_{n-1}, Y_{t_n}). \tag{2.13}$$

The mappings $\mathscr{P}^*$ and $\mathscr{P}$ can be decomposed into two parts. The first part is identical for each of these mappings: the transformation that takes p_{n-1} to p_n^- coincides with the mapping from p_{n-1}^* to p_n^{*-}. In each case it is defined by the Kolmogorov forward equation associated with the diffusion on $[t_{n-1}, t_n)$.

The second part of the mapping is the transformation that takes p_n^{*-} to p_n^*, which is obtained from Bayes' rule: Given the observation Y_{t_n} made at time $t = t_n$,

$$p_n^*(s) = \frac{p_n^{*-}(s) \cdot p_{Y|X}(Y_{t_n}|s)}{p_Y(Y_{t_n})}, \quad s \in \mathbb{R}, \tag{2.14}$$

where p_Y denotes the pdf for Y_{t_n}, and $p_{Y|X}(\,\cdot \mid s)$ denotes the conditional distribution of Y_{t_n} given $X_{t_n} = s$. Applying (2.10) gives,

$$p_{Y|X}(Y_{t_n} \mid s) = \frac{1}{\sqrt{2\pi\sigma_W^2/\triangle}} \exp\left(-\frac{(Y_{t_n} - h(s))^2}{2\sigma_W^2/\triangle}\right).$$

Combining (2.14) with the forward equation defines $\mathscr{P}^*$.

The transformation that takes p_n^- to p_n depends upon the choice of control $U_{t_n}^i$ in (2.12). At time $t = t_n$, we seek a control input $U_{t_n}^i$ that is *admissible*.

Definition 1 (Admissible Input) *The control sequence $\{U_{t_n}^i : n \geq 0\}$ is admissible if there is a sequence of maps $\{v_n(x; y_0^n)\}$ such that $U_{t_n}^i = v_n(X_{t_n^-}^i, Y_{t_0}, \ldots, Y_{t_n})$ for each n, and moreover,*

(i) $\mathsf{E}[|U_{t_n}^i|] < \infty$, *and with probability one,*

$$\lim_{x \to \pm\infty} v_n(x, Y_{t_0}, \ldots, Y_{t_n}) p_n^-(x) = 0.$$

(ii) v_n *is twice continuously differentiable as a function of x.*

(iii) $1 + v_n'(x)$ *is non-zero for all x, where* $v_n'(x) = \frac{\mathrm{d}}{\mathrm{d}x} v_n(x)$.

We will suppress the dependency of v_n on the observations (and often the time-index n), writing $U_{t_n}^i = v(x)$ when $X_{t_n^-}^i = x$. Under the assumption that $1 + v'(x)$ is non-zero for all x, we can write,

$$p_n(x^+) = \frac{p_n^-(x)}{|1 + v'(x)|}, \quad \text{where } x^+ = x + v(x). \tag{2.15}$$

2.2.2 Variational Problem

Our goal is to choose an admissible input so that the mapping $\mathscr{P}$ approximates the mapping $\mathscr{P}^*$ in (2.13). More specifically, given the pdf p_{n-1} we have already defined the mapping $\mathscr{P}$ so that $p_n = \mathscr{P}(p_{n-1}, Y_{t_n})$. We denote $\hat{p}_n^* = \mathscr{P}^*(p_{n-1}, Y_{t_n})$, and choose v_n so that these pdfs are as close as possible. We approach this goal through the formulation of an optimization problem with respect to the KL divergence metric. That is, at time $t = t_n$, the function v_n is the solution to the following optimization problem,

$$v_n(x) = \arg\min_v \mathsf{D}\left(p_n \| \hat{p}_n^*\right). \tag{2.16}$$

Based on the definitions, for any v the KL divergence can be expressed,

$$\mathsf{D}(p_n \| \hat{p}_n^*) = -\int_{\mathbb{R}} p_n^-(x) \Big\{ \ln|1+v'(x)| + \ln\left(p_n^-(x+v(x)) p_{Y|X}(Y_{t_n}|x+v(x))\right) \Big\} \mathrm{d}x + C, \tag{2.17}$$

where $C = \int_{\mathbb{R}} p_n^-(x) \ln(p_n^-(x) p_Y(Y_{t_n}))\,\mathrm{d}x$ is a constant that does not depend on v; cf., App. A.1 for the calculation.

The solution to (2.16) is described in the following proposition, whose proof appears in App. A.2.

Proposition 2.2.1 *Suppose that the admissible input is obtained as the solution to the sequence of optimization problems* (2.16)*. Then for each n, the function $v = v_n$ is a solution of the following Euler-Lagrange (E-L) BVP:*

$$\frac{\mathrm{d}}{\mathrm{d}x}\left(\frac{p_n^-(x)}{|1+v'(x)|}\right) = p_n^-(x) \frac{\partial}{\partial v}\left(\ln(p_n^-(x+v) p_{Y|X}(Y_{t_n}|x+v))\right), \tag{2.18}$$

with boundary condition $\lim_{x\to\pm\infty} v(x) p_n^-(x) = 0$.

We refer to the minimizer as the *optimal control function*. Additional details on the continuous-discrete time filter appear in our conference paper [157].

2.3 Feedback Particle Filter

We now consider the continuous time filtering problem (2.1a, 2.1b) introduced in Sec. 2.1.

2.3.1 Belief State Dynamics and Control Architecture

The model for the particle filter is given by the Itô diffusion,

$$\mathrm{d}X_t^i = a(X_t^i)\,\mathrm{d}t + \sigma_B\,\mathrm{d}B_t^i + \underbrace{u(X_t^i, t)\,\mathrm{d}t + \mathsf{K}(X_t^i, t)\,\mathrm{d}Z_t}_{\mathrm{d}U_t^i}, \tag{2.19}$$

where $X_t^i \in \mathbb{R}$ is the state for the i^{th} particle at time t, and $\{B_t^i\}$ are mutually independent standard Wiener processes. We assume the initial conditions $\{X_0^i\}_{i=1}^N$ are i.i.d., independent of $\{B_t^i\}$, and drawn from the initial distribution $p^*(x,0)$ of X_0. Both $\{B_t^i\}$ and $\{X_0^i\}$ are also assumed to be independent of X_t, Z_t.

As in Sec. 2.2, we impose admissibility requirements on the control input U_t^i in (2.19):

Definition 2 (Admissible Input) *The control input U_t^i is admissible if the random variables $u(x,t)$ and $\mathsf{K}(x,t)$ are $\mathscr{Z}_t = \sigma(Z_s : s \le t)$ measurable for each t. Moreover, each t,*

(i) $\mathsf{E}[|u(X_t^i,t)| + |\mathsf{K}(X_t^i,t)|^2] < \infty$, *and with probability one,*

$$\lim_{x\to\pm\infty} u(x,t)p(x,t) = 0, \tag{2.20a}$$

$$\lim_{x\to\pm\infty} \mathsf{K}(x,t)p(x,t) = 0. \tag{2.20b}$$

where p is the posterior distribution of X_t^i given $\mathscr{Z}_t$, defined in (2.4).

(ii) $u : \mathbb{R}^2 \to \mathbb{R}$, $\mathsf{K} : \mathbb{R}^2 \to \mathbb{R}$ *are twice continuously differentiable in their first arguments.*

The functions $\{u(x,t), \mathsf{K}(x,t)\}$ represent the continuous-time counterparts of the optimal control function $v_n(x)$ (see (2.16)). We say that these functions are *optimal* if $p \equiv p^*$, where recall p^* is the posterior distribution of X_t given $\mathscr{Z}_t$ as defined in (2.2). Given $p^*(\cdot,0) = p(\cdot,0)$, our goal is to choose $\{u,\mathsf{K}\}$ in the feedback particle filter so that the evolution equations of these conditional distributions coincide.

The evolution of $p^*(x,t)$ is described by the Kushner-Stratonovich (K-S) equation:

$$\mathrm{d}p^* = \mathscr{L}^\dagger p^* \,\mathrm{d}t + \frac{1}{\sigma_W^2}(h - \hat{h}_t)(\mathrm{d}Z_t - \hat{h}_t\,\mathrm{d}t)p^*, \tag{2.21}$$

where $\hat{h}_t = \int h(x)p^*(x,t)\,\mathrm{d}x$, and $\mathscr{L}^\dagger p^* = -\frac{\partial(p^*a)}{\partial x} + \frac{\sigma_B^2}{2}\frac{\partial^2 p^*}{\partial x^2}$.

The evolution equation of $p(x,t)$ is described next. The proof appears in App. A.3.

Proposition 2.3.1 *Consider the process X_t^i that evolves according to the particle filter model (2.19). The conditional distribution of X_t^i given the filtration $\mathscr{Z}_t$, $p(x,t)$, satisfies the forward equation*

$$\mathrm{d}p = \mathscr{L}^\dagger p\,\mathrm{d}t - \frac{\partial}{\partial x}(\mathsf{K}p)\,\mathrm{d}Z_t - \frac{\partial}{\partial x}(up)\,\mathrm{d}t + \sigma_W^2\frac{1}{2}\frac{\partial^2}{\partial x^2}\left(p\mathsf{K}^2\right)\mathrm{d}t. \tag{2.22}$$

2.3.2 Consistency with the Nonlinear Filter

The main result of this section is the construction of an optimal pair $\{u,\mathsf{K}\}$ under the following assumption:

Assumption A1 The conditional distributions (p^*, p) are C^2, with $p^*(x,t) > 0$ and $p(x,t) > 0$, for all $x \in \mathbb{R}$, $t > 0$.

We henceforth choose $\{u, \mathsf{K}\}$ as the solution to a certain E-L BVP based on p: the function K is the solution to

$$\frac{\partial}{\partial x}(p\mathsf{K}) = -\frac{1}{\sigma_{\tilde{W}}^2}(h - \hat{h}_t)p, \tag{2.23}$$

with boundary condition (2.20b). The function $u(\cdot,t) : \mathbb{R} \to \mathbb{R}$ is obtained as:

$$u(x,t) = \mathsf{K}(x,t)\left(-\frac{1}{2}(h(x) + \hat{h}_t) + \frac{1}{2}\sigma_{\tilde{W}}^2 \mathsf{K}'(x,t)\right), \tag{2.24}$$

where $\hat{h}_t = \int h(x)p(x,t)\,\mathrm{d}x$. We assume moreover that the control input obtained using $\{u, \mathsf{K}\}$ is admissible. The particular form of u given in (2.24) and the BVP (2.23) is motivated by considering the continuous-time limit of (2.18), obtained on letting $\triangle := t_{n+1} - t_n$ go to zero; the calculations appear in App. A.4.

Existence and uniqueness of $\{u, \mathsf{K}\}$ is obtained in the following proposition — Its proof is given in App. A.5.

Proposition 2.3.2 *Consider the BVP (2.23), subject to Assumption A1. Then,*

1) *There exists a unique solution K, subject to the boundary condition (2.20b).*

2) *The solution satisfies $\mathsf{K}(x,t) \geq 0$ for all x,t, provided $h'(x) \geq 0$ for all x.*

The following theorem shows that the two evolution equations (2.21) and (2.22) are identical. The proof appears in App. A.6.

Theorem 2.3.3 *Consider the two evolution equations for p and p^*, defined according to the solution of the forward equation (2.22) and the K-S equation (2.21), respectively. Suppose that the control functions $u(x,t)$ and $\mathsf{K}(x,t)$ are obtained according to (2.23) and (2.24), respectively. Then, provided $p(x,0) = p^*(x,0)$, we have for all $t \geq 0$,*

$$p(x,t) = p^*(x,t)$$

Remark 1 *Thm. 2.3.3 is based on the ideal setting in which the gain $\mathsf{K}(X_t^i, t)$ is obtained as a function of the posterior $p = p^*$ for X_t^i. In practice the algorithm is applied with p replaced by the empirical distribution of the N particles.*

In this ideal setting, the empirical distribution of the particle system will approximate the posterior distribution $p^*(x,t)$ as $N \to \infty$. The convergence is in the weak sense in general. To obtain almost sure convergence, it is necessary to obtain sample path representations of the solution to the stochastic differential equation for each i (see e.g. [99]).

Under these conditions the solution to the SDE (2.3) for each i has a functional representation,

$$X_t^i = F(X_0^i, B_{[0,t]}^i; Z_{[0,t]}),$$

where the notation $Z_{[0,t]}$ signifies the entire sample path $\{Z_s : 0 \le s \le t\}$ for a stochastic process Z; F is a continuous functional (in the uniform topology) of the sample paths $\{B_{[0,t]}^i, Z_{[0,t]}\}$ along with the initial condition X_0^i. It follows that the empirical distribution has a functional representation,

$$p^{(N)}(A,t) = \frac{1}{N}\sum_{i=1}^{N} \mathbb{1}\{F(X_0^i, B_{[0,t]}^i; Z_{[0,t]}) \in A\}$$

The sequence $\{(X_0^i, B_{[0,t]}^i) : i = 1, \ldots\}$ is i.i.d. and independent of Z. It follows that the summand $\{\mathbb{1}\{F(X_0^i, B_{[0,t]}^i; Z_{[0,t]}) : i = 1, \ldots\}$ is also i.i.d. given $Z_{[0,t]}$. Almost sure convergence follows from the Law of Large Numbers for scalar i.i.d. sequences.

In current research we are considering the more difficult problem of performance bounds for the approximate implementations described in Sec. 2.4.

Remark 2 *Although the methodology and the filter is presented for Gaussian process and observation noise, the case of non-Gaussian process noise is easily handled – simply replace the noise model in the filter with the appropriate model of the process noise.*

For other types of observation noise, one would modify the conditional distribution $p_{Y|X}$ in the optimization problem (2.16). The derivation of filter would then proceed by consideration of the first variation (see App. A.4).

2.3.3 Example: Linear Model

It is helpful to consider the feedback particle filter in the following simple linear setting,

$$\mathrm{d}X_t = \alpha\, X_t\, \mathrm{d}t + \sigma_B\, \mathrm{d}B_t, \tag{2.25a}$$

$$\mathrm{d}Z_t = \gamma\, X_t\, \mathrm{d}t + \sigma_W\, \mathrm{d}W_t, \tag{2.25b}$$

where α, γ are real numbers. The initial distribution $p^*(x,0)$ is assumed to be Gaussian with mean μ_0 and variance Σ_0.

The following lemma provides the solution of the gain function $\mathsf{K}(x,t)$ in the linear Gaussian case.

Lemma 2.3.4 *Consider the linear observation equation (2.25b). If $p(x,t)$ is assumed to be Gaussian with mean μ_t*

and variance Σ_t, then the solution of E-L BVP (2.8) is given by:

$$\mathsf{K}(x,t) = \frac{\Sigma_t \gamma}{\sigma_W^2}. \tag{2.26}$$

The formula (2.26) is verified by direct substitution in the ODE (2.8) where the distribution p is Gaussian.

The optimal control yields the following form for the particle filter in this linear Gaussian model:

$$\mathrm{d}X_t^i = \alpha\, X_t^i\, \mathrm{d}t + \sigma_B\, \mathrm{d}B_t^i + \frac{\Sigma_t \gamma}{\sigma_W^2}\left(\mathrm{d}Z_t - \gamma \frac{X_t^i + \mu_t}{2}\, \mathrm{d}t\right). \tag{2.27}$$

Now we show that $p = p^*$ in this case. That is, the conditional distributions of X_t and X_t^i coincide, and are defined by the well-known dynamic equations that characterize the mean and the variance of the continuous-time Kalman filter. The proof appears in App. A.7.

Theorem 2.3.5 *Consider the linear Gaussian filtering problem defined by the state-observation equations (2.25a,2.25b). In this case the posterior distributions of X_t and X_t^i are Gaussian, whose conditional mean and covariance are given by the respective SDE and the ODE,*

$$\mathrm{d}\mu_t = \alpha \mu_t\, \mathrm{d}t + \frac{\Sigma_t \gamma}{\sigma_W^2}\Big(\mathrm{d}Z_t - \gamma \mu_t\, \mathrm{d}t\Big) \tag{2.28}$$

$$\frac{\mathrm{d}}{\mathrm{d}t}\Sigma_t = 2\alpha\Sigma_t + \sigma_B^2 - \frac{(\gamma)^2 \Sigma_t^2}{\sigma_W^2} \tag{2.29}$$

Notice that the particle system (2.27) is not practical since it requires computation of the conditional mean and variance $\{\mu_t, \Sigma_t\}$. If we are to compute these quantities, then there is no reason to run a particle filter!

In practice $\{\mu_t, \Sigma_t\}$ are approximated as sample means and sample covariances from the ensemble $\{X_t^i\}_{i=1}^N$:

$$\begin{aligned} \mu_t &\approx \mu_t^{(N)} := \frac{1}{N}\sum_{i=1}^N X_t^i, \\ \Sigma_t &\approx \Sigma_t^{(N)} := \frac{1}{N-1}\sum_{i=1}^N \Big(X_t^i - \mu_t^{(N)}\Big)^2. \end{aligned} \tag{2.30}$$

The resulting equation (2.27) for the i^{th} particle is given by

$$\mathrm{d}X_t^i = \alpha\, X_t^i\, \mathrm{d}t + \sigma_B\, \mathrm{d}B_t^i + \frac{\Sigma_t^{(N)} \gamma}{\sigma_W^2}\left(\mathrm{d}Z_t - \gamma \frac{X_t^i + \mu_t^{(N)}}{2}\, \mathrm{d}t\right). \tag{2.31}$$

It is very similar to the mean-field "synchronization-type" control laws and oblivious equilibria constructions as in [79, 160]. The model (2.27) represents the mean-field approximation obtained by letting $N \to \infty$.

The control term in the linear feedback particle filter (2.30)-(2.31) appears also in the work of Reich [130], where it is referred to as the *ensemble square root filter*.

2.4 Synthesis of the Gain Function

Implementation of the nonlinear filter (2.5) requires solution of the E-L BVP (2.8) to obtain the gain function $\mathsf{K}(x,t)$ for each fixed t.

2.4.1 Direct Numerical Approximation of the BVP Solution

The explicit closed-form formula (A.15) for the solution of the BVP (2.8) can be used to construct a direct numerical approximation of the solution. Using (A.15), we have

$$\mathsf{K}(x,t) = \frac{1}{p(x,t)} \frac{1}{\sigma_W^2} \int_{-\infty}^{x} (\hat{h}_t - h(y)) p(y,t) \, \mathrm{d}y.$$

The approximation involves three steps:

1) Approximation of $\hat{h}_t$ by using a sample mean:

$$\hat{h}_t \approx \frac{1}{N} \sum_{j=1}^{N} h(X_t^j) =: \hat{h}_t^{(N)}.$$

2) Approximation of the integrand:

$$(\hat{h}_t - h(y)) p(y,t) \approx \frac{1}{N} \sum_{j=1}^{N} (\hat{h}_t^{(N)} - h(X_t^j)) \delta(y - X_t^j),$$

where $\delta(\cdot)$ is the Dirac delta function.

3) Approximation of the density $p(x,t)$ in the denominator, e.g., as a sum of Gaussian:

$$p(x,t) \approx \frac{1}{N} \sum_{j=1}^{N} q_t^j(x) =: \tilde{p}(x,t), \tag{2.32}$$

where $q_t^j(x) = q(x; X_t^j, \epsilon) = \frac{1}{\sqrt{2\pi\epsilon}} \exp\left(-\frac{1}{2\epsilon}(x - X_t^j)^2\right)$. The appropriate value of ϵ depends upon the problem. As a function of N, ϵ can be made smaller as N grows; As $N \to \infty$, $\epsilon \to 0$.

This yields the following numerical approximation of the gain function:

$$\mathsf{K}(x,t) = \frac{1}{\tilde{p}(x,t)} \frac{1}{\sigma_W^2} \frac{1}{N} \sum_{j=1}^{N} (\hat{h}_t^{(N)} - h(X_t^j)) H(x - X_t^j), \tag{2.33}$$

where $H(\cdot)$ is the Heaviside function.

Note that the gain function needs to be evaluated only at the particle locations X_t^i. An efficient $O(N^2)$ algorithm is easily constructed to do the same:

$$\begin{aligned} \mathsf{K}(X_t^i,t) &= \frac{1}{\tilde{p}(X_t^i,t)} \frac{1}{\sigma_W^2} \frac{1}{N} \left(\sum_{j:X_t^j<X_t^i} (\hat{h}_t^{(N)} - h(X_t^j)) + \frac{1}{2}(\hat{h}_t^{(N)} - h(X_t^i)) \right) \\ \mathsf{K}'(X_t^i,t) &= \frac{1}{\sigma_W^2}(\hat{h}_t^{(N)} - h(X_t^i)) - \tilde{b}(X_t^i)\mathsf{K}(X_t^i,t), \end{aligned} \tag{2.34}$$

where $\tilde{b}(x) := \frac{\partial}{\partial x}(\ln \tilde{p})(x,t)$. For $\tilde{p}$ defined using the sum of Gaussian approximation (2.32), a closed-form formula for $\tilde{b}(x)$ is easily obtained.

Algorithm 1 Implementation of feedback particle filter

Initialization
for $i = 1$ to N **do**
  Sample X_0^i from $p(x,0)$
end for
Assign value $t = 0$

Iteration [from t to $t + \triangle t$]
Calculate $\hat{h}_t^{(N)} = \frac{1}{N}\sum_{i=1}^N h(X_t^i)$
for $i = 1$ to N **do**
  Generate a sample, $\triangle V$, from $N(0,1)$
  Calculate $\triangle I_t^i = \triangle Z_t - \frac{1}{2}\left(h(X_t^i) + \hat{h}_t^{(N)}\right)\triangle t$
  Calculate the gain function $\mathsf{K}(X_t^i,t)$ (e.g., by using Algo. 2)
  $X_{t+\triangle t}^i = X_t^i + a(X_t^i)\triangle t + \sigma_B\sqrt{\triangle t}\triangle V + \mathsf{K}(X_t^i,t)\triangle I_t^i$
end for
$t = t + \triangle t$

2.4.2 Algorithm

For implementation purposes, we use the Stratonovich form of the filter (see (2.9)) together with an Euler discretization. The resulting discrete-time algorithm appears in Algo. 1. At each time step, the algorithm requires approximation of the gain function. A direct numerical solution-based algorithm for the same is summarized in Algo. 2.

In practice, one can use a less computationally intensive algorithm to approximate the gain function. An algorithm based on sum-of-Gaussian approximation of density appears in our conference paper [156]. In the application example presented in Sec. 2.5.3, the gain function is approximated by using Fourier series.

Algorithm 2 Synthesis of gain function $\mathsf{K}(x,t)$

1: Calculate $\hat{h}_t \approx \hat{h}_t^{(N)}$;
2: Approximate $p(x,t)$ as a sum of Gaussian:

$$p(x,t) \approx \tilde{p}(x,t) = \frac{1}{N}\sum_{j=1}^{N} q_t^j(x),$$

where $q_t^j(x) = \frac{1}{\sqrt{2\pi\epsilon}} \exp\left(-\frac{(x-X_t^j)^2}{2\epsilon}\right)$.
3: Calculate the gain function

$$\mathsf{K}(x,t) = \frac{1}{\tilde{p}(x,t)} \frac{1}{\sigma_W^2} \frac{1}{N} \sum_{j=1}^{N} \left(\hat{h}_t^{(N)} - h(X_t^j)\right) H(x - X_t^j),$$

where $H(\cdot)$ is the Heaviside function.

2.4.3 Further Remarks on the BVP

Recall that the solution of the nonlinear filtering problem is given by the Kushner-Stratonovich nonlinear evolution PDE. The feedback particle filter instead requires, at each time t, a solution of the linear BVP (2.8) to obtain the gain function K.

We make the following remarks:

1) There are close parallels between the proposed algorithm and the vortex element method (VEM) developed by Chorin and others for solution of the Navier-Stokes evolution equation; cf., [42, 106]. In VEM, as in the feedback particle filter, one obtains the solution of a Navier-Stokes equation by flowing a large number of particles. The vector-field for the particles is obtained by solving a linear BVP at each time.

   Algorithms based on VEM are popular in the large Reynolds number regime when the domain is not too complicated. The latter requirement is necessary to obtain solution of the linear BVP in tractable fashion [75].

2) One may ask what is the benefit, in terms of accuracy and computational cost, of the feedback particle filter-based solution when compared to a direct solution of the nonlinear evolution equation (Kushner-Stratonovich PDE), or even its linear counterpart (Zakai equation)?

   The key point, we believe, is robustness on account of the feedback control structure. Specifically, the self-correcting property of the feedback provides robustness, allowing one to tolerate a degree of uncertainty inherent in any model or approximation scheme. This is expected to yield accurate solutions in a computationally efficient manner. A complete answer will require further analysis, and as such reflects an important future direction.

3) The biggest computational cost of our approach is the need to solve the BVP at each time-step, that additionally requires one to approximate the density. We are encouraged however by the extensive set of tools in feedback

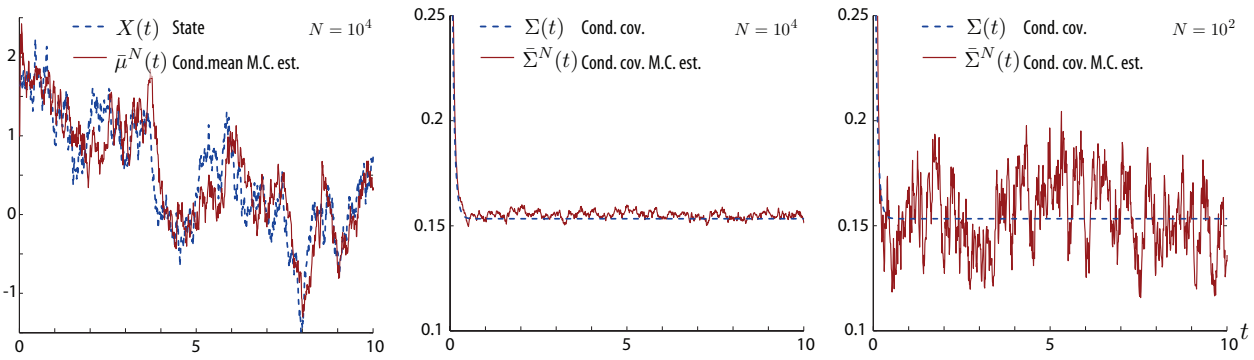

Figure 2.2: (a) Comparison of the true state $\{X_t\}$ and the conditional mean $\{\bar{\mu}_t^{(N)}\}$. (b) and (c) Plots of estimated conditional covariance with $N = 10,000$ and $N = 100$ particles, respectively. For comparison, the true conditional covariance obtained using Kalman filtering equations is also shown.

control: after all, one rarely needs to solve the HJB equations in closed-form to obtain a reasonable feedback control law. Moreover, there are many approaches in nonlinear and adaptive control to both approximate control laws as well as learn/adapt these in online fashion; cf., [14].

2.5 Numerics

2.5.1 Linear Gaussian Case

Consider the linear system:

$$\mathrm{d}X_t = \alpha\, X_t\, \mathrm{d}t + \mathrm{d}B_t, \tag{2.35a}$$

$$\mathrm{d}Z_t = \gamma\, X_t\, \mathrm{d}t + \sigma_W\, \mathrm{d}W_t, \qquad X_0 \sim N(1,1)\,, \tag{2.35b}$$

where $\{B_t\}, \{W_t\}$ are mutually independent standard Wiener process, and parameters $\alpha = -0.5$, $\gamma = 3$ and $\sigma_W = 0.5$.

Each of the N particles is described by the linear SDE,

$$\mathrm{d}X_t^i = \alpha\, X_t^i\, \mathrm{d}t + \mathrm{d}B_t^i + \frac{\gamma\, \bar{\Sigma}_t^{(N)}}{\sigma_W^2}\big[\mathrm{d}Z_t - \gamma\frac{X_t^i + \bar{\mu}_t^{(N)}}{2}\,\mathrm{d}t\big]\,, \tag{2.36}$$

where $\{B_t^i\}$ are mutually independent standard Wiener process; the particle system is initialized by drawing initial conditions $\{X_0^i\}_{i=1}^N$ from the distribution $\boldsymbol{N}(1,1)$, and the parameter values are chosen according to the model.

In the simulation discussed next, the mean $\bar{\mu}_t^{(N)}$ and the variance $\bar{\Sigma}_t^{(N)}$ are obtained from the ensemble $\{X_t^i\}_{i=1}^N$ according to (2.30).

Fig. 2.2 summarizes some of the results of the numerical experiments: Part (a) depicts a sample path of the state $\{X_t\}$ and the mean $\{\bar{\mu}_t^{(N)}\}$ obtained using a particle filter with $N = 10,000$ particles. Part (b) provides a comparison

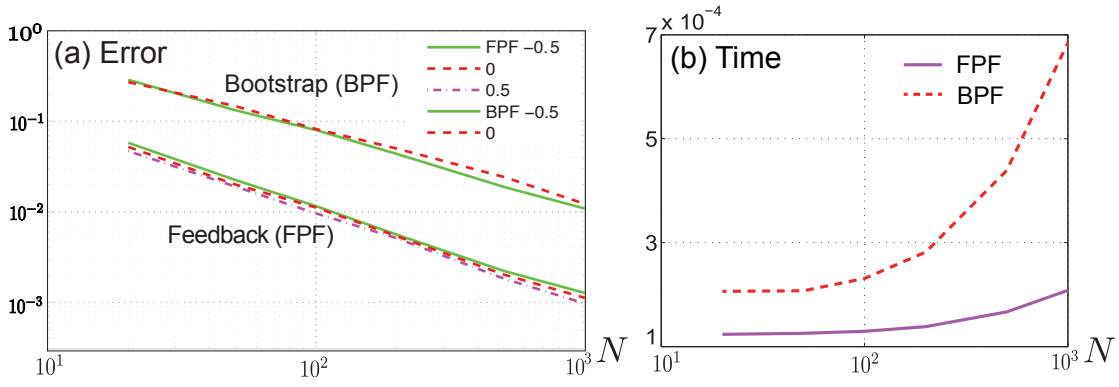

Figure 2.3: Comparison of (a) the *mse*, (b) the computational time using feedback particle filter and the bootstrap particle filter.

between the estimated variance $\bar{\Sigma}_t^{(N)}$ and the true error variance Σ_t that one would obtain by using the Kalman filtering equations. The accuracy of the results is sensitive to the number of particles. For example, part (c) of the figure provides a comparison of the variance with $N = 100$ particles.

Comparison with the bootstrap filter: We next provide a performance comparison between the feedback particle filter and the bootstrap particle filter for the linear problem (2.35a, 2.35b) in regard to both error and running time.

For the linear filtering problem, the optimal solution is given by the Kalman filter. We use this solution to define the relative mean-squared error:

$$mse = \frac{1}{T}\int_0^T \left(\frac{\Sigma_t^{(N)} - \Sigma_t}{\Sigma_t}\right)^2 \mathrm{d}t, \tag{2.37}$$

where Σ_t is the error covariance using the Kalman filter, and $\Sigma_t^{(N)}$ is its approximation using the particle filter.

Fig. 2.3(a) depicts a comparison between *mse* obtained using the feedback particle filter (2.36) and the bootstrap filter. The latter implementation is based on an algorithm taken from Ch. 9 of [7]. For simulation purposes, we used a range of values of $\alpha \in \{-0.5, 0, 0.5\}$, $\gamma = 3$, $\sigma_B = 1$, $\sigma_W = 0.5$, $\triangle t = 0.01$, and $T = 50$. The plot is generated using simulations with $N = 20, 50, 100, 200, 500, 1000$ particles.

These numerical results suggest that feedback can help reduce the high variance that is sometimes observed with the conventional particle filter. The variance issue can be especially severe if the signal process (2.1a) is unstable (e.g., $\alpha > 0$ in (2.35a)). In this case, individual particles can exhibit numerical instabilities due to time-discretization, floating point representation etc. With $\alpha > 0$, our numerical simulations with the bootstrap filter "blew-up" (similar conclusions were also arrived independently in [51]) while the feedback particle filter is provably stable based on observability of the model (2.35a)-(2.35b) (see Fig. 2.3 mse plot with $\alpha = 0.5$).

Fig. 2.3(b) depicts a comparison between computational time for the two filtering algorithms on the same problem. The time is given in terms of computation time per iteration cycle (see Algo. 1 in Sec. 2.4.2) averaged over 100 trials.

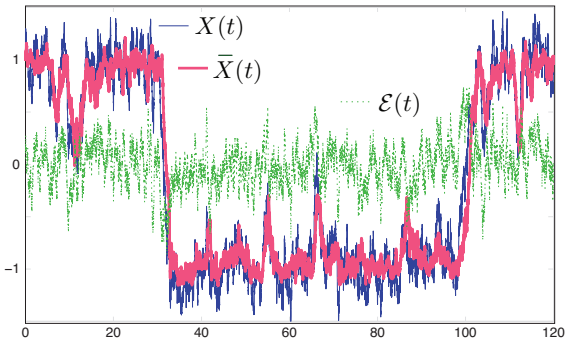

Figure 2.4: Comparison of the true state $X(t)$ and the conditional mean $\bar{X}(t)$ by using the feedback particle filter. The error $\mathscr{E}(t) = X(t) - \bar{X}(t)$ remains small even during a transition of the state.

For simulation purpose, we use MATLAB R2011b (7.13.0.564) on a 2.66GHz iMac as our test platform.

These numerical results suggest that, for a linear Gaussian implementation, the feedback particle filter has a lower computational cost compared to the conventional bootstrap particle filter. The main reason is that the feedback particle filter avoids the computationally expensive resampling procedure.

We also carried out simulations where the gain function is approximated using Algo. 2. In this case, the mse of the filter is comparable to the mse depicted in Fig. 2.3(a). However, the computation time is larger than the bootstrap particle filter. This is primarily on account of the evaluation of the exponentials in computing $\tilde{p}(x,t)$. Detailed comparisons between the feedback particle filter and the bootstrap particle filter will appear elsewhere.

In general, the main computational burden of the feedback particle filter is to obtain gain function which can be made efficient by using various approximation approaches; cf., [154].

2.5.2 Nonlinear Example

This nonlinear SDE is chosen to illustrate the tracking capability of the filter in highly nonlinear settings,

$$\mathrm{d}X_t = X_t(1 - X_t^2)\,\mathrm{d}t + \sigma_B\,\mathrm{d}B_t, \tag{2.38a}$$

$$\mathrm{d}Z_t = X_t\,\mathrm{d}t + \sigma_W\,\mathrm{d}W_t\,. \tag{2.38b}$$

When $\sigma_B = 0$, the ODE (2.38a) has two stable equilibria at ± 1. With $\sigma_B > 0$, the state of the SDE "transitions" between these two "equilibria".

Fig. 2.4 depicts the simulation results obtained using the nonlinear feedback particle filter (2.5), with $\sigma_B = 0.4$, $\sigma_W = 0.2$. The implementation is based on an algorithm described in Sec. IV of [156], and the details are omitted here. We initialize the simulation with two Gaussian clusters. After a brief period of transients, these clusters merge

into a single cluster, which adequately tracks the true state including the transition events.

2.5.3 Application: Nonlinear Oscillators

We consider the filtering problem for a nonlinear oscillator:

$$\mathrm{d}\theta_t = \omega\,\mathrm{d}t + \sigma_B\,\mathrm{d}B_t \mod 2\pi, \tag{2.39}$$

$$\mathrm{d}Z_t = h(\theta_t)\,\mathrm{d}t + \sigma_W\,\mathrm{d}W_t, \tag{2.40}$$

where ω is the frequency, $h(\theta) = \frac{1}{2}[1+\cos(\theta)]$, and $\{B_t\}$ and $\{W_t\}$ are mutually independent standard Wiener process. For numerical simulations, we pick $\omega = 1$ and the standard deviation parameters $\sigma_B = 0.5$ and $\sigma_W = 0.4$. We consider oscillator models because of their significance to applications including neuroscience; cf., [160].

The feedback particle filter is given by:

$$\mathrm{d}\theta_t^i = \omega\,\mathrm{d}t + \sigma_B\,\mathrm{d}B_t^i + \mathsf{K}(\theta_t^i,t)\circ\left[\mathrm{d}Z_t - \frac{1}{2}(h(\theta_t^i)+\hat{h}_t)\,\mathrm{d}t\right] \mod 2\pi, \tag{2.41}$$

$i = 1,\ldots,N$, where the function $\mathsf{K}(\theta,t)$ is obtained via the solution of the E-L equation:

$$-\frac{\partial}{\partial\theta}\left(\frac{1}{p(\theta,t)}\frac{\partial}{\partial\theta}\{p(\theta,t)\mathsf{K}(\theta,t)\}\right) = -\frac{\sin\theta}{2\sigma_W^2}. \tag{2.42}$$

Although the equation (2.42) can be solved numerically to obtain the optimal control function $\mathsf{K}(\theta,t)$, here we investigate a solution based on perturbation method. Suppose, at some time t, $p(\theta,t) = \frac{1}{2\pi} =: p_0$, the uniform density. In this case, the E-L equation is given by:

$$\partial_{\theta\theta}\mathsf{K} = \frac{\sin\theta}{2\sigma_W^2}.$$

A straightforward calculation shows that the solution in this case is given by

$$\mathsf{K}(\theta,t) = -\frac{\sin\theta}{2\sigma_W^2} =: \mathsf{K}_0(\theta). \tag{2.43}$$

To obtain the solution of the E-L equation (2.42), we assume that the density $p(\theta,t)$ is a small harmonic perturbation of the uniform density. In particular, we express $p(\theta,t)$ as:

$$p(\theta,t) = p_0 + \varepsilon\tilde{p}(\theta,t), \tag{2.44}$$

where ε is a small perturbation parameter. Since $p(\theta,t)$ is a density, $\int_0^{2\pi}\tilde{p}(\theta,t)\,\mathrm{d}\theta = 0$.

We are interested in obtaining a solution of the form:

$$\mathsf{K}(\theta,t) = \mathsf{K}_0(\theta) + \varepsilon\tilde{\mathsf{K}}(\theta,t). \tag{2.45}$$

On substituting the ansatz (2.44) and (2.45) in (2.42), and retaining only $O(\varepsilon)$ term, we obtain the following linearized equation:

$$\partial_{\theta\theta}\tilde{\mathsf{K}} = -2\pi\partial_\theta[(\partial_\theta\tilde{p})\mathsf{K}_0]. \tag{2.46}$$

The linearized E-L equation (2.46) can be solved easily by considering a Fourier series expansion of $\varepsilon\tilde{p}(\theta,t)$:

$$\varepsilon\tilde{p}(\theta,t) = P_c(t)\cos\theta + P_s(t)\sin\theta + \text{h.o.h}, \tag{2.47}$$

where "h.o.h" denotes the terms due to higher order harmonics. The Fourier coefficients are given by,

$$P_c(t) = \frac{1}{\pi}\int_0^{2\pi} p(\theta,t)\cos\theta\,\mathrm{d}\theta,\ P_s(t) = \frac{1}{\pi}\int_0^{2\pi} p(\theta,t)\sin\theta\,\mathrm{d}\theta.$$

For a harmonic perturbation, the solution of the linearized E-L equation (2.46) is given by:

$$\begin{aligned}\varepsilon\tilde{\mathsf{K}}(\theta,t) &= \frac{\pi}{4\sigma_{\tilde{W}}^2}\left(P_c(t)\sin 2\theta - P_s(t)\cos 2\theta\right)\\ &=: \mathsf{K}_1(\theta;P_c(t),P_s(t))\end{aligned} \tag{2.48}$$

For "h.o.h" terms in the Fourier series expansion (2.47) of the density in $p(\theta,t)$, the linearized E-L equation (2.46) can be solved in a similar manner. In numerical simulation provided here, we ignore the higher order harmonics, and use a control input as summarized in the following proposition:

Proposition 2.5.1 *Consider the E-L equation (2.42) where the density $p(\theta,t)$ is assumed to be a small harmonic perturbation of the uniform density $\frac{1}{2\pi}$, as defined by (2.44) and (2.47). As $\varepsilon\to 0$, the gain function is given by the following asymptotic formula:*

$$\mathsf{K}(\theta,t) = \mathsf{K}_0(\theta) + \mathsf{K}_1(\theta;P_c(t),P_s(t)) + o(\varepsilon), \tag{2.49}$$

where $P_c(t),P_s(t)$ denote the harmonic coefficients of density $p(\theta,t)$. For large N, these are approximated by using the formulae:

$$P_c(t) \approx \frac{1}{\pi N}\sum_{j=1}^N \cos\theta_j(t), \quad P_s(t) \approx \frac{1}{\pi N}\sum_{j=1}^N \sin\theta_j(t). \tag{2.50}$$

We next discuss the result of numerical experiments. The particle filter model is given by (2.41) with gain function

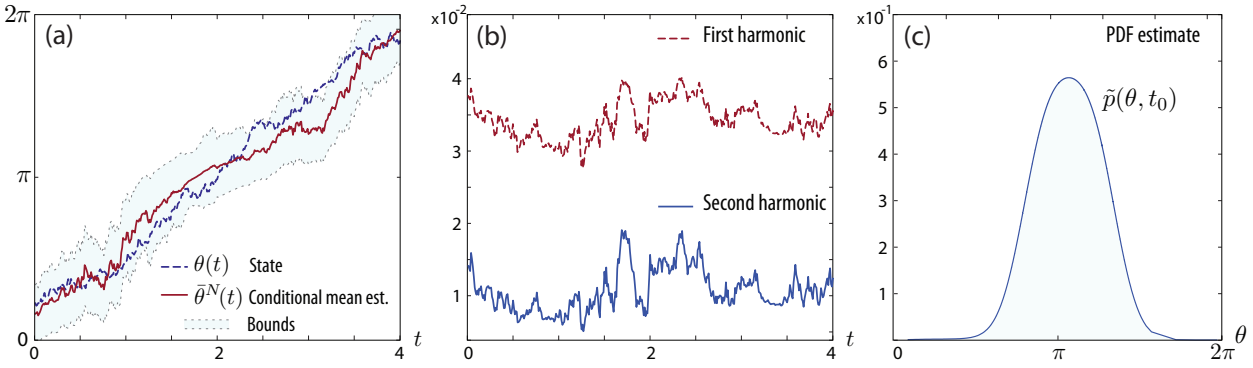

Figure 2.5: Summary of the numerical experiments with the nonlinear oscillator filter: (a) Comparison of the true state $\{\theta_t\}$ and the conditional mean $\{\bar{\theta}_t^N\}$. (b) The mean-squared estimate of the first and second harmonics of the density $p(\theta,t)$ and (c) a plot of a typical empirical distribution.

$K(\theta_t^i,t)$, obtained using formula (2.49). The number of particles $N = 10,000$ and their initial condition $\{\theta_0^i\}_{i=1}^N$ was sampled from a uniform distribution on circle $[0,2\pi]$.

Fig. 2.5 summarizes some of the results of the numerical simulation. For illustration purposes, we depict only a single cycle from a time-window after transients due to initial condition have converged. Part (a) of the figure compares the sample path of the actual state $\{\theta_t\}$ (as a dashed line) with the estimated mean $\{\bar{\theta}_t^{(N)}\}$ (as a solid line). The shaded area indicates $\pm$ one standard deviation bounds. Part (b) of the figure provides a comparison of the magnitude of the first and the second harmonics (as dashed and solid lines, respectively) of the density $p(\theta,t)$. The density at any time instant during the time-window is approximately harmonic (see also part (c) where the density at one typical time instant is shown).

Note that at each time instant t, the estimated mean, the bounds and the density $p(\theta,t)$ shown here are all approximated from the ensemble $\{\theta_t^i\}_{i=1}^N$. For the sake of illustration, we have used a Gaussian mixture approximation to construct a smooth approximation of the density.

The reader is referred to our papers [139,140] for additional applications involving nonlinear filtering with coupled oscillator models. In these papers, Galerkin approaches are described for the approximation of the gain function.

2.6 Conclusions

In this chapter, we introduced a new formulation of the nonlinear filter, referred to as the *feedback particle filter*. The feedback particle filter provides for a generalization of the Kalman filter to a general class of nonlinear non-Gaussian problems. The feedback particle filter inherits many of the properties that has made the Kalman filter so widely applicable over the past five decades, including innovation error and the feedback structure (see Fig. 2.1).

Feedback is important on account of the issue of *robustness*. In particular, feedback can help reduce the high

variance that is sometimes observed in the conventional particle filter. Numerical results are presented to support this claim (see Fig. 2.3).

Even more significantly, the structural aspects of the Kalman filter have been as important as the algorithm itself in design, integration, testing and operation of a larger system involving filtering problems (e.g., navigation systems). We show in later chapters that the feedback particle filter similarly provides an integrated framework, now for nonlinear non-Gaussian problems. Details on the feedback particle filter-based algorithms for nonlinear filtering with additional uncertainty are described in Chap. 6, Chap. 7.

Chapter 3

Existence, Uniqueness and Admissibility*

3.1 Introduction

In this chapter, we generalize the scalar feedback particle filter in Chap. 2 to the general multivariable case. Specifically, we consider the multivariable filtering problem:

$$\mathrm{d}X_t = a(X_t)\,\mathrm{d}t + \sigma(X_t)\,\mathrm{d}B_t, \tag{3.1a}$$

$$\mathrm{d}Z_t = h(X_t)\,\mathrm{d}t + \mathrm{d}W_t, \tag{3.1b}$$

where $X_t \in \mathbb{R}^d$ is the state at time t, $Z_t \in \mathbb{R}^m$ is the observation vector, and $\{B_t\}$, $\{W_t\}$ are two mutually independent Wiener processes taking values in $\mathbb{R}^d$ and $\mathbb{R}^m$. The mappings $a(\cdot) : \mathbb{R}^d \to \mathbb{R}^d$, $h(\cdot) : \mathbb{R}^d \to \mathbb{R}^m$ and $\sigma(\cdot) : \mathbb{R}^d \to \mathbb{R}^{d\times d}$ are C^1 functions. The covariance matrix of the observation noise $\{W_t\}$ is assumed to be positive definite. The function h is a column vector whose j-th coordinate is denoted as h_j (i.e., $h = (h_1, h_2, \ldots, h_m)^T$). For notational ease, the process noise $\{B_t\}$ is assumed to be a standard Wiener process. By scaling, we may assume without loss of generality that the covariance matrices associated with $\{B_t\}$, $\{W_t\}$ are identity matrices.

The objective of the filtering problem is to estimate the posterior distribution of X_t given the history $\mathscr{Z}_t := \sigma(Z_s : 0 \le s \le t)$. The posterior is denoted by p^* as defined in (1.2).

The multivariable feedback particle filter is a controlled system. The dynamics of the i^{th} particle have the following gain feedback form,

$$\mathrm{d}X_t^i = a(X_t^i)\,\mathrm{d}t + \sigma(X_t^i)\,\mathrm{d}B_t^i + \mathsf{K}(X_t^i, t)\,\mathrm{d}I_t^i + \Omega(X_t^i, t)\,\mathrm{d}t, \tag{3.2}$$

where $\{B_t^i\}$ are mutually independent standard Wiener processes, I^i is similar to the *innovation process* that appears in the nonlinear filter,

$$\mathrm{d}I_t^i := \mathrm{d}Z_t - \frac{1}{2}(h(X_t^i) + \hat{h})\,\mathrm{d}t, \tag{3.3}$$

where $\hat{h} := \mathsf{E}[h(X_t^i)|\mathscr{Z}_t]$. In a numerical implementation, we approximate $\hat{h} \approx \frac{1}{N}\sum_{i=1}^N h(X_t^i) =: \hat{h}^{(N)}$.

*This chapter is an extension of the published paper [154].

The gain function K is obtained as a solution to an Euler-Lagrange boundary value problem (E-L BVP): For $j = 1,2,\ldots,m$, the function ϕ_j is a solution to the second-order differential equation,

$$\begin{aligned} \nabla\cdot(p(x,t)\nabla\phi_j(x,t)) &= -(h_j(x)-\hat{h}_j)p(x,t), \\ \int \phi_j(x,t)p(x,t)\,\mathrm{d}x &= 0, \end{aligned} \tag{3.4}$$

where p denotes the conditional distribution of X_t^i given $\mathscr{Z}_t$. In terms of these solutions, the gain function is given by

$$[\mathsf{K}]_{lj} = \frac{\partial\phi_j}{\partial x_l}\,. \tag{3.5}$$

Note that the gain function needs to be obtained for each value of time t.

Finally, $\Omega = (\Omega_1,\Omega_2,...,\Omega_d)^T$ is the Wong-Zakai correction term:

$$\Omega_l(x,t) := \frac{1}{2}\sum_{k=1}^{d}\sum_{s=1}^{m}\mathsf{K}_{ks}(x,t)\frac{\partial\mathsf{K}_{ls}}{\partial x_k}(x,t). \tag{3.6}$$

The controlled system (3.2)-(3.6) is called the *multivariable feedback particle filter*.

The main results of this chapter are as follows:

• **Consistency.** The feedback particle filter (3.2) is consistent with the nonlinear filter, given consistent initializations $p(\cdot,0) = p^*(\cdot,0)$.

Consequently, if the initial conditions $\{X_0^i\}_{i=1}^N$ are drawn from the initial distribution $p^*(\cdot,0)$ of X_0, then, as $N\to\infty$, the empirical distribution of the particle system approximates the posterior distribution $p^*(\cdot,t)$ for each t.

• **Well-posedness.** A weak formulation of (3.4) is introduced, and used to prove an existence-uniqueness result for ϕ_j in a suitable function space. Certain apriori bounds are derived for the gain function to show that the resulting control input in (3.2) is admissible (That is, the filter (3.2) is well-posed in the Itô sense).

• **Numerical algorithms.** Based on the weak formulation, a Galerkin finite-element algorithm is proposed for approximation of the gain function $\mathsf{K}(x,t)$. The algorithm is completely adapted to data (That is, it does not require an explicit approximation of $p(x,t)$ or computation of derivatives). Certain closed-form expressions for gain function are derived in certain special cases. The conclusions are illustrated with numerical examples.

• **Characterization of the feedback gain.** The *Smoluchowski equation* models a d-dimensional gradient flow with "noise":

$$\mathrm{d}\Phi_t = -\nabla\mathscr{G}(\Phi_t)\,\mathrm{d}t + \sqrt{2}\,\mathrm{d}\xi_t, \tag{3.7}$$

where ξ is a standard Wiener process. It is regarded as the original MCMC algorithm: Under general conditions it is

ergodic, with (unnormalized) stationary distribution $e^{-\mathscr{G}}$. The BVP (3.4) can be expressed as an instance of Poisson's equation for this diffusion,

$$\mathscr{D}\phi_j = -(h_j - \hat{h}_j), \quad 1 \le j \le m, \tag{3.8}$$

where $\mathscr{D}$ is the differential generator for the Smoluchowski equation, with potential $\mathscr{G} = -\log p$. Subject to growth conditions on h and p, this implies the mean-integral representation for the vector-valued function,

$$\phi_j(x) = \int_0^\infty \mathsf{E}[h_j(\Phi_t) - \hat{h}_j \mid \Phi_0 = x] \, \mathrm{d}t. \tag{3.9}$$

This representation also suggests an alternate proof of well-posedness and construction of numerical algorithms; cf., [71]. This will be the subject of future work.

3.1.1 Comparison with Relevant Literature

The feedback particle filter is originally motivated by recent development in mean-field games, but the focus there has been primarily on optimal control [79, 160].

In nonlinear filtering, there are two directly related works: Crisan and Xiong [45], and Mitter and Newton [117]. In each of these papers, a controlled system is introduced, of the form

$$\mathrm{d}X_t^i = \big(a(X_t^i) + u(X_t^i, t)\big) \, \mathrm{d}t + \sigma_B(X_t^i) \, \mathrm{d}B_t^i.$$

The objective is to choose the control input to obtain a solution of the nonlinear filtering problem.

The approach in [117] is based on consideration of a finite-horizon optimal control problem. It leads to an HJB equation whose solution yields the optimal control input.

The work of Crisan and Xiong is closer to ours in terms of both goals and approaches. Although we were not aware of their work prior to submission of our original conference papers [156, 157], Crisan and Xiong provide an explicit expression for a control law that is similar to the feedback particle filter, with some important differences. One, the considerations of Crisan and Xiong (and also of Newton and Mitter) require introduction of a *smooth approximation* of the process "$\frac{\mathrm{d}Z}{\mathrm{d}t} - \hat{h}_t$," which we avoid with our formulation. Two, the filter derived in Crisan and Xiong has a structure based on a gain feedback with respect to the smooth approximation, while the feedback particle filter is based on a modified formula for the innovation error I_t^i as given in (3.3). This formula is fundamental to construction of particle filters in continuous time settings. We clarify here that the formula for innovation error is *not* assumed, rather it comes about as a result of the analysis of the variational problem.

Remarkably, both the feedback particle filter and Crisan and Xiong's filter require solution of the same boundary

value problem, and as such have the same computational complexity. The BVP is solved to obtain the gain function. However, the particular solution described in Crisan and Xiong for the BVP may not work in all cases, including the linear Gaussian case. Additional discussion appears in Sec. 3.2.4.

Apart from these works, Daum and Huang have introduced the *information flow filter* for the continuous-discrete time filtering problem [51]. Although an explicit formula for the filter is difficult to obtain, a closely related form of the boundary value problem appears in their work. There is also an important discussion of both the limitations of the conventional particle filter, and the need to incorporate feedback to ameliorate these issues. Several numerical experiments are presented that describe high variance and robustness issues, especially where signal models are unstable. These results provide significant motivation to the work described here.

3.1.2 Outline

The outline of the remainder of this chapter is as follows. The nonlinear filter is introduced in Sec. 3.2. Consistency result is shown in Sec. 3.2.3, followed by a comparison with Crisan and Xiong's filter in Sec. 3.2.4. The weak formulation of the BVP appears in Sec. 3.3 where well-posedness results are also derived. Algorithms are discussed in Sec. 3.4 and numerical examples in Sec. 3.5.

3.2 Multivariable Feedback Particle Filter

Consider the continuous time filtering problem (3.1a, 3.1b) introduced in Sec. 3.1.

We denote as $p^*(x,t)$ the conditional distribution of X_t given $\mathscr{Z}_t = \sigma(Z_s : s \le t)$. The evolution of $p^*(x,t)$ is described by the Kushner-Stratonovich (K-S) equation:

$$\mathrm{d}p^* = \mathscr{L}^\dagger p^* \,\mathrm{d}t + (h - \hat{h})^T (\mathrm{d}Z_t - \hat{h}\,\mathrm{d}t) p^*, \tag{3.10}$$

where $\hat{h} = \int h(x) p^*(x,t)\,\mathrm{d}x$ and $\mathscr{L}^\dagger p^* = -\nabla\cdot(p^* a) + \frac{1}{2}\sum_{l,k=1}^{d} \frac{\partial^2}{\partial x_l \partial x_k}\left(p^*[\sigma\sigma^T]_{lk}\right)$.

3.2.1 Belief State Dynamics & Control Architecture

The model for the particle filter is given by,

$$\mathrm{d}X_t^i = a(X_t^i)\,\mathrm{d}t + \sigma(X_t^i)\,\mathrm{d}B_t^i + \underbrace{u(X_t^i,t)\,\mathrm{d}t + \mathsf{K}(X_t^i,t)\,\mathrm{d}Z_t}_{\mathrm{d}U_t^i}, \tag{3.11}$$

where $X_t^i \in \mathbb{R}^d$ is the state for the i^{th} particle at time t, and $\{B_t^i\}$ are mutually independent standard Wiener processes. We assume the initial conditions $\{X_0^i\}_{i=1}^N$ are i.i.d., independent of $\{B_t^i\}$, and drawn from the initial distribution $p^*(x,0)$ of X_0. Both $\{B_t^i\}$ and $\{X_0^i\}$ are also assumed to be independent of X_t, Z_t. Note that the gain function $\mathsf{K}(x,t)$ is a $d \times m$ matrix and $u(x,t) \in \mathbb{R}^d$.

We impose admissibility requirements on the control input U_t^i in (3.11):

Definition 3 (Admissible Input) *The control input U_t^i is* admissible *if the random variables $u(x,t)$ and $\mathsf{K}(x,t)$ are $\mathscr{Z}_t = \sigma(Z_s : s \le t)$ measurable for each t. And for each t, $\mathsf{E}[|u|] := \mathsf{E}[\sum_l |u_l(X_t^i,t)|] < \infty$ and $\mathsf{E}[|\mathsf{K}|^2] := \mathsf{E}[\sum_{lj} |\mathsf{K}_{lj}(X_t^i,t)|^2] < \infty$.*

Recall that there are two types of conditional distributions of interest in our analysis:

1. $p(x,t)$: Defines the conditional dist. of X_t^i given $\mathscr{Z}_t$.
2. $p^*(x,t)$: Defines the conditional dist. of X_t given $\mathscr{Z}_t$.

The functions $\{u(x,t), \mathsf{K}(x,t)\}$ are said to be *optimal* if $p \equiv p^*$. That is, given $p^*(\cdot,0) = p(\cdot,0)$, our goal is to choose $\{u, \mathsf{K}\}$ in the feedback particle filter so that the evolution equations of these conditional distributions coincide (see (3.10) and (3.12)).

The evolution equation for the belief state is described in the next result. The proof is identical to the proof in the scalar case (see Proposition 2 in [156]). It is omitted here.

Proposition 3.2.1 *Consider the process X_t^i that evolves according to the particle filter model (3.11). The conditional distribution of X_t^i given the filtration $\mathscr{Z}_t$, $p(x,t)$, satisfies the forward equation*

$$\mathrm{d}p = \mathscr{L}^\dagger p \,\mathrm{d}t - \nabla \cdot (p\mathsf{K})\,\mathrm{d}Z_t - \nabla \cdot (pu)\,\mathrm{d}t + \frac{1}{2}\sum_{l,k=1}^{d} \frac{\partial^2}{\partial x_l \partial x_k}\left(p[\mathsf{K}\mathsf{K}^T]_{lk}\right)\,\mathrm{d}t. \tag{3.12}$$

3.2.2 General Form of the Feedback Particle Filter

The general form of the feedback particle filter is obtained by choosing $\{u, \mathsf{K}\}$ as the solution to a certain E-L BVP based on p. The function K is a solution to

$$\nabla \cdot (p\mathsf{K}) = -(h - \hat{h})^T p, \tag{3.13}$$

and the function u is obtained as

$$u(x,t) = -\frac{1}{2}\mathsf{K}(x,t)\left(h(x) + \hat{h}\right) + \Omega(x,t). \tag{3.14}$$

The reader is referred to our earlier paper [156] for additional justification regarding these choices.

If one further *assumes* that the control input U_t^i is admissible, a short calculation shows that the feedback particle filter is consistent with the choice of $\{u, \mathsf{K}\}$ given by (3.13)-(3.14). This calculation appears in App. B.1.

3.2.3 Consistency with the Nonlinear Filter

To establish admissibility of the input U_t^i requires additional assumptions on the density p and function h:

(i) ***Assumption A1*** The probability density $p(x,t)$ is of the form $p(x,t) = e^{-\mathscr{G}(x,t)}$, where $\mathscr{G}(x,t)$ is a twice continuously differentiable function with

$$|\nabla \mathscr{G}|^2 - 2\Delta \mathscr{G} \to \infty \quad \text{as } |x| \to \infty. \tag{3.15}$$

(ii) ***Assumption A2*** The function h satisfies,

$$\int |h(x)|^2 p(x,t)\, \mathrm{d}x < \infty,$$

where $|h(x)|^2 := \sum_j |h_j(x)|^2$. For admissibility of u, our arguments require additional assumptions:

(iii) ***Assumption A3*** The second derivatives of $\mathscr{G}(x,t)$ with respect to x are uniformly bounded at each t, i.e., $|\frac{\partial^2 \mathscr{G}}{\partial x_j \partial x_k}(x,t)| \leq c_2(t)$ for all $x \in \mathbb{R}^d$, $t > 0$.

(iv) ***Assumption A4*** The first (weak) derivatives of h satisfy

$$\int |\nabla h(x)|^2 p(x,t)\, \mathrm{d}x < \infty,$$

where $|\nabla h(x)|^2 := \sum_{jk} |\frac{\partial h_j}{\partial x_k}(x)|^2$.

Under these assumptions, it is shown in Theorem 3.3.1 that the gradient-form representation (3.4) of the E-L BVP (3.13) is uniquely obtained to give ϕ and thence K.

The admissibility of the resulting control input is established in Corollary 3.3.1. Theorem 3.3.1 and Corollary 3.3.1 are stated and proved in Sec. 3.3.

The following theorem then shows that the two evolution equations (3.10) and (3.12) are identical. The proof appears in App. B.1.

Theorem 3.2.2 *Consider the two evolution equations for p and p^*, defined according to the solution of the forward equation (3.12) and the K-S equation (3.10), respectively. Suppose that the gain function $\mathsf{K}(x,t)$ is obtained according to (3.4)-(3.5). Then, provided $p(\cdot,0) = p^*(\cdot,0)$, we have for all $t \geq 0$,*

$$p(\cdot,t) = p^*(\cdot,t).$$

3.2.4 Comparison with Crisan and Xiong's Filter

For ease of presentation, consider the model (3.1a)-(3.1b) where the observation process $Z_t \in \mathbb{R}$ is real-valued. To aid comparison with Crisan and Xiong's work, we express the feedback particle filter in its Stratonovich form:

$$\mathrm{d}X_t^i = a(X_t^i)\,\mathrm{d}t + \sigma(X_t^i)\,\mathrm{d}B_t^i + \mathsf{K}(X_t^i,t) \circ \mathrm{d}I_t^i, \tag{3.16}$$

where the gain function $\mathsf{K}(x,t) = (\mathsf{K}_1, \mathsf{K}_2, ..., \mathsf{K}_d)^T$ is vector-valued. It is given by the solution of a BVP:

$$\nabla \cdot (p\mathsf{K}) = -(h - \hat{h}_t)p. \tag{3.17}$$

Following the work of Crisan and Xiong [45], we might assume the following representation in an attempt to solve (3.17),

$$p\mathsf{K} = \nabla\phi. \tag{3.18}$$

where ϕ is assumed to be sufficiently smooth. Substituting (3.18) in (3.17) yields the Poisson equation,

$$\Delta\phi = -(h - \hat{h}_t)p\,. \tag{3.19}$$

A solution to Poisson's equation with $d \geq 2$ can be expressed in terms of Green's function:

$$G(r) = \begin{cases} \frac{1}{2\pi}\ln(r) & \text{for } d = 2; \\ \frac{1}{d(2-d)\omega_d} r^{2-d} & \text{for } d > 2\,, \end{cases}$$

where ω_d is the volume of the unit ball in $\mathbb{R}^d$. A solution to (3.19) is then given by,

$$\phi(x) = -\frac{1}{\sigma_W^2}\int_{\mathbb{R}^d} G(|y-x|)(h(y) - \hat{h}_t)p(y,t)\,\mathrm{d}y,$$

where $|y-x| := \left(\sum_{j=1}^d (y_j - x_j)^2\right)^{\frac{1}{2}}$ is the Euclidean distance.

On taking the gradient and using (3.18), one obtains an explicit formula for the gain function:

$$\mathsf{K}(x,t) = \frac{\Gamma(p,h)(x)}{p(x,t)} =: \mathsf{K}_g(x,t), \tag{3.20}$$

where $\Gamma(p,g)(x) := \frac{1}{d\omega_d}\int \frac{y-x}{|y-x|^d}(g(y) - \hat{g})p(y)\,\mathrm{d}y$.

While this leads to a solution to (3.17), it may not lead to an admissible control law. This difficulty arises in the

prior work of Crisan and Xiong. In [45] and in Sec. 4 of [150], a particle filter of the following form is presented by the authors:

$$\mathrm{d}X_t^i = a(X_t^i)\,\mathrm{d}t + \sigma(X_t^i)\,\mathrm{d}B_t^i + \mathsf{K}_g(X_t^i,t)\Big(\frac{\mathrm{d}}{\mathrm{d}t}\tilde{I}_t\Big)\,\mathrm{d}t, \tag{3.21}$$

where $\tilde{I}_t$ is a certain smooth approximation obtained from the standard form of the innovation error $I_t := Z_t - \int_0^t \hat{h}_t\,\mathrm{d}t$. A consistency result is described for this filter.

We make the following comparisons:

1) Without taking a smooth approximation, the filter (3.21) is formally equivalent to the following SDE expressed here in its Stratonovich form:

$$\mathrm{d}X_t^i = a(X_t^i)\,\mathrm{d}t + \sigma(X_t^i)\,\mathrm{d}B_t^i + \mathsf{K}_g(X_t^i,t)\circ\Big(\mathrm{d}Z_t - \hat{h}_t\,\mathrm{d}t\Big). \tag{3.22}$$

In this case, using (3.12), it is straightforward to show that the consistency result *does not hold*. In particular, there is an extra second order term that is not present in the K-S equation for evolution of the true posterior $p^*(x,t)$.

2) The proposed feedback particle filter does not require a smooth approximation and yet achieves consistency. The key breakthrough is the modified definition of the innovation error (compare (3.22) with (3.16)). Note that the innovation error (3.3) is not assumed apriori but comes about via analysis of the variational problem. This is one utility of introducing the variational formulation. Once the feedback particle filter has been derived, it is straightforward to prove consistency (see the Proof of Thm. 3.2.2).

3) The computational overhead for the feedback particle filter and the filter of Crisan and Xiong are equal. Both require the approximation of the integral (3.20), and division by (a suitable regularized approximation of) $p(x,t)$. Numerically, the Poisson equation formulation (3.19) of the E-L BVP (3.17) is convenient. There exist efficient numerical algorithms to approximate the integral solution (3.20) for a system of N particles in arbitrary dimension; cf., [75].

However, while appealing, the function K_g is *not* the correct form of the gain function in the multivariable case, even for the linear Gaussian model: It is straightforward to verify that the Kalman gain is a solution of the boundary value problem (3.17). Using the Kalman gain for the gain function in (3.16) yields the feedback particle filter for the multivariable linear Gaussian case. The filter is described in Sec. 3.3.4.

However, the Kalman gain solution is not of the form (3.18). Thus, the integral solution (3.20) does *not* equal the Kalman gain in the linear Gaussian case (for $d \geq 2$).

Moreover, the gradient form solution is unbounded: $|\mathsf{K}_g(x,t)| \to \infty$ as $|x| \to \infty$, and $\mathsf{E}[|\mathsf{K}_g|] = \mathsf{E}[|\mathsf{K}_g|^2] = \infty$. A proof is given in App. B.2.

It follows that the control input obtained using K_g is not admissible, and hence the Kolmogorov forward operator

is no longer valid. Filter implementations using K_g suffer from numerical issues on account of large unbounded gains. In contrast, the feedback particle filter using the Kalman gain works both in theory and in practice.

The choice of gain function in the multivariable case requires careful consideration of the uniqueness of the solutions of the BVP: The solution of (3.17) is not unique, even though uniqueness holds when $p\mathsf{K}$ is assumed to be of a gradient-form. More details on the well-posedness result appear in Sec. 3.3.

Before closing this section, we note that [45, Proposition 2.4] concerns another filter that does not rely on smooth approximation,

$$\mathrm{d}X_t^i = a(X_t^i)\,\mathrm{d}t + \sigma(X_t^i)\,\mathrm{d}B_t^i + \mathsf{K}_g(X_t^i,t)\circ\mathrm{d}Z_t - \frac{1}{\sigma_W^2}\frac{\Gamma(p,\frac{1}{2}|h|^2)(X_t^i)}{p(X_t^i,t)}\,\mathrm{d}t.$$

Our calculations indicate that consistency is also an issue for this filter. The issue with K_g also applies to this filter. A more complete comparison needs further investigation.

3.3 Existence, Uniqueness and Admissibility

The aim of this section is to introduce a particular *gradient-form solution* of the BVP (3.13). The gradient-form solution is obtained in terms of m real-valued functions $\{\phi_1(\cdot,t),\phi_2(\cdot,t),\ldots,\phi_m(\cdot,t)\}$. For $j=1,2,\ldots,m$, the function ϕ_j is a solution to,

$$\begin{aligned}\nabla\cdot(p(x,t)\nabla\phi_j(x,t)) &= -(h_j(x)-\hat{h}_j)p(x,t),\\ \int \phi_j(x,t)p(x,t)\,\mathrm{d}x &= 0.\end{aligned} \tag{3.23}$$

The normalization $\int\phi_j(x,t)p(x,t)\,\mathrm{d}x=0$ is for convenience: If ϕ_j^o is a solution to the differential equation (3.23), we obtain the desired normalization on subtracting its mean.

In terms of these solutions, the gain function is given by,

$$\mathsf{K}_{lj}(x,t) = \frac{\partial\phi_j}{\partial x_l}(x,t)\,,\quad x\in\mathbb{R}^d\,. \tag{3.24}$$

It is straightforward to verify that K thus defined is a particular solution of the BVP (3.13).

3.3.1 Poisson's Equation Interpretation

The differential equation (3.23) is solved for each t to give the m functions $\{\phi_j(\cdot,t):1\le j\le m\}$. On dividing each side of this equation by p, elementary calculus leads to the equivalent equation (3.8), with generator $\mathscr{D}$ defined for C^2 functions f via,

$$\mathscr{D}f = -\nabla\mathscr{G}\cdot\nabla f + \Delta f$$

and with $\mathscr{G}(\cdot) = -\log p(\cdot, t)$. This is the differential generator for the Smoluchowski equation (3.7). It is shown in [81] that this diffusion is exponentially ergodic under mild conditions on $\mathscr{G}$. Consequently, $\mathsf{E}[h_j(\Phi_t) - \hat{h}_j \mid \Phi_0 = x]$ converges to zero exponentially fast, subject to growth conditions on h_j, and from this we can conclude that (3.9) is well defined, and provides a solution to Poisson's equation (3.8) [71].

Poisson's equation can be regarded as the *value function* that arises in average-cost optimal control, and this is the object of interest in the approximation techniques used in TD-learning for average-cost optimal control [114]. The integral representation (3.9) suggests approximation techniques based on approximate models for the diffusion Φ.

The remainder of this section is devoted to showing existence and uniqueness of the solution of (3.23), and admissibility of the resulting control input, obtained using gain function defined by (3.24).

3.3.2 Weak Formulation

Further analysis of this problem requires introduction of Hilbert spaces: $L^2(\mathbb{R}^d; p)$ is used to denote the Hilbert space of functions on $\mathbb{R}^d$ that are square-integrable with respect to density $p(\cdot, t)$ (for a fixed time t); $H^k(\mathbb{R}^d; p)$ is used to denote the Hilbert space of functions whose first k-derivatives (defined in the weak sense) are in $L^2(\mathbb{R}^d; p)$. Denote

$$H_0^1(\mathbb{R}^d; p) := \left\{ \phi \in H^1(\mathbb{R}^d; p) \,\middle|\, \int \phi(x) p(x,t)\, \mathrm{d}x = 0 \right\}.$$

A function $\phi_j \in H_0^1(\mathbb{R}^d; p)$ is said to be a weak solution of the BVP (3.23) if

$$\int \nabla \phi_j(x,t) \cdot \nabla \psi(x) p(x,t)\, \mathrm{d}x = \int (h_j(x) - \hat{h}_j) \psi(x) p(x,t)\, \mathrm{d}x, \tag{3.25}$$

for all $\psi \in H^1(\mathbb{R}^d; p)$.

Denoting $\mathsf{E}[\cdot] := \int \cdot\, p(x,t)\, \mathrm{d}x$, the weak form of the BVP (3.23) can also be expressed as

$$\mathsf{E}[\nabla \phi_j \cdot \nabla \psi] = \mathsf{E}[(h_j - \hat{h}_j)\psi], \quad \forall\, \psi \in H^1(\mathbb{R}^d; p). \tag{3.26}$$

This representation is useful for the numerical algorithm described in Sec. 3.4.

3.3.3 Main Results

The existence-uniqueness result for the BVP (3.23) is described next — Its proof is given in App. B.3.

Theorem 3.3.1 *Under Assumptions A1-A2, the BVP* (3.23) *possesses a unique weak solution* $\phi_j \in H_0^1(\mathbb{R}^d; p)$*, satis-*

fying

$$\int |\nabla\phi_j(x)|^2 p(x,t)\,\mathrm{d}x \le \frac{1}{\lambda}\int |h_j(x)-\hat{h}_j|^2 p(x,t)\,\mathrm{d}x. \tag{3.27}$$

If in addition Assumptions A3-A4 hold, then $\phi_j \in H^2(\mathbb{R}^d;p)$ *with*

$$\int \left|(D^2\phi_j)(\nabla\phi_j)\right| p(x,t)\,\mathrm{d}x \le C(\lambda;p)\int |\nabla h_j|^2 p(x,t)\,\mathrm{d}x, \tag{3.28}$$

where λ *is (spectral gap) constant (see App. B.3) and* $C(\lambda;p) = \frac{1}{\lambda^{3/2}}\left(\frac{\|D^2(\log p)\|_{L^\infty}}{\lambda}+1\right)^{1/2}$.

The apriori bounds (3.27)-(3.28) are used to show that the control input for the feedback particle filter is admissible. The proof is omitted.

Corollary 3.3.1 *Suppose* ϕ_j *is the weak solution of BVP (3.23) as described in Theorem 3.3.1. The gain function* K *is obtained using (3.24) and* u *is given by (3.14). Then*

$$\begin{aligned}
\mathsf{E}[|\mathsf{K}|^2] &\le \frac{1}{\lambda}\sum_{j=1}^m \int |h_j(x)|^2 p(x,t)\,\mathrm{d}x,\\
\mathsf{E}[|u|] &\le \left(\frac{1}{\lambda}+C(\lambda;p)\right)\sum_{j=1}^m \int \left(|h_j(x)|^2+|\nabla h_j|^2\right) p(x,t)\,\mathrm{d}x,
\end{aligned}$$

where $C(\lambda;p)$ *is given in Theorem 3.3.1. That is, the resulting control input in (3.24) is admissible.*

3.3.4 Linear Gaussian Case

Consider the linear system,

$$\mathrm{d}X_t = A\,X_t\,\mathrm{d}t + \mathrm{d}B_t \tag{3.29a}$$

$$\mathrm{d}Z_t = H\,X_t\,\mathrm{d}t + \mathrm{d}W_t \tag{3.29b}$$

where A is an $d\times d$ matrix, and H is an $m\times d$ matrix. The initial distribution $p^*(x,0)$ is Gaussian with mean vector μ_0 and covariance matrix Σ_0.

The following proposition shows that the Kalman gain is a gradient-form solution of the multivariable BVP (3.13):

Proposition 3.3.2 *Consider the d-dimensional linear system (3.29a)-(3.29b). Suppose* $p(x,t)$ *is assumed to be Gaussian:* $p(x,t) = \frac{1}{(2\pi)^{\frac{d}{2}}|\Sigma_t|^{\frac{1}{2}}}\exp\left(-\frac{1}{2}(x-\mu_t)^T\Sigma_t^{-1}(x-\mu_t)\right)$, *where* $x=(x_1,x_2,...,x_d)^T$, $\mu_t=(\mu_{1t},\mu_{2t},\ldots,\mu_{dt})^T$ *is the*

mean, Σ_t is the covariance matrix, and $|\Sigma_t| > 0$ denotes the determinant. A solution of the BVP (3.23) is given by,

$$\phi_j(x,t) = \sum_{k=1}^{d} [\Sigma_t H^T]_{kj}(x_k - \mu_{kt}). \tag{3.30}$$

Using (3.24), $\mathsf{K}(x,t) = \Sigma_t H^T$ (the Kalman gain) is the gradient form solution of (3.13).

The formula (3.30) is verified by direct substitution in the BVP (3.23) where the distribution p is multivariable Gaussian.

The gain function yields the following form for the particle filter in this linear Gaussian model:

$$\mathrm{d}X_t^i = A\, X_t^i\, \mathrm{d}t + \mathrm{d}B_t^i + \Sigma_t H^T \left(\mathrm{d}Z_t - H \frac{X_t^i + \mu_t}{2}\, \mathrm{d}t \right). \tag{3.31}$$

Now we show that $p = p^*$ in this case. That is, the conditional distributions of X and X^i coincide, and are defined by the well-known dynamic equations that characterize the mean and the variance of the continuous-time Kalman filter.

Theorem 3.3.3 *Consider the linear Gaussian filtering problem defined by the state-observation equations (3.29a)-(3.29b). In this case the posterior distributions of X_t and X_t^i are Gaussian, whose conditional mean and covariance are given by the respective SDE and the ODE,*

$$\begin{aligned} \mathrm{d}\mu_t &= A\mu_t\, \mathrm{d}t + \Sigma_t H^T \Big(\mathrm{d}Z_t - H\mu_t\, \mathrm{d}t \Big) \\ \frac{\mathrm{d}}{\mathrm{d}t}\Sigma_t &= A\Sigma_t + \Sigma_t A^T + I - \Sigma_t H^T H \Sigma_t \end{aligned}$$

The result is verified by substituting $p(x,t) = (2\pi)^{-\frac{d}{2}} |\Sigma_t|^{-\frac{1}{2}} \exp\left[-\frac{1}{2}(x-\mu_t)^T \Sigma_t^{-1}(x-\mu_t)\right]$ in the forward equation (3.12). The details are omitted, and because the result is a special case of Theorem 3.2.2.

In practice $\{\mu_t, \Sigma_t\}$ are approximated as sample means and sample covariances from the ensemble $\{X_t^i\}_{i=1}^N$:

$$\begin{aligned} \mu_t &\approx \mu_t^{(N)} := \frac{1}{N} \sum_{i=1}^{N} X_t^i, \\ \Sigma_t &\approx \Sigma_t^{(N)} := \frac{1}{N-1} \sum_{i=1}^{N} (X_t^i - \mu_t^{(N)})^2. \end{aligned}$$

The resulting equation (3.31) for the i^{th} particle is given by

$$\mathrm{d}X_t^i = A\, X_t^i\, \mathrm{d}t + \mathrm{d}B_t^i + \Sigma_t^{(N)} H^T \left(\mathrm{d}Z_t - H \frac{X_t^i + \mu_t^{(N)}}{2}\, \mathrm{d}t \right).$$

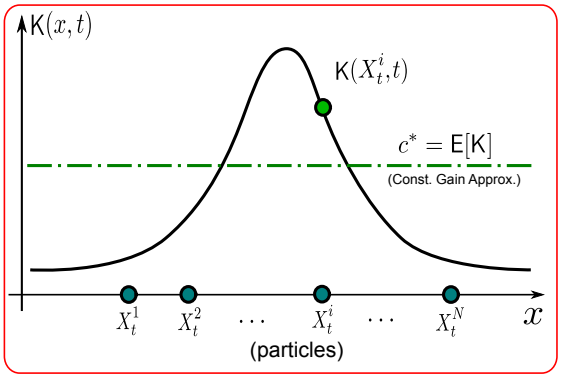

Figure 3.1: Approximating nonlinear K by its expected value $\mathsf{E}[\mathsf{K}]$. For simplicity, the scalar case is depicted (i.e., $X_t \in \mathbb{R}$).

As $N \to \infty$, the empirical distribution of the particle system approximates the posterior distribution $p^*(x,t)$ (by Theorem 3.3.3).

3.4 Finite-Element Algorithm

In this section, a Galerkin finite-element algorithm is described to construct an approximate solution of (3.25). Since there are m uncoupled BVPs, without loss of generality, we assume scalar-valued observation in this section, with $m = 1$, so that $\mathsf{K} = \nabla\phi$. The time t is fixed. The explicit dependence on time is suppressed for notational ease (That is, $p(x,t)$ is denoted as $p(x)$, $\phi(x,t)$ as $\phi(x)$ etc.).

3.4.1 Galerkin Approximation

For a fixed time t and $j \in \{1,\ldots,s\}$, a vector-valued function $\nabla\phi_j(x,t)$ is said to be a weak solution of the BVP (3.23) if

$$\mathsf{E}\left[\nabla\phi_j \cdot \nabla\psi\right] = \mathsf{E}[(h_j - \hat{h}_j)\psi] \tag{3.32}$$

holds for all $\psi \in H^1(\mathbb{R}^d; p)$ where $\mathsf{E}[\cdot] := \int_{\mathbb{R}^d} \cdot\, p(x,t)\,\mathrm{d}x$ and H^1 is a certain Sobolev space (see [154]).

In general, the weak solution $\nabla\phi_j(\cdot,t)$ of the BVP (3.32) is some, possibly non-constant, vector-valued function of the state (see Fig. 3.1). The existence-uniqueness result for the weak solution appears in [154]; a Galerkin algorithm for numerically approximating the solution is described next:

The function ϕ_j is approximated as,

$$\phi_j(x,t) = \sum_{l=1}^{L} \kappa_j^l(t)\,\psi_l(x),$$

where $\{\psi_l(x)\}_{l=1}^L$ are a given set of basis functions.

The finite-dimensional approximation of (3.32) is to choose constants $\{\kappa_j^l(t)\}_{l=1}^L$ – for each fixed time t – such that

$$\sum_{l=1}^{L} \kappa_j^l(t)\, \mathsf{E}[\nabla\psi_l \cdot \nabla\psi] = \mathsf{E}[(h_j - \hat{h}_j)\psi], \quad \forall\ \psi \in S, \tag{3.33}$$

where $S := \text{span}\{\psi_1, \psi_2, \ldots, \psi_L\} \subset H^1(\mathbb{R}^d; p)$.

Denoting $[A]_{kl} = \mathsf{E}[\nabla\psi_l \cdot \nabla\psi_k]$, $b_j^k = \mathsf{E}[(h_j - \hat{h}_j)\psi_k]$, $b_j = (b_j^1, \ldots, b_j^L)$ and $\kappa_j = (\kappa_j^1, \ldots, \kappa_j^L)$, the finite-dimensional approximation (3.33) is expressed as a linear matrix equation:

$$A\kappa_j = b_j.$$

In a numerical implementation, the matrix A and vector b_j are approximated as,

$$[A]_{kl} = \mathsf{E}[\nabla\psi_l \cdot \nabla\psi_k] \approx \frac{1}{N}\sum_{i=1}^{N} \nabla\psi_l(X_t^i) \cdot \nabla\psi_k(X_t^i), \tag{3.34}$$

$$b_j^k = \mathsf{E}[(h_j - \hat{h}_j)\psi_k] \approx \frac{1}{N}\sum_{i=1}^{N} (h_j(X_t^i) - \hat{h}_j)\psi_k(X_t^i), \tag{3.35}$$

where recall $\hat{h}_j \approx \frac{1}{N}\sum_{i'=1}^{N} h_j(X_t^{i'})$. The important point to note is that the gain function is expressed in terms of averages taken over the population.

3.4.2 Example 1: Constant Gain Approximation

Suppose $\chi_l = e_l$, the canonical coordinate vector with value 1 for the l^{th} coordinate and zero otherwise. The test functions are the coordinate functions $\psi_k(x) = x_k$ for $k = 1, 2, \ldots, d$. Denoting $\psi(x) = (\psi_1, \psi_2, \ldots, \psi_d)^T = x$,

$$\kappa = \mathsf{E}[\mathsf{K}] = \mathsf{E}[(h - \hat{h})\psi] = \int (h(x) - \hat{h})\psi(x)p(x)\,\mathrm{d}x \approx \frac{1}{N}\sum_{i=1}^{N} (h(X_t^i) - \hat{h})X_t^i. \tag{3.36}$$

This formula yields the *constant-gain approximation* of the gain function.

The constant gain approximation is obtained by using the coordinate functions $(x_1, x_2, \ldots, x_d)$ as basis functions. In this case,

$$\kappa_j = \mathsf{E}[(h_j - \hat{h}_j)x] \approx \frac{1}{N}\sum_{i=1}^{N} X_t^i \left(h_j(X_t^i) - \frac{1}{N}\sum_{i'=1}^{N} h_j(X_t^{i'}) \right) =: c_j^{(N)}. \tag{3.37}$$

Denoting $C := [c_1^{(N)}, \ldots, c_s^{(N)}]$, where $c_j^{(N)}$ is a column vector for $j \in \{1, \ldots, s\}$, the gain function is succinctly expressed as:

$$\mathsf{K} = C. \tag{3.38}$$

We refer to this solution as the *constant gain approximation*.

Remark 3 *There is also a variational interpretation of these solutions. The constant gain approximation, formula (3.38), is the best – in the least-square sense – constant approximation of the gain function (see Fig. 3.1). Precisely, consider the following least-square optimization problem:*

$$c_j^* = \arg\min_{c_j \in \mathbb{R}^d} \mathsf{E}[|\nabla\phi_j - c_j|^2].$$

By using a standard sum of square argument, we have

$$c_j^* = \mathsf{E}[\nabla\phi_j].$$

Even though ϕ_j is unknown, a closed-form formula for constant vector c_j^* can easily be obtained by using (3.32). Specifically, by substituting $\psi(x) = x = (x_1, x_2, \ldots, x_d)$ in (3.32):

$$\mathsf{E}[\nabla\phi_j] = \mathsf{E}[(h_j - \hat{h}_j)\psi] = \int_{\mathbb{R}^d} (h_j(x) - \hat{h}_j)\, x\, p(x,t)\, \mathrm{d}x.$$

This is also the first equality in (3.37).

Likewise, the Galerkin solution is the optimal least-square approximation in the function space S.

Remark 4 *It is noted that if p is Gaussian and h is linear then, in the limit as $N \to \infty$, the constant gain approximation equals the Kalman gain (see Sec. 3.3.4).*

3.4.3 Example 2: Single-State Case

Consider a scalar example, where the density is a sum of Gaussian,

$$p(x) \approx \sum_{j=1}^{3} \lambda^j q^j(x),$$

where $q^j(x) = q(x; \mu^j, \Sigma^j) = \frac{1}{\sqrt{2\pi\Sigma^j}} \exp(-\frac{(x-\mu^j)^2}{2\Sigma^j})$, $\lambda^j > 0$, $\sum \lambda^j = 1$. The parameter values for $\lambda^j, \mu^j, \Sigma^j$ are tabulated in Table I.

In the scalar case, a direct numerical solution (DNS) of the gain function is obtained by numerically approximating the integral

$$\mathsf{K}(x) = -\frac{1}{p(x)} \int_{-\infty}^{x} (h(y) - \hat{h}) p(y)\, \mathrm{d}y.$$

The DNS solution is used to provide comparisons with the approximate Galerkin solutions.

(a) Table 1
Parameter Values

j	λ^j	μ^j	Σ^j
1	0.2	-1	0.25
2	0.5	0	0.25
3	0.3	1	0.25

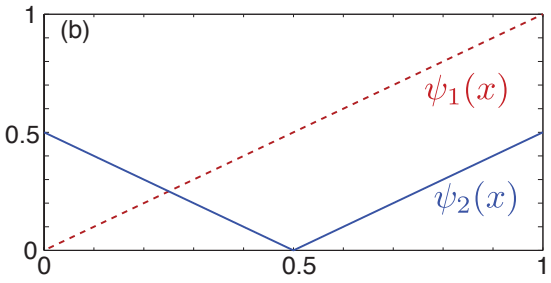

Figure 3.2: (a) Parameter values and (b) (ψ_1, ψ_2) in the Example.

The Galerkin approximation of the gain function is constructed on an interval domain $D \subset \mathbb{R}$. The domain is a union of finitely many non-intersecting intervals $D_l = [a_{l-1}, a_l)$, where $a_0 < a_1 < \ldots < a_L$.

Define for $l = 1, 2, \ldots, L$ and $k = 1, 2, \ldots, L$:

$$\text{Basis functions:} \qquad \chi_l(x) = 1_{D_l}(x),$$

$$\text{Test functions:} \qquad \psi_k(x) = |x - a_k|.$$

Fig. 3.2 depicts the test functions $\{\psi_1(x), \psi_2(x)\}$ for $D = [0,1]$ and $a_0 = 0$, $a_1 = \frac{1}{2}$ and $a_2 = 0$. The basis functions are the indicator functions on $[0, \frac{1}{2})$ and $[\frac{1}{2}, 1)$.

Fig. 3.3 depicts a comparison of the DNS solution and the Galerkin solution for $h(x) = x^2$, $D = [-2, 2]$ and $L = 1, 5, 15$. For a given L, the basis and test functions are constructed for a uniform partition of the domain (That is, $a_l = -2 + \frac{l}{L}4$). The Galerkin solution is obtained using $N = 1000$ particles that are sampled from the distribution p. The particles are used to compute matrix A and vector b, using formulae (3.34) and (3.35), respectively. Since the analytical form of p is known, these matrices can also be assembled by using the integrals:

$$[A]_{kl} = \int \chi_l(x) \cdot \nabla \psi_k(x) p(x) \, \mathrm{d}x, \tag{3.39}$$

$$b_k = \int (h(x) - \hat{h}) \psi_k(x) p(x) \, \mathrm{d}x. \tag{3.40}$$

The figure also depicts the Galerkin solution based on the integral evaluation of the matrix A and vector b.

For $L = 15$, the matrix A was found to be singular for the particle-based implementation. This is because there are no particles in D_{15}. In this case, the Galerkin solution is obtained using only the integral formulae (3.39)-(3.40). These formulae are exact while the particle-based formulae (3.34) and (3.35) are approximations. In the other two cases ($L = 1$ and $L = 5$), the particle-based solution provides a good approximation.

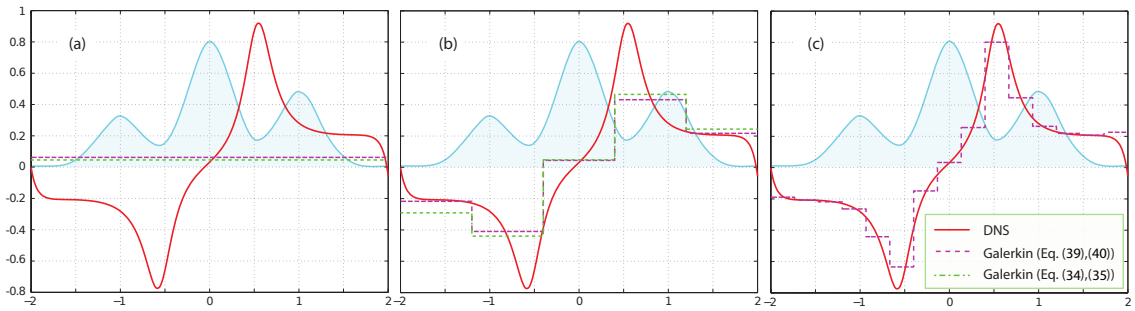

Figure 3.3: Comparison of the DNS and the Galerkin approximations of the gain function for $h(x) = x^2$ and: (a) $L = 1$, (b) $L = 5$ and (c) $L = 15$. The density is depicted as the shaded curve in the background.

3.5 Numerics

We present two numerical examples to illustrate the use of multivariable feedback particle filter: i) A bearing-only tracking problem using Galerkin method, and ii) an application to the high-dimensional systems.

3.5.1 Bearing-only Tracking Example

Consider a target tracking problem with bearing-only measurements [74]. A single target moves in a two-dimensional (2d) plane according to the standard second-order model:

$$\mathrm{d}X_t = AX_t\,\mathrm{d}t + \Gamma\,\mathrm{d}B_t,$$

where $X := (X_1, V_1, X_2, V_2)^T \in \mathbb{R}^4$, (X_1, X_2) denotes the position and (V_1, V_2) denotes the velocity. The matrices,

$$A = \begin{bmatrix} 0 & 1 & 0 & 0 \\ 0 & 0 & 0 & 0 \\ 0 & 0 & 0 & 1 \\ 0 & 0 & 0 & 0 \end{bmatrix}, \qquad \Gamma = \sigma_B \begin{bmatrix} 0 & 0 \\ 1 & 0 \\ 0 & 0 \\ 0 & 1 \end{bmatrix},$$

and $\{B_t\}$ is a standard 2d Wiener process.

Two fixed sensors can take bearing measurements Z_t of the target according to the observation model,

$$\mathrm{d}Z_t = h(X_t)\,\mathrm{d}t + \sigma_W\,\mathrm{d}W_t,$$

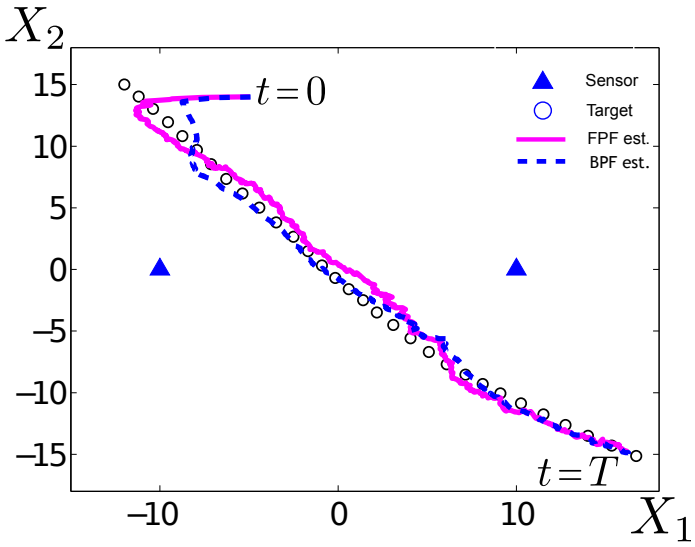

Figure 3.4: Simulation results: Comparison of the true target trajectory with estimated mean obtained using the FPF and the BPF.

where $\{W_t\}$ is a standard 2d Wiener process, $h = (h_1, h_2)^T$ and

$$h_j(x_1, v_1, x_2, v_2) = \arctan\left(\frac{x_2 - x_2^{(\text{sen } j)}}{x_1 - x_1^{(\text{sen } j)}}\right), \quad j = 1, 2,$$

where $(x_1^{(\text{sen } j)}, x_2^{(\text{sen } j)})$ denotes the position of sensor j.

Fig. 3.4 depicts a sample path of the target trajectory obtained for a typical numerical experiment. The sensor location and target trajectory are depicted as triangles and circles, respectively. The simulation parameters are: The actual initial state of the target is $(-12, 4, 15, -5)^T$, and $\sigma_B = 1$; The two sensors are located at fixed points $(-10, 0)^T$ and $(10, 0)^T$, and $\sigma_W = 0.017$. The simulation is carried out in a timeframe $T = 6$ with a discretized time step $\Delta t = 0.01$.

The results of applying the feedback particle filter (FPF) and the bootstrap particle filter (BPF) are also depicted in Fig. 3.4. For the FPF, the gain function is obtained by using the Galerkin method described in Sec. 3.4.1 with polynomial basis functions $\{X_1, V_1, X_2, V_2, X_1^2, V_1^2, X_2^2, V_2^2\}$. This leads to a 8×8 linear matrix problem (**??**), whose solution is obtained numerically. For the BPF, its implementation is based on an algorithm taken from Ch. 9 of [7]. Both particle filters are comprised of $N = 500$ particles whose initial condition is sampled from a multivariate Gaussian distribution with mean vector $\mu_0 = (-5, 3, 14, -6)^T$ and covariance matrix $\Sigma_0 = \text{diag}([1.5^2, 0.05^2, 0.3^2, 0.01^2])$. The sample mean is used as the particle estimate of the actual target state.

The simulation results in Fig. 3.4 show that both filters can adequately track the target, while the FPF estimate (as a solid line) converges to the true trajectory slightly faster than the BPF estimate (as a dashed line). Furthermore, in Fig. 3.5, a scatterplot of particles on the 2d plane is made using samples from the FPF and the BPF respectively at

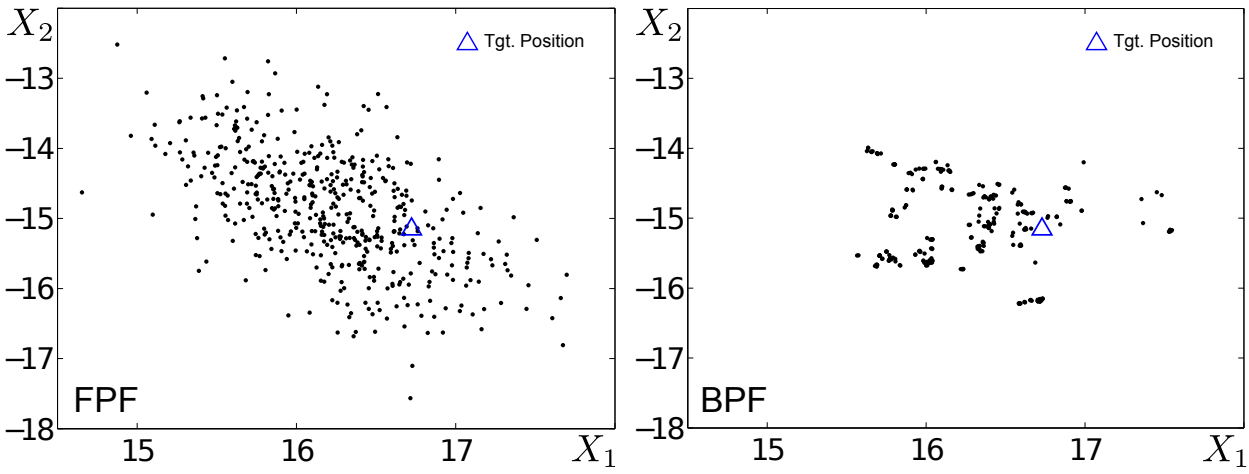

Figure 3.5: Scatterplots of 500 particle samples on the X_1-X_2 plane from the FPF (left) and the BPF (right).

time $t = 6$. The true target position is also depicted as a circle. This result suggests that although the point estimates of both filters are close, the FPF provides a better approximation in terms of the empirical distribution than the BPF.

3.5.2 High-dimensional Systems Example

It has been widely recognized that the conventional particle filter (based on importance sampling) may fail in large scale systems [13]. To shed light on the effects of dimensionality on filter performance, we provide a comparison between the FPF and the bootstrap particle filter BPF with regard to the estimation error. Consider a motivating example from [13]:

$$\mathrm{d}X_t = 0, \tag{3.41}$$

$$\mathrm{d}Z_t = X_t\,\mathrm{d}t + \mathrm{d}W_t, \quad X_0 \sim N(0, I_d), \tag{3.42}$$

where X_t is the d-dimensional state vector, Z_t is the d-dimensional observation vector, I_d denotes the $d \times d$ identity matrix and $\{W_t\}$ is the standard Wiener process with covariance I_d. The prior distribution is assumed to be Gaussian with zero mean vector and covariance matrix $\Sigma_0 = I_d$. These choices of system parameters allow straightforward manipulation of system dimension for simulation purpose.

For the linear filtering problem (3.41)-(3.42), the optimal solution is given by the Kalman filter. We use this solution to define the relative mean-square error:

$$rmse = \frac{1}{T}\int_0^T \frac{\|\mu_t^{(N)} - \mu_t\|^2}{\|\mu_t\|^2}\,\mathrm{d}t, \tag{3.43}$$

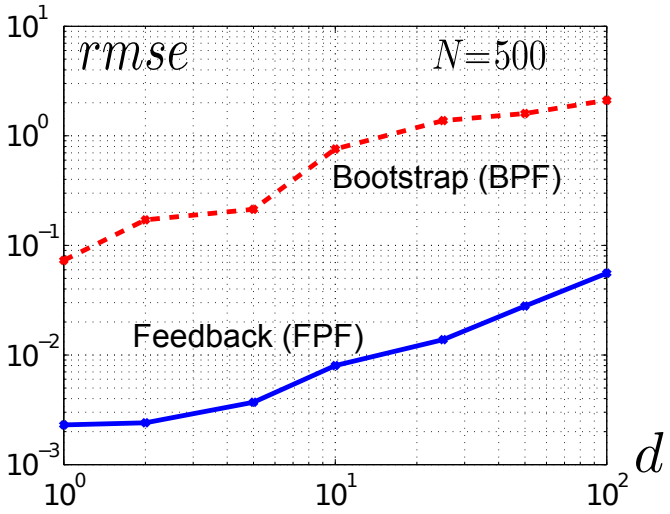

Figure 3.6: Comparisons of the *rmse* using feedback particle filter and the bootstrap particle filter.

where μ_t is the conditional mean vector obtained using the Kalman filter, and $\mu_t^{(N)}$ is calculated as the sample mean of the particles.

Fig. 3.6 depicts the comparison between the *rmse* obtained using the FPF and the BPF. The latter implementation is based on an algorithm taken from Ch. 9 of [7]. For simulation purpose, we use a range of values of system dimension $d \in \{1,2,5,10,25,50,100\}$, $\Delta t = 0.01$, $T = 1$ and a fixed number of particles $N = 500$. The plot is generated by running 100 Monte Carlo simulations.

These simulation results suggest that the feedback can help reduce the high variance that is often observed with the conventional particle filter, especially when the underlying system is of high dimensionality (e.g., $d = 100$). In this case, the bootstrap particle filter suffers from particle degeneracy, i.e., the particle population collapse to one mass point after few iterations. It has been shown that the degeneracy phenomenon is impossible to avoid in importance sampling-based approaches [56]. The root cause for particle degeneracy is the point-by-point multiplication implementation of Bayes' rule; cf., [13, 52, 57]. In the FPF algorithm, the particles are directly "migrated" to the desired regions of the state space by using a feedback control approach, thereby avoiding the degeneracy issues.

It should be noted that there are many "advanced" versions of the BPF algorithm, e.g., the resample-move particle filter [69], the regularized particle filter [119] and the auxiliary particle filter [126]. Although these algorithms show improvement in terms of estimation accuracy as well as computational complexity, they still rely on a good proposal density for importance sampling, or demand a careful design for the resampling procedure, both of which are found difficult in large scale systems. The FPF, unlike the sampling-based methods, is a control-oriented approach to particle filtering. It implements the Bayes' rule via an innovation error-based feedback control structure and requires no importance sampling or resampling. Therefore, the FPF does not suffer sampling-related issues as the conventional

PF does. Rigorous convergence results of the FPF will be the subject of future work.

3.6 Conclusions

In this chapter, we introduce the feedback particle filter in the general multivariable setting. The main conclusions are:

(i) Consistency is established in the multivariate setting, as well as well-posedness of the associated PDE to obtain the filter gain. The admissibility of the control input for the feedback particle filter is also proved.

(ii) The gain can be expressed as the gradient of a function, which is precisely the solution to Poissons equation for a related MCMC diffusion (the Smoluchowski equation). This provides a bridge to MCMC as well as to approximate optimal filtering approaches such as TD-learning, which can in turn be used to approximate the gain.

(iii) Motivated by a weak formulation of Poissons equation, a Galerkin finite-element algorithm is proposed for approximation of the gain. Its performance is illustrated in numerical experiments.

The approximation of the gain function is at the core of the feedback particle filter algorithm. Future research directions regarding the gain function approximation include but not limited to the following:

(i) How to choose the optimal basis function? The performance of FPF clearly depends the choice of basis functions and the best way to do this is not clear.

(ii) Is it possible to write a differential equation for the gain function, i.e., use the gain function at time t to obtain the gain function at time $t + \Delta t$? The Galerkin method, on the other hand, is memoryless (i.e., does not depend on the history).

Chapter 4

Feedback Particle Filter for Continuous-Discrete Time Filtering*

4.1 Introduction

The purpose of the present chapter is to introduce the feedback particle filter algorithm for the continuous-discrete time nonlinear filtering problem. The motivation is two-fold: one is to derive the continuous-discrete time analogue of the feedback control structure present in the continuous-time FPF algorithm. The other is to provide a comparison to existing continuous discrete-time algorithms, specifically the work of Daum and Huang [51].

Filtering Problem: Consider the continuous-discrete time nonlinear filtering problem. The state process evolves in continuous-time according to the stochastic differential equation (SDE) model:

$$\mathrm{d}X_t = a(X_t)\,\mathrm{d}t + \mathrm{d}B_t, \tag{4.1}$$

where $X_t \in \mathbb{R}^d$ is the state at time t, $\{B_t\}$ is a d-dimensional standard Wiener process independent of X_0, and a is assumed to be a known C^1 function so that SDE (4.1) has a pathwise unique solution for each initial X_0.

The observations (measurements) are obtained at discrete-times $t = t_n$ according to the model:

$$Y_n = h(X_{t_n}) + W_n, \tag{4.2}$$

where $Y_n \in \mathbb{R}^m$, $\{t_n;\, n = 1,2,\ldots\}$ is a strictly increasing sequence of observation sampling times, i.e., $t_n > t_{n-1}$, $\forall n \geq 1$; the sequence $\{t_n\}$ is independent of $\{X_t\}$; $\{W_n\}$ is a sequence of m-dimensional variables, each component of which is independent and sampled from the Gaussian distribution; $\{W_n\}$ is also independent of $\{X_t\}$ and of $\{t_n\}$. The function h is a column vector whose j-th coordinate is denoted as h_j (i.e., $h = (h_1, h_2, \ldots, h_m)$). All components of $h(x)$ are assumed to be twice continuously differentiable in x.

The objective of the continuous-discrete time filtering problem (4.1)-(4.2) is to compute the conditional probability density function (posterior) of X_t given the observation history (filtration) $\mathscr{Z}_t := \sigma\{Y_n : \forall n \text{ such that } t_n \in [0,t]\}$. The posterior distribution p^* is defined the same as in (2.2).

*This chapter is an extension of the published paper [152].

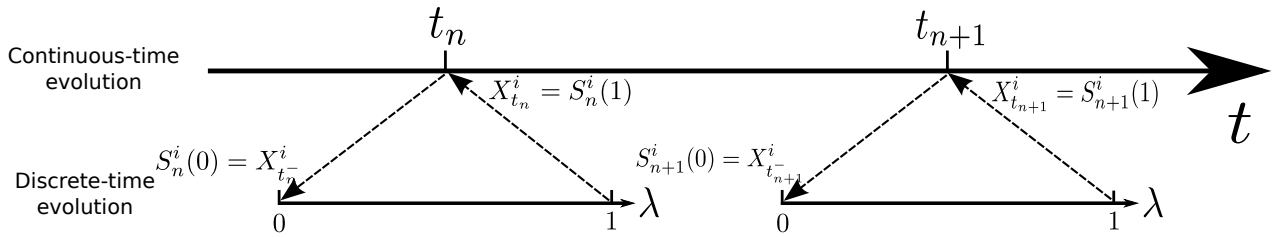

Figure 4.1: An illustration of the two-step evolution structure in the continuous-discrete time feedback particle filter.

The objective of the present chapter is to develop an extension of the previously introduced continuous-time FPF algorithm for the continuous-discrete time filtering problem (4.1)-(4.2). The continuous-discrete FPF is a controlled system where the state evolves in two alternating steps: For $n = 1, 2, 3, \ldots,$

(i) the continuous-time evolution according to (4.1) for values of time $t \in [t_{n-1}, t_n)$;

(ii) the discrete-time evolution to simulate the Bayesian update step at discrete time $t = t_n$.

This two-step structure also exists for the classic continuous-discrete time Kalman filter and the SIR particle filter.

Specifically, the dynamics of the i-th particle have the following form: For time $t \in [t_{n-1}, t_n)$,

$$\mathrm{d}X^i_t = a(X^i_t)\,\mathrm{d}t + \mathrm{d}B^i_t, \tag{4.3}$$

where $X^i_t \in \mathbb{R}^d$ is the state for the i-th particle at time t, $\{B^i_t\}$ are mutually independent standard Wiener processes and initial condition $X^i_{t_{n-1}}$ are known. At time $t = 0$, these are sampled i.i.d. from the prior distribution $p^*(\cdot, 0)$. We denote the right limit as:

$$X^i_{t_n^-} := \lim_{t \nearrow t_n} X^i_t. \tag{4.4}$$

At the discrete time $t = t_n$, the value of the new observation Y_n becomes known. To account for this new observation, one introduces a particle flow (see [51]) defined according to differential equations,

$$\frac{\mathrm{d}S^i_n}{\mathrm{d}\lambda}(\lambda) = U^i_n(\lambda),$$

with initial condition $S^i_n(0) = X^i_{t_n^-}$ for $i = 1, \ldots, N$. The parameter $\lambda \in [0, 1]$ is referred to as the pseudo-time. We present an algorithm to design the control input $U^i_n(\lambda)$ such that the empirical distribution of the ensemble $\{S^i_n(1)\}_{i=1}^N$ approximates the posterior distribution. This in particular allows us to set the initial condition for the next time interval, as $X^i_{t_n} = S^i_n(1)$ for $i = 1, \ldots, N$.

The two-step evolution structure of the continuous-discrete time feedback particle filter is illustrated in Fig. 4.1.

Recall that we denote conditional distribution of a particle X_t^i given $\mathscr{Z}_t$ by p:

$$\int_{x\in A} p(x,t)\,\mathrm{d}x = \mathsf{P}\{X_t^i \in A|\mathscr{Z}_t\},$$

and the empirical distribution formed by the "particle population" by $p^{(N)}$:

$$p^{(N)}(A,t) = \frac{1}{N}\sum_{i=1}^{N} \mathbb{1}\{X_t^i \in A\}.$$

The control problem is to choose the control input $U_n^i(\lambda)$ so that p approximate p^*, and consequently $p^{(N)}$ approximates p^* for large N. The main result of this chapter is to derive an explicit formula for the optimal control input, and demonstrate that under general conditions we obtain an exact match $p = p^*$ under optimal control.

The basic idea of particle flow is borrowed from Daum and Huang [48–51]. The control law – to obtain the control input $U_n^i(\cdot)$ – described in this chapter is somewhat different from Daum and Huang's work. The control law's structure is closer to the innovation-error based feedback control structure of the continuous-time FPF algorithm. A discussion of this appears in Sec. 4.3.

The outline of the remainder of this chapter is as follows: The continuous-discrete time FPF algorithm is derived in Sec. 4.2. A comparison to Daum and Huang's filter appears in Sec. 4.3. Some numerical examples are discussed in Sec. 4.4.

4.2 Continuous-Discrete Time Filtering

4.2.1 Evolution of the Posterior

Given the initial density function $p^*(x,0)$ and an increasing family of filtration $\mathscr{Z}_t$, the evolution of the posterior distribution $p^*(x,t)$ of the diffusion process $\{X_t\}$ is characterized through two alternating steps: For $n = 1,2,3,\ldots$,

(i) Continuous-time evolution of the posterior for $t \in [t_{n-1}, t_n)$;

(ii) Bayesian update step at the discrete time instant $t = t_n$.

Elaboration of these steps leads to the following well-known characterization. Its proof is omitted.

Proposition 4.2.1 *Consider the filtering problem (4.1)-(4.2) over time interval $[t_{n-1}, t_n]$. For $t \in [t_{n-1}, t_n)$, the posterior distribution $p^*(x,t)$ evolves according to:*

$$\frac{\partial p^*}{\partial t}(x,t) = \mathscr{L}^\dagger p^*(x,t), \tag{4.5}$$

where $\mathscr{L}^\dagger p^* = -\nabla\cdot(p^* a) + \frac{1}{2}\Delta p^*$ *is the forward generator of the diffusion process* X_t, Δ *denotes the Laplacian in* $\mathbb{R}^d$ *and the initial condition* $p^*(x,t_{n-1})$ *is given. At time* $t=0$, *it is* $p^*(x,0)$. *We denote the right limit as*

$$p^*(x,t_n^-) := \lim_{t\nearrow t_n} p^*(x,t).$$

Note $p^*(x,t_n^-)$ *is the posterior distribution of* X_{t_n} *given* $\mathscr{Z}_{n-1}$.

At the discrete time instant $t=t_n$ *when the n-th observation is made, the posterior is updated using Bayes' rule:*

$$p^*(x,t_n) = p^*(x,t_n^-)\cdot\exp\left[-\frac{1}{2}(Y_n - h(x))^T(Y_n-h(x))\right]/C_n, \tag{4.6}$$

where C_n *is the normalization constant.*

The two equations (4.5)-(4.6) *define the mapping of* p^* *from* t_{n-1} *to* t_n.

4.2.2 Log-Homotopy Transformation

In this section, we introduce the log-homotopy transformation for the discrete-time Bayesian update step (4.6). The transformation is used to convert its evaluation into a continuous-time process.

On taking a logarithm of both sides in (4.6),

$$\ln p^*(x,t_n) = \ln p^*(x,t_n^-) + h(x)^T\left(Y_n - \frac{1}{2}h(x)\right) - \ln C_n^1,$$

where C_n^1 is a constant that does not depend on x. The constant may be dropped to obtain the recursion for the un-normalized density:

$$\ln q^*(x,t_n) = \ln q^*(x,t_n^-) + h(x)^T\left(Y_n - \frac{1}{2}h(x)\right),$$

where

$$p^*(x,t_n) = \frac{q^*(x,t_n)}{\int q^*(x',t_n)\,\mathrm{d}x'}, \quad p^*(x,t_n^-) = \frac{q^*(x,t_n^-)}{\int q^*(x',t_n^-)\,\mathrm{d}x'}.$$

Next define two homotopy functions $f_n(x,\lambda)$ and $\rho_n(x,\lambda)$ as follows:

$$f_n(x,\lambda) := \ln q^*(x,t_n^-) + \lambda h(x)^T\left(Y_n - \frac{1}{2}h(x)\right), \tag{4.7}$$

$$\rho_n^*(x,\lambda) := \frac{\exp f_n(x,\lambda)}{\int \exp f_n(x',\lambda)\,\mathrm{d}x'}, \tag{4.8}$$

where $\lambda\in[0,1]$ is the *pseudo-time* parameter.

By construction, for $\lambda = 0$ and $\lambda = 1$:

$$f_n(x,0) = \ln q^*(x,t_n^-), \qquad f_n(x,1) = \ln q^*(x,t_n),$$
$$\rho_n^*(x,0) = p^*(x,t_n^-), \qquad \rho_n^*(x,1) = p^*(x,t_n).$$

In words, $\rho_n^*(x,0)$ is the distribution of X_{t_n} just prior to conditioning on the observation Y_n, while $\rho_n^*(x,1)$ is the posterior distribution after conditioning on Y_n.

The evolution of $\rho_n^*(x,\lambda)$, with respect to the pseudo-time parameter λ, is described in the following proposition. Its proof appears in App. C.1.

Proposition 4.2.2 *Consider the normalized density function $\rho_n^*(x,\lambda)$ as defined in (4.7)-(4.8) with $\lambda \in [0,1]$. Then its evolution is given by the following partial differential equation: For $\lambda \in [0,1]$,*

$$\frac{\partial \rho_n^*}{\partial \lambda}(x,\lambda) = \rho_n^*(x,\lambda)\left[(h(x)-\hat{h}(\lambda))^T Y_n - \frac{1}{2}|h(x)|^2 + \frac{1}{2}\widehat{|h|^2}\right], \tag{4.9}$$

where $\hat{h}(\lambda) := \int \rho_n^*(x,\lambda)h(x)\,\mathrm{d}x$, $|h(\cdot)|^2 := h(\cdot)^T h(\cdot)$ and $\widehat{|h|^2} := \int \rho_n^*(x,\lambda)|h(x)|^2\,\mathrm{d}x$.

Remark 5 *By using the log-homotopy transformation, we convert the discrete-time Bayesian update step (4.6) to a continuously evolving process (4.9) with respect to the pseudo-time parameter $\lambda \in [0,1]$. Effectively, given $\rho_n^*(x,0) = p^*(x,t_n^-)$ at the beginning of pseudo-time interval, if $\rho_n^*(x,\lambda)$ evolves according to (4.9), then we have $\rho_n^*(x,1) = p^*(x,t_n)$ at the end, which is the desired posterior distribution.*

4.2.3 Belief State Dynamics & Control Architecture

As described in the Introduction and illustrated in Fig. 4.1, the state evolves in two steps: the continuous-time evolution followed by the discrete-time evolution to simulate the Bayesian update step. In this section, we propose a feedback control structure for the latter.

At discrete time t_n, the i-th particle evolves according to,

$$\frac{\mathrm{d}S_n^i}{\mathrm{d}\lambda}(\lambda) = \underbrace{\mathsf{K}(S_n^i(\lambda),\lambda)Y_n + u(S_n^i(\lambda),\lambda)}_{U_n^i(\lambda)}, \tag{4.10}$$

where $\lambda \in [0,1]$ is the pseudo-time variable and the initial condition $S_n^i(0) := X_{t_n^-}^i$ for $i = 1,\ldots,N$, where $X_{t_n^-}^i$ is the right limit of the continuous-time process X_t^i as defined in (4.4). Note that the gain function $\mathsf{K}(x,\lambda)$ is a $d \times m$ matrix and $u(x,\lambda) \in \mathbb{R}^d$.

Recall that there are two types of density functions of interest in our analysis:

(i) $\rho_n(x,\lambda)$: Defines the distribution of $S_n^i(\lambda)$ as in (4.10).

(ii) $\rho_n^*(x,\lambda)$: Defines the homotopy distribution with $\rho_n^*(x,0) = p^*(x,t_n^-)$ and $\rho_n^*(x,1) = p^*(x,t_n)$.

The functions $\{u(x,\lambda), \mathsf{K}(x,\lambda)\}$ are said to be *optimal* if $\rho_n = \rho_n^*$. That is, given $\rho_n(\cdot,0) = \rho_n^*(\cdot,0)$, our goal is to choose $\{u,\mathsf{K}\}$ in the feedback particle filter so that the evolution equations of these distributions coincide (see (4.9) and (4.11)) and thus $\rho_n(\cdot,1) = p^*(\cdot,t_n)$.

The evolution equation for $\rho_n(x,\lambda)$ is given by the Kolmogorov's forward equation (see [86]):

$$\frac{\partial \rho_n}{\partial \lambda}(x,\lambda) = -\nabla\cdot(\rho_n \mathsf{K}) Y_n - \nabla\cdot(\rho_n u). \tag{4.11}$$

Note that Y_n is a known constant for $\lambda \in [0,1]$.

In the following, we restrict our discussion to a fixed time $t = t_n$ and suppress the subscript in ρ_n^* and ρ_n.

4.2.4 General Form of the Feedback Particle Filter

The general form of the feedback particle filter is obtained by choosing $\{u,\mathsf{K}\}$ as the solution to a certain E-L BVP based on ρ.

For each fixed $\lambda \in [0,1]$, the gain function

$$\mathsf{K} = [\nabla\phi_1^T, \nabla\phi_2^T, \ldots, \nabla\phi_m^T]$$

is obtained as a solution to: For $j = 1,\ldots,m$,

$$\begin{aligned} &\nabla\cdot(\rho\nabla\phi_j) = -(h_j - \hat{h}_j)\rho, \\ &\int \phi_j(x,\lambda)\rho(x,\lambda)\,\mathrm{d}x = 0. \end{aligned} \tag{4.12}$$

The function u is obtained as:

$$u(x,\lambda) = -\frac{1}{2}\mathsf{K}(x,\lambda)\left(h(x) + \hat{h}\right) + \frac{1}{2}\Omega(x,\lambda), \tag{4.13}$$

where $\Omega = \nabla\varphi$ is a solution to:

$$\begin{aligned} &\nabla\cdot(\rho\nabla\varphi) = -(g - \hat{g})\rho, \\ &\int \varphi(x,\lambda)\rho(x,\lambda)\,\mathrm{d}x = 0, \end{aligned} \tag{4.14}$$

where $g := \sum_{j=1}^{m} \nabla\phi_j \cdot \nabla h_j^T$ and $\hat{g} := \int \rho(x,\lambda) g(x)\,\mathrm{d}x = |\hat{h}|^2 - \widehat{|h|^2}$.

Substituting (4.12)-(4.14) into (4.10) gives the feedback particle filter model:

$$\frac{\mathrm{d}S_n^i}{\mathrm{d}\lambda}(\lambda) = \mathsf{K}(S_n^i(\lambda),\lambda)\left[Y_n - \frac{h(S_n^i(\lambda)) + \hat{h}}{2}\right] + \frac{1}{2}\Omega(S_n^i(\lambda),\lambda),$$

with initial condition $S_n^i(0) = X_{t_{n-}}^i$ for $i = 1,\ldots,N$.

Recall that the evolution of $\rho^*(x,\lambda)$ is described by (4.9). The evolution of $\rho(x,\lambda)$ is given by the Kolmogorov forward equation (4.11). The following theorem shows that the evolution equations for ρ and ρ^* are identical. The proof appears in App. C.2.

Theorem 4.2.3 *Consider the two distributions ρ and ρ^*. Suppose that the functions $\{u(x,\lambda),\mathsf{K}(x,\lambda)\}$ are obtained according to (4.12)-(4.14), respectively. Then provided $\rho(x,0) = \rho^*(x,0)$, we have for all $\lambda \in [0,1]$, $\rho(x,\lambda) = \rho^*(x,\lambda)$.*

Remark 6 *Note that the dynamics (4.3) of the i-th particle during $[t_{n-1},t_n)$ coincides with the state process model (4.1). Therefore, given $\rho(x,\lambda) = \rho^*(x,\lambda)$ for all $\lambda \in [0,1]$, we have $p = p^*$ for all t.*

4.2.5 Algorithm

The main difficulty is to obtain a solution of the BVP (4.12) and (4.14) at each pseudo-time λ. The constant gain approximation may be used to approximate these solutions as:

$$\mathsf{K} \approx \frac{1}{N}\sum_{i=1}^{N} S_n^i(\lambda)(h(S_n^i(\lambda)) - \hat{h})^T, \tag{4.15}$$

$$\Omega \approx \frac{1}{N}\sum_{i=1}^{N} S_n^i(\lambda)(g(S_n^i(\lambda)) - \hat{g}), \tag{4.16}$$

where we denote $S_n^i(\lambda)$ to be the state of i-th particle at pseudo-time $\lambda \in [0,1]$.

Apart from the gain function, the algorithm requires approximation of $\hat{h}$ and $\widehat{|h|^2}$. These are obtained in terms of particle as:

$$\hat{h} \approx \frac{1}{N}\sum_{i=1}^{N} h(S_n^i(\lambda)), \quad \widehat{|h|^2} \approx \frac{1}{N}\sum_{i=1}^{N} h(S_n^i(\lambda))^T h(S_n^i(\lambda)).$$

For simulating the continuous-discrete time feedback particle filter, we use an Euler-discretization method for both t and λ. The resulting discrete-time algorithm appears in Algo.1. At each time step, the algorithm requires computation of the gain function, which is obtained using (4.15)-(4.16). Note that the algorithm for pseudo-time variable λ is conceptually the same the algorithm described for the real time variable t as in [158].

Algorithm 3 Continuous-Discrete Time FPF

INITIALIZATION
Set $n = 0$
for $i = 1$ to N **do**
  Sample X_0^i from $p^*(\cdot, 0)$
end for
$t = 0$
$n = n + 1$

ITERATION 1 [$t \in [t_{n-1}, t_n)$]
Set $t = t_{n-1}$
while $t \leq t_n$ **do**
  for $i = 1$ to N **do**
    Generate a sample, ΔV, from $N(0,1)$
    $X_{t+\Delta t}^i = X_t^i + a(X_t^i)\Delta t + \sqrt{\Delta t}\, \Delta V$
  end for
  $t = t + \Delta t$
end while

ITERATION 2 [$t = t_n$]
Set $\lambda = 0$
for $i = 1$ to N **do**
  Set $S_n^i(0) = X_t^i$
end for
while $\lambda \leq 1$ **do**
  Calculate $\hat{h}(\lambda) \approx \frac{1}{N} \sum_{i=1}^N h(S_n^i(\lambda))$
  for $i = 1$ to N **do**
    Calculate $I_n^i(\lambda) = Y_n - \frac{1}{2}\left[h(S_n^i(\lambda)) + \hat{h}(\lambda)\right]$
    Calculate the gain function K (e.g., by using (4.15))
    Calculate the function Ω (e.g., by using (4.16))
    $S_n^i(\lambda + \Delta\lambda) = S_n^i(\lambda) + \left[\mathsf{K}\, I_{t_n}^i(\lambda) + \frac{1}{2}\Omega\right] \Delta\lambda$
  end for
  $\lambda = \lambda + \Delta\lambda$
end while
for $i = 1$ to N **do**
  Set $X_t^i = S_n^i(1)$
end for
$n = n + 1$
goto ITERATION 1

4.2.6 Linear Gaussian Case

In this section, we show that for the linear Gaussian case, a closed-form solution for (4.12)-(4.14) exists which leads to a closed-form continuous-discrete time feedback particle filter. An alternate feedback particle filter algorithm for this case appears in [157].

Consider the continuous-discrete time linear filtering problem,

$$\mathrm{d}X_t = A\,X_t\,\mathrm{d}t + \mathrm{d}B_t, \tag{4.17}$$

$$Y_n = H\,X_{t_n} + W_n, \tag{4.18}$$

where A is a $d \times d$ matrix, and H is an $m \times d$ matrix. The initial distribution $p^*(x,0)$ is Gaussian with mean vector μ_0 and covariance matrix Σ_0.

The following proposition shows that the Kalman gain is the solution of the multivariable BVP (4.12). Its proof appears in App. C.3.

Proposition 4.2.4 *Consider the d-dimensional linear system (4.17)-(4.18). Suppose the homotopy density function ρ is Gaussian, i.e., $\rho(x,\lambda) = \frac{1}{(2\pi)^{\frac{d}{2}}|\Sigma_\lambda|^{\frac{1}{2}}}\exp[-\frac{1}{2}(x-\mu_\lambda)^T\Sigma_\lambda^{-1}(x-\mu_\lambda)]$, where $x=(x_1,\ldots,x_d)$, $\mu_\lambda=(\mu_1(\lambda),\ldots,\mu_d(\lambda))$ is the mean, Σ_λ is the covariance matrix, and $|\Sigma_\lambda|>0$ denotes the determinant. A solution of the BVP (4.12) and (4.14) is given by:*

$$\phi_j(x,\lambda) = \sum_{k=1}^{d}[\Sigma_\lambda H^T]_{kj}(x_k - \mu_k(\lambda)), \quad j=1,\ldots,m \tag{4.19}$$

$$\Omega(x,\lambda) = (0,\ldots,0). \tag{4.20}$$

Using $\mathsf{K} = [\nabla\phi_1^T,\ldots,\nabla\phi_m^T]$, we obtain that $\mathsf{K}(x,\lambda) = \Sigma_\lambda H^T$ (same as Kalman gain in [86]).

The gain function yields the following closed-form feedback particle filter in this linear Gaussian model:

$$t\in[t_{n-1},t_n): \quad \mathrm{d}X_t^i = A\,X_t^i\,\mathrm{d}t + \mathrm{d}B_t^i, \tag{4.21}$$

$$t=t_n: \quad \frac{\mathrm{d}S_n^i}{\mathrm{d}\lambda}(\lambda) = \Sigma_\lambda H^T\left[Y_n - \frac{1}{2}H\left(S_n^i(\lambda)+\mu_\lambda\right)\right], \quad \text{for } \lambda\in[0,1]. \tag{4.22}$$

Now we show that $p=p^*$ in this case. That is, the conditional distributions of X and X^i coincide, and are defined by the well-known dynamic equations that characterize the mean and the variance of the continuous-discrete time Kalman filter. The proof of Theorem 4.2.5 is very similar to the proof in App. E of [157], and thus omitted here.

Theorem 4.2.5 *Consider the linear Gaussian filtering problem defined by the state-observation equations ((4.17),(4.18)). In this case the posterior distributions of X and X^i are Gaussian, whose conditional mean μ_t and covariance matrix Σ_t are given by the following equations of evolution. Between observations, these satisfy the differential equations:*

$$t \in [t_{n-1}, t_n): \quad \begin{aligned} \mathrm{d}\mu_t &= A\,\mu_t\,\mathrm{d}t, \\ \frac{\mathrm{d}\Sigma_t}{\mathrm{d}t} &= A\Sigma_t + \Sigma_t A^T + I, \end{aligned} \tag{4.23}$$

At discrete time instants $t = t_n$, these satisfy the difference equations:

$$t = t_n: \quad \begin{aligned} \mu_{t_n} &= \mu_{t_n^-} + \mathsf{K}_n(Y_n - H\mu_{t_n^-}), \\ \Sigma_{t_n} &= \Sigma_{t_n^-} - \mathsf{K}_n H \Sigma_{t_n^-}, \end{aligned} \tag{4.24}$$

where the gain function $\mathsf{K}_n := \Sigma_{t_n^-} H^T [H\Sigma_{t_n^-} H^T + I]^{-1}$.

Notice that particle system (4.21)-(4.22) is not practical since it requires computation of the conditional mean and variance $\{\mu_\lambda, \Sigma_\lambda\}$. If we are to compute these quantities, then there is no reason to run a particle filter!

In practice $\{\mu_\lambda, \Sigma_\lambda\}$ are approximated as sample means and sample covariances from the ensemble $\{S_n^i(\lambda)\}_{i=1}^N$:

$$\begin{aligned} \mu_\lambda &\approx \bar{\mu}_\lambda^{(N)} := \frac{1}{N}\sum_{i=1}^N S_n^i(\lambda), \\ \Sigma_\lambda &\approx \bar{\Sigma}_\lambda^{(N)} := \frac{1}{N-1}\sum_{i=1}^N \left[S_n^i(\lambda) - \bar{\mu}_\lambda^{(N)}\right]^2. \end{aligned} \tag{4.25}$$

4.3 Comparison with the Particle Flow Filter

Daum and Huang were the first to introduce a particle flow algorithm for the continuous-discrete time filtering problem [48]. The use of homotopy transformation as well as the continuous-time particle flow to implement the Bayesian update step appears in their work (see also [49–51]). In our notation, the particle flow ODEs for Daum-Huang's filter are:

$$\frac{\mathrm{d}S_n^i}{\mathrm{d}\lambda}(\lambda) = u(S_n^i(\lambda), \lambda),$$

where u is obtained by solving the boundary value problem,

$$\nabla \cdot (q_n(x,\lambda)u(x,\lambda)) = -q_n(x,\lambda)\,\ln L(Y_n; x),$$

where q_n is the unnormalized conditional density function and $L(Y_n;x)$ is the likelihood function with $L(Y_n;x) := (2\pi)^{-\frac{d}{2}} \exp\left(-\frac{1}{2}|Y_n - h(x)|^2\right)$.

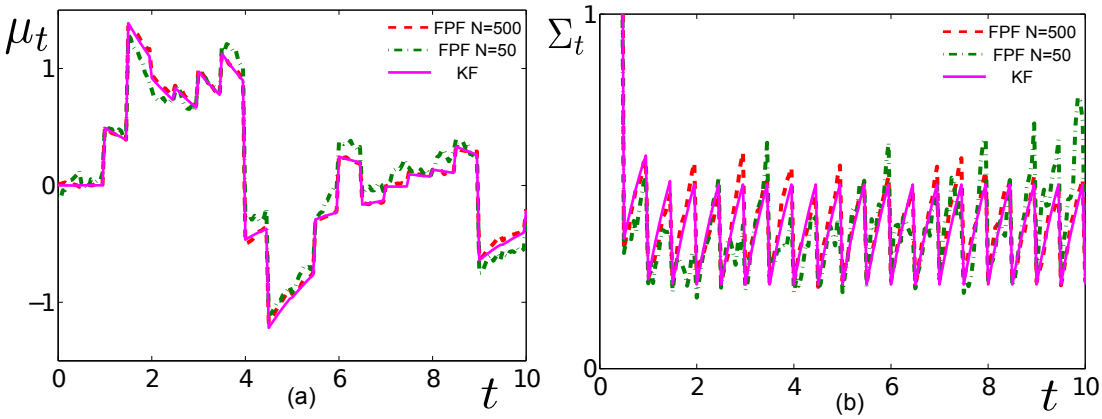

Figure 4.2: Comparison of the Kalman filter and the feedback particle filter with different number of particles: (a) conditional mean; (b) conditional variance.

The main differences between the algorithm presented here and Daum-Huang's filter concern

(i) the structure of the control law, and

(ii) the nature of the boundary value problems solved.

The innovation error-based gain feedback structure proposed here is motivated by the feedback particle filter algorithm in continuous-time. The boundary value problems described in this chapter have a unique solution. This in particular leads to a well-posed construction of the particle flow. Additional discussion of these issues for the continuous-time problem appears in [154, 158].

4.4 Numerics

In this section, we provide numerical verification of the continuous-discrete feedback particle filter for a linear Gaussian system. We provide comparisons with the classic continuous-discrete Kalman filter, which serves as a benchmark.

Consider the continuous-discrete time filtering problem:

$$\mathrm{d}X_t = A\, X_t\, \mathrm{d}t + \sigma_B\, \mathrm{d}B_t,$$

$$Y_n = H\, X_{t_n} + \sigma_W\, W_n,$$

where $A = -0.5$, $H = 3$, $\sigma_B = 1$, $\sigma_W = 2$, $\{B_t\}$ is the standard Wiener process, $\{W_n\}$ is the standard Gaussian white noise, and $\{B_t\}$, $\{W_n\}$ are mutually independent. Observations are available at $t_n = 0.5, 1.0, 1.5, \ldots, 10$.

The continuous-discrete feedback particle filter comprises of N particles where the controlled system of the i-th

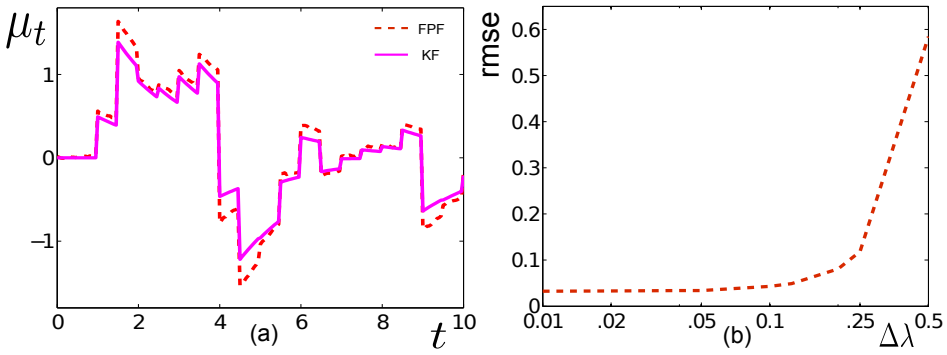

Figure 4.3: (a). Comparison of true mean μ_t and estimated mean $\mu_t^{(N)}$ with $\Delta\lambda = 0.5$; (b). Comparison of the rmse with different choices of $\Delta\lambda$.

particle is given by: For $t \in [t_{n-1}, t_n)$,

$$\mathrm{d}X_t^i = A\, X_t^i\, \mathrm{d}t + \sigma_B\, \mathrm{d}B_t^i,$$

and for $t = t_n$,

$$\frac{\mathrm{d}S_n^i}{\mathrm{d}\lambda}(\lambda) = \frac{H\,\bar{\Sigma}_\lambda^{(N)}}{\sigma_W^2}\left[Y_n - H\,\frac{S_n^i(\lambda) + \bar{\mu}_\lambda^{(N)}}{2}\right],$$

where $\lambda \in [0,1]$ is the pseudo-time, $S_n^i(0) := X_{t_n}^i$, and $\{B_t^i\}$ are mutually independent standard Wiener processes. We initialize the particle system by drawing initial conditions $\{X_0^i\}_{i=1}^N$ from the distribution $N(0,2)$. In the simulation discussed next, the mean $\bar{\mu}_\lambda^{(N)}$ and the variance $\bar{\Sigma}_\lambda^{(N)}$ are obtained from the ensemble $\{S_n^i(\lambda)\}_{i=1}^N$ according to (4.25). The total simulation time is $T = 10$, with real timestep $\Delta t = 0.05$ and the pseudo timestep $\Delta\lambda = 0.05$.

Fig. 4.2 summarizes some of the results of numerical experiments: Part (a) depicts the comparison of the true mean μ_t obtained by Kalman filter and the estimated mean $\{\bar{\mu}_t^{(N)}\}$ obtained using FPF with different number of particles. Similarly, part (b) depicts the comparison of the true variance Σ_t and the estimated variance $\{\bar{\Sigma}_t^{(N)}\}$. The true values of μ_t and Σ_t are obtained by (4.23)-(4.24). It is seen that with $N = 500$ particles the continuous-discrete FPF approximates the continuous-discrete Kalman filter quite well. With fewer particles ($N = 50$), the FPF performance degrades.

Fig. 4.3 depicts the result of a Monte Carlo study of the filter performance as the pseudo timestep $\Delta\lambda$ in Algo. 1 is varied. Part (a) is a sample result using the same parameters as in Fig. 4.2-(a) but with $\Delta\lambda = 0.5$. Part (b) depicts the *root mean square error* (rmse) with different choices of $\Delta\lambda$. The rmse is defined as:

$$\text{rmse} = \sqrt{\frac{1}{T}\int \mathsf{E}\left[\mu_t^{(N)} - \mu_t\right]^2 \mathrm{d}t},$$

where the expectation is calculated over 100 Monte Carlo runs. As expected, the rmse increases as the discretization $\Delta\lambda$ gets coarser.

4.5 Conclusions

In this chapter, the feedback particle filter algorithm is generalized for the continuous-discrete time nonlinear filtering problem. As with the continuous-time FPF, the continuous-discrete time algorithm i) admits an innovation error-based feedback control structure, and ii) requires a solution of an E-L BVP. These solutions are described in closed-form for the linear Gaussian filtering problem. For the general nonlinear non-Gaussian case, an algorithm is described to obtain an approximate solution of the E-L BVP.

The purposes of studying the continuous-discrete time FPF algorithms are two-fold:

1. In many engineering and science applications, observations are only available at certain discrete time instances. Therefore, a continuous-discrete time FPF algorithm is of practical value. The point is the proposed algorithm retain the feedback control structure even for the nonlinear non-Gaussian case.

2. Comparisons are made to the continuous-discrete time particle flow filter algorithm introduced by Daum and Huang [51]. It is shown that the FPF algorithm differs from the particle flow filter in both the structure of the control law and the nature of the BVP solved.

Chapter 5

Feedback Particle Filter for a Continuous-Time Markov Chain*

5.1 Introduction

In this chapter, we introduce the feedback particle filter to the continuous-time discrete-valued state-space nonlinear filtering problem. Consider a Markov chain $(X_t)_{t\geq 0}$ defined on a state-space comprising of standard basis in $\mathbb{R}^d$: $\{e_1, e_2, \ldots, e_d\} =: \mathbb{S}$. The chain is visualized as a directed graph whose edge, (l, l'), denotes possible transition from state $e_l \in \mathbb{S}$ to another state $e_{l'} \in \mathbb{S}/e_l$. The set of all edges is denoted E.

Recall that a continuous time Markov chain with finite state-space can be realized using Poisson counters; cf., Chap. 2 of [32] for notation used in this chapter (see also [120] for a standard reference). The dynamics for the Markovian state are given by,

$$\mathrm{d}X_t = \sum_{(l,l')\in E} A^{ll'} X_t \, \mathrm{d}N_t^{ll'},$$

where $A^{ll'} := (e_{l'} - e_l) \otimes e_l$ is a $d \times d$ matrix, and $N_t^{ll'}$ denotes the state of a Poisson counter with rate $\lambda_{l'l}$. The transition matrix for the Markov chain is then given by,

$$\Lambda = \sum_{(l,l')\in E} \lambda_{l'l} A^{ll'}.$$

The observation process is given by,

$$\mathrm{d}Z_t = h(X_t)\,\mathrm{d}t + \mathrm{d}W_t,$$

where $h : \mathbb{S} \to \mathbb{R}$ and W_t is a standard Wiener process.

The objective of the filtering problem is to compute or approximate the posterior distribution of X_t given the history $\mathscr{Z}_t := \sigma(Z_s : 0 \leq s \leq t)$. The posterior $p_t^* := (p^*(1,t), p^*(2,t), \ldots, p^*(d,t))^T$ is defined as,

$$p^*(l,t) = \mathsf{P}\{X_t = e_l \mid \mathscr{Z}_t\}, \quad l = 1, \ldots, d. \tag{5.1}$$

*This chapter is an extension of the published paper [159].

Its evolution is described by the Wonham filter [148] (see (5.7)).

The objective of this chapter is to introduce a particle approximation of the Wonham filter. As in other particle filtering techniques, the approximate filter is based on the construction of N stochastic processes $\{X_t^i : 1 \le i \le N\}$ [7, 55, 74]. The value $X_t^i \in \mathbb{S}$ is interpreted as the state for the i^{th} particle at time t, and the empirical distribution is used to approximate the conditional distribution. Recall that this is defined as,

$$p^N(l,t) = \frac{1}{N}\sum_{i=1}^{N} \mathbb{1}\{X_t^i = e_l\}. \tag{5.2}$$

The construction is as follows: The model for the i^{th} particle is defined by a controlled system,

$$\mathrm{d}X_t^i = \sum_{(l,l')\in E} A^{ll'} X_t^i \,\mathrm{d}N_t^{ll',i} + \underbrace{\sum_{k=1}^{d} B^k X_t^i \,\mathrm{d}\mathscr{C}_t^{k,i}}_{\text{Control}},$$

where B^k is a $d \times d$ matrix whose only non-zero entires are,

$$\begin{aligned} B^k_{ll} &= -1 \qquad \text{for } l \ne k, \\ B^k_{kl} &= 1 \qquad \text{for } l \ne k \end{aligned} \tag{5.3}$$

and $\mathscr{C}_t^{k,i}$ denotes the state of a time-modulated Poisson counter of the following form: There is an input process $\{U_t^k\}$ and a family of mutually independent Poisson processes $\{\tilde{N}^{k,i}(\cdot)\}$ with constant rate $\lambda = 1$, also independent of Z_t and $\{N_t^{ll',i}\}$, such that

$$\mathscr{C}_t^{k,i} = \tilde{N}^{k,i}(U_t^k), \qquad t \ge 0.$$

The posterior distribution of X_t^i given the history $\mathscr{Z}$ is denoted $p_t := (p(1,t), p(2,t), \ldots, p(d,t))^T$, where

$$p(l,t) = \mathsf{P}\{X_t^i = e_l \mid \mathscr{Z}_t\}, \quad l = 1, \ldots, d. \tag{5.4}$$

The construction of the particle filter is reduced to a control problem: *Choose the control input U_t^k so that p_t is equal to p_t^*, and consequently p_t^N (defined in (5.2)) approximates p_t^* for large N.* The main result of this chapter is the solution of this control problem.

The solution is described as the stochastic differential equation driven by the observations and the particle evolution,

$$\mathrm{d}U_t^k = \mathsf{K}(k,t)(\mathrm{d}Z_t - \hat{h}_t \,\mathrm{d}t),$$

where $\hat{h}_t := \mathsf{E}[h(X_t^i)|\mathscr{Z}_t] = \sum_{l=1}^d h^l p(l,t)$ and $h^l := h(e_l)$. In a numerical implementation, we approximate

$$\hat{h}_t \approx \hat{h}_t^N = \frac{1}{N}\sum_{i=1}^N h(X_t^i)\,.$$

The gain vector, $\mathsf{K}_t := (\mathsf{K}(1,t),\mathsf{K}(2,t),\ldots,\mathsf{K}(d,t))^T$, is the solution of the following linear matrix problem,

$$(p_t \otimes 1 - I)\,\mathsf{K}_t = -(H_t - \hat{h}I)p_t,$$

where $1 := (1,1,\ldots,1)$, I is the $d\times d$ identity matrix, and $H_t := \mathrm{diag}(h^1,\ldots,h^d)$.

The outline of the remainder of this chapter is as follows. The particle filter is introduced in Sec. 5.2, and shown to be consistent with the Wonham filter. An algorithm to simulate the filter is discussed in Sec. 5.3, and illustrated with a numerical example in Sec. 5.4.

5.2 Feedback Particle Filter for Markov Chains

The model for the particle filter is given by the stochastic differential equation,

$$\mathrm{d}X_t^i = \sum_{(l,l')\in E} A^{ll'}X_t^i\,\mathrm{d}N_t^{ll',i} + \underbrace{\sum_{k=1}^d B^k X_t^i\,\mathrm{d}\mathscr{C}_t^{k,i}}_{\text{Control}}, \tag{5.5}$$

where $X_t^i \in \mathbb{S}$ is the state for the i^{th} particle at time t, and $N_t^{ll',i}$ are mutually independent Poisson counters with rates $\lambda_{l'l}$. We assume the initial conditions $\{X_0^i\}_{i=1}^N$ are i.i.d., independent of $N_t^{ll',i}$, and drawn from the initial distribution $p^*(x,0)$ of X_0. Both $N_t^{ll',i}$ and $\{X_0^i\}$ are also assumed to be independent of X_t, Z_t. The matrices $A^{ll'} := (e_{l'} - e_l)\otimes e_l$ and B^k are the $d\times d$ matrices, as defined in Sec. 5.1 (see (5.3)).

For each particle, we introduce d-mutually independent time-modulated Poisson counters, denoted $\{\mathscr{C}_t^{k,i}\}_{k=1}^d$. The k^{th}-counter jumps at times $\{T_1^{k,i}, T_2^{k,i},\ldots,T_j^{k,i},T_{j+1}^{k,i},\ldots,\}$. The time between successive jumps, $T_{j+1}^{k,i} - T_j^{k,i}$, is random. Its law is defined by introducing a time-change process,

$$U_t^k = \int_0^t (\mathsf{K}(k,s)\,\mathrm{d}Z_s + u(k,s)\,\mathrm{d}s)\,. \tag{5.6}$$

In terms of this process, $U_{T_{j+1}^{k,i}} - U_{T_j^{k,i}} \sim \exp(1)$. Introducing a family of mutually independent Poisson processes $\{\tilde{N}^{k,i}(\cdot)\}$ with constant rate $\lambda = 1$, we have that:

$$\mathscr{C}_t^{k,i} = \tilde{N}^{k,i}(U_t^k), \quad t \geq 0.$$

We impose admissibility requirements on the control input U_t^k in (5.6):

Definition 4 (Admissible Input) *The control input* $\{U_t^k\}_{k=1}^d$ *is* admissible *if the random variables*

$$u_t = (u(1,t), u(2,t), \dots, u(d,t))^T,$$
$$\mathsf{K}_t = (\mathsf{K}(1,t), \mathsf{K}(2,t), \dots, \mathsf{K}(d,t))^T$$

are $\mathscr{Z}_t$ *measurable for each* t*. Moreover, at each* t*,*

(i) U_t^k *is non-decreasing with probability one, and*

(ii) $\mathsf{E}[\|u_t\| + \|\mathsf{K}_t\|] < \infty$*, where* $\|u_t\|^2 = |u(1,t)|^2 + \cdots + |u(d,t)|^2$ *and* $\|\mathsf{K}_t\|^2 = |\mathsf{K}(1,t)|^2 + \cdots + |\mathsf{K}(d,t)|^2$.

The filtering problem is to define the control input in terms of $\{u_t, \mathsf{K}_t\}$. We say that these functions are *optimal* if $p_t \equiv p_t^*$, where recall

(i) p_t is the posterior distribution of X_t^i given $\mathscr{Z}_t$ as defined in (5.4).

(ii) p_t^* is the posterior distribution of X_t given $\mathscr{Z}_t$ as defined in (5.1).

Given $p^*(\cdot,0) = p(\cdot,0)$, our goal is to choose $\{u_t, \mathsf{K}_t\}$ in the feedback particle filter so that the evolution equations of these conditional distributions coincide.

The evolution of p_t^* is described by the Wonham filter:

$$\mathrm{d}p_t^* = \Lambda p_t^* \,\mathrm{d}t + (H_t - \hat{h}I)(\mathrm{d}Z_t - \hat{h}\,\mathrm{d}t)p_t^*. \tag{5.7}$$

where $H_t := \mathrm{diag}(h^1, \dots, h^d)$ and I denotes the identity matrix.

The evolution equation of p_t is described next. The proof appears in App. D.1.

Proposition 5.2.1 *Consider the process* X_t^i *that evolves according to the particle filter model* (5.5)*. The conditional distribution of* X_t^i *given the filtration* $\mathscr{Z}_t$*,* p_t*, satisfies the forward equation*

$$\mathrm{d}p_t = \Lambda p_t \,\mathrm{d}t + (I - p_t \otimes 1)(\mathsf{K}_t \,\mathrm{d}Z_t + u_t \,\mathrm{d}t). \tag{5.8}$$

5.2.1 Consistency with the Nonlinear Filter

The main result of this section is the construction of an optimal pair $\{u, \mathsf{K}\}$.

The filter is obtained by comparing (5.7) with (5.8): the vector $\mathsf{K}_t = (\mathsf{K}(1,t), \mathsf{K}(2,t), \ldots, \mathsf{K}(d,t))^T$ is a solution of

$$(p_t \otimes 1 - I)\,\mathsf{K}_t = -(H_t - \hat{h}_t I)p_t, \tag{5.9}$$

and

$$u(k,t) = -\mathsf{K}(k,t)\hat{h}_t.$$

With this choice of $\{u, \mathsf{K}\}$, the control input is given by

$$U_t^k = \int_0^t \mathsf{K}(k,s)(\mathrm{d}Z_s - \hat{h}_s\,\mathrm{d}s). \tag{5.10}$$

The consideration of admissibility requires analysis of solutions of (5.9), described in the following proposition — Its proof is given in App. D.2.

Proposition 5.2.2 *Consider the problem* (5.9)*. Its general solution is given by,*

$$\mathsf{K}_t = H_t p_t + c p_t, \tag{5.11}$$

where c is an arbitrary constant. The minimal 2*-norm solution is given by,*

$$\mathsf{K}_t^0 = H_t p_t + c^0 p_t,$$

where $c^0 = -\langle H_t p_t, p_t\rangle / \|p_t\|^2$, $\langle\cdot,\cdot\rangle$ denotes the standard inner product in $\mathbb{R}^d$ and $\|p_t\|^2 = \langle p_t, p_t\rangle$.

For any solution $\mathsf{K}_t = (\mathsf{K}(1,t), \ldots, \mathsf{K}(d,t))^T$, the following property holds:

$$\textit{If } p(k,t) = 0 \textit{ then } \mathsf{K}(k,t) = 0. \tag{P0}$$

Since $\langle \mathsf{K}_t^0, p_t\rangle = 0$, necessarily, entires of K_t^0 can not all have one sign. This means that the control input U_t^k defined using $\mathsf{K}_t = \mathsf{K}_t^0$ (see (5.10)) is not admissible. In order to obtain an admissible input, we use (5.11) to define two particular solutions of (5.9):

$$\mathsf{K}_t^1 = \mathsf{K}_t^0 + c_t^1 p_t, \tag{5.12a}$$

$$\mathsf{K}_t^2 = \mathsf{K}_t^0 + c_t^2 p_t, \tag{5.12b}$$

where

(i) c_t^1 is chosen so $\mathsf{K}^1(k,t) \geq 0$ for all $k = 1,\ldots,d$ and $\min_k \mathsf{K}^1(k,t) = 0$.

(ii) c_t^2 is chosen so $\mathsf{K}^2(k,t) \leq 0$ for all $k = 1,\ldots,d$ and $\max_k \mathsf{K}^2(k,t) = 0$.

The constants c_t^1, c_t^2 exist because of property (P0).

Using solutions (5.12a)-(5.12b) we define an index vector I_s, taking values in $\{1,2\}$, such that

$$U_t^k = \int_0^t \mathsf{K}^{I_s}(k,s)(\mathrm{d}Z_s - \hat{h}_s \mathrm{d}s) \tag{5.13}$$

is a non-decreasing function of time. The control input defined using (5.13) is admissible by construction – the instantaneous rate of the slowest counter is zero, and the rates of the remaining counters is non-negative. Moreover, the gain function has minimal 2-norm at each time.

The following theorem shows that the two evolution equations (5.7) and (5.8) are identical. The proof is straightforward by direct comparison and thus omitted.

Theorem 5.2.3 *Consider the two evolution equations for p_t and p_t^*, defined according to the solution of the forward equation (5.8) and the Wonham filter (5.7), respectively. Suppose that the control input is obtained according to (5.13). Then, provided $p(\cdot,0) = p^*(\cdot,0)$, we have for all $t \geq 0$,*

$$p(\cdot,t) = p^*(\cdot,t).$$

5.3 Algorithm

In this section, we summarize a practical algorithm for simulating the proposed particle filter. We begin by describing an algorithm for simulating Poisson counters with time-dependent rate.

5.3.1 Poisson Counter with Time-Dependent Rate

In order to implement the particle filter (5.5), we need to sample Poisson counter with time-dependent rates.

Consider a Poisson counter $\mathscr{C}_t$ where the counter jumps at times $\{T_1, T_2, \ldots, T_j, T_{j+1}, \ldots\}$. The time between successive jumps, $T_{j+1} - T_j$, is random and its law is governed by a time-change process:

$$U_t = \int_0^t \mathrm{d}\lambda_s, \tag{5.14}$$

where λ_t is a given time-dependent rate. In term of this process, $U_{T_{j+1}} - U_{T_j} \sim \exp(1)$.

An algorithm to obtain a sample path of $\mathscr{C}_t$ is summarized in Algo. 4. The algorithm is based on Euler discretization of (5.14), and assumes that one can sample from $\exp(1)$.

Algorithm 4 Generate Poisson Counter $\mathscr{C}_t$ with Rate λ_t

INITIALIZATION
$\mathscr{C}_0 = 0$
$T = 0$
$T_{jump} \sim \exp(1)$
ITERATION [t to $t+\Delta t$]
$T = T + \Delta\lambda_t$
if $T > T_{jump}$ **then**
    $\Delta\mathscr{C}_t = 1$
    $T = 0$
    $T_{jump} \sim \exp(1)$
else
    $\Delta\mathscr{C}_t = 0$
end if
$\mathscr{C}_{t+\Delta t} = \mathscr{C}_t + \Delta\mathscr{C}_t$
$t = t + \Delta t$

5.3.2 Implementation of Particle Filter

For simulating the particle filter (5.5), we use an Euler-discretization method. The resulting discrete-time algorithm appears in Algo. 5. At each time step, the algorithm requires computation of the gain function.

5.3.3 Synthesis of Gain Function

In order to solve for the gain function K_t, we need to obtain constants c_t^1, c_t^2 as defined in (5.12a)-(5.12b). These are obtained as solutions of the following two linear programming problems:

$$\min_{c_t^1} \; c_t^1 \quad \text{s.t.: } \mathsf{K}^0(l,t) + c_t^1 p(l,t) \geq 0,\; l = 1,\ldots,d \tag{5.15}$$

$$\max_{c_t^2} \; c_t^2 \quad \text{s.t.: } \mathsf{K}^0(l,t) + c_t^2 p(l,t) \leq 0,\; l = 1,\ldots,d \tag{5.16}$$

Numerous ready-to-use LP algorithms can be applied directly, such as *linprog* in MATLAB. The resulting algorithm for computing the gain function appears in Algo. 6.

5.4 Numerics

In this section, the numerical algorithms are used to simulate the particle filter for a 2-state and a 4-state Markov chain examples.

Algorithm 5 FPF for Continuous-Time Markov chain

INITIALIZATION
for $i = 1$ to N **do**
  Sample X_0^i from $p^*(\cdot, 0)$.
  for $l = 1$ to d **do**
    $T^{i,l} = 0$
    $T^{i,l}_{jump} \sim \exp(1)$
  end for
end for
for $l = 1$ to d **do**
  $p^N(l,0) = \frac{1}{N}\sum_{i=1}^N \mathbb{1}_{e_l}(X_0^i)$
end for

ITERATION [t to $t+\Delta t$]
Calculate $\hat{h}_t^N = \frac{1}{N}\sum_{i=1}^N h(X_t^i)$.
Synthesize the gain function K_t using Algo 6.
for $i = 1$ to N **do**
  $\Delta X_t^i = 0$
  for l, l' in E **do**
    Calculate the Poisson counter increment $\Delta N_t^{ll',i}$ using Algo. 4 with $\Delta\lambda_t = \lambda_{l'l}\Delta t$.
    $\Delta X_t^i = \Delta X_t^i + A^{ll'} X_t^i \Delta N_t^{ll',i}$
  end for
  for $k = 1$ to d **do**
    Calculate $\lambda_t^k = \mathsf{K}(k,t)\left(\frac{\Delta Z_t}{\Delta t} - \hat{h}_t^N\right)$
    Calculate the Poisson counter increment $\Delta\mathscr{C}_t^{k,i}$ using Algo. 4 with $\Delta\lambda_t = \Delta Z_t - \hat{h}_t^N \Delta t$.
    $\Delta X_t^i = \Delta X_t^i + B^k X_t^i \Delta\mathscr{C}_t^{k,i}$.
  end for
  $X_{t+\Delta t}^i = X_t^i + \Delta X_t^i$.
end for
$t = t + \Delta t$
for $l = 1$ to d **do**
  $p^N(l,t) = \frac{1}{N}\sum_{i=1}^N \mathbb{1}_{e_l}(X_t^i)$
end for

Algorithm 6 Synthesis of the Gain Function

ITERATION [t to $t+\Delta t$]
$\mathsf{K}_t^* = h_t p_t$.
$\mathsf{K}_t^0 = \mathsf{K}_t^* - \frac{\langle \mathsf{K}_t^*, p_t\rangle p_t}{\langle p_t, p_t\rangle}$.
if $\lambda_t \geq 0$ **then**
  Solve LP (5.15) for c_t^{1*}.
  $\mathsf{K}_t = \mathsf{K}_t^0 + c_t^{1*} p_t$.
else
  Solve LP (5.16) for c_t^{2*}.
  $\mathsf{K}_t = \mathsf{K}_t^0 + c_t^{2*} p_t$.
end if

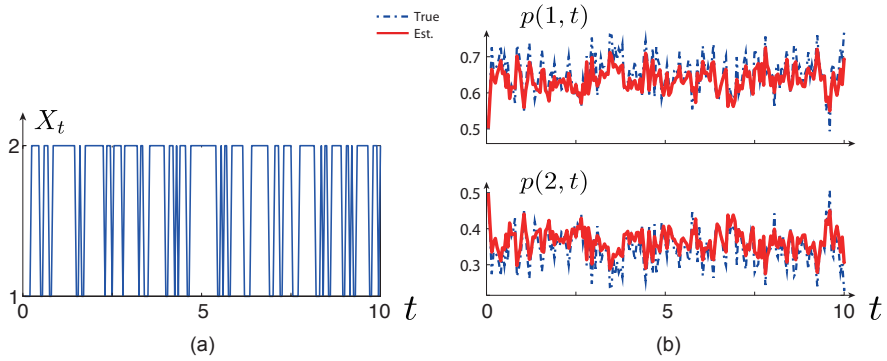

Figure 5.1: Simulation results for Example 1: (a) Sample path X_t; (b) Comparison of $p(\cdot,t)$ obtained using the FPF (Est) and the Wonham filter (True).

5.4.1 Example 1: Markov Chain with Two States

Consider a continuous-time Markov chain with two states: $X_t \in \mathbb{S} = \{e_1, e_2\}$. The signal and observation models are given by:

$$\mathrm{d}X_t = A^{12} X_t \, \mathrm{d}N_t^{12} + A^{21} X_t \, \mathrm{d}N_t^{21},$$

$$\mathrm{d}Z_t = h(X_t)\,\mathrm{d}t + \sigma_W \, \mathrm{d}W_t,$$

where $\{W_t\}$ is a standard Wiener process, and parameters:

$$A^{12} = \begin{bmatrix} 0 & 1 \\ 0 & -1 \end{bmatrix}, \quad A^{21} = \begin{bmatrix} -1 & 0 \\ 1 & 0 \end{bmatrix},$$

$$h(e_l) = l, \quad l = 1, 2.$$

and $\sigma_W = 0.5$.

The transition rate matrix for the Markov chain is:

$$\Lambda = \begin{bmatrix} -5 & 10 \\ 5 & -10 \end{bmatrix},$$

that is N_t^{12} is a Poisson counter with rate $\lambda_{21} = 10$ and N_t^{21} is a Poisson counter with rate $\lambda_{12} = 5$.

In the simulation results described next, $N = 1000$ particles are used with their initial condition X_0^i drawn from a uniform distribution on $\mathbb{S}$. The total simulation time is $T = 10$ with time step $\Delta t = 0.05$.

Fig. 5.1 depicts the result of a single simulation: The state X_t jumps randomly between the two states as depicted

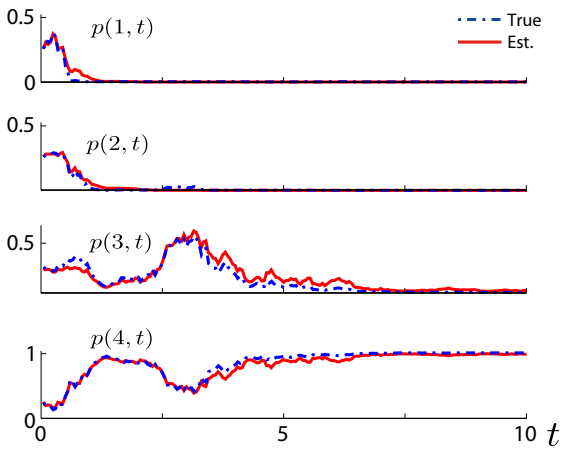

Figure 5.2: Simulation results for Example 2: Comparison of $p(\cdot,t)$ obtained using the feedback particle filter (Est) and the Wonham filter (True).

in Fig. 5.1(a). The distribution obtained using Wonham filter (depicted as dot-dashed line) is compared with the distribution estimated by the feedback particle filter (depicted as solid line) in Fig. 5.1(b).

5.4.2 Example 2: Markov Chain with Four States

Consider a Markov chain with four states: $X_t \in \mathbb{S} = \{e_1, e_2, e_3, e_4\}$ with dynamics,

$$\mathrm{d}X_t = 0.$$

The observation model is as before, where now

$$h(e_l) = l, \quad l = 1,2,3,4,$$

and $\sigma_W = 1$. The initial condition $X_0 = e_4$.

In the simulation results described next, $N = 1000$ particles are used with their initial condition X_0^i drawn from a uniform distribution on $\mathbb{S}$. The total simulation time is $T = 10$ with time step $\Delta t = 0.05$.

Fig. 5.2 depicts the result of a single simulation: The distribution obtained by Wonham filter (depicted as dot-dashed line) is compared to the distribution estimated by the feedback particle filter (depicted as solid line) in Fig. 5.2. After a rapid transient, the particle filter converges to the true state $X_t = e_4$ which is consistent with the calculation using Wonham filter.

5.5 Conclusions

In this chapter, we introduced a feedback particle filter algorithm for approximation of the Wonham filter. The control is realized using Poisson processes. The algorithm is expected to be useful in certain applications:

1. A single Poisson process serves as a reduced order model of the firing of a single neuron [33, 43]. Given the importance of the Bayesian inference paradigm in neuroscience (cf., [58, 105]), the algorithm can be used to develop specific neuromorphic implementations.

2. In problems involving estimation of maneuvering targets, continuous time Markov chains are used to model target maneuvers [10, 19]. The algorithm described here is seen as an intermediate step towards developing particle filter algorithms for such problems.

Both these applications are subject of the ongoing work.

Part II

Applications

Chapter 6

Interacting Multiple Model-Feedback Particle Filter*

6.1 Introduction

In many applications, including air and missile defense systems, remote sensing, autonomous navigation and robotics, additional model uncertainty might enter the system besides the uncertainty associated with signal and observation noise [10]. The uncertainty is typically modeled using a stochastic hybrid system (SHS) framework. Treating the model uncertainty as a discrete variable in the augmented state space, the SHS filtering problem involves the estimation of a partially observed stochastic process with both continuous-valued and discrete-valued states.

An example is to track a maneuvering target (hidden signal) with noisy radar measurements. In this case, the SHS is comprised of the continuous-valued states which represent target positions and velocities, and the discrete-valued states which represent the distinct dynamic model types (e.g., constant velocity or white noise acceleration model) of the target. The discrete signal model types are referred to as *modes*. Since the time of target maneuvers is random, there is *model uncertainty* in the sense that one can not assume, in an apriori fashion, a fixed dynamic model of the target.

Motivated in part by target tracking applications, we consider models of SHS where the continuous-valued state process is modeled using a stochastic differential equation (SDE), and the discrete-valued state process is modeled as a continuous-time Markov chain. The estimation objective is to estimate (filter) the hidden states (both continuous- and discrete-valued state) given noisy observations.

Given the number of applications, algorithms for SHS filtering problems have been extensively studied in the past; cf., [10, 112] and references therein. A typical SHS filtering algorithm is comprised of three parts:

(i) A *filtering* algorithm to estimate the continuous-valued state given the mode,

(ii) An *association* algorithm to associate modes to signal dynamics,

(iii) A *merging process* to combine the results of i) and ii).

Prior to mid-1990s, the primary tool for filtering was a Kalman filter or one of its extensions, e.g., extended

*This chapter is an extension of the published paper [151].

Kalman filter. The limitations of these tools in applications arise on account of nonlinearities, not only in dynamic motion of targets (e.g., drag forces in ballistic targets) but also in the measurement models (e.g., range or bearing). The nonlinearities can lead to a non-Gaussian multimodal conditional distribution. For such cases, Kalman and extended Kalman filters are known to perform poorly; cf., [132]. Since the advent and wide-spread use of particle filters [55], such filters are becoming increasingly relevant to SHS estimation for target tracking applications; cf., [132] and references therein.

The other part is the mode association algorithm. The purpose of the mode association algorithm is to determine the conditional probability for the discrete modes.

In a discrete-time setting, the exact solution to problems (i)-(iii) is given by a Multiple Model (MM) filter which has an (exponentially with time) increasing number of filters, one for each possible mode history. Practically, however, the number of filters has to be limited, which leads to the classical Generalised Pseudo-Bayes estimators of the first and second order (GPB1 and GPB2) and the Interacting Multiple Model (IMM) filter [10]. For some SHS examples, however, it was already shown in [21] that these low-dimensional filters do not always perform well. This has led to the development of two types of particle filters for SHS:

(i) The first approach is to apply the standard particle filtering approach to the joint continuous-valued state and discrete-valued mode process [113], [119].

(ii) The second approach is to exploit Rao-Blackwellization, in the sense of applying particle filtering for the continuous-valued state, and exact filter recursions for the discrete-valued modes [59], [26], [28].

In this chapter, we consider a continuous-time filtering problem for SHS and develop a feedback control-based particle filter algorithm, where the particles represent continuous-valued state components (case (ii)). We refer to the resulting algorithm as the Interacting Multiple Model-Feedback Particle Filter (IMM-FPF). As the name suggests, the proposed algorithm represents a generalization of the Kalman filter-based IMM algorithm to the general nonlinear filtering problem.

One remarkable conclusion is that the IMM-FPF retains the innovation error-based feedback structure even for the nonlinear problem. The interaction/merging process is also handled via a control-based approach. The innovation error-based feedback structure is expected to be useful because of the coupled nature of the filtering and the mode association problem. The theoretical results are illustrated with a numerical example.

The outline of the remainder of this chapter is as follows: The exact filtering equations appear in Sec. 6.2. The IMM-FPF is introduced in Sec. 6.3 and the numerical example is described in Sec. 6.4.

6.2 Problem Formulation and Exact Filtering Equations

In this section, we formulate the continuous-time SHS filtering problem, introduce the notation, and summarize the exact filtering equations (see [20, 108] for standard references). For pedagogical reason, we limit the considerations to scalar-valued signal and observation processes. The generalization to multivariable case is straightforward.

6.2.1 Problem Statement, Assumptions and Notation

The following notation is adopted:

(i) At time t, the signal state is denoted by $X_t \in \mathbb{R}$.

(ii) At time t, the mode random variable is denoted as θ_t, defined on a state-space comprising of the standard basis in $\mathbb{R}^M$: $\{e_1, e_2, \ldots, e_M\} =: \mathbb{S}$. It associates a specific mode to the signal: $\theta_t = e_m$ signifies that the dynamics at time t is described by the m^{th} model.

(iii) At time t, there is only one observation $Z_t \in \mathbb{R}$. The observation history (filtration) is denoted as $\mathscr{Z} := \sigma(Z_s : 0 \leq s \leq t)$.

The following models are assumed for the three stochastic processes:

(i) The evolution of the continuous-valued state X_t is described by a stochastic differential equation with discrete-valued coefficients:

$$\mathrm{d}X_t = a(X_t, \theta_t)\,\mathrm{d}t + \sigma(\theta_t)\,\mathrm{d}B_t, \tag{6.1}$$

where B_t is a standard Wiener process. We denote $a^m(x) := a(x, e_m)$ and $\sigma^m := \sigma(e_m)$.

(ii) The discrete-valued state (mode) θ_t evolves as a Markov chain in continuous-time:

$$\mathsf{P}(\theta_{t+\delta} = e_l | \theta_t = e_m) = q_{ml}\,\delta + o(\delta), \quad m \neq l. \tag{6.2}$$

The generator for this jump process is denoted by a stochastic matrix Q whose ml^{th} entry is q_{ml} for $m \neq l$. The initial distribution is assumed to be given.

(iii) At time t, the observation model is given by,

$$\mathrm{d}Z_t = h(X_t, \theta_t)\,\mathrm{d}t + \mathrm{d}W_t, \tag{6.3}$$

where W_t is a standard Wiener process assumed to be independent of $\{B_t\}$. We denote $h^m(x) := h(x, e_m)$.

The filtering problem is to obtain the posterior distribution of X_t given $\mathscr{Z}$.

6.2.2 Exact Filtering Equations

The following distributions are of interest:

(i) $q_m^*(x,t)$ defines the joint conditional distribution of $(X_t,\theta_t)^T$ given $\mathscr{Z}_t$, i.e.,

$$\int_{x\in A} q_m^*(x,t)\,\mathrm{d}x = \mathsf{P}\{[X_t\in A,\theta_t=e_m]|\mathscr{Z}\},$$

for $A\in\mathscr{B}(\mathbb{R})$ and $m\in\{1,\dots,M\}$. We denote $q^*(x,t) := (q_1^*(x,t),q_2^*(x,t),\dots,q_M^*(x,t))^T$, interpreted as a column vector.

(ii) $p^*(x,t)$ defines the conditional dist. of X_t given $\mathscr{Z}$:

$$\int_{x\in A} p^*(x,t)\,\mathrm{d}x = \mathsf{P}\{X_t\in A|\mathscr{Z}\},\quad A\in\mathscr{B}(\mathbb{R}).$$

By definition, we have $p^*(x,t)=\sum_{m=1}^M q_m^*(x,t)$.

(iii) $\mu_t := (\mu_t^1,\dots,\mu_t^M)^T$ defines the probability mass function of θ_t given $\mathscr{Z}$ where:

$$\mu_t^m = \mathsf{P}\{\theta_t=e_m|\mathscr{Z}\},\quad m=1,\dots,M. \tag{6.4}$$

By definition $\mu_t^m=\int_{\mathbb{R}} q_m^*(x,t)\,\mathrm{d}x$.

(iv) $\rho_m^*(x,t)$ defines the conditional dist. of X_t given $\theta_t=e_m$ and $\mathscr{Z}$. For $\mu_t^m\neq 0$:

$$\rho_m^*(x,t) := \frac{q_m^*(x,t)}{\mu_t^m},\quad m=1,\dots,M, \tag{6.5}$$

Denote $\rho^*(x,t)=(\rho_1^*(x,t),\dots,\rho_M^*(x,t))^T$.

We introduce two more notations before presenting the exact filtering equations for these density functions:

(i) $\hat{h}_t := \mathsf{E}[h(X_t,\theta_t)|\mathscr{Z}] = \sum_{m=1}^M \int_{\mathbb{R}} h^m(x) q_m^*(x,t)\,\mathrm{d}x$;

(ii) $\widehat{h_t^m} := \mathsf{E}[h(X_t,\theta_t)|\theta_t=e_m,\mathscr{Z}] = \int_{\mathbb{R}} h^m(x)\rho_m^*(x,t)\,\mathrm{d}x$.

Note that $\hat{h}_t=\sum_{m=1}^M \mu_t^m\widehat{h_t^m}$.

The following theorem describes the evolution of above-mentioned density functions. A short proof is included in App. E.1.

Theorem 6.2.1 (See also Theorem 1 in [20]) *Consider the hybrid system* (6.1) - (6.3)*:*

(i) *The joint conditional distribution of* $(X_t, \theta_t)^T$ *satisfies:*

$$\mathrm{d}q^* = \mathscr{L}^\dagger(q^*)\,\mathrm{d}t + Q^T q^*\,\mathrm{d}t + (H_t - \hat{h}_t I)(\,\mathrm{d}Z_t - \hat{h}_t\,\mathrm{d}t)q^*, \tag{6.6}$$

where $\mathscr{L}^\dagger = diag\{\mathscr{L}_m^\dagger\}$, $H_t = diag\{h^m\}$, I *is an* $M \times M$ *identity matrix and*

$$\mathscr{L}_m^\dagger q_m^* := -\frac{\partial}{\partial x}(a^m q_m^*) + \frac{1}{2}(\sigma^m)^2 \frac{\partial^2}{\partial x^2} q_m^*.$$

(ii) *The conditional distribution of* θ_t *satisfies:*

$$\mathrm{d}\mu_t = Q^T \mu_t\,\mathrm{d}t + (\widehat{H}_t - \hat{h}_t I)(\,\mathrm{d}Z_t - \hat{h}_t\,\mathrm{d}t)\mu_t, \tag{6.7}$$

where $\widehat{H}_t = diag\{\widehat{h_t^m}\}$.

(iii) *The conditional distribution of* X_t *satisfies:*

$$\mathrm{d}p^* = \sum_{m=1}^{M} \mathscr{L}_m^\dagger(q_m^*)\,\mathrm{d}t + \sum_{m=1}^{M} (h^m - \hat{h}_t)(\,\mathrm{d}Z_t - \hat{h}_t\,\mathrm{d}t)q_m^*. \tag{6.8}$$

(iv) *The conditional distribution of* X_t *given* $\theta_t = e_m$ *satisfies:*

$$\mathrm{d}\rho_m^* = \mathscr{L}_m^\dagger \rho_m^*\,\mathrm{d}t + \frac{1}{\mu_t^m}\sum_{l=1}^{M} q_{lm}\mu_t^l(\rho_l^* - \rho_m^*)\,\mathrm{d}t + (h^m - \widehat{h_t^m})(\,\mathrm{d}Z_t - \widehat{h_t^m}\,\mathrm{d}t)\rho_m^*, \quad m = 1,\ldots,M \tag{6.9}$$

6.3 IMM-Feedback Particle Filter

The IMM-FPF is comprised of M parallel feedback particle filters: The model for the m^{th} particle filter is,

$$\mathrm{d}X_t^{i;m} = a^m(X_t^{i;m})\,\mathrm{d}t + \sigma^m\,\mathrm{d}B_t^{i;m} + \mathrm{d}U_t^{i;m}, \tag{6.10}$$

where $X_t^{i;m} \in \mathbb{R}$ is the state for the i^{th} particle at time t, $U_t^{i;m}$ is its control input, $\{B_t^{i;m}\}_{i=1}^N$ are mutually independent standard Wiener processes and N denotes the number of particles. We assume that the initial conditions $\{X_0^{i;m}\}_{i=1}^N$ are i.i.d., independent of $\{B_t^{i;m}\}$, and drawn from the initial distribution $\rho_m^*(x,0)$ of X_0. Both $\{B_t^{i;m}\}$ and $\{X_0^{i;m}\}$ are assumed to be independent of both X_t and Z_t. Certain additional assumptions are made regarding admissible forms of control input (see [154]).

Remark 7 *The motivation for choosing the parallel structure comes from the conventional IMM filter, which is com-*

prised of M parallel Kalman filters, one for each maneuvering mode $m \in \{1,\dots,M\}$. □

There are two types of conditional distributions of interest in our analysis:

(i) $\rho_m^*(x,t)$: Defines the conditional dist. of X_t given $\theta_t = e_m$ and $\mathscr{Z}$, see (6.5).

(ii) $\rho_m(x,t)$: Defines the conditional dist. of $X_t^{i;m}$ given $\mathscr{Z}$:

$$\int_{x\in A} \rho_m(x,t)\,\mathrm{d}x = \mathsf{P}\{X_t^{i;m} \in A | \mathscr{Z}\}, \quad \forall A \in \mathscr{B}(\mathbb{R}).$$

The control problem is to choose the control inputs $\{U_t^{i;m}\}_{m=1}^M$ so that, ρ_m approximates ρ_m^* for each $m = 1,\dots,M$. Consequently the empirical distribution of the particles approximates ρ_m^* for large number of particles [153].

The main result of this section is to describe an explicit formula for the optimal control input, and demonstrate that under general conditions we obtain an exact match: $\rho_m = \rho_m^*$, under optimal control. The optimally controlled dynamics of the i^{th} particle in the m^{th} FPF have the following Stratonovich form,

$$\mathrm{d}X_t^{i;m} = a^m(X_t^{i;m})\,\mathrm{d}t + \sigma^m\,\mathrm{d}B_t^{i;m} + \mathsf{K}^m(X_t^{i;m},t) \circ \mathrm{d}I_t^{i;m} + u^m(X_t^{i;m}, X_t^{i;-m}, t)\,\mathrm{d}t, \tag{6.11}$$

where $X_t^{i;-m} = \{X_t^{i;l}\}_{l\neq m}$ and $I_t^{i;m}$ is the modified form of *innovation process*,

$$\mathrm{d}I_t^{i;m} := \mathrm{d}Z_t - \frac{1}{2}\left[h^m(X_t^{i;m}) + \widehat{h_t^m}\right]\mathrm{d}t, \tag{6.12}$$

where $\widehat{h_t^m} := \int_{\mathbb{R}} h^m(x)\rho_m(x,t)\,\mathrm{d}x$. The gain function K^m is obtained as a solution of an Euler-Lagrange boundary value problem (E-L BVP):

$$\frac{\partial(\rho_m \mathsf{K}^m)}{\partial x} = -(h^m - \widehat{h_t^m})\rho_m, \tag{6.13}$$

with boundary condition $\lim_{x\to\pm\infty} \rho_m(x,t)\mathsf{K}^m(x,t) = 0$.

The interaction between filters arises as a result of the control term u^m. It is obtained by solving the following BVP:

$$\frac{\partial(\rho_m u^m)}{\partial x} = \sum_{l=1}^M c_{lm}(\rho_m - \rho_l), \tag{6.14}$$

again with boundary condition $\lim_{x\to\pm\infty} \rho_m(x,t)u^m(x,t) = 0$ and $c_{lm} := \frac{q_{lm}\mu_t^l}{\mu_t^m}$.

Recall that the evolution of $\rho_m^*(x,t)$ is described by the modified Kushner-Stratonovich (K-S) equation (6.9). The evolution of ρ_m is given by a forward Kolmogorov operator (derived in App. E.2).

The following theorem shows that the evolution equations for ρ_m and ρ_m^* are identical. The proof appears in App. E.2.

Theorem 6.3.1 *Consider the two distributions ρ_m and ρ_m^*. Suppose that, for $m = 1, \ldots, M$, the gain function $\mathsf{K}^m(x,t)$ and the control term u^m is obtained according to (6.13) and (6.14), respectively. Then provided $\rho_m(x,0) = \rho_m^*(x,0)$, we have for all $t > 0$, $\rho_m(x,t) = \rho_m^*(x,t)$.*

In a numerical implementation, one also needs to estimate μ_t^m, which is done by using the same finite-dimensional filter, as in (6.7):

$$\mathrm{d}\mu_t^m = \sum_{l=1}^{M} q_{lm}\mu_t^l \,\mathrm{d}t + (\widehat{h_t^m} - \hat{h}_t)(\mathrm{d}Z_t - \hat{h}_t \,\mathrm{d}t)\mu_t^m, \tag{6.15}$$

where $\hat{h}_t = \sum_{m=1}^{M} \mu_t^m \widehat{h_t^m}$ and $\widehat{h_t^m} \approx \frac{1}{N}\sum_{i=1}^{N} h^m(X_t^{i;m})$ are approximated with particles.

Remark 8 *The mode association probability filter (6.15) can also be derived by considering a continuous-time limit starting from the continuous-discrete time filter that appears in the classic IMM filter literature [10]. This proof appears in App. E.3. The alternate proof is included because it shows that the filter (6.15) is in fact the continuous-time nonlinear counterpart of the algorithm that is used to obtain association probability in the classical IMM literature. The proof also suggests alternate discrete-time algorithms for evaluating association probabilities in simulations and experiments, where observations are made at discrete sampling times.*

Define $p(x,t) := \sum_{m=1}^{M} \mu_t^m \rho_m(x,t)$ where μ_t^m is defined in (6.4). The following corollary shows that $p(x,t)$ and $p^*(x,t)$ are identical. Its proof is straightforward, by using the definitions, and is thus omitted.

Corollary 6.3.1 *Consider the two distribution $p(x,t)$ and $p^*(x,t)$. Suppose conditions in Thm. 6.3.1 apply, and μ_t^m is obtained using (6.15), then provided $p(x,0) = p^*(x,0)$, we have for all $t > 0$, $p(x,t) = p^*(x,t)$.*

6.3.1 Algorithm

The main difficulty is to obtain a solution of the BVP (6.13) and (6.14) at each time step. A Galerkin algorithm for the same appears in our earlier paper [154]. One particular approximation of the solution, referred to as the *constant gain approximation* is given by:

$$\mathsf{K}^m \approx \frac{1}{N}\sum_{i=1}^{N} (h^m(X_t^{i;m}) - \widehat{h_t^m}) X_t^{i;m}, \tag{6.16}$$

$$u^m \approx \sum_{l=1}^{M} c_{lm} \frac{1}{N} \left(\sum_{i=1}^{N} X_t^{i;l} - \sum_{i=1}^{N} X_t^{i;m} \right), \tag{6.17}$$

which is constant at each given time. The justification of the constant approximation appears in our earlier paper [154].

Apart from the gain function, the algorithm requires approximation of $\hat{h}_t$ and $\widehat{h_t^m}$. These are obtained in terms of

particles as:

$$\widehat{h_t^m} \approx \frac{1}{N}\sum_{i=1}^{N} h^m(X_t^{i;m}), \qquad \hat{h}_t = \sum_{m=1}^{M} \mu_t^m \widehat{h_t^m}.$$

For simulating the IMM-FPF, we use an Euler-discretization method. The resulting discrete-time algorithm appears in Algo.7. At each time step, the algorithm requires computation of the gain function, that is obtained using (6.16)-(6.17).

Algorithm 7 IMM-FPF for SHS

INITIALIZATION
for $m = 1$ to M **do**
  $\mu_0^m = \frac{1}{M}$.
  for $i = 1$ to N **do**
    Sample $X_0^{i;m}$ from $p^*(\cdot, 0)$.
  end for
end for
ITERATION [t to $t+\Delta t$]
for $m = 1$ to M **do**
  Calculate $\widehat{h_t^m} \approx \frac{1}{N}\sum_{i=1}^{N} h^m(X_t^{i;m})$.
end for
Calculate $\hat{h}_t = \sum_{m=1}^{M} \mu_t^m \widehat{h_t^m}$.
for $m = 1$ to M **do**
  for $i = 1$ to N **do**
    Generate a sample, ΔV, from $N(0,1)$
    Calculate $\Delta I_t^{i;m} = \Delta Z_t - \frac{1}{2}\left[h^m(X_t^{i;m}) + \widehat{h_t^m}\right]\Delta t$
    Calculate the gain function K^m (e.g., by using (6.16))
    Calculate the control term u^m (e.g., by using (6.17)).
    $\Delta X_t^{i;m} = a^m(X_t^{i;m})\Delta t + \sigma^m\sqrt{\Delta t}\Delta V + \mathsf{K}^m\Delta I_t^{i;m} + u^m\Delta t$
    $X_{t+\Delta t}^{i;m} = X_t^{i;m} + \Delta X_t^{i;m}$
  end for
  $\mu_{t+\Delta t}^m = \mu_t^m + \sum_{l=1}^{M} q_{lm}\mu_t^l \Delta t + (\widehat{h_t^m} - \hat{h}_t)(\Delta Z_t - \hat{h}_t\Delta t)\mu_t^m$.
end for
$t = t + \Delta t$
$\hat{X}_t := \mathsf{E}[X_t|\mathscr{Z}] \approx \frac{1}{N}\sum_{m=1}^{M}\sum_{i=1}^{N} \mu_t^m X_t^{i;m}$.

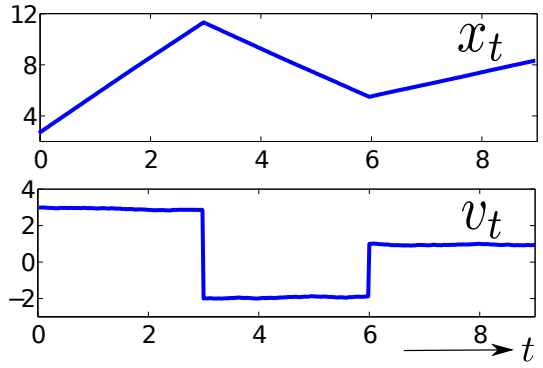

Figure 6.1: Simulation results for a single trial (from top to bottom): (a) Sample position path x_t; (b) Sample velocity path v_t.

6.4 Numerics

6.4.1 Maneuvering Target Tracking with Bearing Measurements

We consider a tracking problem where the target dynamics evolve according to a white noise acceleration model:

$$\mathrm{d}X_t = \begin{bmatrix} 0 & 1 \\ 0 & 0 \end{bmatrix} X_t \,\mathrm{d}t + \sigma_B \,\mathrm{d}B_t, \tag{6.18}$$

$$\mathrm{d}Z_t = h(X_t)\,\mathrm{d}t + \sigma_W \,\mathrm{d}W_t, \tag{6.19}$$

where $X_t = (x_t, v_t)$ denotes the state vector comprising of position and velocity coordinates at time t, Z_t is the observation process, and $\{B_t\}, \{W_t\}$ are mutually independent standard Wiener processes. We consider a bearing-only measurement:

$$h(x,v) = \arctan\left(\frac{x}{L}\right), \tag{6.20}$$

where L is a constant.

In the target trajectory simulation, the following parameter values are used: $\sigma_B = [0, 0.05]$, $\sigma_W = 0.015$, $L = 10$ and initial condition $X_0 = (x_0, v_0) = (2.5, 3)$. The total simulation time is $T = 9$ and the time step for numerical discretization is $\Delta t = 0.02$. At $T_1 = 3$ and $T_2 = 6$, the target instantaneously changes its velocity to $v = -2$ and $v = 1$ respectively. The resulting trajectory is depicted in Fig. 6.1. At each discrete time step, a bearing measurement is obtained according to (6.20). The target is maneuvering in the sense that its velocity switches between three different values $\{3, -2, 1\}$.

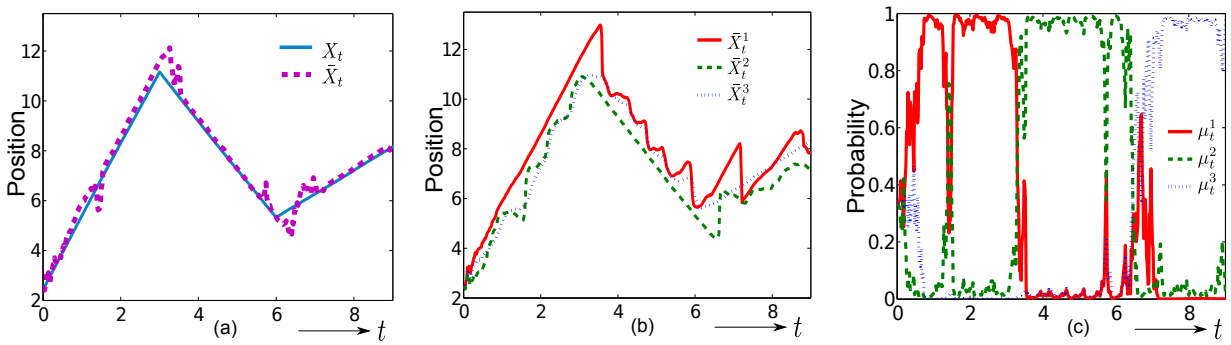

Figure 6.2: Maneuvering target tracking using IMM-FPF: (a) Comparison of IMM-FPF estimated mean $\bar{X}_t$ with target trajectory X_t. (b) Plot of mean trajectories of individual modes. (c) Plot of mode association probability.

6.4.2 Tracking using IMM-FPF

We assume an interacting multiple model architecture as follows:

(i) There are three possible target dynamic modes:

$$\begin{aligned}
\theta_t = 1: &\qquad dX_t = 3\ dt + \sigma_B\, dB_t,\\
\theta_t = 2: &\qquad dX_t = -2\ dt + \sigma_B\, dB_t,\\
\theta_t = 3: &\qquad dX_t = 1\ dt + \sigma_B\, dB_t.
\end{aligned}$$

(ii) θ_t evolves as a continuous-time Markov chain with transition rate matrix Q.

(iii) Observation process is the same as in (6.19)-(6.20).

In the simulation results described next, we use the following parameter values: $\sigma_B = 0.05$, $\sigma_W = 0.015$ and initial condition $X_0 = 2.5$. The total simulation time is $T = 9$ and time step $\Delta t = 0.02$. The transition rate matrix is,

$$Q = \begin{bmatrix} -0.1 & 0.1 & 0 \\ 0.05 & -0.1 & 0.05 \\ 0 & 0.1 & -0.1 \end{bmatrix}$$

The prior mode association probability $\mu_t = (\mu_t^1, \mu_t^2, \mu_t^3)$ at time $t = 0$ is assumed to be $\mu_0 = (1/3, 1/3, 1/3)$.

Fig. 6.2(a) depicts the result of a single simulation: The estimated mean trajectories, depicted as dashed lines, are obtained using the IMM-FPF algorithm described in Sec. 6.3. Fig. 6.2(b) depicts the mean trajectories of individual modes. Fig. 6.2(c) depicts the evolution of association probability $(\mu_t^1, \mu_t^2, \mu_t^3)$ during the simulation run. We see that trajectory probability converges to the correct mode during the three maneuvering periods. For the filter simulation, $N = 500$ particles are used for each mode.

6.5 Conclusions

In this chapter, we introduced a feedback particle filter-based algorithm for the filtering problem with model uncertainty. The additional uncertainty is modeled in a continuous-time SHS framework. The proposed algorithm is shown to be the nonlinear generalization of the conventional Kalman filter-based IMM algorithm. One remarkable conclusion is that the IMM-FPF solution retains the innovation error-based feedback structure even for the nonlinear non-Gaussian case. The interaction/merging process is also handled via a control-based approach. The theoretical results are illustrated with the aid of a numerical example problem from a maneuvering target tracking application.

The ongoing research concerns the following two topics:

(i) Comparison of the IMM-FPF algorithm against the basic particle filter (PF) and the IMM-PF, with respect to estimation accuracy and computational burden.

(ii) Investigation of alternate FPF-based algorithms for SHS estimation. Of particular interest is the filter architecture where particles evolve in the joint state space (analogous to case (i) in Sec. 6.1).

Chapter 7

Probabilistic Data Association-Feedback Particle Filter*

7.1 Introduction

Filtering with data association uncertainty is important to a number of applications, including, air and missile defense systems, air traffic surveillance, weather surveillance, ground mapping, geophysical surveys, remote sensing, autonomous navigation and robotics [8, 137]. One example is the problem of multiple target tracking (MTT) with radar observations. The targets can be multiple aircrafts in air defense, multiple ballistic objects in missile defense, multiple weather cells in weather surveillance, or multiple landmarks in autonomous navigation and robotics. In each of these applications, there exists data association uncertainty in the sense that one can not assign, in an apriori manner, individual observations (measurements) to individual targets.

Given the large number of applications, algorithms for filtering problems with data association uncertainty have been extensively studied in the past; cf., [8, 97, 101, 124] and references therein. A typical algorithm is comprised of two parts:

(i) A *filtering* algorithm for tracking a single target, and

(ii) A *data association* algorithm for associating observations to targets.

Various filtering algorithms have been proposed for the first part, including the classical Kalman filter-based approaches. Amongst them, recent development of particle filters are becoming increasingly relevant to single and multiple target tracking applications; cf., [5, 27–29, 73, 80, 101, 121, 132] and references therein.

The second part is the data association algorithm. The purpose of the data association algorithm is to assign observations to targets. The complications arise due to multiple non-target specific observations (due to multiple targets in the coverage area), missing observations (probability of detection less than one, e.g., due to target occlusion), false alarms (due to clutter) and apriori unknown number of targets (that require track initiation).

The earlier solutions to the data association problem considered assignments in a deterministic manner: These include the simple but non-robust "nearest neighbor" assignment algorithm and the multiple hypothesis testing (MHT)

*This chapter is an extension of the published paper [153].

algorithm, requiring exhaustive enumeration [131]. However, exhaustive enumeration leads to an NP-hard problem because number of associations increases exponentially with time.

The complexity issue led to development of probabilistic approaches: These include the probabilistic MHT or its simpler "single-scan" version, the probabilistic data association (PDA) filter for tracking a single target in clutter, or its extension, the joint PDA (JPDA) filter for tracking multiple targets [9, 97]. These algorithms require computation (or approximation) of the *observation-to-target association probability*. Certain modeling assumptions are necessary to compute these in a tractable manner.

For certain MTT applications, the JPDA filter algorithm was found to coalesce neighboring tracks for closely spaced targets [22, 66]. In order to overcome the track coalescence issue, several extensions of the basic JPDA algorithm have been developed, including the JPDA* filter [18, 22] and the set JPDA (SJPDA) filter [136]. In MTT applications involving multiple maneuvering targets in the presence of clutter, the JPDA algorithm is combined with the interacting multiple model (IMM) approach, which leads to the IMM-JPDA class of filters [23, 41]. Another extension of the JPDA filter for tracking distinctive targets appears in [82]. Even though PDA algorithms have reduced computational complexity, one limitation is that they have been developed primarily in linear settings and rely on Gaussian approximation of the posterior distribution; cf., [8].

Two classes of particle filters for MTT applications with data association uncertainty appear in the literature:

(i) The first approach involves application of the standard particle filtering approach to the joint (multiple target) state. For the joint state space, sequential importance resampling (SIR) particle filter is developed in [5, 73]. Unlike the classical (linear) PDA algorithm, the likelihood of observation needs to be calculated for each particle. This calculation represents the main computational burden. Several extensions have also been considered: For the problem of track coalescence avoidance, a decomposed particle filter is introduced in [29]. For multiple maneuvering target tracking in clutter, the joint IMM-PDA particle filter appears in [24, 25, 27], where the IMM step and the PDA step are performed jointly for all targets.

(ii) The second approach involves evaluation of association probability by using a Markov chain Monte Carlo (MCMC) algorithm, e.g., by randomly sampling from the subset where the posterior is concentrated. This avoids the computationally intensive enumeration of all possible associations. One early contribution is the multi-target particle filter (MTPF) introduced in [80]. In MTPF, samples of the association random variable are obtained iteratively from their joint posterior via the Gibbs sampler. In [121], the Markov chain Monte Carlo data association (MCMCDA) filter is introduced where the association probability is approximated by using the Metropolis-Hastings algorithm.

In applications, the sampling-based approaches may suffer from some the drawbacks of particle filtering, e.g., particle impoverishment and degeneracy, slow convergence rate (particularly for MCMC), robustness issues including

sample variance and numerical instabilities [15, 51, 56]. Moreover, the feedback structure of the Kalman filter-based PDA filter is no longer preserved.

In this chapter, we extend the feedback particle filter algorithms to problems with data association uncertainty. We refer to the resulting algorithm as the probabilistic data association-feedback particle filter (PDA-FPF). As the name suggests, the proposed algorithm represents a generalization of the Kalman filter-based PDA filter now to the general nonlinear non-Gaussian problems. Just as with the classical PDA filter, an extension to multiple target tracking case is also easily obtained. The resulting algorithm is referred to as JPDA-FPF.

One remarkable conclusion is that the PDA-FPF retains the innovation error-based feedback structure even for the nonlinear non-Gaussian problems. The innovation error-based feedback structure is expected to be useful because of the coupled nature of the filtering and the data association problems.

The theoretical results are illustrated with the aid of three numerical examples: i) tracking of a single target in the presence of clutter, ii) tracking of two targets in the presence of data association uncertainty and iii) a multiple target tracking problem involving track coalescence. Comparisons with the sequential importance resampling particle filter (SIR-PF) are also provided.

The outline of the remainder of this chapter is as follows: The PDA-FPF algorithm is described for the problem of tracking single target in the presence of clutter, in Sec. 7.2. The JPDA-FPF for multiple target tracking case follows as a straightforward extension, and is discussed in Sec. 7.3. Numerical examples appear in Sec. 7.4.

7.2 Feedback Particle Filter with Data Association Uncertainty

In this section, we describe the probabilistic data association-feedback particle filter (PDA-FPF) for the problem of tracking a single target with multiple observations. The filter for multiple targets is obtained as an extension, and described in Sec. 7.3.

7.2.1 Problem Statement, Assumptions and Notation

The following notation is adopted:

(i) At time t, the target state is denoted by $X_t \in \mathbb{R}^d$.

(ii) At time t, the observation vector $\underline{Z}_t := (Z_t^1, Z_t^2, \ldots, Z_t^M)$, where M is assumed fixed and $Z_t^m \in \mathbb{R}^s$ for $m \in \{1, \ldots, M\}$. We denote $\underline{\mathscr{Z}}_t := \sigma(\underline{Z}_\tau : \tau \leq t)$ as the history of observations.

(iii) At time t, the association random variable is denoted as $A_t \in \{0, 1, \ldots, M\}$. It is used to associate one observation to the target: $A_t = m$ signifies that the m^{th}-observation Z_t^m is associated with the target, and $A_t = 0$ means that all

observations at time t are due to clutter. It is assumed that the target can give rise to at most one detection. We set the gating and detection probability to be 1 for the ease of presentation. The history of association events is denoted as $\mathscr{A}_t = \sigma(A_\tau : \tau \leq t)$.

The following models are assumed for the three stochastic processes:

(i) The state X_t evolves according to a nonlinear stochastic differential equation (SDE) of the form:

$$\mathrm{d}X_t = a(X_t)\,\mathrm{d}t + \mathrm{d}B_t, \tag{7.1}$$

where the initial condition X_0 is drawn from a known prior distribution $p^*(x,0)$.

(ii) The association random process A_t evolves as a jump Markov process in continuous-time:

$$\mathsf{P}\{A_{t+\Delta t} = m' | A_t = m\} = q\Delta t + o(\Delta t), \quad m' \neq m, \tag{7.2}$$

where, for the ease of presentation, the transition rate is assumed to be a constant q.

(iii) The association probability is defined as the probability of the association $[A_t = m]$ conditioned on $\underline{\mathscr{Z}}_t$:

$$\beta_t^m \triangleq \mathsf{P}\{[A_t = m] | \underline{\mathscr{Z}}_t\}, \quad m = 0, 1, ..., M.$$

Since the events are mutually exclusive and exhaustive, $\sum_{m=0}^{M} \beta_t^m = 1$. The initial distribution is denoted as $\underline{\beta_0}$. It is assumed to be uniform.

(iv) A_t and X_t are assumed to be mutually independent.

(v) At time t, the observation model is given by, for $m = 1, \ldots, M$:

$$\mathrm{d}Z_t^m = 1_{[A_t = m]}\, h(X_t)\,\mathrm{d}t + \mathrm{d}W_t^m, \tag{7.3}$$

where $\{W_t^m\}_{m=1}^M$ are mutually independent standard Wiener processes and

$$1_{[A_t = m]} := \begin{cases} 1 & \text{if } A_t = m \\ 0 & \text{otherwise.} \end{cases}$$

The problem is to obtain the posterior distribution of X_t given the history of observations (filtration), which is denoted as $p^*(x,t)$.

The PDA-FPF methodology comprises of the following two parts:

(i) Evaluation of the association probability, and

(ii) Integration of the association probability into the feedback particle filter.

7.2.2 Approximating Assumption

The PDA-FPF is an *approximate algorithm* to implement the exact nonlinear filter (See App. F.1 for the exact filter). The following approximating assumption is made:

Assumption 7.2.1 *We suppress the dependency on association event history when calculating the posterior distribution of the state, i.e., for any measurable set $A \in \mathbb{R}^d$,*

$$\mathsf{P}\{X_t \in A | \mathscr{C}_t\} = \mathsf{P}\{X_t \in A | \underline{\mathscr{Z}}_t\}, \tag{7.4}$$

where $\mathscr{C}_t := \mathscr{A}_t \vee \underline{\mathscr{Z}}_t$. Recall $\underline{\mathscr{Z}}_t := \sigma(\underline{Z}_\tau : \tau \le t)$ and $\mathscr{A}_t := \sigma(A_\tau : \tau \le t)$.

Assumption. 7.2.1 is the continuous-time analog of the *basic assumption* as in the discrete-time PDAF [8]. In the PDAF, the posterior is a mixture of association-conditioned pdfs, which is approximated by a single Gaussian. For the next time step, each association-conditioned pdf is updated using the *same* prior, which is the posterior of the last time step. Assumption. 7.2.1 represents the continuous-time counterpart with the Gaussian assumption no longer required.

7.2.3 Association Probability for a Single Target

For the single-target-multiple-observation model described above, under Assumption. 7.2.1, the filter for computing association probability is derived in App. F.2. It is of the following form: For $m \in \{1,\dots,M\}$,

$$\mathrm{d}\beta_t^m = q\,[1-(M+1)\beta_t^m]\,\mathrm{d}t + \beta_t^m \hat{h}^T \left(\mathrm{d}Z_t^m - \sum_{j=1}^M \beta_t^j \,\mathrm{d}Z_t^j \right) + \beta_t^m |\hat{h}|^2 \left(\sum_{j=1}^M (\beta_t^j)^2 - \beta_t^m \right) \mathrm{d}t, \tag{7.5}$$

and for $m = 0$,

$$\mathrm{d}\beta_t^0 = q\left[1-(M+1)\beta_t^0\right]\,\mathrm{d}t - \beta_t^0 \hat{h}^T \sum_{j=1}^M \beta_t^j \,\mathrm{d}Z_t^j + \beta_t^0 |\hat{h}|^2 \sum_{j=1}^M (\beta_t^j)^2\,\mathrm{d}t, \tag{7.6}$$

where $\hat{h} = \mathsf{E}[h(X_t)|\underline{\mathscr{Z}}_t]$ and $|\hat{h}|^2 = \hat{h}^T\hat{h}$. This is approximated by using particles:

$$\hat{h} \approx \frac{1}{N}\sum_{i=1}^N h(X_t^i).$$

In practice, one may also wish to consider approaches to reduce filter complexity, e.g., by assigning gating regions for the observations; cf., Sec. 4.2.3 in [9].

Remark 9 *The association probability filter* (7.5)-(7.6) *can also be derived by considering a continuous-time limit starting from the continuous-discrete time filter in literature [9]. This proof appears in App. F.3. The alternate proof is included for the following reasons:*

(i) *The proof helps provide a comparison with the classical PDA filter. This is important because some of the modeling assumptions (e.g., modeling of association A_t via a jump Markov process), at first sight, may appear to be different from those considered in the classical literature.*

(ii) *The proof method suggests alternate discrete-time algorithms for evaluating association probability in simulations and experiments, where observations are made at discrete sampling times.*

In the following, we integrate association probability into the feedback particle filter, which is used to approximate the evolution of the posterior distribution. The algorithmic structure – evaluation of data association probability first, followed by its subsequent inclusion in the filter for approximating posterior – is motivated by the following considerations:

(i) Such an algorithmic structure mirrors the structure used in the classical PDA filtering literature [8, 9, 97].

(ii) The computation of association probability depends upon the details of the clutter model – the present chapter describes this computation for the Gaussian clutter case (see (7.5)-(7.6)). Once the association probability is computed, the filtering equation for the state process does not depend upon the details of the clutter model. It is thus presented separately, and can also be used as such.

(iii) A separate treatment is also useful while considering multiple target tracking problems. For such problems, one can extend algorithms for data association in a straightforward manner, while the algorithm for posterior remains as before. Additional details appear in Sec 7.3.

7.2.4 Probabilistic Data Association-Feedback Particle Filter

Following the feedback particle filter methodology, the model for the particle filter is given by,

$$\mathrm{d}X_t^i = a(X_t^i)\,\mathrm{d}t + \mathrm{d}B_t^i + \mathrm{d}U_t^i,$$

where $X_t^i \in \mathbb{R}^d$ is the state for the i^{th} particle at time t, U_t^i is its control input, and $\{B_t^i\}_{i=1}^N$ are mutually independent standard Wiener processes. We assume the initial conditions $\{X_0^i\}_{i=1}^N$ are i.i.d., independent of $\{B_t^i\}$, and drawn from

the initial distribution $p^*(x,0)$ of X_0. Both $\{B_t^i\}$ and $\{X_0^i\}$ are also assumed to be independent of X_t, $\underline{Z}_t$. Certain additional assumptions are made regarding admissible forms of control input (see [154]).

Recall that there are two types of conditional distributions of interest in our analysis:

(i) $p(x,t)$: Defines the conditional distribution of X_t^i given $\mathscr{Z}_t$.

(ii) $p^*(x,t)$: Defines the conditional distribution of X_t given $\mathscr{Z}_t$.

The control problem is to choose the control input U_t^i so that p approximates p^*, and consequently empirical distribution of the particles approximates p^* for large number of particles.

Under Assumption. 7.2.1, the evolution of $p^*(x,t)$ is described by a modified form of the Kushner-Stratonovich (K-S) equation:

$$\mathrm{d}p^* = \mathscr{L}^\dagger p^* \,\mathrm{d}t + \sum_{m=1}^{M} \beta_t^m (h - \hat{h})^T (\,\mathrm{d}Z_t^m - \hat{h}\,\mathrm{d}t) p^*. \tag{7.7}$$

where $\hat{h} := \mathsf{E}[h(X_t)|\mathscr{Z}_t] = \int_{\mathbb{R}^d} h(x) p^*(x,t)\,\mathrm{d}x$, and $\mathscr{L}^\dagger p^* = -\nabla\cdot(pa) + \frac{1}{2}\Delta p$. The proof appears in App. F.4.

The main result of this section is to describe an explicit formula for the optimal control input, and to demonstrate that under general conditions we obtain an exact match: $p = p^*$ under optimal control. The optimally controlled dynamics of the i^{th} particle have the following Stratonovich form,

$$\mathrm{d}X_t^i = a(X_t^i)\,\mathrm{d}t + \mathrm{d}B_t^i + \underbrace{\sum_{m=1}^{M} \beta_t^m \mathsf{K}(X_t^i,t) \circ \mathrm{d}I_t^{i,m}}_{\mathrm{d}U_t^i}, \tag{7.8}$$

where $I_t^{i,m}$ is a modified form of the *innovation process*,

$$\mathrm{d}I_t^{i,m} := \mathrm{d}Z_t^m - \left[\frac{\beta_t^m}{2} h(X_t^i) + \left(1 - \frac{\beta_t^m}{2}\right)\hat{h}\right] \mathrm{d}t, \tag{7.9}$$

where $\hat{h} := \mathsf{E}[h(X_t^i)|\mathscr{Z}_t] = \int_{\mathbb{R}^d} h(x) p(x,t)\,\mathrm{d}x$.

The gain function $\mathsf{K} = [\nabla\phi_1, \ldots, \nabla\phi_s]$ is a solution of the E-L BVP: For $j = 1, \ldots, s$,

$$\nabla\cdot(p(x,t)\nabla\phi_j(x,t)) = -(h_j(x) - \hat{h}_j) p(x,t). \tag{7.10}$$

The evolution of $p(x,t)$ is described by the forward Kolmogorov operator for (7.8): See App. F.4 for the equations.

The following theorem shows that the two evolution equations for p and p^* are identical. The proof appears in Appendix F.4.

Theorem 7.2.2 *Consider the two evolutions for p and p^*, defined according to the Kolmogorov forward equation (F.15) and modified K-S equation (7.7), respectively. Suppose that the gain function $\mathsf{K}(x,t)$ is obtained according to (7.10). Then provided $p(x,0) = p^*(x,0)$, we have for all $t \geq 0$, $p(x,t) = p^*(x,t)$.*

Example 1 *Consider the problem of tracking a target evolving according to the dynamic model (7.1), in the presence of clutter. At each time t, a single observation is obtained according to the observation model:*

$$\mathrm{d}Z_t = 1_{[A_t=1]}\, h(X_t)\,\mathrm{d}t + \mathrm{d}W_t,$$

where the association variable is denoted as $A_t \in \{0,1\}$: $A_t = 1$ signifies the event that the observation originates from the target and $A_t = 0$ means the observation is due to clutter (model of false alarm).

Let β_t denote the observation-to-target association probability at time t. The probability that the observation originates from the clutter is therefore $1-\beta_t$.

For this problem, the feedback particle filter is given by:

$$\mathrm{d}X_t^i = a(X_t^i)\,\mathrm{d}t + \mathrm{d}B_t^i + \underbrace{\beta_t\,\mathsf{K}(X_t^i,t)\circ \mathrm{d}I_t^i}_{\mathrm{d}U_t^i}, \tag{7.11}$$

where the innovation error I_t^i is given by,

$$\mathrm{d}I_t^i := \mathrm{d}Z_t - \left[\frac{\beta_t}{2}h(X_t^i) + \left(1-\frac{\beta_t}{2}\right)\hat{h}\right]\mathrm{d}t. \tag{7.12}$$

For the two extreme values of β_t, the filter reduces to the known form:

(i) *If $\beta_t = 1$, the observation is associated with the target with probability 1. In this case, the filter is the same as the original form of FPF (2.9) presented in Sec. 2.1.*

(ii) *If $\beta_t = 0$, the observation carries no information and the control input $\mathrm{d}U_t^i = 0$.*

For $\beta_t \in (0,1)$, the control is more interesting. The remarkable fact is that the innovation error-based feedback control structure is preserved. The association probability serves to modify the formula for the gain function and the innovation error:

(i) *The gain function is effectively reduced to $\beta_t\mathsf{K}(X_t^i,t)$. That is, the control gets less aggressive in the presence of possible false alarms due to clutter.*

(ii) *The innovation error is given by a more general formula* (7.12). *The optimal prediction of the* i^{th} *particle is now a weighted average of* $h(X_t^i)$ *and the population prediction* $\hat{h} \approx \frac{1}{N}\sum_{j=1}^{N} h(X_t^j)$. *Effectively, in the presence of possible false alarms, a particle gives more weight to the population in computing its innovation error.*

Table 7.1 provides a comparison of the PDA-FPF and the classical Kalman filter-based PDA filter ([8, 9]). The ODE model is adopted for the ease of presentation. The main point to note is that the feedback particle filter has an innovation error-based structure: In effect, the i^{th} particle makes a prediction $\hat{Y}_t^{i,m}$ as a weighted-average of $h(X_t^i)$ and $\hat{h}$. This is then used to compute an innovation error $I_t^{i,m}$. The Bayes' update step involves gain feedback of the innovation error.

Table 7.1: Comparison of the nonlinear PDA-FPF algorithm with the linear PDAF algorithm

	PDA filter	PDA-FPF
State model	$\dot{X}_t = AX_t + \dot{B}_t$	$\dot{X}_t = a(X_t) + \dot{B}_t$
Observation model	$Y_t = HX_t + \dot{W}_t$	$Y_t = h(X_t) + \dot{W}_t$
Assoc. Prob.	$\beta_t^m := \mathsf{P}\{[A_t = m] \mid \underline{\mathscr{Z}}^t\}$	
Prediction	$\hat{Y}_t = H\hat{X}_t$	$\hat{Y}_t^{i,m} = \frac{\beta_t^m}{2} h(X_t^i) + (1 - \frac{\beta_t^m}{2})\hat{h}$
Innovation error	$I_t^m = Y_t^m - \hat{Y}_t$	$I_t^{i,m} = Y_t^m - \hat{Y}_t^{i,m}$
Feedback control	$U_t^m = \mathsf{K}_g I_t^m$	$U_t^{i,m} = \mathsf{K}(X_t^i, t) I_t^{i,m}$
Gain	K_g: Kalman Gain	$\mathsf{K}(x,t)$: Sol. of a BVP (7.10)
Control input	$\sum_{m=1}^{M} \beta_t^m U_t^m$	$\sum_{m=1}^{M} \beta_t^m U_t^{i,m}$
Filter equation	$\dot{\hat{X}}_t = A\hat{X}_t + \sum_m \beta_t^m U_t^m$	$\dot{X}_t^i = a(X_t^i) + \dot{B}_t^i + \sum_m \beta_t^m U_t^{i,m}$

7.2.5 Algorithm

For implementation purposes, we use an Euler discretization method. The resulting discrete-time algorithm appears in Algo.8.

At each discrete time-step, the algorithm requires approximation of the gain function. The constant gain approximation algorithm is included in Algo.8. One can readily substitute another algorithm for approximating gain function.

The evaluation of association probability is based on the Gaussian clutter assumption. For this or other types of clutter models, one could also substitute a discrete-time algorithm for association probability (see Remark 12 in App. F.3).

Note that the PDA-FPF algorithm propagates an ensemble of particles approximating the posterior distribution at each time step. From the posterior, one can estimate any desired statistic for the state. The formula for the mean (X_t^{est}) is included in Algo.8.

Algorithm 8 PDA-FPF for tracking single target in clutter:

INITIALIZATION
for $i = 1$ to N **do**
  Sample X_0^i from $p(x,0)$
end for
for $m = 0$ to M **do**
  Set $\beta_0^m = \frac{1}{M+1}$.
end for
$p^{(N)}(x,0) = \frac{1}{N}\sum_{i=1}^{N} \delta_{X_0^i}(x)$
$X_0^{\text{est}} = \frac{1}{N}\sum_{i=1}^{N} X_0^i$
ITERATION [t to $t+\Delta t$]
for $i = 1$ to N **do**
  Sample a Gaussian random vector ΔV
  Calculate $\hat{h} = \frac{1}{N}\sum_{i=1}^{N} h(X_t^i)$
  Calculate $|\hat{h}|^2 = \hat{h}^T\hat{h}$
  Calculate the gain function $\mathsf{K} = \frac{1}{N}\sum_{i=1}^{N} X_t^i (h(X_t^i) - \hat{h})^T$
  $X_{t+\Delta t}^i = X_t^i + a(X_t^i)\Delta t + \Delta V\sqrt{\Delta t}$
  for $m = 1$ to M **do**
    Calculate $\Delta I_t^{i,m} = \Delta Z_t^m - \left[\frac{\beta_t^m}{2} h(X_t^i) + (1 - \frac{\beta_t^m}{2})\hat{h}\right]\Delta t$
    $X_{t+\Delta t}^i = X_{t+\Delta t}^i + \beta_t^m \mathsf{K}\Delta I_t^{i,m}$
    $\Delta\beta_t^m = q[1-(M+1)\beta_t^m]\Delta t + \beta_t^m \hat{h}^T\left(\Delta Z_t^m - \sum_{j=1}^{M}\beta_t^j \Delta Z_t^j\right) + \beta_t^m|\hat{h}|^2\left(\sum_{j=1}^{M}(\beta_t^j)^2 - \beta_t^m\right)\Delta t$
    $\beta_{t+\Delta t}^m = \beta_t^m + \Delta\beta_t^m$.
  end for
end for
$t = t + \Delta t$
$p^{(N)}(x,t) = \frac{1}{N}\sum_{i=1}^{N} \delta_{X_t^i}(x)$
$X_t^{\text{est}} = \frac{1}{N}\sum_{i=1}^{N} X_t^i$

7.2.6 Example: Linear Case

In this section, we illustrate the PDA-FPF with the aid of a linear example. The example also serves to provide a comparison to the classic PDA filter. Consider the following linear model:

$$\mathrm{d}X_t = A\,X_t\,\mathrm{d}t + \mathrm{d}B_t, \tag{7.13a}$$

$$\mathrm{d}Z_t^m = 1_{[A_t=m]}\,H\,X_t\,\mathrm{d}t + \mathrm{d}W_t^m, \tag{7.13b}$$

where A is a $d \times d$ matrix and H is an $s \times d$ matrix.

The PDA-FPF is described by (7.8)-(7.10). If we assume the initial distribution $p^*(x,0)$ is Gaussian with mean μ_0 and covariance matrix Σ_0, then the following lemma provides the solution of the gain function $\mathsf{K}(x,t)$ in the linear case.

Lemma 7.2.3 *Consider the linear observation (7.13b). Suppose $p(x,t)$ is assumed to be Gaussian with mean μ_t and variance Σ_t, i.e., $p(x,t) = \frac{1}{(2\pi)^{\frac{d}{2}}|\Sigma_t|^{\frac{1}{2}}}\exp\left[-\frac{1}{2}(x-\mu_t)^T\Sigma_t^{-1}(x-\mu_t)\right]$. Then the solution of the E-L BVP (7.10) is given by:*

$$\mathsf{K}(x,t) = \Sigma_t H^T \tag{7.14}$$

The formula (7.14) is verified by direct substitution in (7.10) where the distribution p is Gaussian.

The linear PDA-FPF is then given by,

$$\mathrm{d}X_t^i = A\,X_t^i\,\mathrm{d}t + \mathrm{d}B_t^i + \Sigma_t H^T \sum_{m=1}^{M} \beta_t^m \left(\mathrm{d}Z_t^m - H\left[\frac{\beta_t^m}{2}X_t^i + \left(1 - \frac{\beta_t^m}{2}\right)\mu_t\right]\mathrm{d}t\right). \tag{7.15}$$

Note that there is no Wong-Zakai correction term since the gain function is constant.

The following theorem states that $p = p^*$ in this case. That is, the conditional distributions of X_t and X_t^i coincide. The proof is a straightforward extension of the proof in App. F.4, and is thus omitted.

Theorem 7.2.4 *Consider the single target tracking problem with a linear model defined by the state-observation equations (7.13a,7.13b). The PDA-FPF is given by (7.15). In this case the posterior distributions of X_t and X_t^i coincide, whose conditional mean and covariance are given by the following,*

$$\mathrm{d}\mu_t = A\mu_t\,\mathrm{d}t + \Sigma_t H^T \sum_{m=1}^{M} \beta_t^m\,(\mathrm{d}Z_t^m - H\mu_t\,\mathrm{d}t), \tag{7.16}$$

$$\frac{\mathrm{d}\Sigma_t}{\mathrm{d}t} = A\Sigma_t + \Sigma_t A^T + I - \sum_{m=1}^{M} (\beta_t^m)^2\,\Sigma_t H^T H \Sigma_t. \tag{7.17}$$

(7.16)-(7.17) *is consistent with the linear PDAF result [9]. In other words, the PDA-FPF reduces to the classic PDAF in the linear case.*

The filter for association probability β_t^m in the linear Gaussian case easily follows from using (7.5). It is of the following form: for $m = 1, \ldots, M$,

$$\mathrm{d}\beta_t^m = q\,[1-(M+1)\beta_t^m]\,\mathrm{d}t + \beta_t^m (H\mu_t)^T \left(\mathrm{d}Z_t^m - \sum_{j=1}^{M} \beta_t^j \,\mathrm{d}Z_t^j \right) + \beta_t^m (H\mu_t)^T (H\mu_t) \left(\sum_{j=1}^{M} (\beta_t^j)^2 - \beta_t^m \right) \mathrm{d}t. \quad (7.18)$$

In practice $\{\mu_t, \Sigma_t\}$ in (7.15)-(7.18) are approximated as sample means and sample covariances from the ensemble $\{X_t^i\}_{i=1}^N$.

$$\mu_t \approx \mu_t^{(N)} := \frac{1}{N} \sum_{i=1}^{N} X_t^i,$$
$$\Sigma_t \approx \Sigma_t^{(N)} := \frac{1}{N-1} \sum_{i=1}^{N} \left(X_t^i - \mu_t^{(N)} \right) \left(X_t^i - \mu_t^{(N)} \right)^T.$$

7.3 Multiple Target Tracking using the Feedback Particle Filter

In this section, we extend the PDA-FPF to the multiple target tracking (MTT) problem. The resulting filter is referred to as the *joint probabilistic data association-feedback particle filter (JPDA-FPF)*. For notational ease, we assume a clutter free scenario where all observations originate from the targets (i.e., there are M targets and M observations at each time). The clutter can be handled in a manner similar to the basic PDA-FPF.

The MTT problem is introduced in Sec. 7.3.1. The algorithm is described *only* for the special case of two targets with two observations ($M = 2$), in Sec. 7.3.2. The algorithm for the general case is conceptually analogous but notationally cumbersome. It appears in Appendix. F.5.

7.3.1 Problem Statement, Assumptions and Notation

The following notation is adopted:

(i) There are M distinct targets. The set of targets is denoted by the index set $\mathscr{M} = \{1, 2, \ldots, M\}$. The set of permutations of $\mathscr{M}$ is denoted by $\Pi(\mathscr{M})$, whose cardinality $|\Pi(\mathscr{M})| = M!$. A typical element of $\Pi(\mathscr{M})$ is denoted as $\underline{\alpha} = (\alpha^1, \alpha^2, \ldots, \alpha^M)$.

(ii) At time t, the state of the n^{th} target is denoted as $X_t^n \in \mathbb{R}^d$ for $n \in \mathscr{M}$.

(iii) At time t, there is exactly one observation per target for a total of M observations, all of which are available in a centralized fashion. The observation vector is denoted by $\underline{Z}_t := (Z_t^1, Z_t^2, \ldots, Z_t^M)$, where the m^{th} entry, $Z_t^m \in \mathbb{R}^s$, originates from one of the targets in $\mathscr{M}$.

(iv) At time t, the association random vector is denoted as $\underline{A}_t \in \Pi(\mathscr{M})$. It is used to associate targets with the observations in a joint manner: $\underline{A}_t := (\alpha_t^1, \alpha_t^2, \ldots, \alpha_t^M) \in \Pi(\mathscr{M})$ signifies that the observation Z_t^1 originates from target α_t^1, Z_t^2 originates from target $\alpha_t^2, \ldots, Z_t^M$ originates from target α_t^M.

The following models are assumed for the three stochastic processes.

(i) The dynamics of the n^{th} target evolves according to the nonlinear SDE:

$$\mathrm{d}X_t^n = a^n(X_t^n)\,\mathrm{d}t + \mathrm{d}B_t^n\,, \tag{7.19}$$

where $\{B_t^n \in \mathbb{R}^d\}$ are mutually independent standard Wiener processes and $n \in \mathscr{M}$.

(ii) The observation model is given by:

$$\begin{bmatrix} \mathrm{d}Z_t^1 \\ \vdots \\ \mathrm{d}Z_t^M \end{bmatrix} = \Psi(\underline{A}_t) \begin{bmatrix} h(X_t^1) \\ \vdots \\ h(X_t^M) \end{bmatrix} \mathrm{d}t + \begin{bmatrix} \mathrm{d}W_t^1 \\ \vdots \\ \mathrm{d}W_t^M \end{bmatrix}, \tag{7.20}$$

where $\Psi(\underline{A}_t)$ is the permutation matrix for association vector $\underline{A}_t$, and $\{W_t^m\}_{m=1}^M$ are mutually independent standard Wiener processes, also assumed to be mutually independent with $\{B_t^n\}$.

(iii) The model for $\underline{A}_t$ is similar to the model assumed in PDA-FPF (see Sec. 7.2) and is described by a continuous-time Markov chain:

$$\mathsf{P}\{[\underline{A}_{t+\Delta t} = \underline{\gamma}] | [\underline{A}_t = \underline{\gamma}']\} = q\Delta t + o(\Delta t), \quad \underline{\gamma} \neq \underline{\gamma}' \in \Pi(\mathscr{M}), \tag{7.21}$$

where, for the ease of presentation, the transition rate is assumed to be a constant q. The initial distribution is assumed given.

(iv) $\underline{A}_t$ and $\underline{X}_t$ are assumed to be mutually independent.

The problem is to design M feedback particle filters, where the n^{th} filter is intended to estimate the posterior distribution of the n^{th} target given the history of all un-associated observations (filtration) $\mathscr{Z}_t := \sigma(Z_\tau : \tau \leq t)$.

The joint association probability is defined as the probability of the joint association event $[\underline{A}_t = \underline{\gamma}]$ conditioned on $\mathscr{Z}_t$:

$$\pi_t^{\underline{\gamma}} := \mathsf{P}\{[\underline{A}_t = \underline{\gamma}] | \mathscr{Z}_t\}, \quad \underline{\gamma} \in \Pi(\mathscr{M}). \tag{7.22}$$

The filter for the joint association probability $\pi_t^{\underline{\gamma}}$ is a notationally tedious but straightforward extension of the association filter in PDA-FPF (7.5). It appears in App. F.5.

The joint association probabilities are then used to obtain association probability for each individual target. Once the observation-to-target association probability is known, its integration into the feedback particle filter is identical to the PDA-FPF (7.8). The complete set of equations for the JPDA-FPF algorithm appear in App. F.5. The $M = 2$ case is illustrated next.

7.3.2 Example: Two-Target Two-Observation Problem

At time t, the target state is denoted as $\underline{X}_t := (X_t^1, X_t^2)$, and the observation vector $\underline{Z}_t := (Z_t^1, Z_t^2)$. The association random vector is denoted as $\underline{A}_t \in \Pi(\{1,2\}) := \{\underline{\gamma}_1, \underline{\gamma}_2\}$, where $\underline{\gamma}_1 := (1,2)$ and $\underline{\gamma}_2 := (2,1)$. It is used to associate observations to targets: $\underline{A}_t = \underline{\gamma}_1$ signifies that Z_t^1 originates from target 1 and Z_t^2 from target 2; $\underline{A}_t = \underline{\gamma}_2$ accounts for the complementary case.

The following models are assumed for the three stochastic processes:

(i) Each element of the state vector $\underline{X}_t$ evolves according to a nonlinear SDE of the form (7.1):

$$\mathrm{d}X_t^n = a^n(X_t^n)\,\mathrm{d}t + \mathrm{d}B_t^n, \quad n \in \{1,2\}, \tag{7.23}$$

where $\{B_t^1\}, \{B_t^2\}$ are mutually independent standard Wiener processes.

(ii) The association random process A_t evolves as a jump Markov process in continuous-time:

$$\mathsf{P}\{[\underline{A}_{t+\Delta t} = \underline{\gamma}_{m'}] | [\underline{A}_t = \underline{\gamma}_m]\} = q\Delta t + o(\Delta t), \quad m' \neq m \in \{1,2\}.$$

The initial distribution is assumed given.

(iii) $\underline{A}_t$ and $\underline{X}_t$ are assumed to be mutually independent.

(iv) At time t, the observation model is given by,

$$\begin{bmatrix} \mathrm{d}Z_t^1 \\ \mathrm{d}Z_t^2 \end{bmatrix} = \Psi(\underline{A}_t) \begin{bmatrix} h(X_t^1) \\ h(X_t^2) \end{bmatrix} \mathrm{d}t + \begin{bmatrix} \mathrm{d}W_t^1 \\ \mathrm{d}W_t^2 \end{bmatrix},$$

where $\{W_t^1\}, \{W_t^2\}$ are mutually independent Wiener processes and $\Psi(\underline{A}_t)$ is a function mapping $\underline{A}_t$ to a permutation matrix:

$$\Psi(\underline{\gamma}_1) = \begin{bmatrix} I_s & 0 \\ 0 & I_s \end{bmatrix}, \quad \Psi(\underline{\gamma}_2) = \begin{bmatrix} 0 & I_s \\ I_s & 0 \end{bmatrix},$$

where I_s is the $s \times s$ identity matrix.

The joint association probability is defined as the probability of the joint association $[\underline{A}_t = \underline{\gamma}]$ conditioned on $\mathscr{Z}_t$:

$$\pi_t^m := \mathsf{P}\{[\underline{A}_t = \underline{\gamma}_m] | \mathscr{Z}_t\}, \quad m \in \{1,2\}.$$

Based on the JPDA-FPF algorithm discussed in App. F.5, the filter for joint association probability π_t^1 is (under Assumption. 7.2.1):

$$\mathrm{d}\pi_t^1 = -q(\pi_t^1 - \pi_t^2)\,\mathrm{d}t + \pi_t^1\pi_t^2\hat{\tilde{h}}^T(\mathrm{d}Z_t^1 - \mathrm{d}Z_t^2) - (\pi_t^1 - \pi_t^2)\pi_t^1\pi_t^2\left|\hat{\tilde{h}}\right|^2\mathrm{d}t,$$

where $\tilde{h}(X_t^1, X_t^2) := h(X_t^1) - h(X_t^2)$, $\hat{\tilde{h}} := \mathsf{E}[\tilde{h}|\mathscr{Z}_t]$ and $\left|\hat{\tilde{h}}\right|^2 = \hat{\tilde{h}}^T\hat{\tilde{h}}$. The expectations are approximated by using particles. Since the joint events are mutually exclusive and exhaustive, we have $\sum_{m=1}^2 \pi_t^m = 1$. Using this, we have $\pi_t^2 = 1 - \pi_t^1$ and $\mathrm{d}\pi_t^2 = -\mathrm{d}\pi_t^1$.

The joint association probabilities π_t^1, π_t^2 are used to obtain association probability for individual target. For example, for target 1: $\beta_t^{1,1} = \pi_t^1$, $\beta_t^{2,1} = \pi_t^2$, where $\beta_t^{m,n}$ denotes the conditional probability that the m^{th} observation originates from the n^{th} target. Once the association probability is known, the feedback particle filter for each target is of the form (7.8). The detailed algorithm for JPDA-FPF is omitted because of its similarity to PDA-FPF.

7.4 Numerics

7.4.1 Single Target Tracking in Clutter

Consider first the problem of tracking a single target in clutter. The target evolves according to a white-noise acceleration model:

$$\mathrm{d}X_t = FX_t\,\mathrm{d}t + \sigma_B\,\mathrm{d}B_t, \tag{7.24}$$

$$\mathrm{d}Z_t = HX_t\,\mathrm{d}t + \sigma_W\,\mathrm{d}W_t, \tag{7.25}$$

where X_t denotes the state vector comprising of position and velocity coordinates at time t, Z_t is the observation process, $\{B_t\}, \{W_t\}$ are mutually independent standard Wiener processes. The two matrices are given by:

$$F = \begin{bmatrix} 0 & 1 \\ 0 & 0 \end{bmatrix}, \quad H = \begin{bmatrix} 1 & 0 \end{bmatrix}.$$

In the simulation results described next, the following parameter values are used: $\sigma_B = (0,1)$, $\sigma_W = 0.06$, and

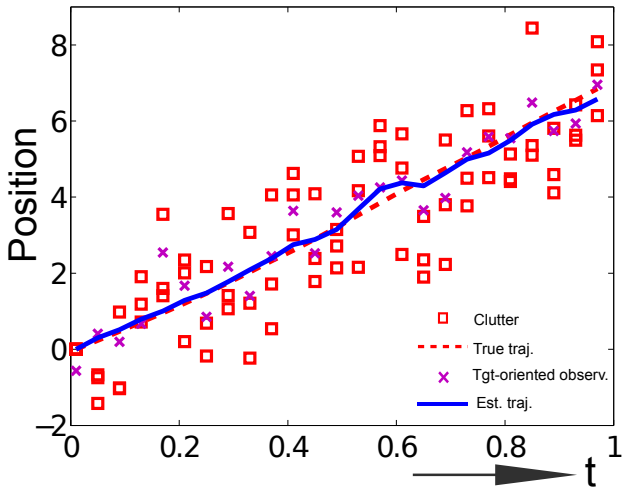

Figure 7.1: Simulation results of single target tracking in clutter using PDA-FPF: Comparison of estimated mean with the true trajectory.

initial condition $X_0 = (0,6)$. The total simulation time $T = 1$ and the discrete time-step $\Delta t = 0.01$. At each discrete-time step, we assume $M = 4$ observations, one due to the target and the others because of clutter. For the clutter observations, the standard discrete-time model from [8] is assumed: The clutter observations are sampled uniformly from a coverage area of radius 2 centered around the target.

Fig. 7.1 depicts the result of a single simulation: True target trajectory is depicted as a dashed line. At each discrete time step, target-oriented observations are depicted as crosses while clutter observations are depicted as squares.

The PDA-FPF is implemented according to Algorithm 1 in Sec. 7.2.5. For the evaluation of association probability, the transition rate parameter of the Markov chain (7.2) is $q = 10$. The output of the algorithm – the estimated mean trajectory – is depicted as a solid line. For the filter simulation, $N = 1000$ particles are used. The initial ensemble of particles are drawn from a Gaussian distribution whose mean is $\mu_0 = X_0$ and covariance matrix is $\Sigma_0 = \begin{bmatrix} 0.1 & 0 \\ 0 & 0.05 \end{bmatrix}$.

7.4.2 Two-Target Tracking Problem

Consider the tracking problem for two targets with two bearing-only sensors as depicted in Fig. 7.2(a). Each target moves in a two-dimensional (2d) plane according to the standard white-noise acceleration model:

$$\mathrm{d}X_t = AX_t\,\mathrm{d}t + \Gamma\,\mathrm{d}B_t,$$

where $X := (X_1, V_1, X_2, V_2) \in \mathbb{R}^4$, (X_1, X_2) denotes the 2d-position of a target and (V_1, V_2) denotes its velocity. The matrices,

$$A = \begin{bmatrix} 0 & 1 & 0 & 0 \\ 0 & 0 & 0 & 0 \\ 0 & 0 & 0 & 1 \\ 0 & 0 & 0 & 0 \end{bmatrix}, \qquad \Gamma = \sigma_B \begin{bmatrix} 0 & 0 \\ 1 & 0 \\ 0 & 0 \\ 0 & 1 \end{bmatrix},$$

and $\{B_t\}$ is a standard 2d Wiener process.

The two bearing-only sensors are also depicted in the figure. At time t, two angle-only observations are made for each target according to the observation model:

$$\mathrm{d}Z_t = h(X_t)\,\mathrm{d}t + \sigma_W\,\mathrm{d}W_t,$$

where $\{W_t\}$ is a standard 2d Wiener process, $h = (h_1, h_2)$ and

$$h_j(x_1, v_1, x_2, v_2) = \arctan\left(\frac{x_2 - x_2^{(\text{sen } j)}}{x_1 - x_1^{(\text{sen } j)}}\right), \quad j \in \{1, 2\},$$

where $(x_1^{(\text{sen } j)}, x_2^{(\text{sen } j)})$ denote the position of sensor j.

There exists data association uncertainty, in the sense that one cannot assign observations to individual targets in an apriori manner. In this particular example, faulty data association can lead to appearance of a "ghost" target (see Fig. 7.2(a)). The "ghost" target position is identified by using the process of triangulation based on angle only observations with the two targets.

In the simulation study described next, we compare performance of the JPDA-FPF algorithm with the sequential importance resampling particle filter (SIR-PF) algorithm. In the SIR-PF implementation, the data association uncertainty is taken into account by updating the particle weights according to the algorithm described in [95].

The performance comparisons are carried out for two distinct filtering scenarios:

(i) The target tracks for the filters are initialized at the true target positions (depicted as black circles in Fig. 7.2(b));

(ii) The target tracks for the filters are initialized at the ghost target position (depicted as black circles in Fig. 7.2(c)).

In the filter implementation, particles are initialized by drawing from a Gaussian distribution whose mean is the initial track position and the covariance matrix $\Sigma_0 = \mathrm{diag}(\{10, 1, 10, 1\})$.

Fig. 7.2 parts (b) and (c) depict the simulation results for the scenarios (i) and (ii), respectively. In each of the figure, the true target track is depicted together with the estimate (mean) from the two filter implementations. In the

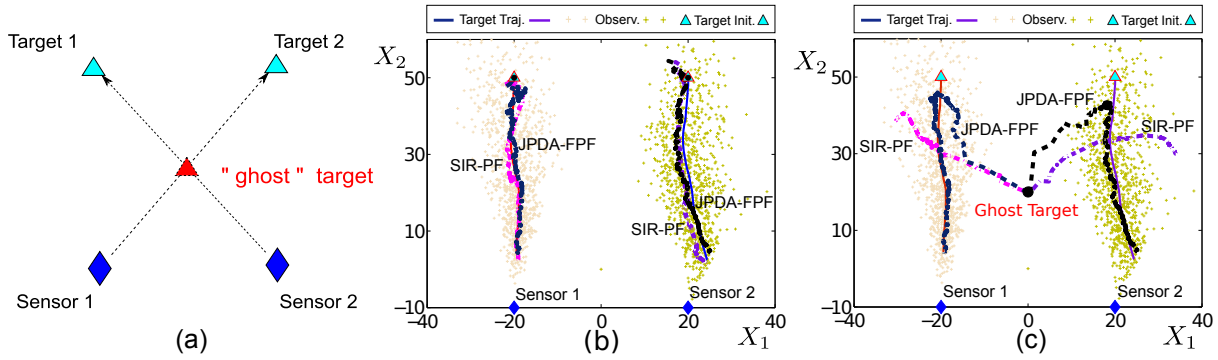

Figure 7.2: (a) Illustration of "ghost" target in the two-sensor two-target case: The ghost appears because of incorrect data association. Simulation results for (b) scenario (i) and (c) scenario (ii).

background, the ensemble of observations are shown. Each point in the ensemble is obtained by using the process of triangulation based on two (noisy) angle observations.

The JPDA-FPF algorithm is based on the methodology described in Sec. 7.3.2, where the PDA-FPF is implemented for each target according to Algorithm 1 in Sec. 7.2.5. At each time t, four association probabilities are approximated for each sensor: $\beta_t^{1,1;1}$, $\beta_t^{2,1;1}$ are the two association probabilities for target 1, and $\beta_t^{1,2;1}$, $\beta_t^{2,2;1}$ are the probabilities for target 2, where $\beta_t^{m,n;r}$ denotes the conditional probability that the m^{th} observation of the r^{th} sensor originates from the n^{th} target.

The simulation parameters are as follows: The two targets start at position $(-20,50)$ and $(20,50)$, respectively. The ghost target location is at $(0,20)$. The initial velocity vectors are $V_0^1 = V_0^2 = (0.0,-5.0)$. The noise parameters $\sigma_B = 0.5$, $\sigma_W = 0.01$ and the number of particles $N = 200$. The total simulation time is $T = 10$ and the fixed discrete time-step $\Delta t = 0.01$. The transition rate of the Markov chain (7.21) is $q = 10$.

The comparison for the two scenarios show that:

(i) If the filter tracks are initialized at the correct locations of the targets, both JPDA-FPF and SIR-PF algorithms are able to track the targets;

(ii) If the tracks are initialized at the incorrect ghost target location, the SIR-PF diverges while the JPDA-FPF can adequately track both targets after a short period of transients.

7.4.3 Track Coalescence

Track coalescence is a well-known problem in multiple target tracking applications. Track coalescence can occur when two closely spaced targets move with approximately the same velocity over a period of time [16, 22]. With a standard implementation of the SIR-PF algorithm, the target tracks are known to coalesce even after the targets have

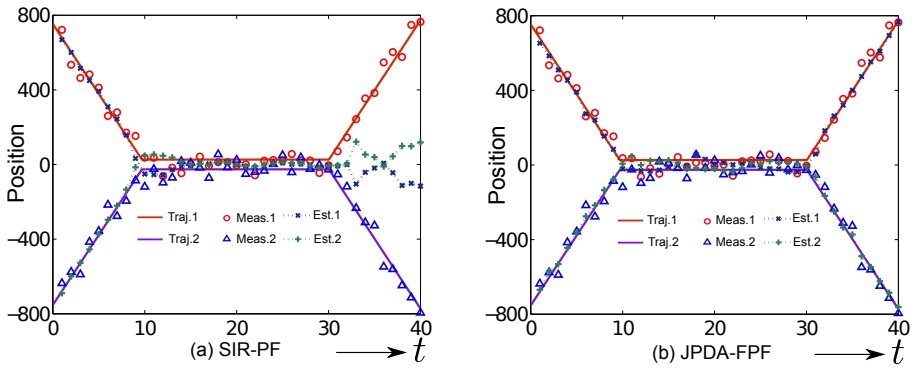

Figure 7.3: (a) Simulation results for SIR-PF; (b) Simulation results for JPDF-FPF.

moved apart [22]. In the following example, simulation results with JPDA-FPF are described for a model problem scenario taken from [27]. The results are compared with the SIR-PF algorithm taken from [5, 95].

The simulation study involves two targets moving on a one-dimension line [27]. At time $t = 0$, the two targets start at position 750 and -750, respectively. They move towards each other according to a white noise acceleration model (7.24) with initial velocity vector -75 and 75, respectively. At time $t = 10$, the distance between the two targets is smaller than $d = 50$, and they come to a stop and maintain position for the next 20 seconds. At time $t = 30$, the two targets move away from each other with velocity 75 and -75, respectively. The resulting position trajectories of the two targets (denoted as X_t^{tgt}) are depicted in Fig. 7.3. The target positions are observed according to the observation model (7.25), again with data association uncertainty.

In the Monte Carlo simulation study described next, the following noise parameters are used: $\sigma_B = (0, 25)$ and $\sigma_W = 10$. One hundred Monte Carlo simulations were performed over a total simulation period $T = 40$ with a fixed discrete time-step $\Delta t = 0.05$. At each discrete time-step, two observations are made but the association is not known in an apriori manner. For the filters, $N = 1000$ particles are initialized by drawing from a Gaussian distribution whose mean is set to be the target's initial position and covariance matrix $\Sigma_0 = \text{diag}(\{100, 10, 100, 10\})$. The JPDA-FPF is implemented as described in Sec. 7.3.2 and the SIR-PF algorithm is taken from [95].

Simulation results are summarized in Fig. 7.3-7.4. Fig. 7.3 parts (a) and (b) depict the typical results for one simulation run with SIR-PF and JPDA-FPF algorithms, respectively. Track coalescence is observed with the SIR-PF algorithm while the JPDA-FPF is able to track the two targets. Fig. 7.4 (a) depicts the corresponding trajectory of the association probability with the JPDA-FPF algorithm. As shown in the figure, the tracks coalesce when the two targets are close. However, the filter is able to recover the target tracks once the targets move away.

Fig. 7.4 (b) depicts a comparison of the root mean square error (RMSE) in position with the SIR-PF and JPDA-FPF

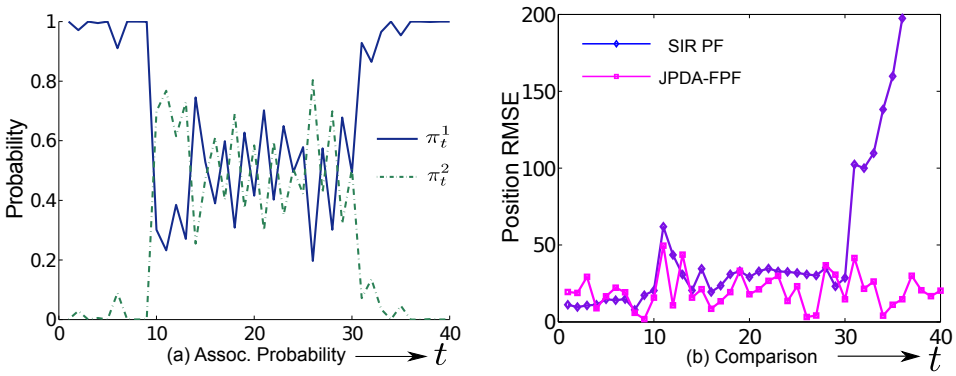

Figure 7.4: (a) Plot of data association probability; (b) Comparison of RMSE with SIR-PF and JPDA-FPF

algorithms. The RMSE at time t is defined as:

$$\text{RMSE}_t = \sqrt{\mathsf{E}\left[\left|X_t^{\text{est}} - X_t^{\text{tgt}}\right|^2\right]},$$

where $\mathsf{E}[\cdot]$ is computed by taking the average of 100 Monte Carlo runs. For $t < 30$, the performance of the two algorithms is comparable. However once the two closely spaced targets depart away from each other, the RMSE of SIR-PF soars while the JPDA-FPF remains relatively stable.

Table 7.2: Comparison between SIR PF and JPDA-FPF

Method	Avg. RMSE	Avg. % Tracks "OK"
SIR-PF	75.40	78
JPDA-FPF	22.86	100

Table 7.2 provides a summary of the performance with the two algorithms. The metrics are average RMSE and the average percentage of the filter tracks being "OK." The average RMSE is calculated as:

$$\text{avg. RMSE} = \sqrt{\frac{1}{T}\int_0^T \mathsf{E}\left[\left|X_t^{\text{est}} - X_t^{\text{tgt}}\right|^2\right] \mathrm{d}t}.$$

A track is said to be "OK" if the average tracking error satisfies:

$$\sqrt{\frac{1}{T}\int_0^T \left|X_t^{\text{est}} - X_t^{\text{tgt}}\right|^2 \mathrm{d}t} \leq 9\sigma_W.$$

The metrics used here are borrowed from [29, 95].

7.5 Conclusion

In this chapter, we introduced a novel feedback control-based particle filter algorithm for the filtering problem with data association uncertainty. The algorithm is referred to as the probabilistic data association-feedback particle filter (PDA-FPF). PDA-FPF provides for a generalization of the Kalman filter-based PDA filter to a general class of non-linear non-Gaussian problems. Our proposed algorithm inherits many of the properties that has made the Kalman filter-based algorithms so widely applicable over the past five decades, including innovation error and the feedback structure (see Fig. 2.1).

The feedback structure is important on account of the issue of robustness. The structural aspects are also expected to be useful for design, integration and testing of the algorithm in a larger system involving filtering problems (e.g., navigation systems).

Several numerical examples were included to illustrate the theoretical results, and provide comparisons with the SIR particle filter. Notably, simulation results suggest that track coalescence, which is a well-known problem in MTT applications, can be avoided by the proposed JPDA-FPF algorithm. A complete numerical comparison, in terms of tracking performance with the existing approaches, for MTT applications is planned for future publications.

Part III

Appendices

Appendix A

Proofs for Chapter 2

A.1 Calculation of K-L divergence

Recall the definition of K-L divergence for densities,

$$\mathsf{D}\,(p_n \| \hat{p}_n^*) = \int_{\mathbb{R}} p_n(s) \ln\Big(\frac{p_n(s)}{\hat{p}_n^*(s)}\Big)\,\mathrm{d}s.$$

We make a co-ordinate transformation $s = x + v(x)$ and use (2.15) to express the K-L divergence as:

$$\mathsf{D}\,(p_n \| \hat{p}_n^*) = \int_{\mathbb{R}} \frac{p_n^-(x)}{|1+v'(x)|} \ln\Big(\frac{p_n^-(x)}{|1+v'(x)|\,\hat{p}_n^*(x+v(x))}\Big)|1+v'(x)|\,\mathrm{d}x$$

The expression for K-L divergence given in (2.17) follows on using (2.14).

A.2 Solution of the Optimization Problem

Denote:

$$\mathscr{L}(x,v,v') = -p_n^-(x)\Big(\ln|1+v'| + \ln(p_n^-(x+v)p_{Y|X}(Y_{t_n}|x+v))\Big). \tag{A.1}$$

The optimization problem (2.16) is a calculus of variation problem:

$$\min_v \int \mathscr{L}(x,v,v')\,\mathrm{d}x.$$

The minimizer is obtained via the analysis of first variation given by the well-known Euler-Lagrange equation:

$$\frac{\partial \mathscr{L}}{\partial v} = \frac{\mathrm{d}}{\mathrm{d}x}\left(\frac{\partial \mathscr{L}}{\partial v'}\right),$$

Explicitly substituting the expression (A.1) for $\mathscr{L}$, we obtain (2.18).

A.3 Derivation of the Forward Equation

We denote the filtration $\mathscr{B}_t = \sigma(X_0^i, B_s^i : s \le t)$, and we recall that $\mathscr{Z}_t = \sigma(Z_s : s \le t)$ for $t \ge 0$. These two filterations are *independent* by construction.

On denoting $\tilde{a}(x,t) = a(x) + u(x,t)$, the particle evolution (2.19) is expressed,

$$X_t^i = X_0^i + \int_0^t \tilde{a}(X_s^i, s)\,\mathrm{d}s + \int_0^t \mathsf{K}(X_s^i, s)\,\mathrm{d}Z(s) + \sigma_B B_t^i. \tag{A.2}$$

By assumption on Lipschitz continuity of $\tilde{a}$ and K, there exists a unique solution that is adapted to the larger filtration $\mathscr{B}_t \vee \mathscr{Z}_t = \sigma(X_0^i, B_s^i, Z_s : s \le t)$. In fact, there is a functional F_t such that,

$$X_t^i = F_t(X_0^i, B_t^i, Z^t), \tag{A.3}$$

where $Z^t := \{Z_s : 0 \le s \le t\}$ denotes the trajectory.

The conditional distribution of X_t^i given $\mathscr{Z}_t = \sigma(Z_s : s \le t)$ was introduced in Sec. 2.2.1: Its density is denoted $p(x,t)$, defined by any bounded and measurable function $f\colon \mathbb{R} \to \mathbb{R}$ via,

$$\mathsf{E}[f(X_t^i) \mid \mathscr{Z}_t] = \int_{\mathbb{R}} p(x,t) f(x)\,\mathrm{d}x =: \langle p_t, f \rangle.$$

We begin with a result that is the key to proving Prop. 2.3.1. The proof of the Lemma A.3.1 below appears in [156]. It is omitted here on account of space.

Lemma A.3.1 *Suppose that f is an $\mathscr{B}_t \vee \mathscr{Z}_t$-adapted process satisfying $\mathsf{E}\int_0^t |f(s)|^2\,\mathrm{d}s < \infty$. Then,*

$$\mathsf{E}\Big[\int_0^t f(s)\,\mathrm{d}s \,|\, \mathscr{Z}_t\Big] = \int_0^t \mathsf{E}[f(s)|\mathscr{Z}_s]\,\mathrm{d}s, \tag{A.4}$$

$$\mathsf{E}\Big[\int_0^t f(s)\,\mathrm{d}Z_s \,|\, \mathscr{Z}_t\Big] = \int_0^t \mathsf{E}[f(s)|\mathscr{Z}_s]\,\mathrm{d}Z_s. \tag{A.5}$$

□

We now provide a proof of the Prop. 2.3.1.

Proof of Proposition 2.3.1 Applying Itô's formula to equation (2.19) gives, for any smooth and bounded function f,

$$\mathrm{d}f(X_t^i) = \mathscr{L} f(X_t^i)\,\mathrm{d}t + \sigma_B \frac{\partial f}{\partial x}(X_t^i)\,\mathrm{d}B_t^i + \mathsf{K}(X_t^i, t)\frac{\partial f}{\partial x}(X_t^i)\,\mathrm{d}Z_t,$$

where $\mathscr{L}f := (a+u)\frac{\partial f}{\partial x} + \frac{1}{2}(\sigma_W^2 \mathsf{K}^2 + \sigma_B^2)\frac{\partial^2 f}{\partial x^2}$. Therefore,

$$f(X_t^i) = f(X_0^i) + \int_0^t \mathscr{L}f(X_s^i)\,\mathrm{d}s + \sigma_B \int_0^t \frac{\partial f}{\partial x}(X_s^i)\,\mathrm{d}B_s^i + \int_0^t \mathsf{K}(X_s^i, s)\frac{\partial f}{\partial x}(X_s^i)\,\mathrm{d}Z_s.$$

Taking conditional expectations on both sides,

$$\langle p_t, f\rangle = \mathsf{E}[f(X_0^i) \mid \mathscr{Z}_t] + \mathsf{E}\Big[\int_0^t \mathscr{L}f(X_s^i)\,\mathrm{d}s|\mathscr{Z}_t\Big] + \sigma_B \mathsf{E}\Big[\int_0^t \frac{\partial f}{\partial x}(X_s^i)\,\mathrm{d}B_s^i \mid \mathscr{Z}_t\Big] + \mathsf{E}\Big[\int_0^t \mathsf{K}(X_s^i, s)\frac{\partial f}{\partial x}(X_s^i)\,\mathrm{d}Z_s \mid \mathscr{Z}_t\Big]$$

On applying Lemma A.3.1, and the fact that B_t^i is a Wiener process, we conclude that

$$\langle p_t, f\rangle = \langle p_0, f\rangle + \int_0^t \langle p_s, Lf\rangle\,\mathrm{d}s + \int_0^t \langle p_s, \mathsf{K}\frac{\partial f}{\partial x}\rangle\,\mathrm{d}Z_s\,.$$

The forward equation (2.22) follows using integration by parts.

A.4 Euler-Lagrange Equation for the Continuous-Time Filter

In this section we describe, formally, the continuous-time limit of the discrete-time E-L BVP (2.18). In the continuous-time case, the control and the observation models are of the form (see (2.19) and (2.1b)):

$$\begin{aligned}\mathrm{d}U_t^i &= u(X_t^i, t)\,\mathrm{d}t + \mathsf{K}(X_t^i, t)\,\mathrm{d}Z_t,\\ \mathrm{d}Z_t &= h(X_t)\,\mathrm{d}t + \sigma_W\,\mathrm{d}W_t.\end{aligned}$$

In discrete-time, these are approximated as

$$\begin{aligned}\triangle U_t^i &= u(X_t^i, t)\triangle t + \mathsf{K}(X_t^i, t)\triangle Z_t,\\ \triangle Z_t &= h(X_t)\triangle t + \sigma_W \triangle W_t,\end{aligned} \tag{A.6}$$

where $\triangle t$ is the small time-increment at t. It follows that the conditional distribution of $Y_t \doteq \frac{\triangle Z_t}{\triangle t}$ given X_t is the density,

$$p_{Y|X}(Y_t|\cdot) = \frac{1}{\sqrt{2\pi\sigma_W^2/\triangle t}} \exp\left(-\frac{(\triangle Z_t - h(\cdot)\triangle t)^2}{2\sigma_W^2 \triangle t}\right). \tag{A.7}$$

Substituting (A.6)-(A.7) in the E-L BVP (2.18) for the continuous-discrete time case, we arrive at the formal

equation:

$$\frac{\partial}{\partial x}\left(\frac{p(x,t)}{1+u'\triangle t+\mathsf{K}'\triangle Z_t}\right)=p(x,t)\frac{\partial}{\partial v}\Big(\ln p(x+v,t)+\ln p_{Y|X}(Y_t\mid x+v)\Big)\Big|_{v=u\triangle t+\mathsf{K}\triangle Z_t}. \tag{A.8}$$

For notational ease, we use primes to denote partial derivatives with respect to x: p is used to denote $p(x,t)$, $p':=\frac{\partial p}{\partial x}(x,t)$, $p'':=\frac{\partial^2 p}{\partial x^2}(x,t)$, $u':=\frac{\partial u}{\partial x}(x,t)$, $\mathsf{K}':=\frac{\partial \mathsf{K}}{\partial x}(x,t)$ etc. Note that the time t is fixed.

A sketch of calculations to obtain (2.23) and (2.24) starting from (A.8) appears in the following three steps:

Step 1: The three terms in (A.8) are simplified as:

$$\begin{aligned}
&\frac{\partial}{\partial x}\left(\frac{p}{1+u'\triangle t+\mathsf{K}'\triangle Z_t}\right)=p'-f_1\triangle t-(p'\mathsf{K}'+p\mathsf{K}'')\triangle Z_t\\
&p\frac{\partial}{\partial v}\ln p(x+v)\Big|_{v=u\triangle t+\mathsf{K}\triangle Z_t}=p'+f_2\triangle t+(p''\mathsf{K}-\frac{p'^2\mathsf{K}}{p})\triangle Z_t\\
&p\frac{\partial}{\partial v}\ln p_{Y|X}(Y_t|x+v)\Big|_{v=u\triangle t+\mathsf{K}\triangle Z_t}=\frac{p}{\sigma_W^2}(h'\triangle Z_t-hh'\triangle t)+ph''\mathsf{K}\triangle t
\end{aligned}$$

where we have used Itô's rules $(\triangle Z_t)^2=\sigma_W^2\triangle t$, $\triangle Z_t\triangle t=0$ etc., and where

$$\begin{aligned}
f_1&=(p'u'+pu'')-\sigma_W^2(p'\mathsf{K}'^2+2p\mathsf{K}'\mathsf{K}''),\\
f_2&=(p''u-\frac{p'^2u}{p})+\sigma_W^2\mathsf{K}^2\left(\frac{1}{2}p'''-\frac{3p'p''}{2p}+\frac{p'^3}{p^2}\right).
\end{aligned}$$

Collecting terms in $O(\triangle Z_t)$ and $O(\triangle t)$, after some simplification, leads to the following ODEs:

$$\mathscr{E}(\mathsf{K})=\frac{1}{\sigma_W^2}h'(x) \tag{A.9}$$

$$\mathscr{E}(u)=-\frac{1}{\sigma_W^2}h(x)h'(x)+h''(x)\mathsf{K}+\sigma_W^2G(x,t) \tag{A.10}$$

where $\mathscr{E}(\mathsf{K})=-\frac{\partial}{\partial x}\left(\frac{1}{p(x,t)}\frac{\partial}{\partial x}\{p(x,t)\mathsf{K}(x,t)\}\right)$, and $G=-2\mathsf{K}'\mathsf{K}''-(\mathsf{K}')^2(\ln p)'+\frac{1}{2}\mathsf{K}^2(\ln p)'''$.

Step 2. Suppose (u,K) are admissible solutions of the E-L BVP (A.9)-(A.10). Then it is claimed that

$$-(p\mathsf{K})'=\frac{h-\hat{h}}{\sigma_W^2}p \tag{A.11}$$

$$-(pu)'=-\frac{(h-\hat{h})\hat{h}}{\sigma_W^2}p-\frac{1}{2}\sigma_W^2(p\mathsf{K}^2)''. \tag{A.12}$$

Recall that admissible here means

$$\lim_{x\to\pm\infty}p(x,t)u(x,t)=0,\quad \lim_{x\to\pm\infty}p(x,t)\mathsf{K}(x,t)=0. \tag{A.13}$$

To show (A.11), integrate (A.9) once to obtain

$$-(p\mathsf{K})' = \frac{1}{\sigma_W^2} hp + Cp,$$

where the constant of integration $C = -\frac{\hat{h}}{\sigma_W^2}$ is obtained by integrating once again between $-\infty$ to ∞ and using the boundary conditions for K (A.13). This gives (A.11).

To show (A.12), we denote its right hand side as $\mathscr{R}$ and claim

$$\left(\frac{\mathscr{R}}{p}\right)' = -\frac{hh'}{\sigma_W^2} + h''\mathsf{K} + \sigma_W^2 G. \tag{A.14}$$

The equation (A.12) then follows by using the ODE (A.10) together with the boundary conditions for u (A.13). The verification of the claim involves a straightforward calculation, where we use (A.9) to obtain expressions for h' and K''. The details of this calculation are omitted on account of space.

Step 3. On integrating (A.9), we obtain the E-L equation for K, which is the same as (2.23). The proof of (2.24) involves a short calculation starting from (A.12), which is simplified to the form (2.24) by using (A.11).

Remark 10 *The derivation of Euler-Lagrange equation, as presented above, is a heuristic on account of Step 1. A similar heuristic also appears in the original paper of Kushner [100]. There, the Kushner-Stratonovich PDE* (2.21) *is derived by considering a continuous-time limit of the Bayes formula* (2.14)*. The Itô's rules are used to obtain the limit. Rigorous justification of the calculation in Step 1, or its replacement by an alternate argument is the subject of future work.*

The calculation in Steps 2 and 3 require additional regularity assumptions on density p and function h: p is C^3 and h is C^2.

A.5 Proof of Prop. 2.3.2.

Consider the ODE (2.23). It is a linear ODE whose unique solution is given by

$$\mathsf{K}(x,t) = \frac{1}{p(x,t)} \left(C_1 + C_2 \int_{-\infty}^{x} p(y,t)\,\mathrm{d}y - \frac{1}{\sigma_W^2} \int_{-\infty}^{x} h(y)p(y,t)\,\mathrm{d}y \right), \tag{A.15}$$

where the constant of integrations $C_1 = 0$ and $C_2 = \frac{\hat{h}_t}{\sigma_W^2}$ because of the boundary conditions for K. Part 2 is an easy consequence of the minimum principle for elliptic PDEs [60].

A.6 Proof of Thm. 2.3.3

It is only necessary to show that with this choice of $\{u, \mathsf{K}\}$, we have $\mathrm{d}p(x,t) = \mathrm{d}p^*(x,t)$, for all x and t, in the sense that they are defined by identical stochastic differential equations. Recall $\mathrm{d}p^*$ is defined according to the K-S equation (2.21), and $\mathrm{d}p$ according to the forward equation (2.22).

If K solves the E-L BVP (2.23) then using (A.15),

$$\frac{\partial}{\partial x}(p\mathsf{K}) = -\frac{1}{\sigma_W^2}(h-\hat{h})p. \tag{A.16}$$

On multiplying both sides of (2.24) by $-p$, we have

$$\begin{aligned} -up &= \frac{1}{2}(h-\hat{h})p\mathsf{K} - \frac{1}{2}\sigma_W^2(p\mathsf{K})\frac{\partial \mathsf{K}}{\partial x} + \hat{h}p\mathsf{K} \\ &= -\frac{1}{2}\sigma_W^2\frac{\partial(p\mathsf{K})}{\partial x}\mathsf{K} - \frac{1}{2}\sigma_W^2(p\mathsf{K})\frac{\partial \mathsf{K}}{\partial x} + \hat{h}p\mathsf{K} \\ &= -\frac{1}{2}\sigma_W^2\frac{\partial}{\partial x}(p\mathsf{K}^2) + \hat{h}p\mathsf{K}, \end{aligned}$$

where we have used (A.16) to obtain the second equality. Differentiating once with respect to x and using (A.16) once again,

$$-\frac{\partial}{\partial x}(up) + \frac{1}{2}\sigma_W^2\frac{\partial^2}{\partial x^2}(p\mathsf{K}^2) = -\frac{\hat{h}}{\sigma_W^2}(h-\hat{h})p. \tag{A.17}$$

Using (A.16)-(A.17) in the forward equation (2.22), we have

$$\mathrm{d}p = \mathscr{L}^\dagger p + \frac{1}{\sigma_W^2}(h-\hat{h})(\mathrm{d}Z_t - \hat{h}\,\mathrm{d}t)p\,.$$

This is precisely the SDE (2.21), as desired.

A.7 Proof of Thm. 2.3.5

The Gaussian density is given by:

$$p(x,t) = \frac{1}{\sqrt{2\pi\Sigma_t}}\exp\left(-\frac{(x-\mu_t)^2}{2\Sigma_t}\right), \tag{A.18}$$

The density (A.18) is a function of the stochastic process μ_t. Using Itô's formula,

$$\mathrm{d}p(x,t) = \frac{\partial p}{\partial \mu}\,\mathrm{d}\mu_t + \frac{\partial p}{\partial \Sigma}\,\mathrm{d}\Sigma_t + \frac{1}{2}\frac{\partial^2 p}{\partial \mu^2}\,\mathrm{d}\mu_t^2,$$

where $\frac{\partial p}{\partial \mu} = \frac{x-\mu_t}{\Sigma_t}p$, $\frac{\partial p}{\partial \Sigma} = \frac{1}{2\Sigma_t}\left(\frac{(x-\mu_t)^2}{\Sigma_t} - 1\right)p$, and $\frac{\partial^2 p}{\partial \mu^2} = \frac{1}{\Sigma_t}\left(\frac{(x-\mu_t)^2}{\Sigma_t} - 1\right)p$. Substituting these into the forward equa-

tion (2.22), we obtain a quadratic equation $Ax^2 + Bx = 0$, where

$$A = \mathrm{d}\Sigma_t - \left(2\alpha\Sigma_t + \sigma_B^2 - \frac{\gamma^2\Sigma_t^2}{\sigma_W^2}\right)\mathrm{d}t,$$
$$B = \mathrm{d}\mu_t - \left(\alpha\mu_t\,\mathrm{d}t + \frac{\gamma\Sigma_t}{\sigma_W^2}(\mathrm{d}Z_t - \gamma\mu_t\,\mathrm{d}t)\right).$$

This leads to the model (2.28) and (2.29). □

Appendix B

Proofs for Chapter 3

B.1 Proof of Thm. 3.2.2

It is only necessary to show that with the choice of $\{u, \mathsf{K}\}$ given by (3.13)-(3.14), we have $\mathrm{d}p(x,t) = \mathrm{d}p^*(x,t)$, for all x and t, in the sense that they are defined by identical stochastic differential equations. Recall $\mathrm{d}p^*$ is defined according to the K-S equation (3.10), and $\mathrm{d}p$ according to the forward equation (3.12).

Recall that the gain function K is a solution of the following BVP:

$$\nabla \cdot (p\mathsf{K}) = -p(h - \hat{h})^T . \tag{B.1}$$

On multiplying both sides of (3.14) by $-p$, we obtain

$$\begin{aligned} -up &= \frac{1}{2} p(h - \hat{h})\mathsf{K} - \Omega p + p\mathsf{K}\hat{h} \\ &= -\frac{1}{2}\mathsf{K}[\nabla \cdot (p\mathsf{K})]^T - \Omega p + p\mathsf{K}\hat{h} \end{aligned} \tag{B.2}$$

where (B.1) is used to obtain the second equality. Denoting $E := \frac{1}{2}\mathsf{K}[\nabla \cdot (p\mathsf{K})]^T$, a direct calculation shows that

$$E_l + \Omega_l p = \sum_{k=1}^{d} \frac{\partial}{\partial x_k} \left(p[\mathsf{K}\mathsf{K}^T]_{lk} \right).$$

Substituting this in (B.2), on taking the divergence of both sides, we obtain

$$-\nabla \cdot (pu) + \frac{1}{2} \sum_{l,k=1}^{d} \frac{\partial^2}{\partial x_l \partial x_k} \left(p[\mathsf{K}\mathsf{K}^T]_{lk} \right) = \nabla \cdot (p\mathsf{K})\, \hat{h}. \tag{B.3}$$

Using (B.1) and (B.3) in the forward equation (3.12),

$$\mathrm{d}p = \mathscr{L}^\dagger p + (h - \hat{h})^T (\mathrm{d}Z_t - \hat{h}\,\mathrm{d}t) p.$$

This is precisely the SDE (3.10), as desired. □

B.2 BVP for the Multivariable Feedback Particle Filter

Consider the multivariable linear system,

$$\mathrm{d}X_t = \alpha X_t\,\mathrm{d}t + \sigma_B\,\mathrm{d}B_t \tag{B.4a}$$

$$\mathrm{d}Z_t = \gamma^T X_t\,\mathrm{d}t + \sigma_W\,\mathrm{d}W_t \tag{B.4b}$$

where $X_t \in \mathbb{R}^d$, $Z_t \in \mathbb{R}^1$, α is an $d \times d$ matrix, γ is an $d \times 1$ vector, $\{B_t\}$ is an $d-$dimensional Wiener process, $\{W_t\}$ is a scalar Wiener process, and $\{B_t\}$,$\{W_t\}$ are assumed to be mutually independent. We assume the initial distribution $p^*(x,0)$ is Gaussian with mean vector μ_0 and variance matrix Σ_0.

The following proposition shows that the Kalman gain is a solution of the multivariable BVP (3.17), the Kalman gain solution does not equal the solution K_g (see (3.20)), and that the solution given by K_g is not integrable with respect to p:

Proposition B.2.1 *Consider the d-dimensional linear system* (B.4a)-(B.4b)*, where $d \geq 2$. Suppose $p(x,t)$ is assumed to be Gaussian: $p(x,t) = \frac{1}{(2\pi)^{\frac{d}{2}}|\Sigma_t|^{\frac{1}{2}}}\exp\left(-\frac{1}{2}(x-\mu_t)^T\Sigma_t^{-1}(x-\mu_t)\right)$, where $x = (x_1,x_2,...,x_d)^T$, μ_t is the mean, Σ_t is the covariance matrix, and $|\Sigma_t| > 0$ denotes the determinant.*

1) *One solution of the BVP* (3.17) *is given by the Kalman gain:*

$$\mathsf{K}(x,t) = \frac{1}{\sigma_W^2}\Sigma_t\gamma \tag{B.5}$$

2) *Suppose that the Kalman gain K given in* (B.5) *is non-zero. For this solution to* (3.17)*, there does not exist a function ϕ such that $p\mathsf{K} = \nabla\phi$.*

3) *Consider the solution $\mathsf{K}_g(x,t)$ of the BVP* (3.17) *as given by* (3.20)*. This gain function is unbounded: $|\mathsf{K}_g(x,t)| \to \infty$ as $|x| \to \infty$, and moreover*

$$\int_{\mathbb{R}^d} |\mathsf{K}_g(x,t)|p(x,t)\,\mathrm{d}x = \infty, \quad \int_{\mathbb{R}^d} |\mathsf{K}_g(x,t)|^2 p(x,t)\,\mathrm{d}x = \infty.$$

□

Proof The Kalman gain solution (B.5) is verified by direct substitution in the BVP (3.17) where the distribution p is Gaussian.

The proof of claim 2 follows by contradiction. Suppose a function ϕ exists such that $p\mathsf{K} = \nabla\phi$, then we have

$$\frac{\partial(\mathsf{K}p)_i}{\partial x_j} = \frac{\partial^2\phi}{\partial x_j\partial x_i} = \frac{\partial^2\phi}{\partial x_i\partial x_j} = \frac{\partial(\mathsf{K}p)_j}{\partial x_i}, \quad \forall i,j \tag{B.6}$$

where $(\mathsf{K}p)_i$ is the i^{th} entry of vector $\mathsf{K}p$. By direct evaluation, we have

$$\frac{\partial(\mathsf{K}p)_i}{\partial x_j} = 2\mathsf{K}_i \cdot \left(\Sigma_t^{-1}(x-\mu_t)\right)_j p.$$

Using (B.6), we obtain

$$\mathsf{K}_i(\Sigma_t^{-1})_{jk} = \mathsf{K}_j(\Sigma_t^{-1})_{ik}, \qquad \forall i,j,k \tag{B.7}$$

Setting $k=i$, summing over the index i and using (B.5), we arrive at

$$\mathrm{tr}(\Sigma_t^{-1})\mathsf{K} = \Sigma_t^{-1}\mathsf{K},$$

where $\mathrm{tr}(\Sigma_t^{-1})$ denotes the trace of the matrix Σ_t^{-1}. This provides a contradiction because $\mathsf{K} \not\equiv 0$ and Σ_t is a positive definite symmetric matrix with $|\Sigma_t| > 0$.

We now establish claim 3. For the solution K_g as given by (3.20):

$$p\mathsf{K}_g(x,t) = \frac{1}{\sigma_W^2}\frac{1}{d\omega_d}\int \frac{y-x}{|y-x|^d}(h(y)-\hat{h})p(y,t)\,\mathrm{d}y$$

For this integral, with $h(y) \equiv \gamma^T y$, we have the following asymptotic formula for $|x| \sim \infty$,

$$p\mathsf{K}_g(x,t) \sim C\frac{1}{|x|^d} + o\left(\frac{1}{|x|^d}\right),$$

where C does not vary as a function of $|x|$ (its value depends only upon the angular coordinates). For example, in dimension $d=2$, C is given by

$$\begin{aligned} C(x_1,x_2) &= C(|x|\cos(\theta), |x|\sin(\theta)) \\ &= -\frac{1}{d\omega_d}\begin{pmatrix} \cos(2\theta) & \sin(2\theta) \\ \sin(2\theta) & \cos(2\theta) \end{pmatrix}\frac{\Sigma_t\gamma}{\sigma_W^2}, \end{aligned}$$

where $\frac{\Sigma_t\gamma}{\sigma_W^2}$ is the Kalman gain vector.

The result follows because $\frac{1}{p|x|^d} \to \infty$ and $\frac{1}{|x|^d}$ is not integrable in $\mathbb{R}^d$. Using the Cauchy-Schwarz inequality,

$$\int |\mathsf{K}_g(x,t)|p(x,t)\,\mathrm{d}x \le \left(\int |\mathsf{K}_g(x,t)|^2 p(x,t)\,\mathrm{d}x\right)^{\frac{1}{2}},$$

which shows that K_g is not square-integrable.

B.3 Proof of Thm. 3.3.1

We omit the subscript "j" in this proof, writing just ϕ and h. We also suppress explicit dependence on time t, writing $p(x)$ instead of $p(x,t)$ and $\phi(x)$ instead of $\phi(x,t)$.

Under Assumption A1, p is known to admit a spectral gap (or Poincaré inequality) with constant $\lambda \geq c_1$ [87]: That is, for all functions $\phi \in H_0^1(\mathbb{R}^d; p)$,

$$\int |\phi(x)|^2 p(x)\,\mathrm{d}x \leq \frac{1}{\lambda} \int |\nabla\phi(x)|^2 p(x)\,\mathrm{d}x. \tag{B.8}$$

Consider now the inner product

$$< \phi, \psi >:= \int \nabla\phi(x) \cdot \nabla\psi(x) p(x)\,\mathrm{d}x.$$

On account of (B.8), the norm defined by using the inner product $< \cdot, \cdot >$ is equivalent to the standard norm in $H^1(\mathbb{R}^d; p)$.

(i) Consider the BVP in its weak form (3.25). The integral on the righthand-side is a bounded linear functional on $\psi \in H_0^1$, since

$$\begin{aligned}\left| \int (h(x) - \hat{h}) \psi(x) p(x)\,\mathrm{d}x \right|^2 &\leq \int |h(x) - \hat{h}|^2 p(x)\,\mathrm{d}x \int |\psi(x)|^2 p(x)\,\mathrm{d}x \\ &\leq (\text{const.}) \int |\nabla\psi(x)|^2 p(x)\,\mathrm{d}x,\end{aligned}$$

where (B.8) is used to obtain the second inequality.

It follows from the Reisz representation theorem that there exists a unique $\phi \in H_0^1$ such that

$$< \phi, \psi >= \int (h(x) - \hat{h}) \psi(x) p(x)\,\mathrm{d}x,$$

for all $\psi \in H_0^1(\mathbb{R}^d; p)$. Thus ϕ is a weak solution of the BVP, satisfying (3.25).

(ii) Suppose ϕ is a weak solution. Using $\psi = \phi$ in (3.25),

$$\begin{aligned}\int |\nabla\phi|^2 p(x)\,\mathrm{d}x = \int (h(x) - \hat{h}) \phi(x) p(x)\,\mathrm{d}x &\leq \left(\int |h(x) - \hat{h}|^2 p(x)\,\mathrm{d}x \right)^{\frac{1}{2}} \left(\int |\phi(x)|^2 p(x)\,\mathrm{d}x \right)^{\frac{1}{2}} \\ &\leq \left(\int |h(x) - \hat{h}|^2 p(x)\,\mathrm{d}x \right)^{\frac{1}{2}} \left(\frac{1}{\lambda} \int |\nabla\phi(x)|^2 p(x)\,\mathrm{d}x \right)^{\frac{1}{2}}\end{aligned}$$

by (B.8). The estimate (3.27) follows.

(iii) For the final estimate (3.28), we need:

Lemma B.3.1 *Under Assumptions A1-A4, the weak solution ϕ of the BVP (3.25) belongs to $H^2(\mathbb{R}^d; p)$, with*

$$\int |D^2\phi|^2 p \, dx \leq \int \nabla\phi \cdot Gp \, dx \tag{B.9}$$

where the vector function $G \in L^2(\mathbb{R}^d; p)$ is defined by

$$G = D^2(\log p)\nabla\phi + \nabla h$$

and where $|D^2\phi|^2 = \sum_{j,k}(\frac{\partial^2\phi}{\partial x_j \partial x_k})^2$.

Proof First note that each entry of the Hessian matrix $D^2(\log p)$ is bounded, by Assumption A3, and that $\nabla h \in L^2(\mathbb{R}^d; p)$ by Assumption A4. Hence $G \in L^2(\mathbb{R}; p)$.

Next, elliptic regularity theory [60, Section 6.3 of the PDE text by Evans] applied to the weak solution $\phi \in H^1(\mathbb{R}^d; p)$ says that $\phi \in H^3_{loc}(\mathbb{R}^d)$. Hence the partial differential equation holds pointwise:

$$-\nabla \cdot (p\nabla\phi) = (h - \hat{h})p. \tag{B.10}$$

We differentiate with respect to x_k to obtain:

$$-\nabla \cdot \left(p\nabla \frac{\partial\phi}{\partial x_k} \right) - \nabla \left(\frac{\partial \log p}{\partial x_k} \right) \cdot (p\nabla\phi) - \frac{\partial \log p}{\partial x_k} \nabla \cdot (p\nabla\phi) = \frac{\partial h}{\partial x_k} p + (h - \hat{h}) \frac{\partial \log p}{\partial x_k} p.$$

The final terms on the left and right sides cancel, by equation (B.10). Thus the preceding formula becomes

$$-\nabla \cdot \left(p\nabla \frac{\partial\phi}{\partial x_k} \right) = G_k p, \tag{B.11}$$

where G_k denotes the kth component of $G(x)$.

Let $\beta(x) \geq 0$ be a smooth, compactly supported "bump" function, meaning $\beta(x)$ is radially decreasing with $\beta(0) = 1$. Let $s > 0$ and multiply (B.11) by $\beta(sx)^2 \frac{\partial\phi}{\partial x_k}$. Integrate by parts on the left side (noting the boundary terms vanish because β has compact support) to obtain

$$\int \nabla \left[\beta(sx)^2 \frac{\partial\phi}{\partial x_k} \right] \cdot (\nabla \frac{\partial\phi}{\partial x_k}) p \, dx = \int \beta(sx)^2 \frac{\partial\phi}{\partial x_k} G_k p \, dx.$$

The right hand side RHS $\to \int \frac{\partial \phi}{\partial x_k} G_k p \, dx$ by dominated convergence as $s \to 0$, since $\beta(0) = 1$. The left side,

$$\text{LHS} = \int \beta(sx)^2 \left| \nabla \frac{\partial \phi}{\partial x_k} \right|^2 p \, dx + 2s \int \frac{\partial \phi}{\partial x_k} \beta(sx) (\nabla \beta)(sx) \cdot \left(\nabla \frac{\partial \phi}{\partial x_k} \right) p \, dx.$$

Clearly the second term is bounded by

$$2s \|\nabla \beta\|_{L^\infty(\mathbb{R}^d)} \int \left| \frac{\partial \phi}{\partial x_k} \right| \beta(sx) \left| \nabla \frac{\partial \phi}{\partial x_k} \right| p \, dx \le s \|\nabla \beta\|_{L^\infty(\mathbb{R}^d)} \int \left[\left(\frac{\partial \phi}{\partial x_k} \right)^2 + \beta(sx)^2 \left| \nabla \frac{\partial \phi}{\partial x_k} \right|^2 \right] p \, dx$$

and so

$$\left(1 - s \|\nabla \beta\|_{L^\infty(\mathbb{R}^d)} \right) \int \beta(sx)^2 \left| \nabla \frac{\partial \phi}{\partial x_k} \right|^2 p \, dx - s \|\nabla \beta\|_{L^\infty(\mathbb{R}^d)} \int \left(\frac{\partial \phi}{\partial x_k} \right)^2 dx \le \text{LHS}.$$

Letting $s \to 0$ in LHS and RHS, and recalling that $\beta(x)$ is radially decreasing, we conclude from the monotone convergence theorem that

$$\int \left| \nabla \frac{\partial \phi}{\partial x_k} \right|^2 p \, dx \le \int \frac{\partial \phi}{\partial x_k} G_k p \, dx.$$

Summing over k completes the proof of the lemma.

Next we prove (3.28). We will use several times that

$$\int |\nabla \phi|^2 p \, dx \le \frac{1}{\lambda} \int |h - \hat{h}|^2 p \, dx \le \frac{1}{\lambda^2} \int |\nabla h|^2 p \, dx, \tag{B.12}$$

by (3.27) followed by (B.8) applied to the function $h - \hat{h} \in H_0^1(\mathbb{R}^d; p)$.

We have

$$\int \left| (D^2 \phi)(\nabla \phi) \right| p \, dx \le \int |D^2 \phi| |\nabla \phi| p \, dx \le \left(\frac{1}{\lambda^2} \int |\nabla h|^2 p \, dx \right)^{3/4} \left(\int |G|^2 p \, dx \right)^{1/4}$$

by Lemma B.3.1, Cauchy–Schwarz, and (B.12). The definition of G, the L^2-triangle inequality and (B.12) show that

$$\begin{aligned} \left(\int |G|^2 p \, dx \right)^{1/2} &\le \|D^2 (\log p)\|_{L^\infty} \left(\int |\nabla \phi|^2 p \, dx \right)^{1/2} + \left(\int |\nabla h|^2 p \, dx \right)^{1/2} \\ &\le \left(\frac{\|D^2 (\log p)\|_{L^\infty}}{\lambda} + 1 \right) \left(\int |\nabla h|^2 p \, dx \right)^{1/2}. \end{aligned}$$

The estimate (3.28) now follows.

Appendix C

Proofs for Chapter 4

C.1 Proof of Prop. 4.2.2

Differentiating $\rho_n^*(x,\lambda)$ in (4.8) with respect to λ, and subsequent evaluation yields:

$$\begin{aligned}
\frac{\partial \rho^*(x,\lambda)}{\partial \lambda} &= \frac{1}{\int \exp f_n(x',\lambda)\,\mathrm{d}x'} \frac{\partial \exp f_n(x,\lambda)}{\partial \lambda} - \frac{\exp f_n(x,\lambda)}{[\int \exp f_n(x',\lambda)\,\mathrm{d}x']^2} \frac{\partial \int \exp f_n(x',\lambda)\,\mathrm{d}x'}{\partial \lambda} \\
&= \frac{\exp f_n(x,\lambda)}{\int \exp f_n(x',\lambda)\,\mathrm{d}x'} \frac{\partial f_n(x,\lambda)}{\partial \lambda} - \frac{\exp f_n(x,\lambda)}{[\int \exp f_n(x',\lambda)\,\mathrm{d}x']^2} \int \exp f_n(x',\lambda) \frac{\partial f_n(x',\lambda)}{\partial \lambda}\,\mathrm{d}x' \\
&= \rho_n^*(x,\lambda) \left[\frac{\partial f_n(x,\lambda)}{\partial \lambda} - \int \rho_n^*(x',\lambda) \frac{\partial f_n(x',\lambda)}{\partial \lambda}\,\mathrm{d}x' \right] \\
&= \rho_n^*(x,\lambda) \cdot \left[h(x)^T [Y_n - \frac{1}{2} h(x)] - \int \rho_n^*(x',\lambda) h(x')^T [Y_n - \frac{1}{2} h(x')]\,\mathrm{d}x' \right] \\
&= \rho_n^*(x,\lambda) \cdot \left[(h(x) - \hat{h}_n(\lambda))^T Y_n - \frac{1}{2}|h(x)|^2 + \frac{1}{2} \int \rho_n^*(x',\lambda) |h(x')|^2\,\mathrm{d}x' \right],
\end{aligned} \tag{C.1}$$

where we define $\hat{h}_n(\lambda) := \int \rho_n^*(x,\lambda) h(x)\,\mathrm{d}x$ and $|h(\cdot)|^2 := h(\cdot)^T h(\cdot)$. Equation (C.1) is exactly (4.9) as desired. □

C.2 Proof of Thm. 4.2.3

It is only necessary to show that with this choice of $\{u, \mathsf{K}\}$ ((4.12)-(4.14)), we have that $\mathrm{d}\rho(x,\lambda) = \mathrm{d}\rho^*(x,\lambda)$, for all x and $\lambda \in [0,1]$, in the sense that they are defined by identical SDEs. Recall that $\mathrm{d}\rho^*$ is described as in (4.9), and $\mathrm{d}\rho$ according to the forward equation (4.11).

If ϕ_j solves the E-L BVP (4.12) then using $\mathsf{K} = [\nabla\phi_1^T, \ldots, \nabla\phi_m^T]$ we have,

$$\nabla \cdot (\rho \mathsf{K}) = -(h(x) - \hat{h})^T \rho. \tag{C.2}$$

On multiplying both sides of (4.13) by $-\rho$ and then taking the gradient, we obtain

$$\begin{aligned}
-\nabla\cdot(\rho u) &= \frac{1}{2}\nabla\cdot(\rho \mathsf{K}(h+\hat{h})) - \frac{1}{2}\nabla\cdot(\rho\Omega) \\
&= -\frac{1}{2}(h-\hat{h})^T(h-\hat{h}) + \frac{1}{2}\rho\sum_{j=1}^{m}\nabla\phi_j\cdot\nabla h_j^T - \frac{1}{2}\nabla\cdot(\rho\Omega) \\
&= -\frac{1}{2}|h|^2 + \frac{1}{2}\widehat{|h|^2},
\end{aligned} \tag{C.3}$$

where we use (C.2) and (4.14) to get the second and third equality, respectively.

Using (C.2)-(C.3) in the forward equation (4.11), we have

$$\mathrm{d}\rho = \rho\left[(h(x)-\hat{h})^T Y_n - \frac{1}{2}\left(|h|^2 - \widehat{|h|^2}\right)\right].$$

This is precisely the SDE (4.9), as desired. □

C.3 Proof of Prop. 4.2.4

Formula (4.19) is verified by direct substitution in the BVP (4.12) where the distribution ρ is multivariate Gaussian. To verify (4.20), first by taking the gradient of (4.19) we obtain:

$$\nabla\phi_j = \left[[\Sigma_\lambda H^T]_{1j},\ldots,[\Sigma_\lambda H^T]_{dj}\right]. \tag{C.4}$$

Substituting (C.4) to (4.14),

$$\nabla\cdot(\rho\Omega) = \frac{1}{2}\left[\mu_\lambda^T H^T H\mu_\lambda - \widehat{X^T H^T H X} + \sum_{j=1}^{m}\sum_{k=1}^{d} H_{jk}[\Sigma_\lambda H^T]_{kj}\right]. \tag{C.5}$$

Recall that:

$$\Sigma_\lambda = \widehat{XX^T} - \mu_\lambda\mu_\lambda^T,$$

and consider the gradient-form solution $\Omega = \nabla\varphi$, we have the RHS of (C.5):

$$\nabla\cdot(\rho\nabla\varphi) = 0.$$

This leads to the unique solution $\Omega = (0,\ldots,0)$ which is (4.20).

Appendix D

Proofs for Chapter 5

D.1 Derivation of the Forward Equation

We denote the filtration $\mathscr{B}_t = \sigma(X_0^i, N_s^{ll',i}, \tilde{N}_s^{k,i} : s \le t)$, where $\tilde{N}_s^{k,i}$ denote the Poisson counters with constant rate $\lambda = 1$, for $k = 1, 2, \ldots, d$. We recall that $\mathscr{Z}_t = \sigma(Z_s : s \le t)$ for $t \ge 0$. These two filtrations are *independent* by construction.

The particle evolution (5.5) is expressed,

$$X_t^i = X_0^i + \sum_{(l,l') \in E} \int_0^t A^{ll'} X_s^i \, \mathrm{d}N_s^{ll',i} + \sum_{k=1}^d \int_0^t B^k X_s^i \, \mathrm{d}\mathscr{C}_s^{k,i}.$$

For the linear system, there exists a unique solution that is adapted to the larger filtration $\mathscr{B}_t \vee \mathscr{Z}_t = \sigma(X_0^i, N_s^{ll',i}, \tilde{N}_s^{k,i}, Z_s : s \le t)$. In fact, there is a functional F_t such that,

$$X_t^i = F_t(X_0^i, N_{[0:t]}^{ll',i}, \tilde{N}_{[0:t]}^{k,i}, Z_{[0:t]}), \tag{D.1}$$

where $Z_{[0:t]} := \{Z_s : 0 \le s \le t\}$ denotes the trajectory.

The conditional distribution of X_t^i given $\mathscr{Z}_t = \sigma(Z_s : s \le t)$ was introduced in Sec. 5.2: Its density is denoted $p(\cdot, t)$, defined by any bounded function $\phi : \mathbb{S} \to \mathbb{R}$ via,

$$\mathsf{E}[\phi(X_t^i) \mid \mathscr{Z}_t] = \sum_{l=1}^d p(l,t)\phi^l =: \langle p_t, \phi \rangle,$$

where $\phi^l := \phi(e_l)$ and with slight abuse of notation we write $\phi = (\phi^1, \phi^2, \ldots, \phi^l)$.

We begin with a result that is the key to proving Prop. 5.2.1.

Lemma D.1.1 *Suppose that f is an $\mathscr{B}_t \vee \mathscr{Z}_t$-adapted process satisfying $\mathsf{E}\int_0^t |f(s)|^2\,\mathrm{d}s < \infty$. Then,*

$$\mathsf{E}\Big[\int_0^t f(s)\,\mathrm{d}s|\mathscr{Z}_t\Big] = \int_0^t \mathsf{E}[f(s)|\mathscr{Z}_s]\,\mathrm{d}s, \tag{D.2}$$

$$\mathsf{E}\Big[\int_0^t f(s)\,\mathrm{d}N_s^{l,l',i}|\mathscr{Z}_t\Big] = \int_0^t \mathsf{E}[f(s)|\mathscr{Z}_s]\lambda_{l'l}\,\mathrm{d}s. \tag{D.3}$$

$$\mathsf{E}\Big[\int_0^t f(s)\,\mathrm{d}\mathscr{C}_s^{k,i}|\mathscr{Z}_t\Big] = \int_0^t \mathsf{E}[f(s)|\mathscr{Z}_s](\mathsf{K}(k,s)\,\mathrm{d}Z_s + u(k,s)\,\mathrm{d}s). \tag{D.4}$$

We now provide a proof of the Proposition 5.2.1.

Proof of Proposition 5.2.1 Applying Itô's Lemma to equation (5.5) gives, for any bounded function $\phi : \mathbb{S} \to \mathbb{R}$,

$$\mathrm{d}\phi(X_t^i) = \mathscr{L}\phi(X_t^i)\,\mathrm{d}t + \sum_{k=1}^d \Big[\phi(X_t^i + B^k X_t^i) - \phi(X_t^i)\Big]\,\mathrm{d}\mathscr{C}_t^{k,i},$$

where $\mathscr{L}\phi(e_l) := \sum_{l'=1}^d \lambda_{l'l}\phi(e_{l'})$. Therefore,

$$\phi(X_t^i) = \phi(X_0^i) + \int_0^t \mathscr{L}\phi(X_s^i)\,\mathrm{d}s + \sum_{k=1}^d \int_0^t \Big[\phi(X_s^i + B^k X_s^i) - \phi(X_s^i)\Big]\,\mathrm{d}\mathscr{C}_s^{k,i}.$$

Taking conditional expectation on both sides,

$$\langle p_t, \phi\rangle = \mathsf{E}[\phi(X_0^i)|\mathscr{Z}] + \mathsf{E}\left[\int_0^t \mathscr{L}\phi(X_s^i)\,\mathrm{d}s|\mathscr{Z}\right] + \sum_{k=1}^d \mathsf{E}\left[\int_0^t [\phi(X_s^i + B^k X_s^i) - \phi(X_s^i)]\,\mathrm{d}\mathscr{C}_s^{k,i}|\mathscr{Z}\right].$$

Using Lemma D.1.1, we have that

$$\langle p_t, \phi\rangle = \langle p_0, \phi\rangle + \int_0^t \langle p_s, \mathscr{L}\phi\rangle\,\mathrm{d}s + \sum_{k=1}^d \int_0^t \langle p_s, \phi(X_s^i + B^k X_s^i) - \phi(X_s^i)\rangle(\mathsf{K}(k,s)\,\mathrm{d}Z_s + u(k,s)\,\mathrm{d}s).$$

Using integration by parts and the definition of B^k we conclude that:

$$\mathrm{d}p(k,t) = \sum_{l=1}^d \lambda_{kl}p(l,t)\,\mathrm{d}t + \sum_{k'\neq k}(\mathsf{K}(k,t)\,\mathrm{d}Z_t + u(k,t)\,\mathrm{d}t)p(k',t) - \sum_{l'\neq k}(\mathsf{K}(l',t)\,\mathrm{d}Z_t + u(l',t)\,\mathrm{d}t)p(k,t),\ k = 1,\ldots,d. \tag{D.5}$$

The forward equation (5.8) follows by expressing equation (D.5) in the vector form. □

We now provide a proof of Lemma D.1.1.

Proof of Lemma D.1.1 The key is the functional form (D.1) of the solution X_t^i: It says that apart from the past values of $\mathscr{Z}_t$, the solution depends only upon initial condition X_0^i and time homogeneous Poisson process $\tilde{N}_t^{k,i}$ and $N_t^{ll',i}$ that are all independent of $\mathscr{Z}_t$.

First we suppose that f, K and u are simple, i.e.,

$$f(s) = \sum_{j=1}^{m} F_j 1_{(a_j,b_j]}(s),$$
$$\mathsf{K}(k,s) = \sum_{j=1}^{m} \mathsf{K}_j^k 1_{(a_j,b_j]}(s), \quad u(k,s) = \sum_{j=1}^{m} u_j^k 1_{(a_j,b_j]}(s).$$

where $(a_j,b_j]$ are disjoint intervals of $[0,t]$. For general f, K and u satisfying the assumptions of the lemma, the result will then follow via an application of the dominated convergence theorem.

Once we restrict to simple functions, the essence of the proof is to establish the identity,

$$\mathsf{E}(F_j|\mathscr{Z}_t) = \mathsf{E}(F_j|\mathscr{Z}_{a_j}). \tag{D.6}$$

Under the measurability assumption we can write $F_j = \Psi(\zeta,\xi)$, where $\zeta \in \mathscr{Z}_{a_j}$, $\xi \in \mathscr{B}_{a_j}$ are random variables, and Ψ is a real-valued function. The random variable ξ is independent of $\mathscr{Z}_t$, so that

$$\mathsf{E}(F_j|\mathscr{Z}_t) = \mathsf{E}(\bar{\Psi}(\zeta)|\mathscr{Z}_t),$$

with $\bar{\Psi}(\,\cdot\,) = \mathsf{E}[\Psi(\,\cdot\,,\xi)]$. Using the fact that $\zeta \in \mathscr{Z}_{a_j} \subset \mathscr{Z}_t$ we obtain (D.6):

$$\mathsf{E}(F_j|\mathscr{Z}_t) = \mathsf{E}(\bar{\Psi}(\zeta)|\mathscr{Z}_t) = \mathsf{E}(F_j|\mathscr{Z}_{a_j}).$$

The desired results follow easily from (D.6): To obtain (D.2),

$$\begin{aligned}\mathsf{E}\Big(\int_0^t f(s)\,\mathrm{d}s \mid \mathscr{Z}_t\Big) &= \sum_{j=1}^{m} \mathsf{E}(F_j(b_j-a_j) \mid \mathscr{Z}_t) = \sum_{j=1}^{m} \mathsf{E}(F_j \mid \mathscr{Z}_{a_j})(b_j-a_j)\\ &= \int_0^t \mathsf{E}(f(s) \mid \mathscr{Z}_s)\,\mathrm{d}s,\end{aligned}$$

To obtain (D.3):

$$\begin{aligned}\mathsf{E}\Big[\int_0^t f(s)\,\mathrm{d}N_s^{ll',i} \mid \mathscr{Z}_t\Big] &= \sum_{j=1}^{m} \mathsf{E}[F_j(N_{b_j}^{ll',i} - N_{a_j}^{ll',i}) \mid \mathscr{Z}_t] = \sum_{j=1}^{m} \mathsf{E}[F_j \mid \mathscr{Z}_{a_j}]\mathsf{E}[N_{b_j}^{ll',i} - N_{a_j}^{ll',i}]\\ &= \sum_{j=1}^{m} \mathsf{E}[F_j \mid \mathscr{Z}_{a_j}]\lambda_{l'l}(b_j-a_j)\\ &= \int_0^t \mathsf{E}[f(s) \mid \mathscr{Z}_s]\lambda_{l'l}\,\mathrm{d}s,\end{aligned}$$

where the third equality uses the facts $N_t^{ll',i}$ is a homogeneous Poisson process with rate $\lambda_{l'l}$. The proof of (D.4) is

similar:

$$\begin{aligned}\mathsf{E}\Big[\int_0^t f(s)\,\mathrm{d}\mathscr{C}_s^{k,i} \mid \mathscr{Z}_t\Big] &= \sum_{j=1}^m \mathsf{E}[F_j(\mathscr{C}_{b_j}^{k,i} - \mathscr{C}_{a_j}^{k,i}) \mid \mathscr{Z}_t] = \sum_{j=1}^m \mathsf{E}[F_j \mid \mathscr{Z}_{a_j}]\mathsf{E}[\mathscr{C}_{b_j}^{k,i} - \mathscr{C}_{a_j}^{k,i} \mid \mathscr{Z}_t] \\ &= \sum_{j=1}^m \mathsf{E}[F_j \mid \mathscr{Z}_{a_j}][\mathsf{K}_j^k(Z_{b_j} - Z_{a_j}) + u_j^k(b_j - a_j)] \\ &= \int_0^t \mathsf{E}[f(s) \mid \mathscr{Z}_s](\mathsf{K}(k,s)\,\mathrm{d}Z_s + u(k,s)\,\mathrm{d}s).\end{aligned}$$

where the third equality follows from the following facts that: (i) $\mathscr{C}_t^{k,i}$ is a non-homogeneous Poisson process with $\mathsf{E}[\mathscr{C}_t^{k,i} - \mathscr{C}_s^{k,i} \mid \mathscr{Z}_t] = \int_s^t \mathsf{K}(k,\tau)\,\mathrm{d}Z_\tau + u(k,\tau)\,\mathrm{d}\tau$; (ii) Z_t is adapted to $\mathscr{Z}_t$, and $a_i < b_i \le t$ for each i. □

D.2 Proof of Prop. 5.2.2.

The matrix, $D := (p_t \otimes 1 - I)$, has rank $d-1$ with null-space $\mathscr{N}(D) = \mathrm{span}\{p_t\}$ and $\mathscr{N}(D^T) = \mathrm{span}\{1\}$. By the application of the closed-range theorem:

(i) A solution exists because the righthand-side, $-H_t p_t$, lies in the complement of $\mathscr{N}(D^T)$:

$$\langle 1, -H_t p_t\rangle = -\sum_{l=1}^d (h(l) - \hat{h}_t)p(l,t) = 0.$$

(ii) A unique solution exists in the complement of $\mathscr{N}(D)$. Denote it as K_t^0. By construction $\langle \mathsf{K}_t^0, p_t\rangle = 0$ and it is the minimal 2-norm solution.

That $H_t p_t$ is a particular solution is verified by direct substitution. The form of the general solution (5.11) then follows. The explicit formula for K_t^0 is obtained by choosing c such that $\langle \mathsf{K}_t^0, p_t\rangle = \langle H_t p_t + c p_t, p_t\rangle = 0$.

The property (P0) is verified by direct substitution. For $p(k,t) = 0$, the k^{th} equation of (5.9) is given by,

$$-\mathsf{K}(k,t) = 0.$$

Appendix E

Proofs for Chapter 6

E.1 Derivation of the Exact Filtering Equations (6.6)-(6.9)

Derivation of (6.6): For each fixed mode $\theta_t = e_m \in \{e_1, e_2, \ldots, e_M\}$, the state process X_t is a Markov process with Kolmogorov forward operator $\mathscr{L}_m^\dagger$. Therefore, the joint process $(X_t, \theta_t)^T$ is a Markov process with generator $\mathscr{L}^\dagger + Q$ where $\mathscr{L}^\dagger := \text{diag}\{\mathscr{L}_m^\dagger\}$. Defining $\int_A \pi_m^*(x,t)\,\mathrm{d}x := \mathsf{P}\{X_t \in A, \theta_t = e_m\}$ and $\pi^*(x,t) := (\pi_1^*(x,t), \cdots, \pi_M^*(x,t))^T$ we have that

$$\frac{\partial \pi^*}{\partial t}(x,t) = \mathscr{L}^\dagger \pi^*(x,t) + Q^T \pi^*(x,t).$$

Recall that the posterior distribution was defined by $\int_A q_m^*(x,t)\,\mathrm{d}x := \mathsf{P}\{[X_t \in A, \theta_t = e_m] | \mathscr{Z}\}$. By applying the fundamental filtering theorem for Gaussian observations (see [107]) to (6.3) we have:

$$\mathrm{d}q_m^* = \mathscr{L}_m^\dagger(q_m^*)\,\mathrm{d}t + \sum_{l=1}^M q_{lm} q_l^*\,\mathrm{d}t + (h^m - \hat{h}_t)(\mathrm{d}Z_t - \hat{h}_t\,\mathrm{d}t) q_m^*,$$

where $\hat{h}_t := \sum_{m=1}^M \int_{\mathbb{R}} h^m(x) q_m^*(x,t)\,\mathrm{d}x$. □

Derivation of (6.7) and (6.8): By definition, we have,

$$p^*(x,t) = \sum_{m=1}^M q_m^*(x,t), \tag{E.1}$$

$$\mu_t^m = \int_{\mathbb{R}} q_m^*(x,t)\,\mathrm{d}x. \tag{E.2}$$

Taking derivatives on both sides of (E.1) and (E.2) gives the desired result. □

Derivation of (6.9): By definition $q_m^* = \rho_m^* \mu_t^m$. Applying Itô's differentiation rule we have:

$$\mathrm{d}\rho_m^* = \frac{\mathrm{d}q_m^*}{\mu_t^m} + q_m^*\,\mathrm{d}\left(\frac{1}{\mu_t^m}\right) + \mathrm{d}q_m^*\,\mathrm{d}\left(\frac{1}{\mu_t^m}\right), \tag{E.3}$$

where $\mathrm{d}\left(\frac{1}{\mu_t^m}\right) = -\frac{\mathrm{d}\mu_t^m}{(\mu_t^m)^2} + \frac{(\mathrm{d}\mu_t^m)^2}{(\mu_t^m)^3}$. Substituting (6.6) and (6.7) into (E.3) we obtain the desired result. □

E.2 Proof of Consistency for IMM-FPF

We express the feedback particle filter (6.11) as:

$$\mathrm{d}X_t^{i;m} = a^m(X_t^{i;m})\,\mathrm{d}t + \sigma^m\,\mathrm{d}B_t^{i;m} + \mathsf{K}^m(X_t^{i;m},t)\,\mathrm{d}Z_t + \tilde{u}(X_t^{i;m},t)\,\mathrm{d}t + u^m(X_t^{i;m},X_t^{i;-m})\,\mathrm{d}t,$$

where

$$\tilde{u}(x,t) = -\frac{1}{2}\mathsf{K}^m(x,t)(h^m(x)+\widehat{h_t^m}) + \Omega(x,t), \tag{E.4}$$

and $\Omega := \frac{1}{2}\mathsf{K}^m(\mathsf{K}^m)'$ is the Wong-Zakai correction term for (6.11). The evolution equation for ρ_m is given by:

$$\mathrm{d}\rho_m = \mathscr{L}_m^\dagger\rho_m\,\mathrm{d}t - \frac{\partial}{\partial x}(\rho_m\mathsf{K}^m)\,\mathrm{d}Z_t - \frac{\partial}{\partial x}(\rho_m\tilde{u})\,\mathrm{d}t - \frac{\partial}{\partial x}(\rho_m u^m)\,\mathrm{d}t + \frac{1}{2}\frac{\partial^2}{\partial x^2}\left(\rho_m(\mathsf{K}^m)^2\right)\mathrm{d}t. \tag{E.5}$$

The derivation of this equation is similar to the basic FPF case (see Proposition 2 in [156]) and thus omitted here.

It is only necessary to show that with the choice of $\{\mathsf{K}^m, u^m\}$ according to (6.13)-(6.14), we have $\mathrm{d}\rho_m(x,t) = \mathrm{d}\rho_m^*(x,t)$, for all x and t, in the sense that they are defined by identical stochastic differential equations. Recall $\mathrm{d}\rho_m^*$ is defined according to the modified K-S equation (6.9), and $\mathrm{d}\rho_m$ according to the forward equation (E.5).

If K^m solves the E-L BVP (6.13) then we have:

$$\frac{\partial}{\partial x}(\rho_m\mathsf{K}^m) = -(h^m - \widehat{h_t^m})\rho_m. \tag{E.6}$$

On multiplying both sides of (E.4) by $-\rho_m$, we have:

$$\begin{aligned}
-\rho_m\tilde{u} &= \frac{1}{2}(h^m-\widehat{h_t^m})\rho_m\mathsf{K}^m - \frac{1}{2}(\rho_m\mathsf{K}^m)\frac{\partial\mathsf{K}^m}{\partial x} + \widehat{h_t^m}\rho_m\mathsf{K}^m \\
&= -\frac{1}{2}\frac{\partial(\rho_m\mathsf{K}^m)}{\partial x}\mathsf{K}^m - \frac{1}{2}(\rho_m\mathsf{K}^m)\frac{\partial\mathsf{K}^m}{\partial x} + \widehat{h_t^m}\rho_m\mathsf{K}^m \\
&= -\frac{1}{2}\frac{\partial}{\partial x}\left(\rho_m(\mathsf{K}^m)^2\right) + \widehat{h_t^m}\rho_m\mathsf{K}^m
\end{aligned}$$

where we used (E.6) to obtain the second equality. Differentiating once with respect to x and using (E.6) once again,

$$-\frac{\partial}{\partial x}(\rho_m\tilde{u}) + \frac{1}{2}\frac{\partial^2}{\partial x^2}\left(\rho_m(\mathsf{K}^m)^2\right) = -\widehat{h_t^m}(h^m-\widehat{h_t^m})\rho_m. \tag{E.7}$$

Substituting (6.13), (6.14) and (E.7) to (E.5) and after some simplifications, we obtain:

$$\mathrm{d}\hat{p}_m = \mathscr{L}_m^\dagger\hat{p}_m\,\mathrm{d}t + (h^m-\widehat{h_t^m})(\mathrm{d}Z_t - \widehat{h_t^m}\,\mathrm{d}t)\hat{p}_m + \frac{1}{\mu_t^m}\sum_{l=1}^M q_{lm}\mu_t^l(\rho_l-\rho_m)\,\mathrm{d}t.$$

This is precisely the SDE (6.9), as desired.

E.3 Alternate Derivation of (6.15)

The aim of this section is to derive, formally, the update part of the continuous time filter (6.15) by taking a continuous time limit of the discrete-time algorithm for evaluation of association probability. The procedure for taking the limit is similar to Sec 6.8 in [86] for derivation of the K-S equation.

At time t, we have M possible modes for the SHS. The discrete-time filter for mode association probability is obtained by using Bayes' rule (see [10]):

$$\mathsf{P}\{\theta_t = e_m | \mathscr{Z}, \Delta Z_t\} = \frac{\mathsf{P}\{\Delta Z_t | \theta_t = e_m\} \mathsf{P}\{\theta_t = e_m | \mathscr{Z}\}}{\sum_{l=1}^{M} \mathsf{P}\{\Delta Z_t | \theta_t = e_l\} \mathsf{P}\{\theta_t = e_l | \mathscr{Z}\}}. \tag{E.8}$$

Rewrite:

$$\begin{aligned} \mathsf{P}\{\Delta Z_t | \theta_t = e_m\} &= \int \mathsf{P}\{\Delta Z_t | \theta_t = e_m, X_t = x\} \rho_m(x,t)\, \mathrm{d}x \\ &= L_m(\Delta Z_t). \end{aligned} \tag{E.9}$$

where $L_m(\Delta Z_t) := \frac{1}{\sqrt{2\pi\Delta t}} \int_{\mathbb{R}} \exp\left[-\frac{(\Delta Z_t - h^m(x)\Delta t)^2}{2\Delta t} \right] \rho_m(x,t)\, \mathrm{d}x$.

Now, recall $\mu_t^m = \mathsf{P}\{\theta_t = e_m | \mathscr{Z}\}$, the increment in the measurement update step (see Sec 6.8 in [86]) is given by

$$\Delta\mu_t^m := \mathsf{P}\{\theta_t = e_m | \mathscr{Z}, \Delta Z_t\} - \mathsf{P}\{\theta_t = e_m | \mathscr{Z}\}. \tag{E.10}$$

Using (E.8) and (E.10), we have:

$$\Delta\mu_t^m = E^m(\Delta t, \Delta Z_t)\mu_t^m - \mu_t^m, \tag{E.11}$$

where

$$E^m(\Delta t, \Delta Z_t) = \frac{\mathsf{P}\{\theta_t = e_m | \mathscr{Z}, \Delta Z_t\}}{\mathsf{P}\{\theta_t = e_m | \mathscr{Z}\}}. \tag{E.12}$$

We expand $E^m(\Delta t, \Delta Z_t)$ as a multivariate series about $(0,0)$:

$$E^m(\Delta t, \Delta Z_t) = E^m(0,0) + E^m_{\Delta t}(0,0)\Delta t + E^m_{\Delta Z_t}(0,0)\Delta Z_t + \frac{1}{2} E^m_{\Delta Z_t, \Delta Z_t}(0,0)\, \mathrm{d}Z_t^2 + o(\Delta t). \tag{E.13}$$

By direct evaluation, we obtain:

$$
\begin{aligned}
&E^m(0,0) = 1, \\
&E^m_{\Delta t}(0,0) = \frac{1}{2}\left(\widehat{h_t^2} - \widehat{(h_t^m)^2}\right), \qquad E^m_{\Delta Z_t}(0,0) = \widehat{h_t^m} - \hat{h}_t \\
&E^m_{\Delta Z_t, \Delta Z_t}(0,0) = \widehat{(h_t^m)^2} - 2\widehat{h_t^m}\hat{h}_t + 2\hat{h}_t^2 - \widehat{h_t^2}
\end{aligned}
$$

where $\widehat{(h_t^m)^2} := \int_{\mathbb{R}} (h^m(x))^2 \rho_m(x,t)\,\mathrm{d}x$ and $\widehat{h_t^2} := \sum_{m=1}^M \mu_t^m \widehat{(h_t^m)^2}$.

By using Itô's rules,

$$\mathsf{E}[\Delta Z_t \Delta Z_t] = \Delta t.$$

This gives

$$E^m(\Delta t, \Delta Z_t) = 1 + (\widehat{h_t^m} - \hat{h}_t)(\Delta Z_t - \hat{h}_t \Delta t) \tag{E.14}$$

Substituting (E.14) to (F.11) we obtain the expression for $\Delta\mu_t^m$, which equals the measurement update part of the continuous-time filter.

Remark 11 *During a discrete-time implementation, one can use* (E.8)-(F.7) *to obtain association probability. In* (E.8)*,* $L_m(\mathrm{d}Z_t)$ *is approximated by using particles:*

$$L_m(\Delta Z_t) \approx \frac{1}{N}\frac{1}{\sqrt{2\pi\Delta t}} \sum_{i=1}^N \exp\left[-\frac{(\Delta Z_t - h^m(X_t^{i;m})\Delta t)^2}{2\Delta t}\right].$$

Appendix F

Proofs for Chapter 7

F.1 Exact Filter for p^*

The exact nonlinear filter for p^* is derived as an application of IMM-FPF, which is described in Sec. 6.2.

Rewrite (7.3) in the vector form:

$$\mathrm{d}\underline{Z}_t = \underline{\chi}(A_t)h(X_t)\,\mathrm{d}t + \mathrm{d}\underline{W}_t,$$

where $\underline{Z}_t := (Z_t^1,\ldots,Z_t^M)$, $\underline{\chi}(A_t) := (\chi_t^1,...,\chi_t^M)$, $\chi_t^m = 1_{[A_t=m]}$, and $\underline{W}_t := (W_t^1,...,W_t^M)$.

On applying Thm. 6.2.1, the conditional distribution of X_t satisfies:

$$\mathrm{d}p^* = \mathscr{L}^\dagger p^*\,\mathrm{d}t + \sum_{m=1}^{M}(\underline{\chi}(m)h - \underline{\hat{h}}_t)^T(\mathrm{d}\underline{Z}_t - \underline{\hat{h}}_t\,\mathrm{d}t)\beta_t^m\rho_m^*, \tag{F.1}$$

where $\beta_t^m := \mathsf{P}\{[A_t=m]|\underline{\mathscr{Z}}_t\}$, $\rho_m^*(\cdot,t) := \mathsf{P}\{\cdot|[A_t=m],\underline{\mathscr{Z}}_t\}$, $\underline{\hat{h}}_t := \mathsf{E}[\underline{\chi}(A_t)h(X_t)|\underline{\mathscr{Z}}_t] = (\beta_t^1\widehat{h_t^1},\ldots,\beta_t^M\widehat{h_t^M})$ and $\widehat{h_t^m} := \int h(x)\rho_m^*(x,t)\,\mathrm{d}x$. Simplification of (F.1) leads to:

$$\mathrm{d}p^* = \mathscr{L}^\dagger(p^*)\,\mathrm{d}t + \sum_{m=1}^{M}\beta_t^m(h\rho_m^* - \widehat{h_t^m}p^*)\,(\mathrm{d}Z_t^m - \beta_t^m\widehat{h_t^m}). \tag{F.2}$$

In (F.2) p^* is coupled with the mode probability β_t^m and the mode conditional distribution ρ_m^*. The exact filtering equations of β_t^m and ρ_m^* can be similarly derived using Thm. 6.2.1 and thus are omitted here.

F.2 Association Probability Filter for β_t^m

For the sake of notational simplicity, we will work with one-dimensional observations, i.e., $h:\mathbb{R}^d\to\mathbb{R}$. Extension to higher dimensions is straightforward.

The transition intensity matrix for the jump Markov process A_t is denoted as Λ with

$$\Lambda_{mm'} = \begin{cases} -Mq & \text{if } m = m' \\ q & \text{if } m \neq m'. \end{cases} \tag{F.3}$$

On applying Thm. 6.2.1, the conditional distribution of A_t satisfies:

$$\mathrm{d}\beta_t^m = \sum_{l=0}^{M} \Lambda_{lm}\beta_t^l \,\mathrm{d}t + (\widehat{\underline{h}_t^m} - \hat{\underline{h}}_t)^T (\mathrm{d}\underline{Z}_t - \hat{\underline{h}}_t \,\mathrm{d}t)\beta_t^m, \tag{F.4}$$

where $\widehat{\underline{h}_t^m} := \widehat{h_t^m}\underline{\chi}(m)$. Substituting (F.3) to (F.4):

$$\mathrm{d}\beta_t^m = q[1-(M+1)\beta_t^m]\,\mathrm{d}t + \beta_t^m \left(\widehat{h_t^m}\,\mathrm{d}Z_t^m - \sum_{j=1}^{M} \beta_t^j \widehat{h_t^j}\,\mathrm{d}Z_t^j \right) + \beta_t^m \left[\sum_{j=1}^{M} (\beta_t^j)^2 \left(\widehat{h_t^j}\right)^2 - \beta_t^m (\widehat{h_t^m})^2 \right] \mathrm{d}t. \tag{F.5}$$

Under Assumption. 7.2.1, we have $\widehat{h_t^m} := \mathsf{E}[h(X_t)|[A_t = m], \underline{\mathscr{Z}}_t] \approx \mathsf{E}[h(X_t)|\underline{\mathscr{Z}}_t] =: \hat{h}$ for all $m \in \{1,\ldots,M\}$. This simplifies (F.5) to (7.5)-(7.6), as desired.

F.3 An Alternate Derivation of (7.5)-(7.6)

The aim of this section is to formally derive the update part of the continuous-time filter (7.5)-(7.6) by taking a continuous-time limit of the discrete-time algorithm for evaluation of association probability. The procedure for taking the limit is identical to the original proof of the K-S equation in [100], and the proof in Sec 6.8 of the classical text [86].

At time t, we have M observations $\Delta\underline{Z}_t = (\Delta Z_t^1, \Delta Z_t^2, ..., \Delta Z_t^M)$, at most one of which originates from the target. The discrete-time filter for association probability is obtained by using the Bayes' rule:

$$\mathsf{P}\{[A_t = m]|\mathscr{Z}_t, \Delta\underline{Z}_t\} = \frac{\mathsf{P}\{\Delta\underline{Z}_t|[A_t = m]\}\mathsf{P}\{[A_t = m]|\mathscr{Z}_t\}}{\sum_{j=0}^{M} \mathsf{P}\{\Delta\underline{Z}_t|[A_t = j]\}\mathsf{P}\{[A_t = j]|\mathscr{Z}_t\}}. \tag{F.6}$$

This equation appears also in the derivation of the classical discrete-time PDA algorithm (equation (6-32) in [9]). The conditional probabilities are evaluated as: for $m = 1,\ldots,M$,

$$\mathsf{P}\{\Delta\underline{Z}_t|[A_t = m]\} = \mathsf{P}\{\Delta Z_t^m|[A_t = m]\} \prod_{j \neq m} \mathsf{P}_0\{\Delta Z_t^j\}, \tag{F.7}$$

and for $m = 0$,

$$\mathsf{P}\{\Delta\underline{Z}_t|[A_t = 0]\} = \prod_{j=1}^{M} \mathsf{P}_0\{\Delta Z_t^j\}, \tag{F.8}$$

where

$$\begin{aligned}\mathsf{P}\{\Delta Z_t^m|[A_t = m]\} &= \frac{1}{(2\pi)^{\frac{s}{2}}\sqrt{\Delta t}} \int_{\mathbb{R}^d} \exp\left[-\frac{|\Delta Z_t^m - h(x)\Delta t|^2}{2\Delta t}\right] p(x,t)\,\mathrm{d}x, \\ \mathsf{P}_0\{\Delta Z_t^j\} &= \frac{1}{(2\pi)^{\frac{s}{2}}\sqrt{\Delta t}} \exp\left[-\frac{|\Delta Z_t^j|^2}{2\Delta t}\right],\end{aligned} \tag{F.9}$$

where Assumption. 7.2.1 is used to obtain (F.9). The formula for P_0 is based on the assumption of the Gaussian clutter model (see Sec. 7.2.1). This is different from the more standard model of clutter, popular in discrete-time settings, whereby the independent observations are uniformly and independently distributed in a "coverage area" V (see [8,9]).

Denote $\beta_t^m = \mathsf{P}\{[A_t = m]|\mathscr{Z}_t\}$, the increment in the observation update step (see Sec 6.8 in [86]) is given by

$$\Delta\beta_t^m := \mathsf{P}\{[A_t = m]|\mathscr{Z}_t, \Delta Z_t\} - \mathsf{P}\{[A_t = m]|\mathscr{Z}_t\}. \tag{F.10}$$

Using (F.6) and (F.10), we have:

$$\Delta\beta_t^m = E^m(\Delta t, \Delta\underline{Z}_t)\beta_t^m - \beta_t^m, \tag{F.11}$$

where

$$E^m(\Delta t, \Delta\underline{Z}_t) := \frac{\mathsf{P}\{[A_t = m]|\mathscr{Z}_t, \Delta\underline{Z}_t\}}{\mathsf{P}\{[A_t = m]|\mathscr{Z}_t\}} = \frac{\mathsf{P}\{\Delta\underline{Z}_t|[A_t = m]}{\sum_{j=0}^{M} \mathsf{P}\{\Delta\underline{Z}_t|[A_t = j]\}\mathsf{P}\{[A_t = j]|\mathscr{Z}_t\}}.$$

Using Itô's rule,

$$(\Delta Z_t^j)^T \Delta Z_t^k = \begin{cases} \Delta t, & \text{if j = k,} \\ 0, & \text{otherwise,} \end{cases}$$

we have for $m = 1, \ldots, M$,

$$E^m(\Delta t, \Delta\underline{Z}_t) = \frac{\int \exp\left[h^T(x)\Delta Z_t^m - \frac{1}{2}h^T(x)h(x)\Delta t\right] p(x,t)\,\mathrm{d}x}{\sum_{l=1}^{M} \beta_t^l \int \exp\left[(h^T(x)\Delta Z_t^l - \frac{1}{2}h^T(x)h(x)\Delta t\right] p(x,t)\,\mathrm{d}x + \beta_t^0},$$

and for $m = 0$,

$$E^0(\Delta t, \Delta\underline{Z}_t) = \frac{1}{\sum_{l=1}^{M} \beta_t^l \int \exp\left[(h^T(x)\Delta Z_t^l - \frac{1}{2}h^T(x)h(x)\Delta t\right] p(x,t)\,\mathrm{d}x + \beta_t^0}.$$

Following the derivation procedure in [86], we expand $E^m(\Delta t, \Delta\underline{Z}_t)$ as a multivariate series about $(0, \underline{0})$:

$$E^m(\Delta t, \Delta\underline{Z}_t) = E^m(0,\underline{0}) + E^m_{\Delta t}(0,\underline{0})\Delta t + \sum_{j=1}^{M} E^m_{\Delta Z_t^j}(0,\underline{0})\Delta Z_t^j + \frac{1}{2}\sum_{j,k=1}^{M} (\Delta Z_t^j)^T E^m_{\Delta Z_t^j, \Delta Z_t^k}(0,\underline{0})\Delta Z_t^k + o(\Delta t).$$

By direct evaluation, we obtain: for $m = 1, \ldots, M$,

$$E^m(0,\underline{0}) = 1, \quad E^m_{\Delta t}(0,\underline{0}) = -\frac{1}{2}\beta_t^0 \widehat{|h^2|},$$
$$E^m_{\Delta Z_t^j}(0,\underline{0}) = -\beta_t^j \hat{h}^T, \quad E^m_{\Delta Z_t^j, \Delta Z_t^j}(0,\underline{0}) = 2(\beta_t^j)^2 |\hat{h}|^2 - \beta_t^j \widehat{|h^2|}, \quad j \neq m,$$
$$E^m_{\Delta Z_t^m}(0,\underline{0}) = (1-\beta_t^m)\hat{h}^T, \quad E^m_{\Delta Z_t^m, \Delta Z_t^m}(0,\underline{0}) = (1-\beta_t^m)\widehat{|h^2|} - 2\beta_t^m(1-\beta_t^m)|\hat{h}|^2,$$

and for $m = 0$,

$$E^0(0,\underline{0}) = 1, \quad E^0_{\Delta t}(0,\underline{0}) = \frac{1}{2}(1-\beta_t^0)\widehat{|h^2|},$$
$$E^0_{\Delta Z_t^j}(0,\underline{0}) = -\beta_t^j \hat{h}^T, \quad E^0_{\Delta Z_t^j, \Delta Z_t^j}(0,\underline{0}) = 2(\beta_t^j)^2 |\hat{h}|^2 - \beta_t^j \widehat{|h^2|}, \quad j = 1, \ldots, M,$$

where $\hat{h} := \mathsf{E}[h(X_t)|\mathscr{Z}_t]$, $|\hat{h}|^2 := \hat{h}^T\hat{h}$ and $\widehat{|h^2|} := \mathsf{E}[|h(X_t)|^2|\mathscr{Z}_t]$.

By using Itô's rule again, we obtain the simplified expression: for $m = 1, \ldots, M$,

$$E^m(\Delta t, \Delta \underline{Z}_t) = 1 + \hat{h}^T \left(\Delta Z_t^m - \sum_{j=1}^M \beta_t^j \Delta Z_t^j \right) + |\hat{h}|^2 \left(\sum_{j=1}^M (\beta_t^j)^2 - \beta_t^m \right) \Delta t, \tag{F.12}$$

and for $m = 0$,

$$E^0(\Delta t, \Delta \underline{Z}_t) = 1 - \hat{h}^T \sum_{m=1}^M \beta_t^m \Delta Z_t^m + |\hat{h}|^2 \sum_{m=1}^M (\beta_t^m)^2 \Delta t. \tag{F.13}$$

Substituting (F.12)-(F.13) into (F.11), we obtain the expression for $\Delta\beta_t^m$. This is identical to the observation update part of the continuous-time filter (7.5)-(7.6).

Remark 12 *In a discrete-time implementation, one can use* (F.6)-(F.8) *to compute the association probability. In the evaluation of* (F.7), $\mathsf{P}\{\Delta Z_t^m | [A_t = m]\}$ *is approximated by using particles:*

$$\mathsf{P}\{\Delta Z_t^m | [A_t = m]\} \approx \frac{1}{N} \frac{1}{(2\pi)^{\frac{s}{2}}\sqrt{\Delta t}} \sum_{i=1}^N \exp\left[-\frac{|\Delta Z_t^m - h(X_t^i)\Delta t|^2}{2\Delta t} \right].$$

In this case, the formula for Gaussian clutter observation density, $\mathsf{P}_0\{\Delta Z_t^j\}$ *in* (F.7)-(F.8)*, can be replaced another commonly used clutter observation density model, e.g., uniform distribution in a "coverage area" V [8, 9]. One can also incorporate gating and detection probability into* (F.6)-(F.8) *as in the classical literature.*

The important point is that once the association probability is computed, the filtering equation for the state process – the PDA-FPF algorithm – does not *depend upon the details of the clutter model. The Gaussian clutter model assumption is primarily used here in the derivation of the continuous-time filter* (7.5)-(7.6) *for computing the association probability.*

F.4 Consistency Proof of p and p^*

Evolution equation for p^*: Recall $\underline{\mathscr{Z}}_t := \sigma(\underline{Z}_\tau : \tau \le t)$, $\mathscr{A}_t := \sigma(A_\tau : \tau \le t)$. We denote $\mathscr{C}_t := \mathscr{A}_t \vee \underline{\mathscr{Z}}_t$. The derivation is based on the property of the conditional expectation:

$$\mathsf{E}[\varphi(X_t)|\underline{\mathscr{Z}}_t] = \mathsf{E}\left[\mathsf{E}[\varphi(X_t)|\mathscr{C}_t]|\underline{\mathscr{Z}}_t\right].$$

The sde for evolution of $\mathsf{E}[\varphi(X_t)|\mathscr{C}_t]$ is described by the standard nonlinear:

$$\mathsf{E}[\varphi(X_t)|\mathscr{C}_t] = \mathsf{E}[\varphi(X_0)] + \int_0^t \mathsf{E}[\mathscr{L}\varphi(X_\tau)|\mathscr{C}_\tau]\,\mathrm{d}\tau + \sum_{m=1}^M \int_0^t \mathsf{E}[(h-\hat{h}_c)^T\varphi(X_\tau)|\mathscr{C}_\tau]\chi_\tau^m(\mathrm{d}Z_\tau^m - \chi_\tau^m\hat{h}_c\,\mathrm{d}\tau),$$

where $\chi_t^m = 1_{[A_t=m]}$, $\hat{h}_c = \mathsf{E}[h(X_t)|\mathscr{C}_t]$, and $\mathscr{L}$ denotes the Kolmogorov's backward operator for the diffusion (7.1) (the adjoint of $\mathscr{L}^\dagger$).

Under Assumption. 7.2.1, taking $\mathsf{E}[\cdot|\underline{\mathscr{Z}}_t]$ gives the desired result since $\hat{h}_c = \hat{h}$, $\mathsf{E}[(h-\hat{h}_c)^T\varphi(X_\tau)|\mathscr{C}_\tau] = \mathsf{E}[(h-\hat{h})^T\varphi(X_\tau)|\underline{\mathscr{Z}}_\tau]$, and $\mathsf{E}[\chi_\tau^m|\underline{\mathscr{Z}}_\tau] = \mathsf{E}[(\chi_\tau^m)^2|\underline{\mathscr{Z}}_\tau] = \mathsf{P}\{[A_\tau = m]|\underline{\mathscr{Z}}_\tau\} =: \beta_\tau^m$.

Evolution equation for p: We express the feedback particle filter (7.8) as:

$$\mathrm{d}X_t^i = a(X_t^i)\,\mathrm{d}t + \sigma_B\,\mathrm{d}B_t^i + \mathsf{K}(X_t^i,t)\sum_{m=1}^M \beta_t^m\,\mathrm{d}Z_t^m + u(X_t^i,t)\,\mathrm{d}t,$$

where

$$u(x,t) := -\sum_{m=1}^M \beta_t^m \mathsf{K}(x,t)\left[\frac{\beta_t^m}{2}h + (1-\frac{\beta_t^m}{2})\hat{h}\right] + \sum_{m=1}^M (\beta_t^m)^2\Omega(x,t), \tag{F.14}$$

and $\Omega(x,t) = (\Omega_1,\Omega_2,\ldots,\Omega_d)$ is the Wong-Zakai correction term for (7.8):

$$\Omega_l(x,t) := \frac{1}{2}\sum_{k=1}^d\sum_{j=1}^s \mathsf{K}_{kj}(x,t)\frac{\partial \mathsf{K}_{lj}}{\partial x_k}(x,t), \text{ for } l \in \{1,\ldots,d\}.$$

The evolution equation for p now follows:

$$\mathrm{d}p = \mathscr{L}^\dagger p\,\mathrm{d}t - \nabla\cdot(pu)\,\mathrm{d}t - \sum_{m=1}^M \beta_t^m\nabla\cdot(p\mathsf{K})\,\mathrm{d}Z_t^m + \sum_{m=1}^M(\beta_t^m)^2\left(\frac{1}{2}\sum_{l,k=1}^d \frac{\partial^2}{\partial x_l\partial x_k}(p[\mathsf{K}\mathsf{K}^T]_{lk})\right)\mathrm{d}t. \tag{F.15}$$

Proof of consistency: The proof follows closely the consistency proof for the multivariable feedback particle filter (see Appendix. A in [154]). If K solves the E-L BVP then

$$\nabla\cdot(p\mathsf{K}) = -(h-\hat{h})^T p. \tag{F.16}$$

On multiplying both sides of (F.14) by $-p$ and simplifying (by using (F.16)), we obtain

$$\begin{aligned} -up &= \sum_{m=1}^{M} \frac{1}{2}(\beta_t^m)^2 \mathsf{K}(h-\hat{h})p + \sum_{m=1}^{M} \beta_t^m p\mathsf{K}\hat{h} - \sum_{m=1}^{M} (\beta_t^m)^2 p\Omega(x,t) \\ &= -\sum_{m=1}^{M} \frac{1}{2}(\beta_t^m)^2 \mathsf{K}\left[\nabla\cdot(p\mathsf{K})\right]^T - \sum_{m=1}^{M} (\beta_t^m)^2 p\Omega + \sum_{m=1}^{M} \beta_t^m p\mathsf{K}\hat{h}, \end{aligned} \tag{F.17}$$

where (F.16) is used to obtain the second equality. Denoting $E := \frac{1}{2}\mathsf{K}[\nabla\cdot(p\mathsf{K})]^T$, a direct calculation shows that

$$E_l + \Omega_l p = \frac{1}{2}\sum_{k=1}^{d} \frac{\partial}{\partial x_k}\left(p[\mathsf{K}\mathsf{K}^T]_{lk}\right).$$

Substituting this in (F.17), on taking the divergence of both sides, we obtain:

$$-\nabla\cdot(pu) + \sum_{m=1}^{M} (\beta_t^m)^2 \frac{1}{2}\sum_{l,k=1}^{d} \frac{\partial^2}{\partial x_l \partial x_k}\left(p[\mathsf{K}\mathsf{K}^T]_{lk}\right) = \sum_{m=1}^{M} \beta_t^m \nabla\cdot(p\mathsf{K})\hat{h}. \tag{F.18}$$

Using (F.16) and (F.18) in the forward equation (F.15), we obtain:

$$\mathrm{d}p = \mathscr{L}^\dagger p\,\mathrm{d}t + \sum_{j=1}^{M} \beta_t^m (h-\hat{h})^T(\mathrm{d}Z_t^m - \hat{h}\,\mathrm{d}t)p.$$

This is precisely the SDE (7.7), as desired.

F.5 Joint Probabilistic Data Association-Feedback Particle Filter

By repeating the steps of the proof in Appendix. F.2, the filter for the joint association probability $\pi_t^{\underline{\gamma}}$ (defined as in (7.22)) is of the following form:

$$\mathrm{d}\pi_t^{\underline{\gamma}} = q\left[1 - M!\,\pi_t^{\underline{\gamma}}\right]\mathrm{d}t + \pi_t^{\underline{\gamma}} \sum_{m=1}^{M} \left[\widehat{h(X_t^{\gamma^m})} - \widehat{\tilde{H}_t^m}\right]^T \mathrm{d}Z_t^m - \pi_t^{\underline{\gamma}} \sum_{m=1}^{M} \left[\widehat{h(X_t^{\gamma^m})}^T \widehat{\tilde{H}_t^m} - \left|\widehat{\tilde{H}_t^m}\right|^2\right]\mathrm{d}t, \tag{F.19}$$

where $\tilde{H}_t = (\tilde{H}_t^1, \ldots, \tilde{H}_t^M) := \sum_{\{\underline{\gamma}\in\Pi(\mathscr{M})\}} \pi_t^{\underline{\gamma}} H(\underline{\gamma})$, $H(\underline{\gamma}) := \left(h(X_t^{\gamma^1}), \ldots, h(X_t^{\gamma^M})\right)$, $\widehat{h(X_t^{\gamma^m})} := \mathsf{E}[h(X_t^{\gamma^m})|\mathscr{Z}_t]$, $\widehat{\tilde{H}_t^m} := \mathsf{E}[\tilde{H}_t^m|\mathscr{Z}_t]$ and $\left|\widehat{\tilde{H}_t^m}\right|^2 := \widehat{\tilde{H}_t^m}^T \widehat{\tilde{H}_t^m}$. All the conditional expectation are approximated by using particles.

Denote $\beta_t^{m,n}$ to be the conditional probability that the m^{th} observation originates from the n^{th} target:

$$\beta_t^{m,n} := \mathsf{P}\{[\alpha_t^m = n]|\mathscr{Z}_t\}.$$

It is obtained by using joint association probability $\pi_t^{\underline{\gamma}}$:

$$\beta_t^{m,n} = \sum_{\{\underline{\gamma} \in \Pi(\mathscr{M}) : \gamma^m = n\}} \pi_t^{\underline{\gamma}}.$$

The JPDA-FPF for the n^{th} target is given by the following controlled system:

$$\mathrm{d}X_t^{i;n} = a^n(X_t^{i;n})\,\mathrm{d}t + \mathrm{d}B_t^{i;n} + \sum_{m=1}^{M} \beta_t^{m,n}\, \mathsf{K}^n(X_t^{i;n}, t) \circ \mathrm{d}I_t^{i,m;n}, \tag{F.20}$$

where $X_t^{i;n} \in \mathbb{R}^d$ is the state for the i^{th} particle at time t for the n^{th} target, $\{B_t^{i;n}\}$ are mutually independent standard Wiener processes, $I_t^{i,m;n}$ is a modified form of the *innovation process*,

$$\mathrm{d}I_t^{i,m;n} := \mathrm{d}Z_t^m - \left[\frac{\beta_t^{m,n}}{2} h(X_t^{i;n}) + \left(1 - \frac{\beta_t^{m,n}}{2}\right) \hat{h}^n\right] \mathrm{d}t, \tag{F.21}$$

where $\hat{h}^n := \mathsf{E}[h(X_t^{i;n}) | \mathscr{Z}_t] = \int_{\mathbb{R}^d} h(x) p_n(x,t)\,\mathrm{d}x \approx \frac{1}{N}\sum_{j=1}^N h(X_t^{j;n})$ and $p_n(x,t)$ denotes the conditional distribution of $X_t^{i;n}$ given $\mathscr{Z}_t$.

The gain function $\mathsf{K}^n = [\nabla\phi_1^n, \ldots, \nabla\phi_s^n]$ is a solution of a certain E-L BVP: for $j \in \{1, \ldots, s\}$,

$$\nabla \cdot (p_n \nabla \phi_j^n) = -(h_j - \hat{h}_j^n) p_n. \tag{F.22}$$

Remark 13 *In a discrete-time implementation, one can use the following heuristic to obtain association probability:*

$$\begin{aligned}
\pi_t^{\underline{\gamma}} &= \prod_{m=1}^{M} \mathsf{P}\{[\alpha_t^m = \gamma^m] | \mathscr{Z}_t\} \ \ (\textit{Assoc. events are independent}) \\
&\propto \prod_{m=1}^{M} \mathsf{P}\left\{ Y_t^m \,\middle|\, [\alpha_t^m = \gamma^m] \right\} \\
&= \frac{1}{(2\pi)^{\frac{s}{2}}} \prod_{m=1}^{M} \left(\int_{\mathbb{R}^d} \exp\left[-\frac{1}{2} |Y_t^m - h(x)|^2 \right] p_{\gamma^m}(x,t)\,\mathrm{d}x \right) \\
&\approx \frac{1}{(2\pi)^{\frac{s}{2}}} \prod_{m=1}^{M} \left(\frac{1}{N} \sum_{i=1}^{N} \exp\left[-\frac{1}{2} \left| Y_t^m - h(X_t^{i;\gamma^m}) \right|^2 \right] \right).
\end{aligned}$$

References

[1] B. D. O. Anderson and J. B. Moore. *Optimal Filtering*. Dover Books on Electrical Engineering. Dover Publications, 2012.

[2] J. L. Anderson and S. L. Anderson. A Monte Carlo implementation of the nonlinear filtering problem to produce ensemble assimilations and forecasts. *Monthly Weather Review*, 127(12):2741–2758, 1999.

[3] C. Andrieu, A. Doucet, S. S. Singh, and V. B. Tadic. Particle methods for change detection, system identification, and control. *Proc. IEEE*, 92(3):423–438, Mar 2004.

[4] M. S. Arulampalam, S. Maskell, N. Gordon, and T. Clapp. A tutorial on particle filters for online nonlinear/non-Gaussian Bayesian tracking. *IEEE Trans. Signal Process.*, 50(2):174–188.

[5] D. Avitzour. Stochastic simulation Bayesian approach to multitarget tracking. In *IEE Proc. of Radar, Sonar and Navigation*, volume 142, pages 41–44, 1995.

[6] B. Azimi-Sadjadi and P. S. Krishnaprasad. Approximate nonlinear filtering and its application in navigation. *Automatica*, 41:945–956, 2005.

[7] A. Bain and D. Crisan. *Fundamentals of Stochastic Filtering*. Springer, Cambridge, Mass, 2010.

[8] Y. Bar-Shalom, F. Daum, and J. Huang. The probabilistic data association filter. *IEEE Control Systems Magazine*, 29(6):82–100, Dec 2009.

[9] Y. Bar-Shalom and T. E. Fortmann. *Tracking and data association*, volume 179 of *Mathematics in Science and Engineering*. Academic Press Inc., San Diego, CA, 1988.

[10] Y. Bar-Shalom, X.-R. Li, and T. Kirubarajan. *Estimation with Applications to Tracking and Navigation*. John Wiley & Sons, Inc., New York, NY, USA, 2001.

[11] A. Baumberg and D. Hogg. Generating spatio-temporal models from examples. *Image and Vision Computing*, 14(8):525–532, 1996. 6th British Machine Vision Conference.

[12] V. E. Beneš. Exact finite-dimensional filters for certain diffusions with nonlinear drift. *Stochastics*, 5:65–92, 1981.

[13] T. Bengtsson, P. Bickel, and B. Li. Curse-of-dimensionality revisited: Collapse of the particle filter in very large scale systems. *ArXiv e-prints*, May 2008.

[14] D. P. Bertsekas and J. N. Tsitsiklis. *Neuro-Dynamic Programming*. Atena Scientific, Cambridge, Mass, 1996.

[15] P. Bickel, B. Li, and T. Bengtsson. Sharp failure rates for the bootstrap particle filter in high dimensions. *IMS Collections*, 3:318–329, 2008.

[16] S. S. Blackman. *Multiple-Target Tracking with Radar Applications*. Artech House, Boston, MA, 1986.

[17] A. Blake, R. Curwen, and A. Zisserman. A framework for spatio-temporal control in the tracking of visual contours. *International Journal of Computer Vision*, 11(2):127–145, 1993.

[18] E. A. Bloem and H. A. P Blom. Joint probabilistic data association methods avoiding track coalescence. In *Proc. of* 34^{th} *IEEE Conf. Decision and Contr.*, volume 3, pages 2752–2757, 1995.

[19] H. A. P. Blom. Markov jump-diffusion models and decision-making-free filtering. In *Proc. of* 6^{th} *International Conf. Analysis and Optimization of Systems*, volume 62, pages 568–580, 1984.

[20] H. A. P. Blom. The continuous time roots of the interacting multiple model filter. In *Proc.* 51^{st} *IEEE Conf. Decision Contr.*, pages 6015–6021, Maui, Hawaii, Dec 2012.

[21] H. A. P. Blom and Y. Bar-Shalom. The interacting multiple model algorithm for systems with Markovian switching coefficients. *IEEE Trans. Autom. Control*, 33(8):780–783, 1988.

[22] H. A. P. Blom and E. A. Bloem. Probabilistic data association avoiding track coalescence. *IEEE Trans. Autom. Control*, 45(2):247–259, 2000.

[23] H. A. P Blom and E. A. Bloem. Combining IMM and JPDA for tracking multiple maneuvering targets in clutter. In *Proc.* 5^{th} *Int. Conf. on Inf. Fusion*, volume 1, pages 705–712, 2002.

[24] H. A. P Blom and E. A. Bloem. Interacting multiple model joint probabilistic data association avoiding track coalescence. In *Proc.* 41^{st} *IEEE Conf. Decision Contr.*, volume 3, pages 3408–3415, 2002.

[25] H. A. P Blom and E. A. Bloem. Joint IMMPDA particle filter. In *Proc.* 6^{th} *Int. Conf. on Inf. Fusion*, volume 2, pages 785–792, 2003.

[26] H. A. P. Blom and E. A. Bloem. Particle filtering for stochastic hybrid systems. In *Proc.* 43^{rd} *IEEE Conf. Decision and Contr.*, pages 3221–3226, Dec. 2004.

[27] H. A. P. Blom and E. A. Bloem. Joint particle filtering of multiple maneuvering targets from unassociated measurements. *Journal of Advancement Information Fusion*, 1:15–36, 2006.

[28] H. A. P. Blom and E. A. Bloem. Exact Bayesian and particle filtering of stochastic hybrid systems. *IEEE Trans. Aerosp. Electron. Syst.*, 43(1):55–70, 2007.

[29] H. A. P. Blom and E. A. Bloem. Decomposed particle filtering and track swap estimation in tracking two closely spaced targets. In *Proc.* 14^{th} *Int. Conf. on Inf. Fusion*, pages 1–8, Jul. 2011.

[30] V. S. Borkar and S. K. Mitter. A note on stochastic dissipativeness. In A. Rantzer and C. I. Byrnes, editors, *Directions in Mathematical Systems Theory and Optimization*, in honor of Professor Anders Lindquist's 60th birthday, pages 41–49. Springer-Verlag, 2002.

[31] D. Brigo, B. Hanzon, and F. LeGland. A differential geometric approach to nonlinear filtering: the projection filter. *IEEE Trans. Autom. Control*, 43(2):247–252, Feb 1998.

[32] R. W. Brockett. *Stochastic control (lecture notes)*. Harvard University, Cambridge, MA., April 2009.

[33] E. N. Brown, R. Barbieri, V. Ventura, R. E. Kass, and L. M. Frank. The time-rescaling theorem and its applications to neural spike train data analysis. *Neural Computation*, 14:325–346, 2002.

[34] R. S. Bucy. Nonlinear filtering theory. *IEEE Trans. Autom. Control*, 10:198, 1965.

[35] R. S. Bucy and P. D. Joseph. *Filtering for stochastic processes with applications to guidance*. Chelsea Publishing Co., New York, 1987.

[36] A. Budhiraja, L. Chen, and C. Lee. A survey of numerical methods for nonlinear filtering problems. *Physica D: Nonlinear Phenomena*, 230(1-2):27–36, 2007.

[37] P. Bui Quang, C. Musso, and F. Le Gland. An insight into the issue of dimensionality in particle filtering. In *Proc.* 13^{th} *Int. Conf. on Inf. Fusion*, pages 1–8, July 2010.

[38] Z. Cai, F. Le Gland, and H. Zhang. An adaptive local grid refinement method for nonlinear filtering. Technical report, INRIA, 1995.

[39] O. Cappe, S.J. Godsill, and E. Moulines. An overview of existing methods and recent advances in sequential monte carlo. *Proc. IEEE*, 95(5):899–924, May 2007.

[40] H. Carvalho, P. Del Moral, A. Monin, and G. Salut. Optimal nonlinear filtering in GPS/INS integration. *IEEE Trans. Aerosp. Electron. Syst.*, 33(3):835–850, July 1997.

[41] B. Chen and J. K. Tugnait. Tracking of multiple maneuvering targets in clutter using IMM/JPDA filtering and fixed-lag smoothing. *Automatica*, 37(2):239–249, 2001.

[42] A. J. Chorin. Numerical study of slightly viscous flow. *J. Fluid Mech.*, 57:785–796, 1973.

[43] T. P. Coleman and S. Sarma. A computationally efficient method for modeling neural spiking activity with point processes nonparametrically. In *Proc.* 46^{th} *IEEE Conf. Decision Contr.*, pages 5800–5805, December 2007.

[44] D. Crisan and A. Doucet. A survey of convergence results on particle filtering methods for practitioners. *IEEE Trans. Signal Process.*, 50(3):736–746, 2002.

[45] D. Crisan and J. Xiong. Approximate McKean-Vlasov representations for a class of SPDEs. *Stochastics: An International Journal of Probability and Stochastic Processes*, pages 1–16, 2009.

[46] J. Cvitanic, R. Lipster, and B. Rozovskii. A filtering approach to tracking volatility from prices observed at random times. *Ann. Appl. Probab.*, 16:1633–1652, 2006.

[47] F. Daum and J. Huang. Curse of dimensionality and particle filters. In *IEEE Proc. Aerosp. Conf.*, volume 4, pages 4–1979–4–1993, March 2003.

[48] F. Daum and J. Huang. Nonlinear filters with log-homotopy. In *Proc. SPIE*, volume 6699, pages 669918–669918–15, Orlando, FL, March 2007.

[49] F. Daum and J. Huang. Particle flow for nonlinear filters with log-homotopy. In *Proc. SPIE*, volume 6969, pages 696918–696918–12, Orlando, FL, March 2008.

[50] F. Daum and J. Huang. Nonlinear filters with particle flow induced by log-homotopy. In *Proc. SPIE*, volume 7336, pages 733603–733603–12, Orlando, FL, April 2009.

[51] F. Daum and J. Huang. Generalized particle flow for nonlinear filters. In *Proc. SPIE*, pages 76980I–76980I–12, 2010.

[52] F. Daum and J. Huang. Particle degeneracy: root cause and solution. In *Proc. SPIE*, volume 8050, May 2011.

[53] F. Daum, J. Huang, and A. Noushin. Exact particle flow for nonlinear filters. In *Proc. SPIE*, volume 7697, pages 769704–769704–19, Orlando, FL, 2010.

[54] P. Del Moral. *Feynman-Kac Formulae: Genealogical and Interacting Particle Systems with Applications*. Probability and Its Applications. Springer, 2004.

[55] A. Doucet, N. de Freitas, and N. Gordon. *Sequential Monte-Carlo Methods in Practice*. Springer-Verlag, April 2001.

[56] A. Doucet, S. Godsill, and C. Andrieu. On sequential Monte Carlo sampling methods for Bayesian filtering. *Statistics and computing*, 10(3):197–208, 2000.

[57] A. Doucet and A. M. Johansen. A tutorial on particle filtering and smoothing: fifteen years later. In *OXFORD Handbook of Nonlinear Filtering*, pages 656–704, 2011.

[58] K. Doya, S. Ishii, A. Pouget, and R. P. N. Rao. *Bayesian Brain*. Comput. Neurosci. MIT Press, Cambridge, MA, 2007.

[59] H. Driessen and Y. Boers. An efficient particle filter for jump Markov nonlinear systems. In *Proc. IEE Colloquium on Target Tracking*, March 2004.

[60] L. C. Evans. *Partial differential equations*. American Mathematical Society, Providence, RI, 1998.

[61] L. C. Evans. Partial differential equations and Monge–Kantorovich mass transfer, 2001. Lecture notes.

[62] G. Evensen. Sequential data assimilation with nonlinear quasi-geostrophic model using monte carlo methods to forecast error statistics. *Journal of Geophysical Research*, 99(C5):143–162, 1994.

[63] G. Evensen. *Data assimilation : The ensemble Kalman filter*. Springer, Berlin, 2007.

[64] M. Fallah, R. Malhamé, and F. Martinelli. Decentralized estimation in a class of measurements induced mean field control problems. In *Proc. 52nd IEEE Conf. Decision Contr.*, 2013.

[65] M. A. Fallah, R. P Malhame, and F. Martinelli. Distributed estimation and control for large population stochastic multi-agent systems with coupling in the measurements. In *Proc. European Control Conf.*, pages 4353–4358, 2013.

[66] R.J. Fitzgerald. Track biases and coalescence with probabilistic data association. *IEEE Trans. Aerosp. Electron. Syst.*, AES-21(6):822–825, 1985.

[67] W. Fleming and S. Mitter. Optimal control and nonlinear filtering for nondegenerate diffusion processes. *Stochastics*, 8:63–77, 1982.

[68] D. A. Forsyth and J. Ponce. *Computer vision: a modern approach*. Prentice Hall Professional Technical Reference, 2002.

[69] W. R. Gilks and C. Berzuini. Following a moving target – Monte Carlo inference for dynamic Bayesian models. *J. R. Statist. Soc. B*, 63(1):127–146, 2001.

[70] D. Givon, P. Stinis, and J. Weare. Variance reduction for particle filters of systems with time scale separation. *IEEE Trans. Signal Process.*, 57(2):424–435, 2009.

[71] P. W. Glynn and S. P. Meyn. A Liapounov bound for solutions of the Poisson equation. *Ann. Appl. Probab.*, 24(2):916–931, 1996.

[72] T. Gneiting and A. E. Raftery. Weather forecasting with ensemble methods. *Science*, 310(5746):248–249, 2005.

[73] N. Gordon, D. Salmond, and D. Fisher. Bayesian target tracking after group pattern distortion. In *Proc. SPIE*, pages 238–248, 1997.

[74] N. J. Gordon, D. J. Salmond, and A. F. M. Smith. Novel approach to nonlinear/non-Gaussian Bayesian state estimation. *IEE Proc. F Radar and Signal Processing*, 140(2):107–113, 1993.

[75] L. Greengard and V. Rokhlin. A fast algorithm for particle simulations. *J. Comput. Phys.*, 73:325–348, December 1987.

[76] Y. Gu and D. S. Oliver. History matching of the PUNQ-S3 reservoir model using the ensemble Kalman filter. *SPE J.*, 10(2):217–224, 2005.

[77] F. Gustafsson, F. Gunnarsson, N. Bergman, U. Forssell, J. Jansson, R. Karlsson, and P.-J. Nordlund. Particle filters for positioning, navigation and tracking. *IEEE Trans. Signal Process.*, 50:425–437, 2002.

[78] J. E. Handschin and D. Q. Mayne. Monte Carlo techniques to estimate the conditional expectation in multi-stage nonlinear filtering. *International Journal of Control*, 9(5):547–559, 1969.

[79] M. Huang, P. E. Caines, and R. P. Malhame. Large-population cost-coupled LQG problems with nonuniform agents: Individual-mass behavior and decentralized ϵ-Nash equilibria. *IEEE Trans. Autom. Control*, 52(9):1560–1571, 2007.

[80] C. Hue, J.-P. Le Cadre, and P. Perez. Sequential Monte Carlo methods for multiple target tracking and data fusion. *IEEE Trans. Signal Process.*, 50(2):309–325, 2002.

[81] W. Huisinga, S. Meyn, and C. Schütte. Phase transitions and metastability in Markovian and molecular systems. *Ann. Appl. Probab.*, 14(1):419–458, 2004.

[82] I. Hwang, H. Balakrishnan, K. Roy, and C. Tomlin. Multiple-target tracking and identity management in clutter for air traffic control. In *Proc. Amer. Control Conf.*, volume 4, pages 3422–3428, Boston, MA, 2004.

[83] M. Isard and A. Blake. Contour tracking by stochastic propagation of conditional density. In *European Conf. Computer Vision*, pages 343–356, 1996.

[84] M. Isard and A. Blake. Condensation - conditional density propagation for visual tracking. *International Journal of Computer Vision*, 29:5–28, 1998.

[85] M. Isard and A. Blake. A mixed-state condensation tracker with automatic model-switching. In 6^{th} *International Conf. Computer Vision*, pages 107–112, Jan 1998.

[86] A. H. Jazwinski. *Stochastic Processes and Filtering theory*. Academic Press, New York, 1970.

[87] J. Johnsen. On the spectral properties of Witten-Laplacians, their range projections and Brascamp-Lieb's inequality. *Integral Equations Operator Theory*, 36(3):288–324, 2000.

[88] R. Jordan, D. Kinderlehrer, and F. Otto. The variational formulation of the Fokker-Planck equation. *SIAM J. Math. Anal*, 29:1–17, 1999.

[89] S. J. Julier and J. K. Uhlmann. A New Extension of the Kalman Filter to Nonlinear Systems. In *International Symposium Aerospace/Defense Sensing, Simulation and Controls*, volume 3068, pages 182–193, 1997.

[90] T. Kailath, A. H. Sayed, and B. Hassibi. *Linear estimation*. Prentice-Hall information and system sciences series. Prentice Hall, 2000.

[91] G. Kallianpur. *Stochastic filtering theory*. Springer-Verlag, New York, 1980.

[92] R. E. Kalman. A new approach to linear filtering and prediction problems. *Trans. ASME ser. D*, 82:35–45, 1960.

[93] R. E. Kalman. New methods in wiener filtering theory. In *Proc. of* 1^{st} *symposium on engineering applications of random function theory and probability*, pages 270–388, 1963.

[94] R. E. Kalman and R. S. Bucy. New results in linear filtering and prediction theory. *Trans. ASME ser. D*, 83:95–107, 1961.

[95] R. Karlsoon and F. Gustafsson. Monte Carlo data association for multiple target tracking. In *Proc. IEE Target Tracking: Algorithms Appl.*, Amsterdam, The Netherlands, 2001.

[96] S. Kichenassamy, A. Kumar, P. Olver, A. Tannenbaum, and A. Yezzi. Gradient flows and geometric active contour models. In *Proc.* 5^{th} *International Conf. Computer Vision*, pages 810–815, 1995.

[97] T. Kirubarajan and Y. Bar-Shalom. Probabilistic data association techniques for target tracking in clutter. *Proc. IEEE*, 92(3):536–557, 2004.

[98] D. Knill and A. Pouget. The Bayesian brain: the role of uncertainty in neural coding and computation. *Trends in Neuroscience*, 27(12):712–719, 2004.

[99] H. Kunita. *Stochastic Flows and Stochastic Differential Equations*. Cambridge University Press, Cambridge, 1990.

[100] H. J. Kushner. On the differential equations satisfied by conditional probability densities of Markov processes. *SIAM J. Control*, 2:106–119, 1964.

[101] I. Kyriakides, D. Morrell, and A. Papandreou-Suppappola. Sequential Monte Carlo methods for tracking multiple targets with deterministic and stochastic constraints. *IEEE Trans. Signal Process.*, 56(3):937–948, 2008.

[102] S. Lankton and A. Tannenbaum. Localizing region-based active contours. *IEEE Trans. Image Process.*, 17(11):2029–2039, 2008.

[103] J. M. Lasry and P. L. Lions. Mean field games. *Japanese Journal of Mathematics*, 2(1):229–260, 2007.

[104] R. S. Laugesen, P. G. Mehta, S. P. Meyn, and M. Raginsky. Poisson's equation in nonlinear filtering. *SIAM J. Control and Optimization*, 2013. Submitted.

[105] T. S. Lee and D. Mumford. Hierarchical Bayesian inference in the visual cortex. *Journal of the Optical Society of America, A*, 20(7):1434–1448, 2003.

[106] A. Leonard. Vortex method for flow simulation. *Journal of Computational Physics*, 37:289–335, 1980.

[107] R. S. Liptser and A. N. Shiryayev. *Statistics of Random Processes*. Springer Verlag, 1977.

[108] K. A. Loparo, Z. Roth, and S. J. Eckert. Nonlinear filtering for systems with random structure. *IEEE Trans. Autom. Control*, 31(11):1064–1068, November 1986.

[109] S. Lototsky, R. Mikulevicius, and B. L. Rozovskii. Nonlinear filtering revisited: A spectral approach. *SIAM J. Control and Optimization*, 35(2):435–461, 1997.

[110] R. Ma and T. P. Coleman. Generalizing the posterior matching scheme to higher dimensions via optimal transportation. In *Allerton Conf. on Communication, Control and Computing*, pages 96–102, 2011.

[111] W. J. Ma, J. Beck, P. Latham, and A. Pouget. Bayesian inference with probabilistic population codes. *Nature Neuroscience*, 9(11):1432–1438, 2006.

[112] E. Mazor, A. Averbuch, Y. Bar-Shalom, and J. Dayan. Interacting multiple model methods in target tracking: A survey. *IEEE Trans. Aerosp. Electron. Syst.*, 34(1):103–123, 1998.

[113] S. McGinnity and G. W. Irwin. Multiple model bootstrap filter for maneuvering target tracking. *IEEE Trans. Aerosp. Electron. Syst.*, 36(3):1006–1012, 2000.

[114] S. P. Meyn. *Control Techniques for Complex Networks*. Cambridge University Press, Cambridge, 2007.

[115] O. Michailovich, Y. Rathi, and A. Tannenbaum. Image segmentation using active contours driven by the Bhattacharyya gradient flow. *IEEE Trans. Image Process.*, 16(11):2787–2801, 2007.

[116] S. K. Mitter and N. J. Newton. The duality between estimation and control. In J. L. Menaldi, E. Rofman, and A. Sulem, editors, *Optimal Control and Partial Differential Equations*, In honor of Professor Alain Bensoussan's 60th anniversary. IOS Press, Amsterdam, 2000.

[117] S. K. Mitter and N. J. Newton. A variational approach to nonlinear estimation. *SIAM J. Control and Optimization*, 42(5):1813–1833, 2003.

[118] S. K. Mitter and N. J. Newton. Information and entropy flow in the Kalman-Bucy filter. *Journal of Statistical Physics*, 118(1-2):145–176, 2005.

[119] C. Musso, N. Oudjane, and F. Le Gland. Improving regularized particle filters. In A. Doucet, N. de Freitas, and N. Gordon, editors, *Sequential Monte Carlo methods in practice*, pages 247–271. Springer, 2001.

[120] J. R. Norris. *Markov Chains*. Cambridge University Press, 1998.

[121] S. Oh, S. Russell, and S. Sastry. Markov chain Monte Carlo data association for multi-target tracking. *IEEE Trans. Autom. Control*, 54(3):481–497, 2009.

[122] B. Øksendal. *Stochastic Differential Equations (6th ed.): An Introduction with Applications*. Springer-Verlag, Inc., New York, NY, USA, 2005.

[123] D. S. Oliver and Y. Chen. Recent progress on reservoir history matching: a review. *Comput. Geosci.*, 15:185–221, 2011.

[124] K. R. Pattipati, R. L. Popp, and T. Kirubarajan. Survey of assignment techniques for multitarget tracking. In Y. Bar-Shalom and W. D. Blair, editors, *Multitarget-Multisensor Tracking: Application and Advances*. Artech, Boston, 2000.

[125] S. Pequito, A. Aguiar, B. Sinopoli, and D. A. Gomes. Nonlinear estimation using mean field games. In *Proc. 5th International Conf. Network Games, Control and Optimization*, pages 1–5, 2011.

[126] M. K. Pitt and N. Shephard. Filtering via simulation: auxiliary particle filters. *J. Amer. Statist. Assoc.*, 94(446):590–599, 1999.

[127] B. R. Rambharat. American option valuation with particle filters. In R. A. Carmona, P. Del Moral, P. Hu, and N. Oudjane, editors, *Numerical Methods in Finance*, volume 12 of *Springer Proceedings in Mathematics*, pages 51–82. Springer Berlin Heidelberg, 2012.

[128] R. P. N. Rao, B. A. Olshausen, and M. S. Lewicki. *Probabilistic Models of the Brain*. MIT Press, Cambridge, MA, 2002.

[129] Rajesh P. N. Rao. Neural models of Bayesian belief propagation. In *Bayesian Brain*, Comput. Neurosci., pages 239–267. MIT Press, Cambridge, MA, 2007.

[130] Sebastian Reich. A dynamical systems framework for intermittent data assimilation. *BIT Numerical Mathematics*, 51(1):235–249, 2011.

[131] D. B. Reid. An algorithm for tracking multiple targets. *IEEE Trans. Autom. Control*, 24:843–854, 1979.

[132] B. Ristic, S. Arulampalam, and N. Gordon. *Beyond the Kalman Filter: Particle Filters for Tracking Applications*. Artech House, 2004.

[133] Y. Sato, T. Toyoizumi, and K. Aihara. Bayesian inference explains perception of unity and ventriloquism aftereffect: identification of common sources of audiovisual stimuli. *Neural Comput.*, 19:3335–55, 2007.

[134] P. M. Stano, A. K Tilton, and R. BabuKska. Estimation of the soil-dependent time-varying parameters of the hopper sedimentation model: The FPF versus the BPF. *Control Engineering Practice*, 24:67–78, 2014.

[135] R. L. Stratonovich. Conditional markov processes. *Teor. Verojatnost. i Primenen*, 5:172–195, 1960.

[136] L. Svensson, D. Svensson, M. Guerriero, and P. Willett. Set JPDA filter for multitarget tracking. *IEEE Trans. Signal Process.*, 59(10):4677–4691, 2011.

[137] S. Thrun. Probabilistic robotics. *Commun. ACM*, 45:52–57, March 2002.

[138] A. K. Tilton, S. Ghiotto, and P. G. Mehta. A comparative study of nonlinar filtering techniques. In *Proc. 16th Int. Conf. on Inf. Fusion*, pages 1827–1834, July 2013.

[139] A. K. Tilton, E. T. Hsiao-Wecksler, and P. G. Mehta. Filtering with rhythms: Application of the feedback particle filter to estimation of human gait cycle. In *Proc. Amer. Control Conf.*, pages 3433–3438, Montréal, Canada, June 2012.

[140] A. K. Tilton, P. G. Mehta, and S. P. Meyn. Multi-dimensional feedback particle filter for coupled oscillators. In *Proc. Amer. Control Conf.*, pages 2415–2421, Washington D.C., June 2013.

[141] S. T. Tsay. *Analysis of Financial Time Series*. Wiley, 2002.

[142] R. van Handel. Discrete time nonlinear filters with informative observations are stable. *Elect. Comm. in Probab.*, 13:562–575, 2008.

[143] P. J. van Leeuwen. A variance-minimizing filter for large-scale applications. *Monthly Weather Review*, 131:2071–2084, 2003.

[144] P. J. van Leeuwen and G. Evensen. Data assimilation and inverse methods in terms of probabilities formulation. *Monthly Weather Review*, 124:2898–2913, 1996.

[145] C. Villani. *Topics in Optimal Transportation*. American Mathematical Society, Providence, RI, 2003.

[146] E. A. Wan and R. van der Merwe. The unscented kalman filter for nonlinear estimation. In *Proc. ASPCC*, pages 153–158, 2000.

[147] X.-H. Wen and W. H. Chen. Real-time reservoir model updating using ensemble Kalman filter. *SPE J.*, 11(4):431–442, 2006.

[148] W. M. Wonham. Some applications of stochastic differential equations to optimal nonlinear filtering. *SIAM J. Control*, 2:347–369, 1965.

[149] J. Xiong. *An introduction to Stochastic filtering theory*. Oxford University Press, Oxford, UK, 2008.

[150] J. Xiong. Particle approximations to the filtering problem in continuous time. In D. Crisan and B. Rozovskii, editors, *The Oxford Handbook of Nonlinear Filtering*. Oxford University Press, 2011.

[151] T. Yang, H. A. P. Blom, and P. G. Mehta. Interacting multiple model-feedback particle filter for stochastic hybrid systems. In *Proc. 52nd IEEE Conf. Decision Contr.*, pages 7065–7070, Florence, Italy, Dec 2013.

[152] T. Yang, H. A. P. Blom, and P. G. Mehta. The continuous-discrete time feedback particle filter. In *Proc. Amer. Control Conf.*, pages 648–653, Portland, OR, June 2014.

[153] T. Yang, G. Huang, and P. G. Mehta. Joint probabilistic data association-feedback particle filter for multi-target tracking application. In *Proc. Amer. Control Conf.*, pages 820–826, Montréal, Canada, June 2012.

[154] T. Yang, R. S. Laugesen, P. G. Mehta, and S. P. Meyn. Multivariable feedback particle filter. In *Proc. 51st IEEE Conf. Decision Contr.*, pages 4063–4070, Maui, HI, Dec 2012.

[155] T. Yang and P. G. Mehta. Probabilistic Data Association-Feedback Particle Filter for Multiple Target Tracking Applications . *ArXiv e-prints*, 2014.

[156] T. Yang, P. G. Mehta, and S. P. Meyn. Feedback particle filter with mean-field coupling. In *Proc. 50th IEEE Conf. Decision Contr.*, pages 7909–7916, Orlando, FL, December 2011.

[157] T. Yang, P. G. Mehta, and S. P. Meyn. A mean-field control-oriented approach for particle filtering. In *Proc. Amer. Control Conf.*, pages 2037–2043, San Francisco, June 2011.

[158] T. Yang, P. G. Mehta, and S. P. Meyn. Feedback particle filter. *IEEE Trans. Autom. Control*, 58(10):2465–2480, October 2013.

[159] T. Yang, P. G. Mehta, and S. P. Meyn. The feedback particle filter for a continuous-time Markov chain. In *Proc. Amer. Control Conf.*, Washington D.C., June 2013.

[160] H. Yin, P. G. Mehta, S. P. Meyn, and U. V. Shanbhag. Synchronization of coupled oscillator is a game. *IEEE Trans. Autom. Control*, 57(4):920–935, 2012.